

703<sup>e</sup>

ARCHEOMETRY OF PLEISTOCENE SITES

ARCHEOMETRY OF FIVE PLEISTOCENE SITES  
AS INFERRED FROM  
URANIUM AND THORIUM  
ISOTOPIC ABUNDANCES IN TRAVERTINE

by

BONNIE BLACKWELL, B.A.

A Thesis

submitted to the Department of Geology  
in Partial Fulfilment of the Requirements

for the Degree  
Master of Sciences

McMaster University

September 1980

MASTER OF SCIENCE (1980)

McMASTER UNIVERSITY

(geology)

Hamilton, Ontario.

Title: Archeometry of Five Pleistocene Sites as inferred  
from Uranium and Thorium Isotopic Abundences in  
Travertine

Author: Bonnie Blackwell, B.A.

Supervisor: Dr. H. P. Schwarcz

Number of Pages: xxix, 538

## ABSTRACT

The U/Th dating method has been applied to five archeological sites in France. The U/Th method relies upon the coprecipitation of uranium with calcium carbonate in speleothems formed in caves. Because  $^{230}\text{Th}$  forms in the calcite from the decay of  $^{234}\text{U}$  a radiometric clock is begun in the newly deposited calcite. Dates are derived from measuring the isotopic abundances of the uranium and thorium in the calcite. For many archeological samples, pre-roasting of the sample before analysis is necessary to improve the yields.

Normally, relative dates for archeological sites are derived from the comparison of paleoclimatic interpretations determined from sedimentological, faunal, and palynological studies of the cave sediments with global climatic records. These methods have established that the Mousterian culture and Neanderthals appeared in Europe at the beginning of the Wurm, 80 Ka BP.

Absolute dates determined for samples from Lachaise, Montgaudier, Pech de l'Aze, Abri Vaufrey, and Grotte 13, where archeological or faunal material is associated stratigraphically with speleothems sampled, have established that there were several regional climatic phenomena experienced in southern France. These events are dated at 80 to 120 Ka BP, interpreted to be the Riss/Würm interglacial, and at 38 to 50 Ka, interpreted to be the Würm I/II interstadial. Furthermore, archeological materials and human skeletal remains associated with these sites and the spel-

eothers therein, have proven that the Neanderthals must have evolved prior to 150 Ka BP, but that they did not develop their Mousterian culture until about 125 Ka BP.

## ACKNOWLEDGEMENTS

It was only with the help and assistance of many people that this work was successfully completed. Therefore, I wish to express my thanks to the following people.

Without the help, encouragement, and financial support of my supervisor, Dr. Henry P. Schwarcz, this research would not have been possible. The initial sample collections in France were made by Dr. Schwarcz, with the help of Professor François Bordes, Henri Laville, Andre Debenath, and Jean-Philippe Rigaud. In addition, I must thank Messrs. Debenath and Rigaud for their aid in my own sample collections.

Ada Dixon, and Marija Smith, the laboratory technicians provided excellent technical advice, and helped in innumerable small ways. Both Mel Gascoyne and Alf Latham listened to my problems and offered stimulation, criticism when it was sorely needed, and assistance of all kinds. Mr. Jack Whorwood provided the photographic assistance.

Finally, my deepest gratitude to Val Li who tirelessly keypunched data, proofread the copy, and helped in the drafting, in addition to supporting and encouraging me at every step.



It's Time Again To Change  
THE COUNTERS!

## TABLE OF CONTENTS

	<u>Page</u>
ABSTRACT	v
1. INTRODUCTION	1
2. THE THEORY	12
2.1 The Geological Cycle	12
2.1.1 The Uranium Cycle	12
2.1.2 The Thorium Cycle	19
2.1.3 Isotopic Fractionation of Uranium	22
2.2 Cave Systems	25
2.2.1 The Carbonate System	25
2.2.2 Cave Genesis and Evolution	29
2.2.3 Abri Genesis and Evolution	30
2.2.4 Speleothem Morphology	33
2.3 Radioactive Decay	36
2.4 The Uranium-Thorium Decay Series	38
2.5 The Theoretical Principles of U/Th Dating	43
3. THE METHOD	48
3.1 The Chemical Analysis	48
3.1.1 Detrital Contamination	52



	<u>Page</u>
3.1.2 The Roasting Technique	59
3.1.2.1 Problems with Roasted Samples	60
3.1.2.2 Results upon Roasting	64
3.2 Computing the Uranium Thorium Relationship	66
3.3 Calibration of the Method	73
3.4 The Application of the Dating Method to Archeology	75
3.5 Limitations of the Method	82
4. ARCHEOLOGICAL METHODS	93
4.1 Sedimentology	93
4.1.1 Global Granulometry	94
4.1.2 Element Separation	94
4.1.3 Granulometry of the Pebbles	99
4.1.4 Morphoscopy	99
4.1.4.1 The Effects of Frost	99
4.1.4.2 The Effects of Humidity	105
4.1.5 Fines Analysis	118
4.1.5.1 Calcimetry	119
4.1.5.2 Granulometry and Densitometry	119
4.1.5.3 pH of the Fines	119
4.1.5.4 Morphoscopy	124
4.1.5.5 Other Methods	124
4.1.6 Summary	124

	<u>Page</u>	
4.2	Palynology	124
4.3	Faunal Analysis	128
4.4	Intrepreting the Paleoclimatological Data	142
4.5	Archeological Techniques	143
4.5.1	Excavation	143
4.5.2	Typological Analysis	146
4.5.2.1	Cores or Nuclei	147
4.5.2.2	Debitage	147
4.5.2.3	Retouched Tools	152
4.5.2.4	Other Tools	158
4.5.2.5	Typological Indices	161
4.5.3	Technical Indices	161
4.5.4	Representing the Archeological Data	163
4.6	Absolute Dating Methods Used by Archeo- logists	166
4.6.1	<sup>14</sup> C Dating	166
4.6.2	K/Ar Dating	168
4.6.3	Thermoluminescence	169
5.	PEOPLES AND CULTURES OF THE MIDDLE AND UPPER PLEISTOCENE	170
5.1	Terminology for the Pleistocene	170
5.2	Climate	176
5.3	Pleistocene Hominids	177
5.3.1	<u>Homo erectus</u>	180

	<u>Page</u>
5.3.2 Neanderthals	185
5.3.2.1 "Classic" Neanderthal Morphology	186
5.3.2.2 Other Neanderthals	189
5.3.3 <u>Homo sapiens sapiens</u>	196
5.4 Pleistocene Cultures	196
5.4.1 The Acheulian	196
5.4.2 The Mousterian	202
5.4.2.1 Significance of the Mousterian Assemblages	206
5.4.3 The Upper Paleolithic	208
6. THE SITES IN THE CHARENTE	211
6.1 Geography	211
6.2 Geology	214
6.2.1 The Charente Karst	215
6.3 Lachaise	218
6.3.1 The History of Excavation at Lachaise	218
6.3.2 General Description	219
6.3.3 Stratigraphy	224
6.3.3.1 Bourgeois-Delaunay	224
6.3.3.2 Suard	237
6.3.3.3 Comparison between Bourgeois-Delaunay and Suard	242

	<u>Page</u>
6.3.4 Archeology	243
6.3.4.1 Suard	243
6.3.4.2 Bourgeois-Delaunay	266
6.3.5 Human Remains at Lachaise	291
6.3.5.1 Suard	291
6.3.5.2 Bourgeois-Delaunay	291
6.3.6 Paleoenvironments	296
6.3.6.1 Fauna	296
6.3.6.2 Interpretations	296
6.3.7 Other Absolute Dates for Lachaise	300
6.3.8 Sample Description	300
6.3.8.1 Bourgeois-Delaunay	320
6.3.8.2 Suard	320
6.3.8.3 <u>Couloir</u>	321
6.3.9 Results	323
6.3.9.1 Bourgeois-Delaunay	323
6.3.9.2 Suard	324
6.3.9.3 <u>Couloir</u>	325
6.3.10 Conclusions	325
6.4 Montgaudier	331
6.4.1 The History of Excavation	332
6.4.2 General Description	332
6.4.3 Stratigraphy	339
6.4.3.1 The Grand Porche	339

	<u>Page</u>
6.4.3.2 The Balcony	340
6.4.3.3 Abri Lartet	341
6.4.3.4 Abri Gaudry	346
6.4.3.5 Abri Paignon	346
6.4.4 Archeology	348
6.4.4.1 Lower Paleolithic	348
6.4.4.2 The Mousterian	348
6.4.4.3 Perigordina and Aurignacian	352
6.4.4.4 Solutrean	352
6.4.4.5 Magdalenian	354
6.4.5 Human Remains at Montgaudier	362
6.4.6 Paleoenvironments	362
6.4.7 Sample Descriptions	369
6.4.8 Results	370
6.4.8.1 Abri Lartet	372
6.4.8.2 Abri Gaudry	390
6.4.8.3 New Hall	390
6.4.8.4 Cave Bear Alley	391
6.4.8.5 The Grand Porche	391
6.4.9 Conclusions	391
6.5 Conclusions	393
7. THE SITES IN THE DORDOGNE	395
7.1 Geography	395

7.2	Geology	
7.3	Pech de l'Azé	
7.3.1	The History of Excavation	
7.3.2	General Description	
7.3.3	Stratigraphy	
7.3.3.1	Pech de l'Azé I	
7.3.3.2	Pech de l'Azé II	
7.3.3.3	Pech de l'Azé IV	
7.3.4	Archeology	
7.3.4.1	Pech de l'Azé I	
7.3.4.2	Pech de l'Azé II	
7.3.4.3	Pech de l'Azé IV	
7.3.5	Human Remains at Pech de l'Azé	
7.3.6	Paleoenvironments	
7.3.7	Results	
7.3.7.1	Pech de l'Azé IV	
7.3.7.2	Pech de l'Azé I	
7.3.7.	Pech de l'Azé II	
7.3.8	Conclusions	
7.4	The Castelnaud Caves	
7.4.1	The History of Excavation	
7.4.2	The Fromation of the Caves	
7.4.3	Abri Vaufrey	
7.4.3.1	General Description	

- 7.4.3.2 Stratigraphy
- 7.4.3.3 Archeology and Fauna
- 7.4.3.4 Human Remains
- 7.4.3.5 Paleoenvironments
- 7.4.3.6 Sample Descriptions
- 7.4.3.7 Results
- 7.4.3.8 Conclusions

7.4.4. Grotte Treize

- 7.4.4.1 General Description
- 7.4.4.2 Stratigraphy
- 7.4.4.3 Paleoenvironments
- 7.4.4.4 Sample Descriptions
- 7.4.4.5 Results
- 7.4.4.6 Conclusions

7.5 Conclusions

8. CONCLUSIONS

REFERENCES

## LIST OF TABLES

<u>Table</u>	<u>Page</u>
2.1 Important Aqueous Uranium Species	14
3.1 Comparison of Roasted and Unroasted Samples	65
4.1 Chronology of the Pleistocene Mammals	137
4.2 Bordes' List of Mousterian Tool Types	
4.3 Index Definitions	162
5.1 Terminology from the Pleistocene	172
5.2 Chronology of the Pleistocene	173
5.3 Differences between "Classic" and Eastern Neanderthals and <u>Homo sapiens sapiens</u>	191
5.4 Chronology of the Upper Paleolithic Cultures	209
6.1 Correspondence between the Excavations of David and Debenath in Abri Bourgeois-Delaunay	236
6.2 Debenath's Chronology for Lachaise Sediments	244
6.3 Tool Typology, Couche I, Abri Suard, Lachaise	245
6.4 Tool Typology, Couche II, Abri Suard, Lachaise	246
6.5 Technical and Typological Indices and Characteristic Groups, Couche II, Abri Suard, Lachaise	247



	<u>Page</u>
6.6 Tool Typology, Couche III, Abri Suard Lachaise	247
6.7 Technical and Typological Indices and Characteristic Groups, Couche III, Abri Suard, Lachaise	249
6.8 Tool Typology, Couche IV, Abri Suard Lachaise	249
6.9 Technical and Typological Indices and Characteristic Groups, Couche IV, Abri Suard, Lachaise	251
6.10 Tool Typology, Couche V, Abri Suard, Lachaise	251
6.11 Technical and Typological Indices and Characteristic Groups, Couche V, Abri Suard, Lachaise	253
6.12 Tool Typology, Couche VI, Abri Suard, Lachaise	253
6.13 Technical and Typological Indices and Characterist Groups, Couche VI, Abri Suard, Lachaise	255
6.14 Tool Typology, Couche V-VI, Abri Suard, Lachaise	255
6.15 Technical and Typological Indices and Characteristic Groups, Couche V-VI, Abri Suard, Lachaise	257
6.16 Tool Typology, Couche VIII, Abri Suard, Lachaise	257
6.17 Tool Typology, Couche 51, Abri Suard, Lachaise	259
6.18 Technical and Typological Indices and Characteristic Groups, Abri Suard, La- chaise	260

	<u>Page</u>
6.19 Tool Typology, Couche 52, Abri Suard, Lachaise	260
6.20 Technical and Typological Indices and Characteristic Groups, Couche 52, Abri Suard, Lachaise	262
6.21 Tool Typology, Couche 53, Abri Suard, Lachaise	262
6.22 Technical and Typological,Indices and Characteristic Groups, Abri Suard, Lachaise	264
6.23 Tool Typology, Couche 5, Abri Bourgeois-Delaunay, Lachaise	264
6.24 Technical and Typological Indices and Characteristic Groups, Couche 5, Abri Bourgeois- Delaunay, Lachaise	277
6.25 Tool Typology, Couche 6, Abri Bourgeois Bourgeois-Delaunay, Lachaise Delaunay, Lachaise	277
6.26 Technical and Typological Indices and Characteristic Groups, Abri Bourgeois-Delaunay, Lachaise	279
6.27 Tool Typology, Couche 8 a-d, Abri Bourgeois-Delaunay, Lachaise	279
6.28 Technical and Typological Indices and Characteristic Groups, Lachaise	281
6.29 Tool Typology, Couche 8e, Abri Bourgeois-Delaunay, Lachaise	281
6.30 Technical and Typological Indices and Characteristic Groups, Couche 8e, Lachaise	282
6.31 Tool Typology, Couche 9, Lachaise	282
6.32 Technical and Typological Indices and Characteristic Groups, couche 9a,b Abri Bourgeois-Delaunay, Lachaise	284

	<u>Page</u>
6.33 Tool Typology, couche 9c, Abri Bourgeois-Deluanay, Lachaise	284
6.34 Piece Typology, couche 9c, Abri Bourgeois-Delaunay, Lachaise	285
6.35 Tool Typology, couche 9, Abri Bourgeois-Delaunay, Lachaise	285
6.36 Tool Typology, couche 10, Abri Bourgeois-Delaunay, Lachaise	287
6.37 Technical and Typological Indices and Characteristic Groups, couche 10, Abri Bourgeois-Delanay, Lachaise	288
6.38 Paleoenvironmental Data for Lachaise	297
6.39 Sample Descriptions, Lachaise	301
6.40 Correlation of Data from 79LC11, 79LC12	324
6.41 Correlation of Data from 77LC1	325
6.42 Correlation of Data from 79LC13	326
6.43 Correlation of Data from 79LC14	327
6.44 Correlation of Data from 79LC15	328
6.45 Correlation of Data from 79LC16	328
6.46 Correlation of Data from 79LC18	329
6.47 Correlation of Data from 77LC3	330
6.48 Correlation of Data from 79LC19	331
6.49 Correlation of Data from 79LC20	332
6.50 Tool Typology, Couche 1, Abri Lartet	348
6.51 Piece Typology, Couche 1, Abri Lartet	348
6.52 Technical and Typological Indices and Characteristic Groups, Couche 1, Abri Lartet	349

	<u>Page</u>
6.53 Piece Typology, couche 2, Abri Lartet	350
6.54 Tool Typology, couche 2, Abri Lartet	350
6.55 Technical and Typological Indices and Characteristic Groups, Couche 2, Abri Lartet	351
6.56 Tool Typology, Abri Paignon, couche 4	351
6.57 Piece Typology, Abri Paignon, couche 4	351
6.58 Paleoenvironments at Montgaudier	365
6.59 Sample Descriptions	371
6.60 Correlation of Data from 78MG4	372
6.61 Correlation of Data from couche 3, Lartet	372
6.62 Correlation of Data from 78MG14	373
6.63 Correlation of Data from couche 6, Lartet	373
6.64 Correlation of Data from couche 2, Gaudry	374
6.65 Correlation of Data from 78MG12	375
6.66 Correlation of Data from New Hall	376
6.67 Correlation of Data from Cave Bear Alley	377
6.68 Correlation of Data from 78MG18	377
7.1 The Straea of Pech II	414
7.2 Tool Typology couche 4, Pech I	422
7.3 Piece Typology, couche 4 Pech I	423
7.4 Raw Material, couche 4, Pech I	424
7.5 Nuclear form, couche 4, Pech I	425
7.6 Characteristic Techniques, couche 4, Pech I	426

	<u>Page</u>
7.7 Characteristic Techniques, couche 4, Pech I	426
7.8 Technical and Typological Indices and Characteristic Groups, couche A, Pech I	427
7.9 Technical and Typological Indices and Characteristic Groups, couche 9, Pech I	427
7.10 Technical and Typological Indices and Characteristic Groups, couche 7c Pech II	431
7.11 Technical and Typological Indices and Characteristic Groups, couche 4b2, Pech II	431
7.12 Technical and Typological Indices and Characteristic Groups, couche 4b , Pech II	432
7.13 Technical and Typological Indices and Characteristic Groups, couche 3, Pech II	432
7.14 Technical and Typological Indices and Characteristic Groups, couche F, Pech IV	434
7.15 Technical and Typological Indices and Characteristic Groups, couche F , Pech IV	434
7.16 Technical and Typological Indices and Characteristic Groups couche F1, Pech IV	434
7.17 Technical and Typological Indices and Characteristic Groups, couche F3, Pech IV	435
7.18 Technical and Typological Indices and Characteristic Groups, couche F4, Pech IV	435
7.19 Technical and Typological Indices and Characteristic Groups couche I1, Pech IV	436
7.20 Technical and Typological Indices and Characeteristic Groups, couche I2, Pech IV	436
7.21 Technical and Typological Indices and Characteristic Groups, couche J3, Pech IV	437
7.22 Technical and Typological Indices and Characteristic Groups, couche J3a, Pech IV	437

	<u>Page</u>
7.23 Technical and Typological Indices and Characteristic Groups, couche J3b, Pech IV	438
7.24 Technical and Typological Indices and Characteristic Groups, couche J3c, Pech IV	438
7.25 Technical and Typological Indices and Characteristic Groups, couche X, Pech IV	439
7.26 Technical and Typological Indices and Characteristic Groups, couche Y, Pech IV	439
7.27 Technical and Typological Indices and Characteristic Groups, couche Z, Pech IV	440
7.28 Sample Descriptions	450
7.30 Correlation of Data from 77Pa2	451
7.31 Correlation of Data from Outer Breccia	451
7.32 Correlation of Data from Inner Breccia	452
7.33 Correlation of Data from 77PA14	453
7.34 Correlation of Data from 77PA12	454
7.35 Correlation of Data from 77PA13	454
7.36 Correlation of Data from couche 6, Pech II	455
7.37 Correlation of Data from couche 8, Pech II	456
7.38 Sample Descriptions from Abri Vaufrey	500
7.39 Correlation of data from 78AV1	503
7.40 Correlation of Data from couche 7	504
7.41 Correlation of Data from couche 9	505
7.42 Correlation of Data from couche 10	506
7.43 Correlation of Data from above Datum	507

	<u>Page</u>
7.44 Correlation of Data from couche II, Grotte 13	523
7.45 Corelation of Data from couche I, Grotte 13	524
7.46 Correlation of Data from Diverticule 1, Grotte 13	524
7.47 Sample Descriptions from .Grotte 13	

## LIST OF FIGURES

<u>Figure</u>	<u>Page</u>
1.1 The sampling localities	6
1.2 The logic which is used to establish absolute dates and paleoclimatic interpretations for archeological sites	10
2.1 The dissolved uranium species in a typical ground water	18
2.2 The geochemical cycle of uranium and thorium	21
2.3 Uranium concentrations and $^{234}\text{U}/^{238}\text{U}$ ratios in the hydrologic cycle	24
2.4 The process leading to the deposition of speleothems in caves	28
2.5 Formation and evolution of an abri	32
2.6 The $^{238}\text{U}$ and $^{232}\text{Th}$ decay series	40
2.7 The $\alpha$ particle energies of the $^{238}\text{U}$ and $^{232}\text{Th}$ decay series isotopes	42
2.8 The relationship between the activity ratios $^{230}\text{Th}/^{234}\text{U}$ and $^{234}\text{U}/^{238}\text{U}$ for systems with no initial thorium	46
3.1 The chemical procedure	54
3.2 The chemical analysis for the separation of uranium and thorium from calcite	56
3.3 Typical emission spectra showing the energies and relative abundences	58
3.4 The roasting technique	62
3.5 The relationship between travertine and sediments in archeological cave sites	77
3.6 A typical computer printout	81
3.7 A flowchart for the archeological application of U/Th dating	84



	<u>Page</u>
4.1 The analysis of cave sediments	96
4.2 Granulometry of Pech de l'Azé I, upper levels	98
4.3 Plaquettes found in sediments	101
4.4 Percentage of plaquettes vs. depth, Pech de l'Azé I, upper levels	104
4.5 Pebbles affected by frost action	107
4.6 The bluntness index references	110
4.7 Effects of humidity on cave sediments	113
4.8 Pebbles affected by humidity and cryoturbation	115
4.9 Illuvial concretions in cave sediments	117
4.10 Analysis of the fines	121
4.11 Granulometry and densitometry of the fines	123
4.12 The palynology of Combe-Grenal couches 36 to 55	127
4.13 European mammal fauna during the Villefranchian	130
4.14 European mammal fauna from the Middle Pleistocene	132
4.15 European mammal fauna from the Upper Pleistocene	134
4.16 Evolution of the elephants and bears during the Quaternary	136
4.17 European bioherms during the Upper Pleistocene	141
4.18 The grid system in Abri Vaufray	145
4.19 Core typology	149

	<u>Page</u>	
4.20	Mousterian cores	151
4.21	Debitage description	154
4.22	Modification and retouch categories for retouched tools	156
4.23	Other artefacts often found in tool assem- blages	160
4.24	Cumulative graphs of tool typologies	166
5.1	Deep sea core record for temperature change during the late Pleistocene	175
5.2	Climatic zones during the Wurm glaciation	179
5.3	<u>Homo erectus</u>	182
5.4	<u>Homo erectus</u> in Europe	184
5.5	Neanderthal sites	188
5.6	Comparative anatomy for <u>Homo sapiens</u> subspecies	188
5.7	<u>Homo sapiens neanderthalensis</u>	193
5.8	An Eastern Neanderthal	195
5.9	The Cro-Magnon skull, <u>H. sapiens sapiens</u>	198
5.10	Distribution of Lower Paleolithic indust- ries	200
5.11	The production of Levallois flakes	204
6.1	The Charente France	213
6.2	The Charente Karst	217
6.3	Lachaise Chateau	221
6.4	Plan view of Lachaise	223
6.5	Active speleothem in deposition in Lachaise	226

	<u>Page</u>
6.6 Stratigraphy of Bourgeois-Delaunay	228
6.7 Stratigraphic section of cut 5, Abri Bourgeois-Delaunay,	235
6.8 Stratigraphy of Abri Suard, Lachaise	239
6.9 Tools from Facies A	268
6.10 Tools from Facies B	270
6.11 Tools from Facies C	272
6.12 The structure made of reindeer antlers in couche 51, Abri Suard	274
6.13 Incised bone from Abri Suard,	276
6.14 Tools from Bourgeois-Delaunay	278
6.15 Human Remains from Abri Suard	293
6.16 An Infant mandible from Lachaise	295
6.17 Lachaise: ideal for hunting and shelter	302
6.18 79LC11, couche 7, Bourgeois-Delaunay	307
6.19 79LC13, couche 11, Bourgeois-Delaunay	309
6.20 79LC15 and 79LC16, <u>plancher superieur</u>	311
6.21 79LC17, couche 53', Suard	313
6.22 79LC18, <u>plancher superieur</u> , Suard	314
6.23 79LC19, near <u>puits</u> , Abri Suard,	317
6.24 79LC20, in the <u>couloir</u>	317
6.25 Sample locations in Bourgeois-Delaunay	319
6.26 An interpretation of the depositional history of Lachaise	327
6.27 Montgaudier, near Vouthon	334

	<u>Page</u>
6.28 An overview of Montgaudier	337
6.29 Plan view of Abri Lartet	343
6.30 Stratigraphy of the west cut in Abri Lartet	345
6.31 Incised and engraved bones from Montgaudier	353B
6.32 Pig skeletons in Abri Lartet	353D
6.33 The Upper Paleolithic in Montgaudier	354C
6.34 The <u>Baton de Commandement</u> , Montgaudier	354E
6.35 Magdalenian pieces from Montgaudier	358
6.36 Magdalenian engraved reindeer scapula	360
6.37 Mandible from Montgaudier	364
6.38 The river Tardoire as seen from Montgaudier	368
6.39 78MG1, couche 3, Abri Lartet	368
6.40 78MG4, couche 2, Abri Lartet	379
6.41 Couche 6, Abri Lartet, Montgaudier	381
6.42 78MG11, New Hall, Abri Gaudry, Montgaudier	383
6.43 78MG12, couche 4, Abri Gaudry, Montgaudier	383
6.44 79MG14, couche 4, Abri Lartet	385
6.45 79MG15, stalagmitic <u>plancher</u> , Cave Bear Alley, the Balcony, Montgaudier	385
6.46 Couche 2, Abri Gaudry, Montgaudier	387
6.47 Sample locations within Montgaudier	389

	<u>Page</u>
7.1 The Peridord, France	397
7.2 The escarpments of the Dordogne	400
7.3 The geology of the Dordogne	402
7.4 Plan view of Pech de l'Azé I and II	407
7.5 The stratigraphy in Pech de l'Azé IV	409
7.6 The strigraphic section in Pech I	412
7.7 Pech I	413
7.8 Tools from Pech I	423
7.9 Worked bones from Pech II	425
7.10 Tools from Pech II, Mousterian of Acheulian Tradition A	432
7.11 Tools from Pech II, Mousterian of Acheulian Tradition B	434
7.12 Tools from Pech IV	436
7.13 The history of Pech I and II	458
7.14 77PA1, calcite cemented sand in Würm layers, Pech IV	460
7.15 The outer breccia Mass, Pech I	461
7.16 The inner breccia mass, Pech I	463
7.17 Couche 3 and 4, Pech II	465
7.18 77PA14, couche 4, Pech II	469
7.19 77PA15, couche 9, Pech II	471
7.20 77PA16, Pech II.	472
7.21 The cliffs near Vaufrey	477
7.22 Stopping of the roof in Abri Vaufrey	480

	<u>Page</u>
7.23 Three caves near Abri Vaufrey	480
7.24 The two faults on which Abri Vaufrey is situated	481
7.25 A diagrammatic representation of the stratigraphy in Vaufrey	484
7.26 Couches IV through VI	486
7.27 Couche XI, filled by plaquettes from the roof	489
7.28 The stratigraphy of Vaufrey in the pit at back	491
7.29 The view from the cliffs at Castelnaud	494
7.30 The stalagmitic mound in Abri Vaufrey	496
7.31 Plan view of Grotte 13	514
7.32 Actively growing stalactites in Diverticule 1, Grotte 13	516
7.33 The Mindel/Riss boundary, couche II, Main Gallery, Grotte 13	516
7.34 Stratigraphy in Grotte 13	519C
7.35 Couche II, Grotte 13	528

## INTRODUCTION

For nearly thirty years, certain time foci of archeology and physical anthropology have enjoyed the benefits of absolute dating, thereby allowing their students to state with reasonable accuracy the period of occupation of a site, or the age of a skeleton or tool. For those focusing on people and cultures prior to 400,000 years BP, potassium-argon dating has served well, while those focusing on anything more recent than 40,000 years BP have had their information supplied by the radiocarbon method. Unfortunately for those who wished to focus on that interim period, 400,000 to 40,000 years BP, there has been no absolute method, only relative ones, such as faunal, palynological, or stratigraphic analysis and comparison.

Recently, however, a host of new dating techniques have been developed to fill this gap. For example, amino acid racemization, magnetostratigraphy, thermoluminescence (TL), and the various uranium series disequilibrium methods have enjoyed intensive study to determine their efficacy, and in the case of some of these methods, their applicability to anthropology. Because the uranium series disequilibrium methods have the potential to date the entire gap from 40,000 to 400,000 years BP (and perhaps even as far back as 1,000,000 years BP for certain special applications of one method), this group of methods, when perfected,

may prove to be the most informative of the new methods. They may also prove to have other factors in their favor: all the uranium series disequilibrium methods are relatively inexpensive to perform (unlike some of the other methods); they do not require samples bored from priceless fossils; no expensive equipment is required in the field, nor are any difficult calculations of sample orientations needed; finally, they use calcium carbonate, very frequently found near open air spring sites, and almost always found in caves, where ancient man often took shelter. Therefore, the uranium series disequilibrium methods should be applied to more archeological sites, in an attempt to solve some of the many problems which plague archeologists in this period.

There are almost as many uranium series disequilibrium method used for dating as there are isotopes of the various elements in the uranium and thorium decay series. Some of these include the  $^{230}\text{Th}/^{231}\text{Pa}$  method, for dating sea cores, the unsupported isotope methods, utilizing either  $^{230}\text{Th}$  or  $^{231}\text{Pa}$  in dating deep sea sediments and ferromanganese nodules, the  $^{230}\text{Th}/^{232}\text{Th}$  method applied somewhat unsuccessfully to marine cores, the Ra/U method used originally to date uranium minerals, the unsupported  $^{210}\text{Pb}$  methods, used to date lake sediments, marine shores, permanent snow fields, and paintings to test for forgeries, the  $^{228}\text{Th}/^{232}\text{Th}$  method used to determine dates for deep marine cores, the  $^{234}\text{U}/^{238}\text{U}$  method utilizing excess  $^{234}\text{U}$  found in sea water, best applied unaltered fossil corals, the unsupported  $^{228}\text{Ra}$  method, applied to coral skeletal growth band dating, the  $^{231}\text{Pa}/^{235}\text{U}$  method



used to date cave deposits, and finally, the  $^{230}\text{Th}/^{234}\text{U}$  method also used to date cave and spring deposits. Both Ku (1976) and Cherdyn-tsev (1971) give excellent discussions of the above methods, commenting upon their limitations, and the results achieved by these methods. Furthermore, these latter two methods offer the most obvious applications to archeology and physical anthropology.

Although the  $^{230}\text{Th}/^{234}\text{U}$ , or simply U/Th, method was potentially available for use in the 1930's, when the relationships between the isotopes were first understood, the method was not seriously applied until the late 1950's, when it was used to date everything from deep marine sediments to bones, including corals, oolites, speleothems, even those now found in submarine caves, mollusc shells, marls, desert calcretes, and bones (Ku, 1976). In the case of mollusc shells and bones, however, there is a discrepancy in the age on the order of 50%, suspected to be due to the geochemical factors influencing uranium incorporation into the material and diagenetic movement of the uranium (Ku, 1976; Szabo et al., 1969). Certainly, the most consistent results for the method arise from the coral and speleothem samples.

Very few workers have actually tried to date deposits related to archeological sites. Cherdyntsev et al. (1976) attempted to analyze, without much success, the Ehringsdorf material, also attempted in Blackwell (1978), while Schwarcz et al. (1978) have dated Nahal Zin in Israel. Schwarcz (1980) reports dates for several sites around the world. In Schwarcz et al. (1980), dates are given

for Petrolona in Greece, and Schwarcz and Debénath (1978) reported dates for Lachaise in France. Recently, Harmon et al. (1980) have dated the Bilzingsleben material.

Because the dates reported in Schwarcz and Debénath (1978) were controversial, it was decided to collect more material. The original 1977 collection was made by Andre Debénath, who assisted the author during the 1980 collection. Several other French sites are also problematic. Figure 1.1 shows the locations of the other two sample localities. In the Charente, the northern region, is the type locality for the Quina and Ferrassie Mousterian assemblages, while the Dordogne contains the type localities for the other Mousterian assemblages.

In the Charente, Montgaudier is very near Lachaise, but its character of deposition is completely different. While Lachaise is a small but deep cave complex, Montgaudier is a huge abri complex. While the former is filled by calcite-cemented breccias and stalagmitic material is a well-understood stratigraphy, the latter has deposits which have slid as slump blocks from one place to another intermixed with normal sediment sequences, resulting in a baffling stratigraphic jigsaw puzzle. Yet both contain Mousterian cultural material and hominid fossils. The 1978 collection at Montgaudier was made H. Schwarcz, assisted by Louis Duport, and the 1979 collection was by the author, assisted by Debénath and Duport.

In the Dordogne, Pech de l'Azé Cave (foot of the ass in old Bordelais), containing Acheulian and Mousterian industries, has been extensively studied by Bordes (1972, 1976). In one section

Figure 1.1

The sampling localities

A. The Charente

B. The Dordogne

(modified from Smith, 1964)



of the cave, the paleoclimatology is extremely well-understood, but is not related to any absolute dates. This paleoclimatological sequence has been used to correlate this site with other local sites. Samples there were collected by H. Schwarcz with the help of François Bordes in 1977, and two other samples were collected in 1978. Near Bergerac, a rich network of caves can be found in the cliffs overlooking the Dordogne. Of these, two are presently being excavated. Abri Vaufrey contains several metres of sedimentary fill all containing a Typical Mousterian industry which has been attributed the Würm I stadial. It is surprising that so thick a section should be deposited so quickly. Therefore, absolute dates here would be especially helpful to confirm the paleoclimatic interpretations. A nearby cave, Grotte 13, contains no cultural material, but does contain Ursus deningeri, the extinction of which is used to determine the Mindel/Riss boundary. Because no dates had been established yet for the extinction of U. deningeri, and because of its wide use as an index fossil, an absolute age for this level would be of great interest.

In this study, all the absolute dates, however, have been related to the paleoclimatic interpretations of the deposits in the caves. Sedimentological characteristics of the deposits (granulometry, carbonate content, pH, etc.) are used along with the faunal and palynological analysis to establish the paleoclimates for the sediment sequence. These data are then compared to regional and global glacial/interglacial sequences, such as the oceanic core isotope data, attempting to match the local climatic sequence

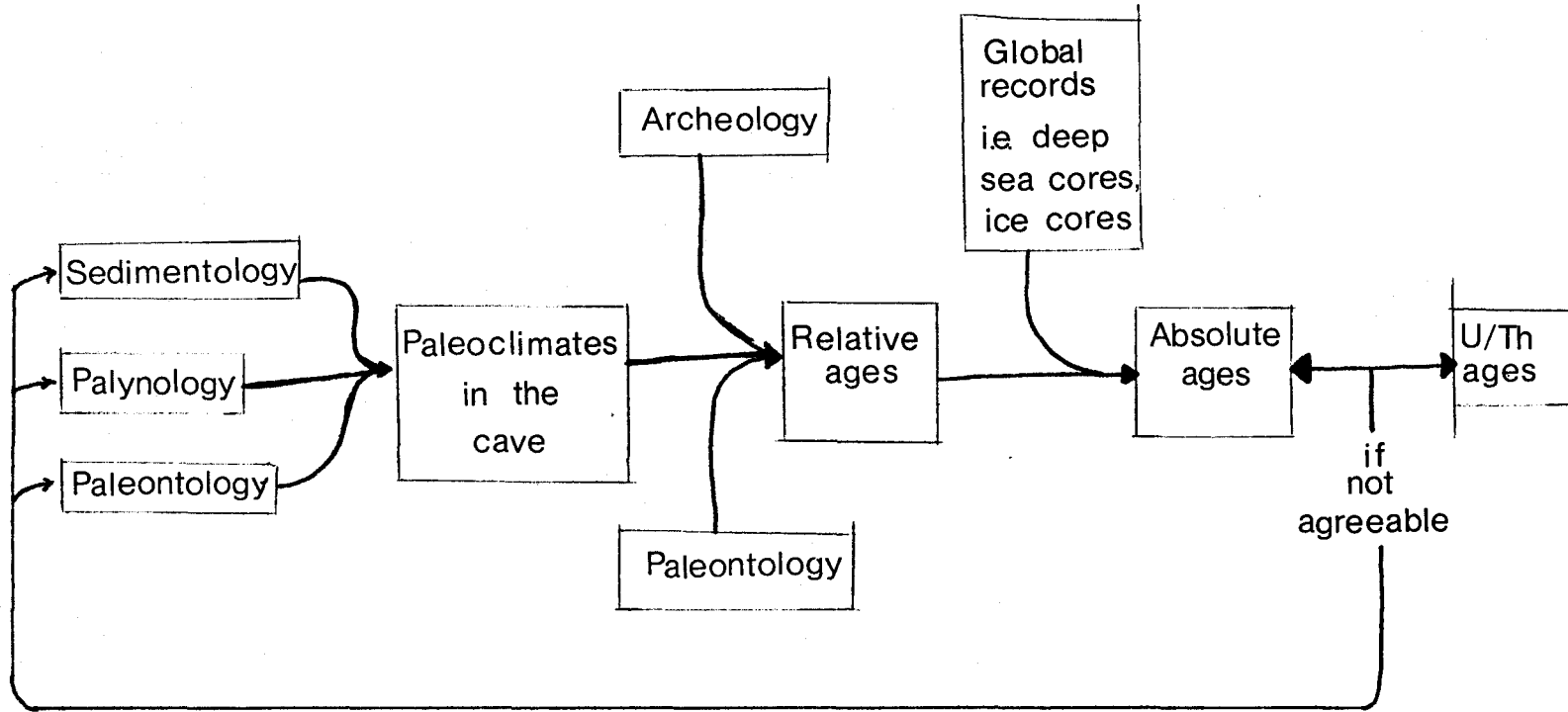
with that of the global sequence, thereby to derive a relative date for the sequence. In some cases, these relative dates can be related to an absolute age. For example, the Würm III/IV interstadial has been established at approximately 20 Ka, the Würm II/III at 27 Ka, and the Würm I/II at 38 Ka (Smith, 1964). Beyond that no dates have been firmly established, however, it is generally agreed among archeologists that the Würm I begins at about 80 Ka, the end of isotopic stage 5, and that the Riss ends at about 130 Ka, the end of stage 7. Using these conventions, the absolute dates derived for travertines are related to the paleoclimatic interpretations made by the archeologists. It is then possible to estimate the accuracy of their interpretations (Figure 1.2).

Therefore, for each of the caves from which samples have been collected for dating, the sedimentology, archeology and paleoclimatic interpretations have been summarized. In the stratigraphic sections, the French word plancher (literally, floor) has been used to describe sheets of calcitic flowstone up to several centimetres thick commonly covering the entire floor of a cave at a stratigraphic level. All the sections are listed from the top, by convention. Unfortunately, there are no thickness listed for many sections in their original published descriptions. In the cases of the Mousterian cultures in the caves, tool lists and lists of the important indices have been included because these are not published in any of the English literature.

Generally, the dates herein have proven to be older than

Figure 1.2

The logic which is used to establish the absolute dates and paleoclimatic interpretation for archeological sites.





the chronological interpretations made by the archeologists who have studied the sites. Few dates, however, were obtained for the Dordogne region. Caves in this area seem poor in travertine, and what is present contains low concentrations of uranium. In the Charente, the samples from Lachaise gave excellent results, but raised almost as many questions as they answered, while the chronology of Montgaudier is still a problem, as is the history of its occupation by man.

From the few conclusive dates, however, Neanderthals, as a group appear to be much older than formerly thought, as is the Mousterian culture with which they are associated.

Before discussing each site in detail, the theory and methodology of U/Th dating should be discussed, followed by a brief summary of the paleoclimatological methods, and the background into which these sites fit, the Pleistocene.

## THE THEORY

Before discussing the application of the uranium-thorium method to archeology, it is necessary to first outline the theory underlying the method. Uranium and thorium behave differently in the geologic cycle, resulting in a separation of the daughter products from the parent uranium. Therefore, when a travertine is deposited in a cave as a result of percolation of groundwater, uranium, but usually no thorium, will be coprecipitated with the calcite. Thus, a natural clock is started as the decay products grow back into secular equilibrium with the parent uranium, and that disequilibrium can be measured by separating the uranium and thorium and measuring the abundance of the various isotopes.

### 2.1 The Geological Cycle

Both uranium and thorium originally enter the crust as a result of igneous activity. Thereafter, however, these two actinide elements behave differently as they pass through the geologic cycle.

#### 2.1.1 The Uranium Cycle

Most of the uranium in igneous rocks is almost insoluble in 4+ valence state. Upon exposure to the atmosphere, the uranium can be oxidized to the soluble U(VI) state. The solubility can be increased further by the presence of CO<sub>2</sub>, or phosphates in the groundwaters. Solubility is also affected by the presence of

vanadates, silicates, and arsenates (Langmuir, 1978).

Once in solution, uranium may form several different aqueous species, depending on the Eh, pH, and the concentrations of various ions in solution. Some of the important ions include carbonates, fluoride, phosphate, sulphate, silicates, hydroxide and chloride with which uranium can complex. Some of the important aqueous uranium species are listed in Table 2.1, along with their ranges of stability vs. pH. According to Langmuir (1978), only the uranyl carbonates,  $UO_2^+$ , and  $U(OH)_5^-$  are significant in natural waters. In the presence of phosphate, however,  $UO_2(HPO_4)_2^{2-}$  will predominate in the range  $4 < pH < 10$ , the normal pH range for natural waters. This becomes significant in caves with bones or teeth exposed to acidic cave waters which can dissolve the hydroxyapatite,  $Ca_3(PO_4)_2 \cdot CaCO_3$ , thereby releasing large amounts of phosphate into the cave waters. Figure 2.1 shows a typical distribution of aqueous uranium species vs. pH for a natural water.

The amount of uranium dissolved in the water has been related to several factors, including:

1. the uranium content of the source (allogenic rock, authigenic rock, sediment, soil)
2. the leachability of the uranium
3. the proximity of the water to the source when tested
4. climatic effects, their variability, and their influence on evaporation and transpiration, which in turn influence:
5. the Eh and pH of the water

Table 2.1 Important Aqueous Uranium Species.

Aqueous Species	$G_f^\circ$ (kcal/mol)	Stability Range (pH)	Conditions
$U^{3+}$	-114.9		
$U^{4+}$	-126.9	< 1	$\Sigma U = 10^{-6}$ M, $P_{CO_2} = 10^{-2}$ atm
$UOH^{3+}$	-187.2	1-2	$\Sigma U = 10^{-6}$ M, $P_{CO_2} = 10^{-2}$ atm
$U(OH)_2^{2+}$	-237.2	2-4.2	$\Sigma F = .2$ ppm, $\Sigma Cl = 10$ ppm, $\Sigma SO_4 = 100$ ppm, $\Sigma PO_4 = .1$ ppm
$U(OH)_3^+$	-290.3	2-4.8	$\Sigma F = .2$ ppm, $\Sigma Cl = 10$ ppm, $\Sigma SO_4 = 100$ ppm, $\Sigma PO_4 = .1$ ppm
$U(OH)_4^0$	-342.0	2-6	$\Sigma F = .2$ ppm, $\Sigma Cl = 10$ ppm, $\Sigma SO_4 = 100$ ppm, $\Sigma PO_4 = .1$ ppm
$U(OH)_5^-$	-392.4	5-9.5	$\Sigma U = 10^{-6}$ M, $P_{CO_2} = 10^{-2}$ atm
$U_6(OH)_{15}^{9+}$	-1588.2		
$UF_3^+$	-206.0	< 3	$\Sigma F = .2$ ppm, $\Sigma Cl = 10$ ppm, $\Sigma SO_4 = 100$ ppm, $\Sigma PO_4 = .1$ ppm
$UF_2^{2+}$	-281.3	< 3.5	$\Sigma F = .2$ ppm, $\Sigma Cl = 10$ ppm, $\Sigma SO_4 = 100$ ppm, $\Sigma PO_4 = .1$ ppm
$UF_3^+$	-355.0	< 3.2	$\Sigma F = .2$ ppm, $\Sigma Cl = 10$ ppm, $\Sigma SO_4 = 100$ ppm, $\Sigma PO_4 = .1$ ppm
$UF_4^0$	-428.5	1-3	$\Sigma F = .2$ ppm, $\Sigma Cl = 10$ ppm, $\Sigma SO_4 = 100$ ppm, $\Sigma PO_4 = .1$ ppm
$UF_5^-$	-498.0		
$UF_6^{2-}$	-568.7		
$UCl_3^+$	-160.1		
$USO_4^{2-}$	-312.3		
$U(SO_4)_2^0$	-496.1		

Table 2.1 (continued)

Aqueous Species	G <sub>f</sub> <sup>o</sup> (kcal/mol)	Stability Range (pH)	Conditions
UHPO <sub>4</sub> <sup>2+</sup>	-403.6		
U(HPO <sub>4</sub> ) <sub>2</sub> <sup>o</sup>	-677.6		
U(HPO <sub>4</sub> ) <sub>3</sub> <sup>2-</sup>	-949.7		
U(HPO <sub>4</sub> ) <sub>4</sub> <sup>4-</sup>	-1221.0		
UO <sub>2</sub> <sup>+</sup>	-231.5	1-7	ΣU = 10 <sup>-6</sup> M, P <sub>CO<sub>2</sub></sub> = 10 <sup>-2</sup> atm
UO <sub>2</sub> <sup>2+</sup>	-227.7	>7	ΣU = 10 <sup>-8</sup> M, T = 25°C
UO <sub>2</sub> OH <sup>+</sup>	-276.5	4-7	ΣU = 10 <sup>-8</sup> M, T = 25°C
(UO <sub>2</sub> ) <sub>2</sub> (OH) <sub>2</sub> <sup>2+</sup>	-561.1	5-7	ΣU = 10 <sup>-8</sup> M, ΣSO <sub>4</sub> = 10 <sup>-3</sup> M, T = 25°C
(UO <sub>2</sub> ) <sub>3</sub> (OH) <sub>5</sub> <sup>+</sup>	-945.2	>6	ΣU = 10 <sup>-8</sup> M
UO <sub>2</sub> CO <sub>3</sub> <sup>o</sup>	-367.6	4-7.5	ΣU = 10 <sup>-8</sup> M, P <sub>CO<sub>2</sub></sub> = 10 <sup>-2</sup> atm, T = 25°C
UO <sub>2</sub> (CO <sub>3</sub> ) <sub>2</sub> <sup>2-</sup>	-503.2	5-9	ΣU = 10 <sup>-8</sup> M, P <sub>CO<sub>2</sub></sub> = 10 <sup>-2</sup> atm, T = 25°C
		7-9	ΣPO <sub>4</sub> = .1 ppm, P <sub>CO<sub>2</sub></sub> = 10 <sup>-2</sup> atm
UO <sub>2</sub> (CO <sub>3</sub> ) <sub>3</sub> <sup>4-</sup>	-635.4	>7	ΣU = 10 <sup>-8</sup> M, T = 25°C
UO <sub>2</sub> F <sup>+</sup>	-302.0	<5	ΣF = .3 ppm
UO <sub>2</sub> F <sub>2</sub> <sup>o</sup>	-374.6	<5	ΣF = .3 ppm
UO <sub>2</sub> F <sub>3</sub> <sup>-</sup>	-445.2		
UO <sub>2</sub> F <sub>4</sub> <sup>2-</sup>	-514.2		
UO <sub>2</sub> Cl <sup>+</sup>	-259.4		
UO <sub>2</sub> SO <sub>4</sub> <sup>o</sup>	-409.4	<6.8	ΣU = 10 <sup>-8</sup> M, ΣSO <sub>4</sub> = 10 <sup>-3</sup> M

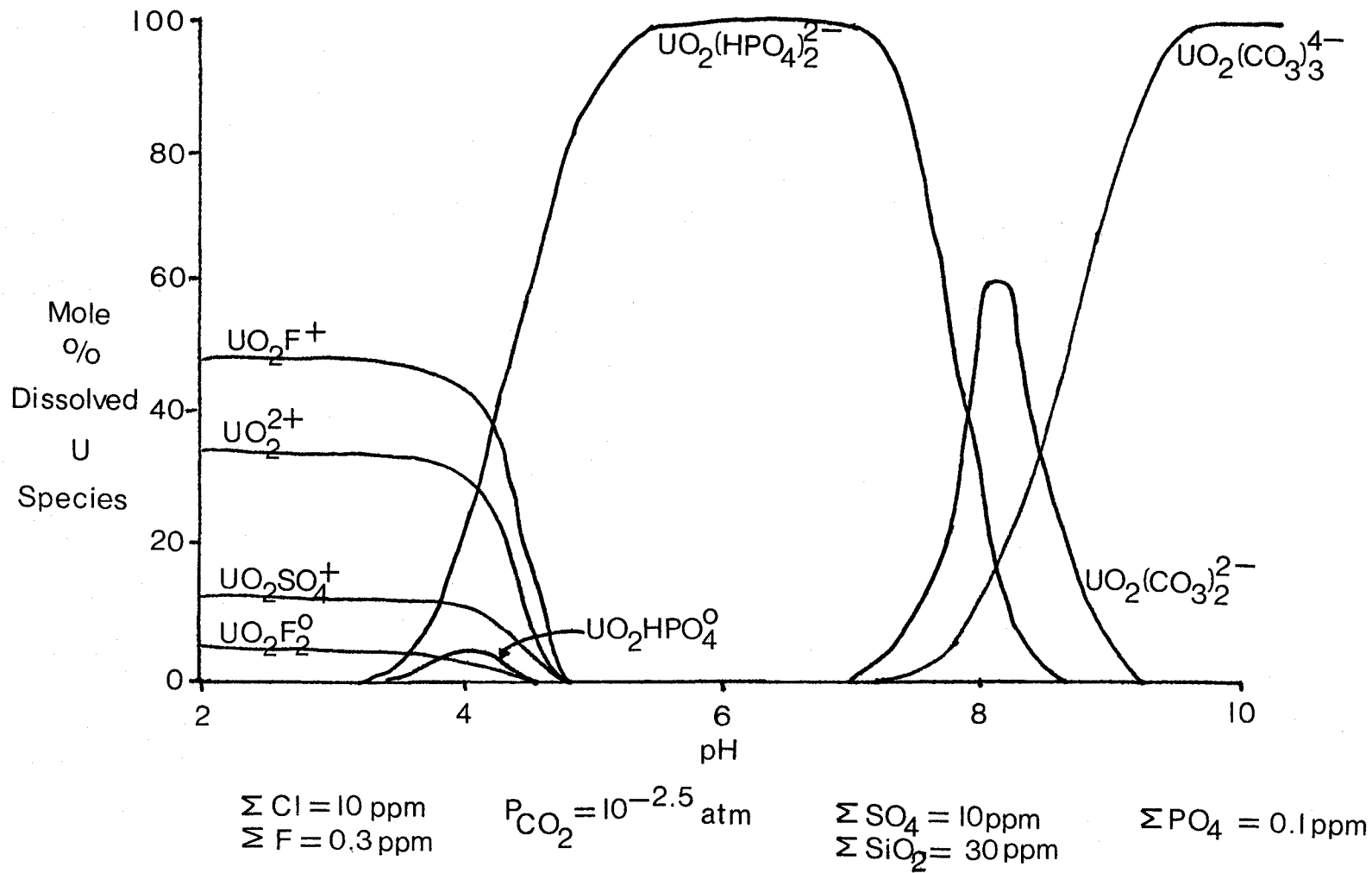
Table 2.1 (continued)

Aqueous Species	$G_f^\circ$ (kcal/mol)	Stability Range (pH)	Conditions
$UO_2(SO_4)_2^{2-}$	-589.4		
$UO_2HPO_4^0$	-499.5	3-5	$\Sigma PO_4 = .1$ ppm
$UO_2(HPO_4)_2^{2-}$	-773.7	3-8	$\Sigma PO_4 = .1$ ppm
$UO_2H_2PO_4^+$	-502.0		
$UO_2(H_2PO_4)_2^0$	-775.5		
$UO_2(H_2PO_4)_3^-$	-1048.0		
$UO_2SiO(OH)_3^+$	-537.0	3.8-7	$\Sigma U = 10^{-8}$ M, $\Sigma SiO_2 = 10^{-3}$ M $T = 25^\circ C$

(adapted from Langmuir, 1978).

Figure 2.1

The dissolved uranium species in a typical ground  
water (after Langmuir, 1978)





6. the concentrations of the aforementioned ions
7. the presence of highly adsorptive materials such as organic compounds, oxides of iron(III), manganese, and titanium, and clay minerals
8. the amount of dilution of the water by non-uranium bearing waters.

(Langmuir, 1978).

After the uranium has been complexed in the water, it will move through the soil or aquifer with the water. In karst systems, the stability of the uranium species, particularly the carbonate-complexed species, is dependent upon the partial pressure of carbon dioxide,  $P_{CO_2}$ . In the formation of a speleothem, as discussed in Chapter 2.2,  $CO_2$  degassing or evaporation of the water will result in coprecipitation of the uranium with the calcite. Much of the uranium in the speleothem will probably have originated in the limestone itself or the interbedded shales (Gascoyne, 1979), but the amount dissolved in the water, and hence the final concentration in the speleothem depends on the factors listed above. Uranium concentrations in speleothems can vary from  $<0.01$  to  $>100$  ppm, averaging about 0.5 to 1.5 ppm.

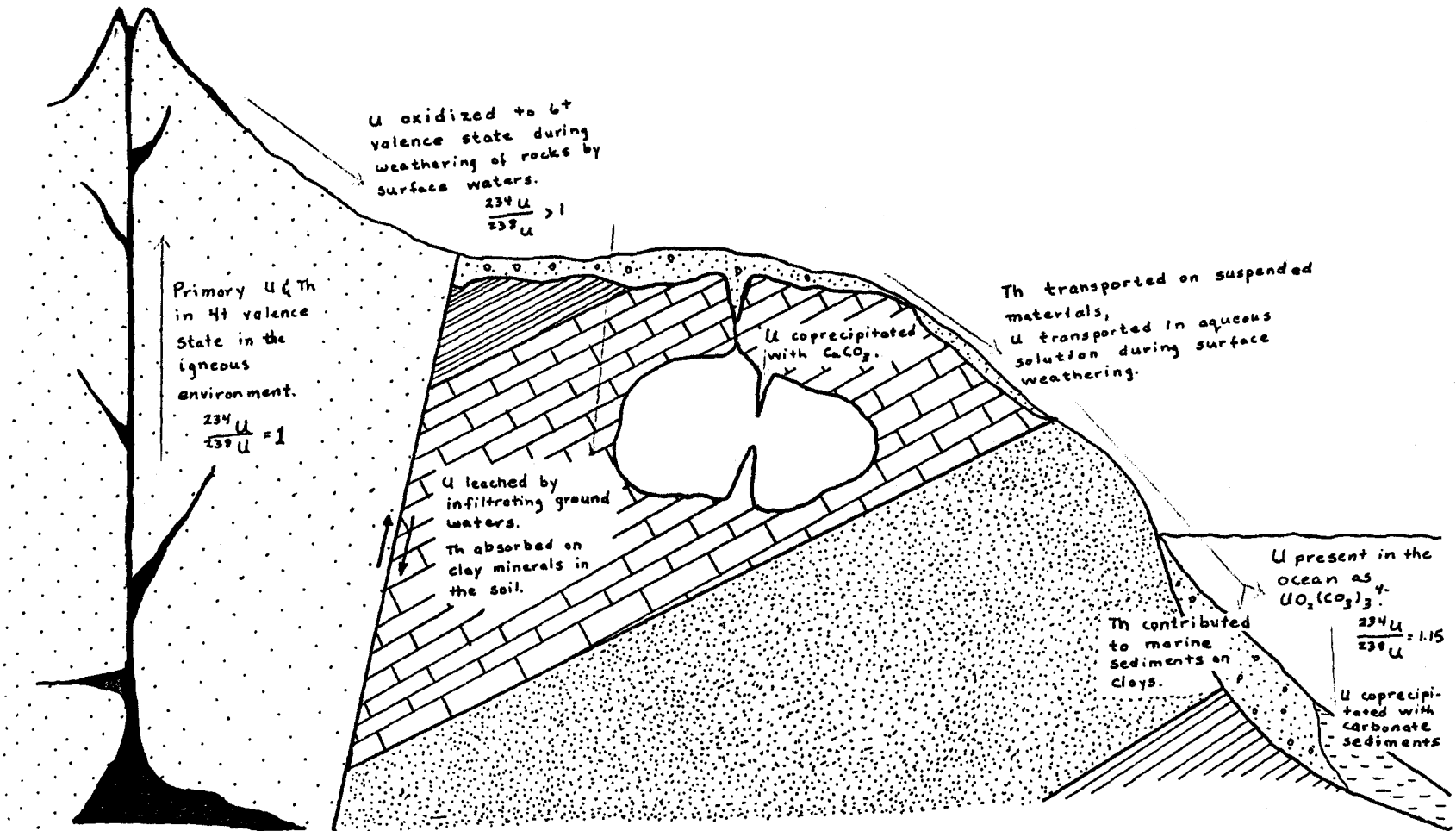
Figure 2.2 summarizes the geochemical cycle of uranium and thorium.

#### 2.1.2 The Thorium Cycle

Although thorium is approximately four times more abundant than uranium in crustal rocks, the Th/U ratio in seawater is ap-

Figure 2.2

The geochemical cycle of uranium and thorium  
(from Blackwell, 1978, after Harmon, 1975)



U oxidized to 6+ valence state during weathering of rocks by surface waters.  
 $\frac{^{234}\text{U}}{^{238}\text{U}} > 1$

Primary U & Th in 4+ valence state in the igneous environment.  
 $\frac{^{234}\text{U}}{^{238}\text{U}} = 1$

U leached by infiltrating ground waters.  
 Th absorbed on clay minerals in the soil.

U coprecipitated with  $\text{CaCO}_3$ .

Th transported on suspended materials, U transported in aqueous solution during surface weathering.

Th contributed to marine sediments on clays.

U present in the ocean as  $\text{UO}_2(\text{CO}_3)_3$ .  
 $\frac{^{234}\text{U}}{^{238}\text{U}} = 1.15$

U coprecipitated with carbonate sediments

proximately 1/200. This is a direct result of the significantly lower solubility of thorium (Gascoyne, 1979). What little thorium does dissolve, unlike uranium remains in the 4+ valence state, and is usually quickly adsorbed onto the surface of clays and other detritus. Therefore, very little dissolved thorium is found in natural waters, although some studies have shown some thorium may be dissolved in water (Thompson, 1973).

### 2.1.3 Isotopic Fractionation of Uranium

Because the long-lived daughter of  $^{238}\text{U}$  is the same element, namely  $^{234}\text{U}$ , one might expect these two isotopes to exist in secular equilibrium in most natural waters, i.e.  $^{234}\text{U}/^{238}\text{U}^* = 1.0$ . Such, however, is usually not the case.  $^{234}\text{U}$  is preferentially dissolved from uranium-bearing minerals. The reason for this is still not certain; however, the following explanations have been proposed:

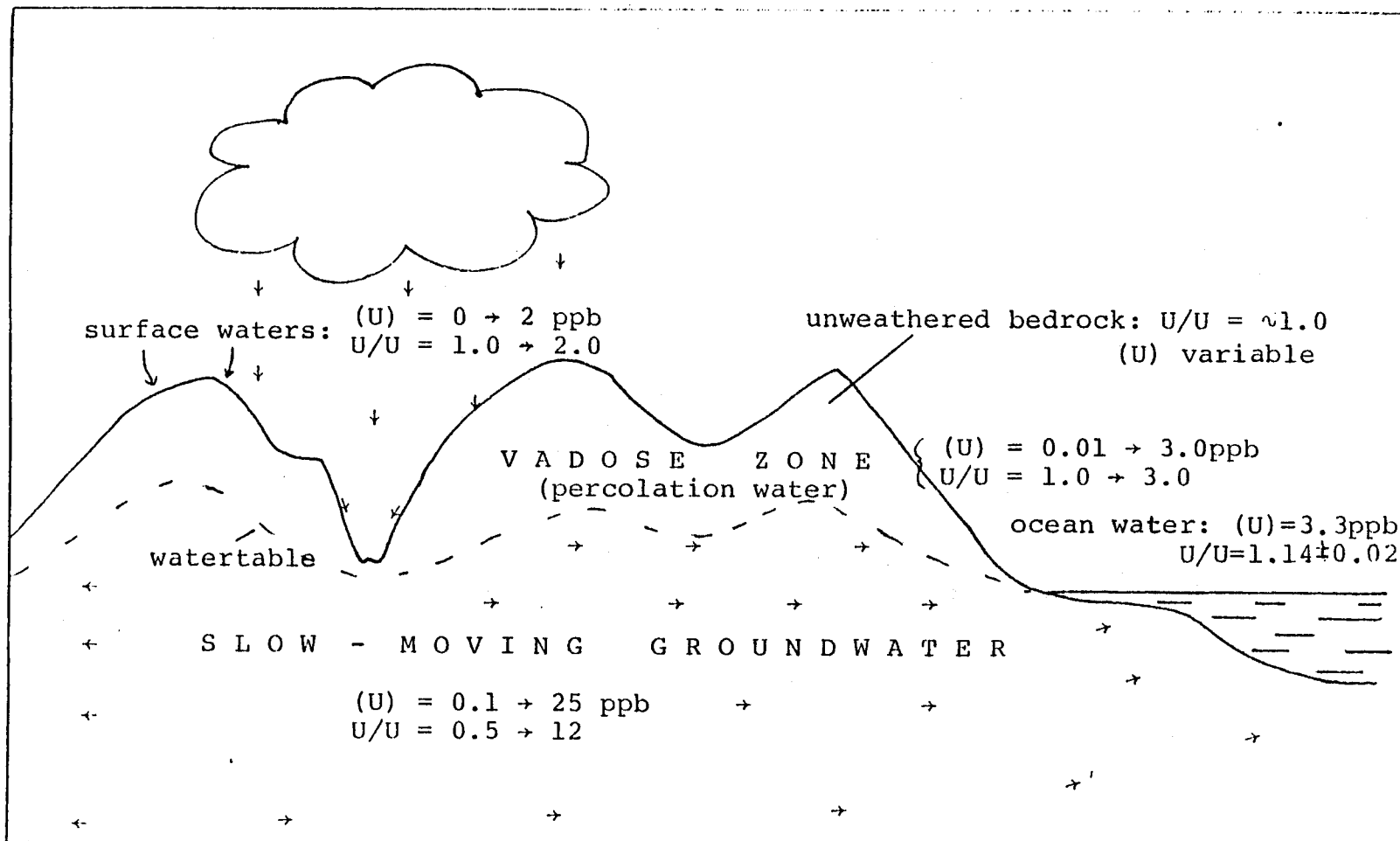
1. The crystal lattice is dislocated as the  $^{238}\text{U}$  atom emits the high energy  $\alpha$  and  $\beta$  particles to decay to  $^{234}\text{U}$ .
2. The oxidation state of  $^{238}\text{U}$  may change from U(IV) to U(VI) because of stripping of the orbital electrons by the emitted  $\alpha$ . This will increase the solubility of the resultant  $^{234}\text{U}$ .
3. During decay of nuclide at the surface of a grain, the  $\alpha$  emission may cause the daughter to recoil from the solid phase into the liquid phase (Gascoyne, 1979).

Therefore, the  $^{234}\text{U}/^{238}\text{U}$  ratios may vary considerably from  $< 1.0$  to 12 in ground water (Figure 2.3). Seawater, however, has a con-

\* All references to nuclides means the activity, i.e.  $^{234}\text{U} = \lambda_{234} N_{234}$

Figure 2.3

Uranium concentrations and  $^{234}\text{U}/^{238}\text{U}$  ratios in the hydrologic cycle (after Gascoyne, 1979)



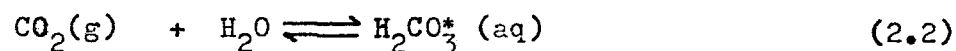
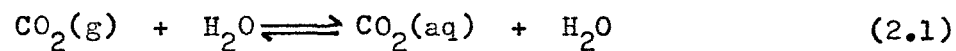
stant ratio of  $1.14 \pm 0.02$ .

## 2.2 Cave Systems

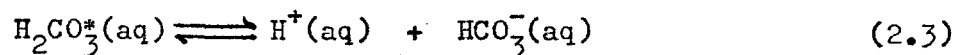
Because of the presence of carbon dioxide in the atmosphere, limestone formations are subject to erosion causing cave formation. Within these caves, speleothems may be deposited bearing uranium.

### 2.2.1 The Carbonate System

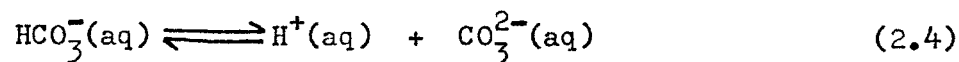
When carbon dioxide gas comes into contact with water and calcite, the carbonate system of chemical reactions is established:



$$K_{\text{CO}_2} = \frac{(\text{H}_2\text{CO}_3^*)}{P_{\text{CO}_2}}$$



$$K_1 = \frac{(\text{H}^+) (\text{HCO}_3^-)}{(\text{H}_2\text{CO}_3^*)}$$



$$K_2 = \frac{(\text{H}^+) (\text{CO}_3^{2-})}{(\text{HCO}_3^-)}$$

Water also can dissociate:

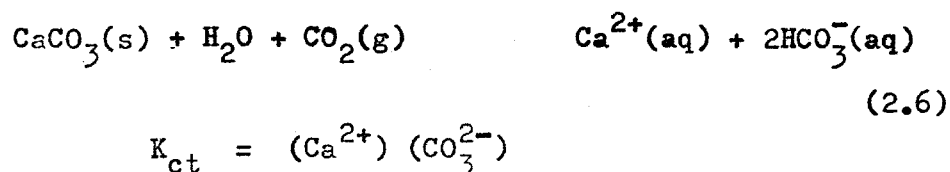


$$K_{H_2O} = (H^+) (OH^-)$$

Since all the above equilibrium constants are **parameters** dependent upon temperature, the above equilibrium depends on the partial pressure of carbon dioxide,  $P_{CO_2}$ ; temperature, and the concentration of other ions in solution, especially  $Na^+$ ,  $Cl^-$ ,  $SO_4^{2-}$ .

When a water equilibrated with the atmosphere,  $P_{CO_2} = 10^{-3.5}$  atm., passes into the soil it may come in contact with soil gases whose  $P_{CO_2}$  is as high as  $10^{-2.0}$  atm. A new equilibrium will be established with much more of the ions  $H_2CO_3^*$ ,  $HCO_3^-$ ,  $H^+$ , and  $CO_3^{2-}$ , making the water more acidic, and therefore, more capable of dissolving limestone.

Most limestone is almost pure calcite which will dissolve according to

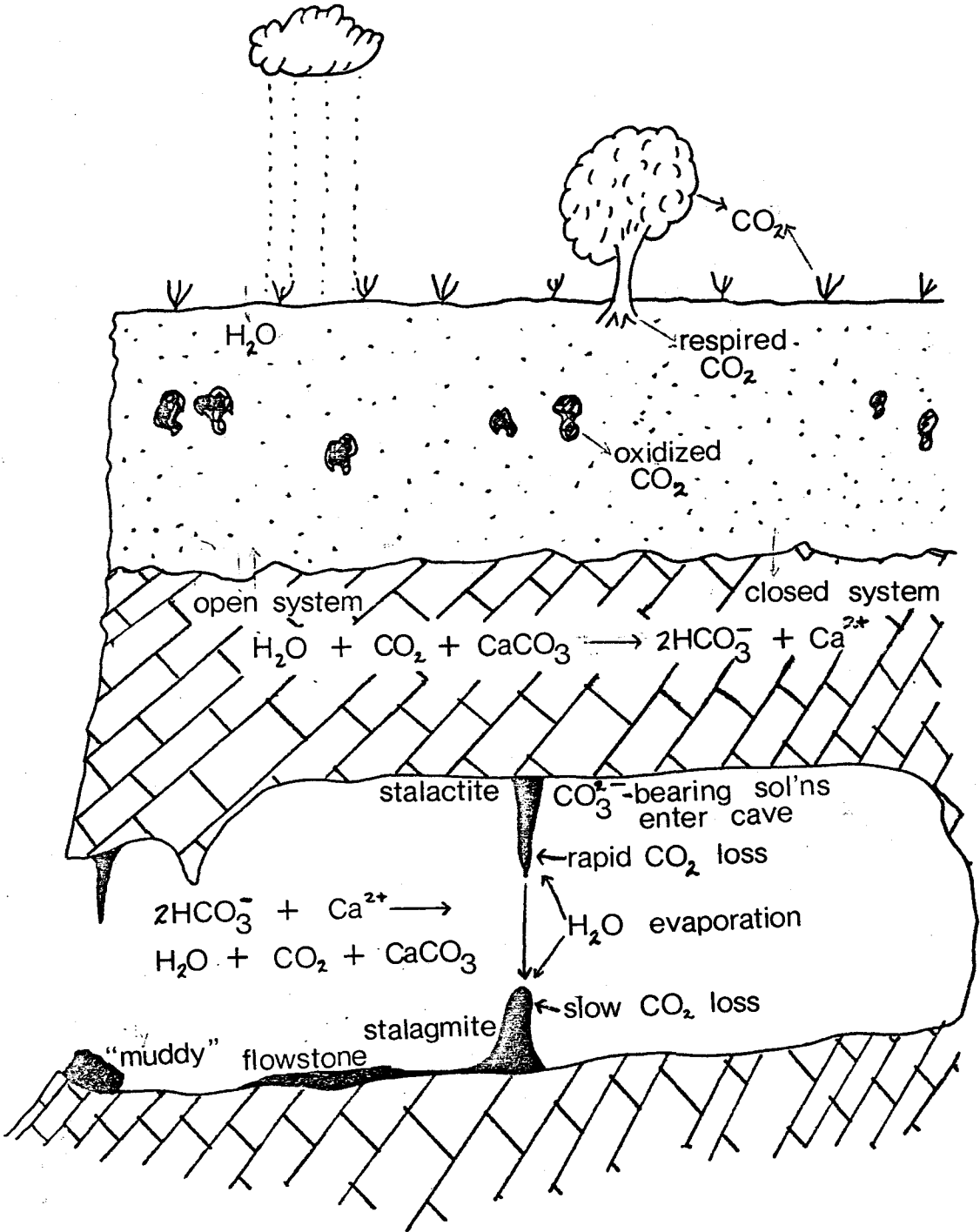


By reversing the above reaction it is possible to precipitate calcite. This may be possible if the water containing the ions is evaporated, or if the water comes in contact with air which has a lower  $P_{CO_2}$ . This latter condition often occurs when water which has been previously equilibrated with soil gases, comes in contact with the atmosphere again, either in a ventilated cave, or at the resurgence point. See Figure 2.4.



Figure 2.4

The process leading to the deposition of speleothems  
in caves (after Hendy, 1971)



### 2.2.2 Cave Genesis and Evolution

A karst cave is defined as a solution cavity  $> 5$  to 16 mm in diameter (Ford & Ewers, 1977); however, for archeological purposes, a cave shall be considered a room within the limestone in which a person can sit or stand, and which has significantly greater dimensions than the opening which leads to the room. If the entrance is of the same dimensions as the room itself, it shall be called an abri (also known in English as rock shelters).

Caves form as a result of the dissolution of the limestone due to the passage of acidic waters equilibrated with soil gases, as described above. Eventually due to some minor lithologic differences, or because of jointing which routes the water along certain courses, a conduit will be dissolved from the host rock. Thereafter, the conduit will receive more dissolution than the surrounding areas, resulting in more rapid enlargement of the conduit. It will continue to carry more water as it scavenges water from other less developed passages. At some point, the conduit will become a cave through successive enlargement.

Continued evolution of the cave may result in the formation of speleothems by the process of precipitation described above. Because of weakening of the roof rock by continued seepage of water, the roof may partially collapse into the cave; the roof thus slopes upward.

In archeological caves, the occupation is seldom very deep in the cave, while the cave is usually located on a ridge overlooking a river valley, because of the obvious hunting advantage this

provides. Over time, speleothems formed on the roof or walls, during interglacials or interstadials are more apt to be spalled off in the colder but variable periods preceding major glaciations. Furthermore, the cave entrance will be prone to rock falls, as the ridge erodes back from the valley. Therefore, the strata in the front of the cave will be a complex mixture of archeological material, clastic sediments, and roof debris. There may also be stalagmitic "planchers" or floors developed at times when the cave was very wet. Excavation of the archeological layers, then, can provide information about the history of the cave development, in addition to the archeological insights.

### 2.2.3 Abri Genesis and Evolution

An abri is formed by erosion of the lower or middle levels of a cliff, while the upper levels remain as an overhang. Abris may also form if a cave entrance collapses back to the point where the main chamber opens directly to the cliff face.

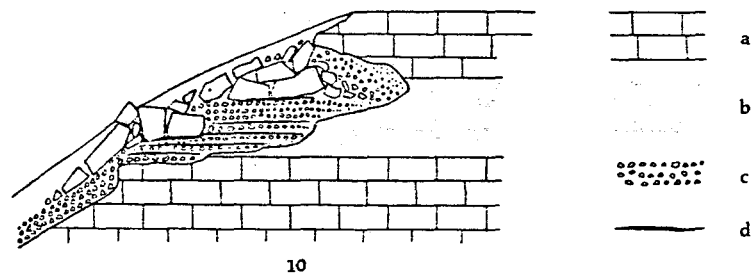
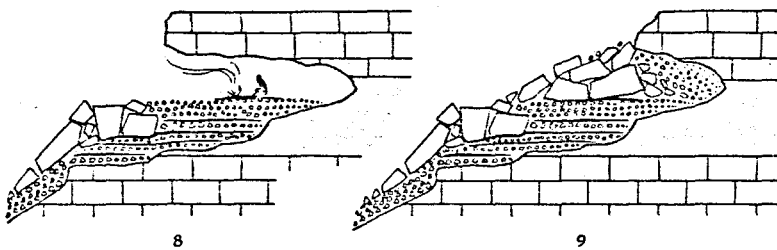
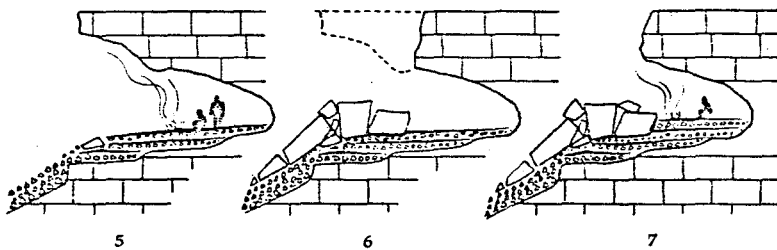
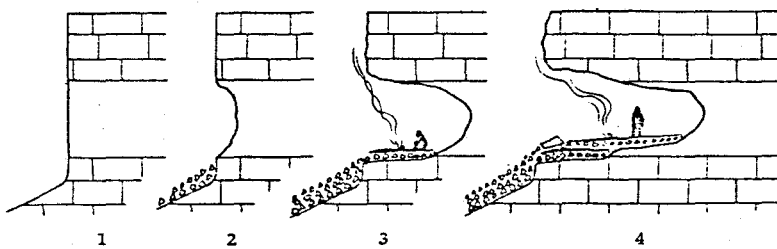
Once it is formed, the evolution of an abri is significantly different from a cave. While the back of the abri continues to erode back into the rock, the overhanging roof will continue to collapse onto the area which was the floor of the abri. Therefore, there is a steady regression of the abri with its associated sediments (Bordes, 1972; Figure 2.5). In abris, it is very common for "muddy" flowstones, planchers, and breccias to form. These latter may be composed of a mixture of archeological material, roof spall, and clastic sediments cemented by calcite during wetter peri-

Figure 2.5

Formation and evolution of an abri:

- a. Compact limestone
- b. Porous or frost-sensitive limestone
- c. Eboulis
- d. Archeological layers

When damp conditions, or those with abundant frosts, an embryonic abri is formed (2) which becomes deep enough to be inhabited (3). As the cryoturbation continues, the shelter becomes deeper, but the rock beneath the eboulis is not eroded further, producing "steps" in the level of the cave floor (4, 5). As deepening continues, the roof eventually caves in (6) partially, momentarily halting human habitation. The process of deepening and partial collapse (7, 8) continues until the roof finally collapses completely, ending habitation of the cave. Finally, colluvium covers the whole cave opening (after Bordes, 1972).



ods, in which the abri may act as a local spring, or as a result of seepage of water down the cliff face. Therefore, the travertine in abris is likely to be less pure than that of caves.

#### 2.2.4 Speleothem Morphology

A speleothem, as defined by Moore (1952), is a naturally formed, unitary, coherent body of mineral material deposited within a cave. Stalactites and stalagmites, the most common types, form with the precipitation of calcite from the water entering the cave which has a lower  $P_{CO_2}$  than the that which the water was previously equilibrated, or by evaporation of the water. The rate of deposition will depend on the degree of air circulation, the internal climate of the cave, particularly the rate of evaporation, and the characteristics of the wafer. Flowstones are laminar deposits formed on walls or the floor. Planchers are formed from standing or slowly flowing water in the cave, resulting in a calcite "floor" being deposited over the previous cave floor.

Open air travertine, though not strictly speleothems by definition, may closely resemble those of the caves. These deposits form where saturated waters resurge to the surface, causing deposition of travertines in many shapes, with flowstone one of the most common.

To precipitate a stalactite, the drip rate must be sufficiently slow to allow precipitation of the calcite before the drip falls. Prolonged precipitation will produce a conical stalactite composed of wedge-shaped crystals growing perpendicular to long axis (Moore, 1962). In the initial stages of growth, the

stalactite will have a pipe-like shape often referred to as a "soda straw" As the speleothem grows, however, this will be filled as well.

Alternatively, when a drip lands on the floor, the water spreads out radially with the precipitation being greatest at the centre of impact. In time, this results in a columnar form composed of radial crystals oriented perpendicular to the growth surfaces (Harmon, 1975). Crystals in stalagmites are usually somewhat larger than those in stalactites, because, in the former, most of the growth occurs in one plane. In stalagmites, larger than average crystals usually indicate slower growth accompanied by fewer impurities.

Flowstone forms as water flows over a surface resulting in thinly laminated sheet-like deposits with the crystals oriented perpendicular to the growth surface. Planchers are very similar, with crystals oriented perpendicular to the growth surface. These form over entire cave floors when a film of slowly flowing water allows precipitation over the entire floor. Often stalagmites may form the upper surface of a stalagmitic plancher. Fallen stalactites might be embedded in the calcite, as well.

All these speleothems are characterized by growth rings or laminations, comparable to those found in trees. These, however, are not necessarily annual, but can represent up to several thousand years of growth for one "band". Frequently, these growth horizons exhibit colour banding and differences in opacity, in many instances, due to fluid inclusions, inclusions of fine-grained

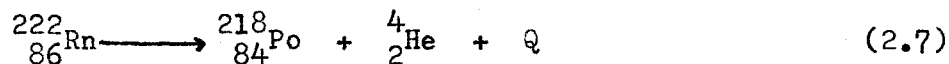


detritus, differences in chemical composition, especially of trace elements, or surface effects from irregular deposition rates (Harmon, 1975).

The shape of speleothems directly reflects the depositional conditions under which they grew. Under uniform growth conditions, a stalagmite will have a constant diameter, while a flowstone will be evenly laminated. Furthermore, both will likely be macrocrystalline, high in fluid inclusions, and low in detritus. Irregular growth rates, however, alter both internal and external appearances. Often, as a result of a hiatus in growth, a sand or silt horizon will be formed. Under conditions of rapid evaporation or loss of carbon dioxide, as often occur at cave entrances, or in abris, porous microcrystalline speleothems are formed with randomly oriented crystals. Often containing large amounts of detritus, these deposits are "muddy" in appearance, and normally should be avoided when collecting calcite for dating. Unfortunately, however, it is often these deposits which have the closest association with archeological material because the occupants of the cave seldom went deep inside. To be avoided at all times when selecting calcite for dating are the calcite-cemented breccias, which may contain limestone from the host rock which will be infinite in age compared with the formation of the breccia which is the date of interest. With properly selected calcite, it is possible to date the time of the formation of the speleothem by utilizing the radioactive decay of the uranium in it.

### 2.3 Radioactive Decay

Many radionuclides with atomic number  $> 58$ , and a few of very low atomic number decay by spontaneous emission of an  $\alpha$  particles,  ${}^4_2\text{He}$ . The  $\alpha$  particles emitted may be either of a discrete energy, or of slightly varying energies. In the latter case,  $\gamma$  rays will also be emitted to return the nucleus from its excited state to its ground state. Because the  $\alpha$  has a mass of 4 amu., it can cause the nucleus to recoil with an energy of about 0.1 MeV. For example,



$$Q_{\text{total}} = 5.5904 \text{ MeV}$$

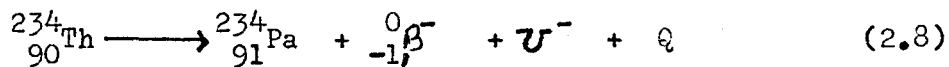
$$Q_{\alpha} = 5.4897$$

$$Q_{\gamma} = 0.51$$

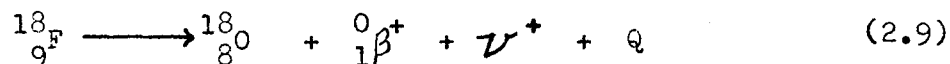
$$Q_{\text{recoil}} = 0.4907$$

(Faure, 1977).

Some nuclei with an excess of neutrons may undergo  $\beta^-$ ,  ${}^0_1\text{e}^-$ , emission (also known as negatron emission), usually accompanied by  $\gamma$  ray emission, i.e.



Some nuclei, on the other hand, with a low atomic number and a deficiency of neutrons will emit  $\beta^+$ ,  ${}^0_1\text{e}^+$ , particles, i.e.



(Faure, 1977).

All radioactive decay obeys the law

$$\frac{dN(t)}{dt} = -\lambda t \quad (2.10)$$

where  $N(t)$ , a function of time, is the number of atoms at time  $t$ , and  $\lambda$  is the decay constant.

Assuming the daughter product from the radioactive decay is initially absent, the decay of the parent atom obeys the following equation

$$N(t) = N_0 e^{-\lambda t} \quad (2.11)$$

where  $N_0$  is the number of atoms at time 0, i.e. the time of formation of the material. Under these conditions, the age of the deposit can be determined by solving the following for  $t$

$$N_b = N_a (1 - e^{-\lambda_a t}) \quad (2.12)$$

where  $N_a$  and  $N_b$  are the amounts of the parent and daughter nuclides respectively at time  $t$  (now), and  $\lambda_a$  is the decay constant of the parent atom. If, however, the daughter atom is also radioactive, the equation must consider this. If the parent is longer-lived than the daughter, i.e.  $\lambda_a \ll \lambda_b$ , the system will eventually reach secular equilibrium, where the decay of the daughter is as rapid as its formation from the parent. Under these conditions,

$$\frac{\lambda_b N_b}{\lambda_a N_a} = 1.00 \quad (2.13)$$

Therefore, by knowing the initial amounts of the two atoms, in this case, the age of the deposit can be determined from

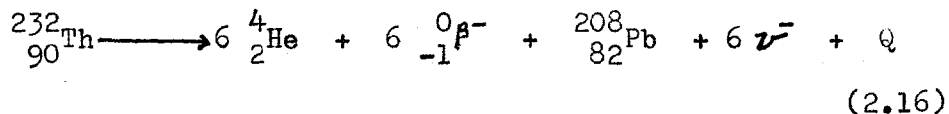
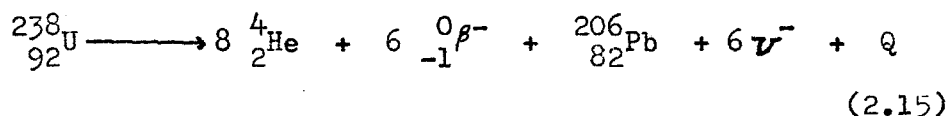
$$N_b = N_a^0 \frac{\lambda_a}{\lambda_b - \lambda_a} (e^{-\lambda_a t} - e^{-\lambda_b t}) + N_b^0 e^{-\lambda_b t} \quad (2.14)$$

where  $N_a^0$  and  $N_b^0$  are respectively the initial amounts of the parent and daughter nuclides. If such a system is disturbed from equilibrium by removal of the daughter, the subsequent return to equilibrium can be applied as radiometric clock to date the time of the disturbance.

#### 2.4 The Uranium-Thorium Decay Series

$^{238}\text{U}$  and  $^{232}\text{Th}$  both decay by  $\alpha$  and  $\beta^-$  emission, as described above, in a complicated multistep pattern shown in Figure 2.6.

$^{238}\text{U}$  eventually decays to  $^{206}\text{Pb}$ , while  $^{232}\text{Th}$  decays to  $^{208}\text{Pb}$ :



In the U/Th method, only the decay of  $^{238}\text{U}$  as far as  $^{230}\text{Th}$ , and  $^{232}\text{Th}$  as far as  $^{228}\text{Th}$  are of interest. Other dating methods based on these schemes, and that of  $^{235}\text{U}$  employ different parts of the decay pattern and the different properties of the elements involved.

While the decay from  $^{234}\text{Th}$  to  $^{234}\text{U}$  is fast (the half-life

**Figure 2.6**

The  $^{238}\text{U}$  and  $^{232}\text{Th}$  decay series

Shown in the diagram are the decay paths, the partitioning in the case of multiple decay pathways, the halflives, and the mode of decay (after Ku, 1976; Faure, 1977; Weast, 1972)



is less than 25 days), that from  $^{234}\text{U}$  to  $^{230}\text{Th}$  and from  $^{230}\text{Th}$  to  $^{226}\text{Ra}$  is slow ( $t_{1/2} = 2.48$  and  $0.75 \times 10^5$  y). Should unsupported  $^{234}\text{U}$  be incorporated into a speleothem, the  $^{234}\text{U}$  will not reach equilibrium with the  $^{230}\text{Th}$  it produces until approximately 700,000 years (700 ka) after the initial deposition, while the  $^{238}\text{U}$  will reach equilibrium about 2.5 million years after deposition, providing the  $^{234}\text{U}$  is not preferentially dissolved out, as discussed above. Theoretically, until 700 ka, the relative ratios  $^{234}\text{U}/^{238}\text{U}$  and  $^{230}\text{Th}/^{234}\text{U}$  can be used to measure the time elapsed from the time of deposition, but after 350 ka, the latter ratio approximately equals one (equilibrium).

The  $^{232}\text{Th}$  series acts as a tracer for the presence of allogenic thorium. If  $^{232}\text{Th}$  appears in thorium emission spectrum, this implies that thorium of all isotopes has been incorporated into the calcite. Another problem which this implies is that if the thorium is present due to detrital inclusions in the calcite, that same detritus may contain allogenic uranium which has a significantly different activity ratio than that of the calcite. These two problems will be discussed in greater detail in the next chapter. The absence of  $^{232}\text{Th}$  ensures that the initial  $^{230}\text{Th}$  concentration was zero, because the half-life of  $^{232}\text{Th}$  is much longer than that of  $^{230}\text{Th}$ .

Each of the  $\alpha$  particles emitted in the decay series has a specific energy associated with it which is characteristic of the nucleus whence it came. The  $\alpha$  particle energies for the uranium and thorium decay series are shown in Figure 2.7. The problem,

Figure 2.7

The  $\alpha$  particle energies of the  $^{238}\text{U}$  and  $^{232}\text{Th}$   
decay series isotopes (after Harmon, 1975, from  
Lederer et al., 1966)



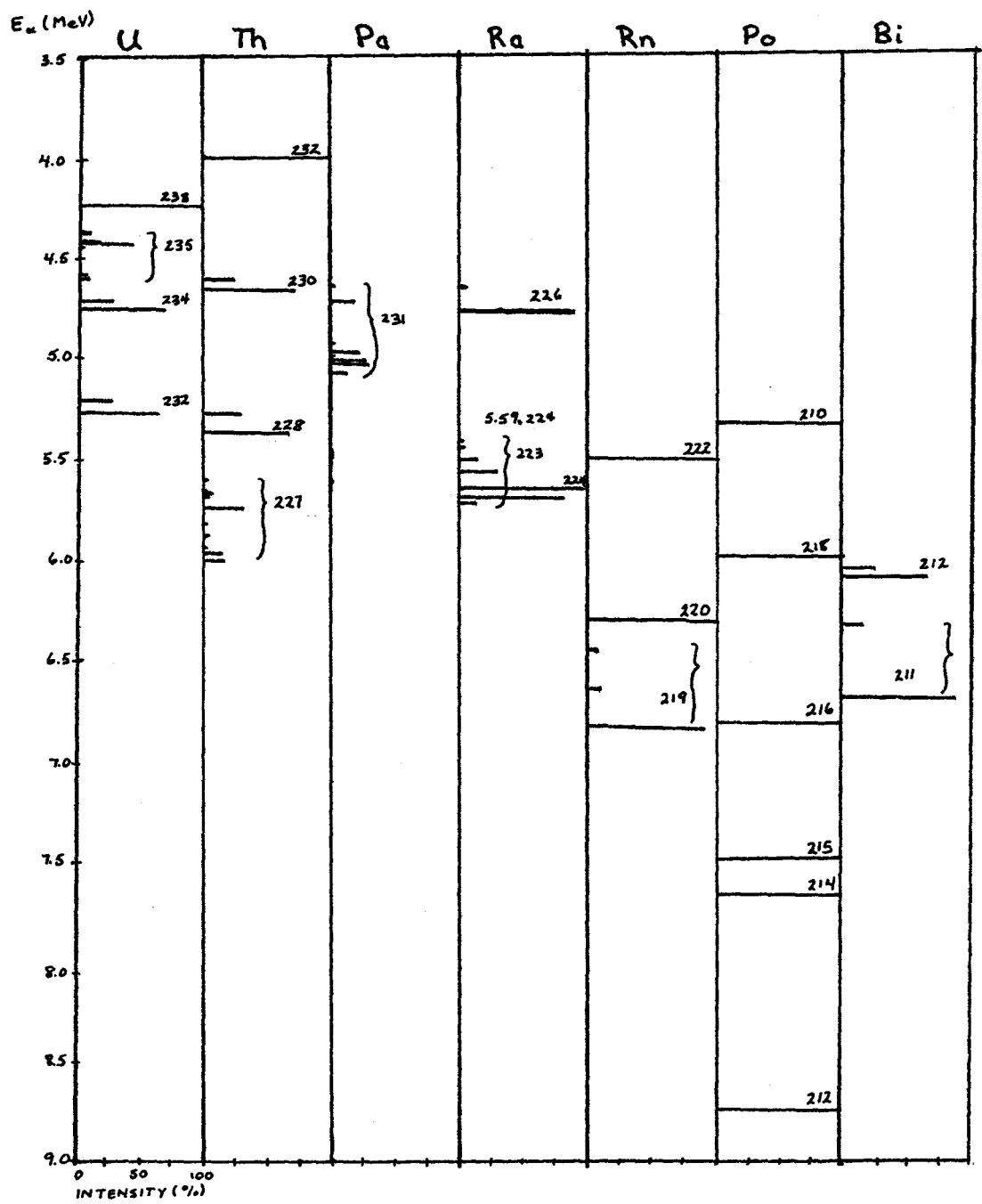


Figure 2.3

however, is somewhat complicated in that the particles may be emitted in any direction, and may reflect off any other substance in the counting chamber, thereby reducing their initial maximum energy. Therefore, when a sample is counted in an  $\alpha$  counter, it is necessary to assume that a range of energies exists for each nucleo-specific  $\alpha$ . Therefore, it is necessary to separate the the various elements whose  $\alpha$  particle energies could overlap in the final spectrum.

In the U/Th method, the activity of the various isotopes is used to determine the ratios of the isotopes present in the sample. Because only the isotopes of uranium and thorium are of interest, only these elements are counted.

## 2.5 The Theoretical Principles of U/Th Dating

When dating the time of deposition of a speleothem, it is assumed that there was no thorium, especially  $^{230}\text{Th}$ , present initially. Because this requires that no thorium be present in the groundwater, it is necessary to test this assumption. Present day groundwaters contain only about  $1/10^4$  as much thorium as uranium. Since thorium is removed from the groundwater by adsorption onto clays, etc., this U/Th ratio is found to be fairly constant for waters throughout the world (Thompson, 1973). Furthermore, no evidence exists to suggest the past ratio should not be similar for the Quaternary. Calcite crystallographically incorporates uranium into the crystal lattice as  $\text{UO}_2\text{CO}_3$ , but thorium is adsorbed on the surface of clay detritus which is a minimum in

clean speleothems. Therefore, pure calcium carbonate should contain no radiogenic thorium detectable by present techniques of measurement.

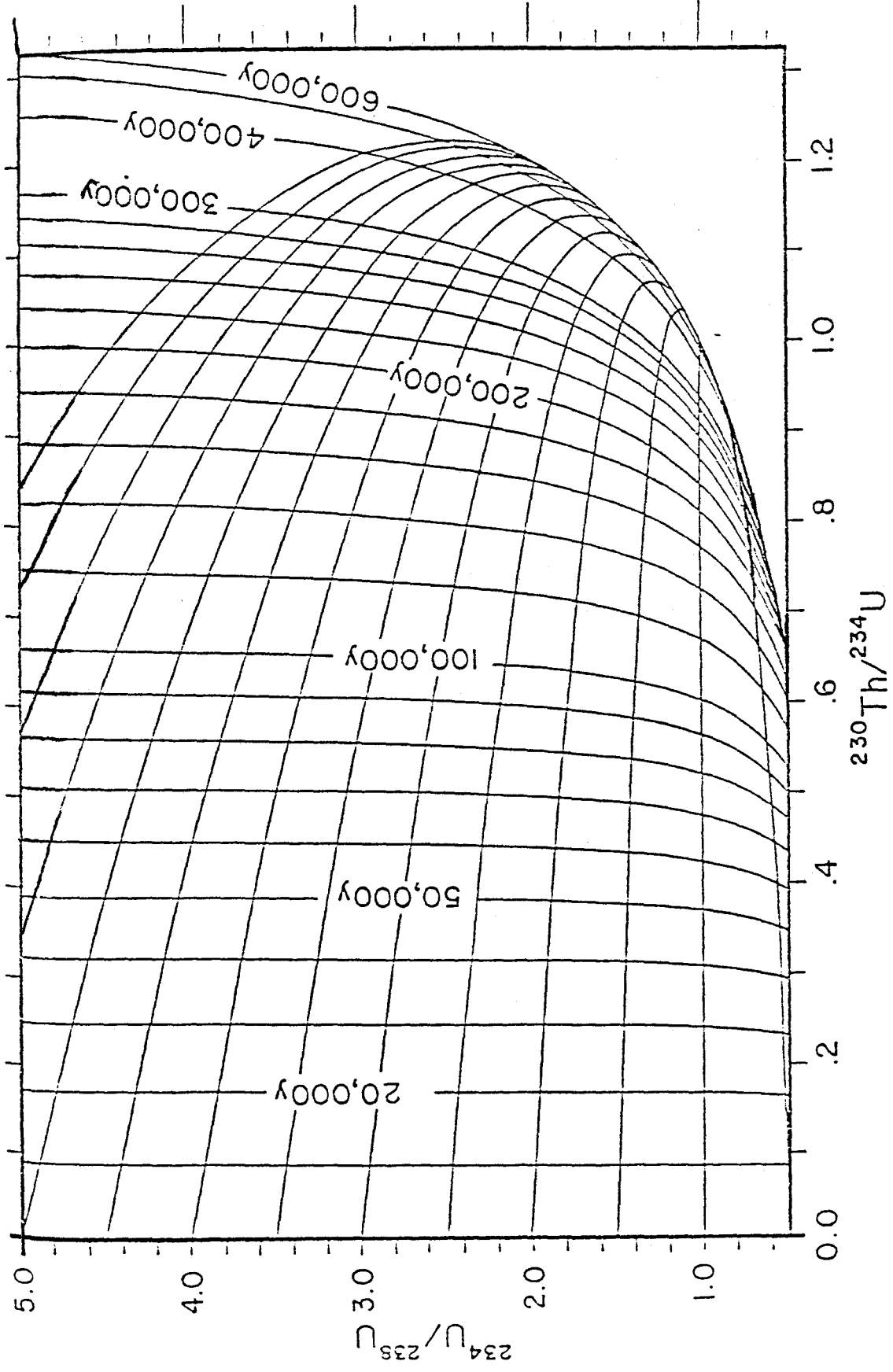
Once the speleothem has been deposited with x ppm of uranium and no thorium, both  $^{238}\text{U}$  and  $^{234}\text{U}$  will decay, while  $^{230}\text{Th}$  ingrows. The uranium will have been deposited in the calcite in the activity ratio which it had in the water, because these nuclides are too heavy for isotopic fractionation to occur. The ratio will slowly change until equilibrium is reached; however, this process is slow compared with the change in the  $^{230}\text{Th}/^{234}\text{U}$  ratio which reaches equilibrium in about 700 ka. **Until 350 or 400 Ka after the time of deposition, determination of the  $^{230}\text{Th}/^{234}\text{U}$  ratio is sufficiently accurate to discriminate the age of the deposit.** Beyond that, the ratio is so close to equilibrium that it is difficult to distinguish the true age from an infinite one. The relationship between  $^{230}\text{Th}/^{234}\text{U}$  and  $^{234}\text{U}/^{238}\text{U}$  and time is shown in Figure 2.8

Should there be any initial allogenic thorium present in the calcite, the applicability of the method depends on the reliability with which the initial  $^{230}\text{Th}/^{232}\text{Th}$  and the initial amount added can be determined. **Since no calcite is absolutely pure, thorium could be from several sources, including mineral inclusions, particularly clays, as well as occlusion.** By assuming that the  $^{232}\text{Th}$  has remained constant since the deposition (the half-life is  $1.4 \times 10^{10}$  years), and assuming an initial  $^{230}\text{Th}/^{232}\text{Th}$  ratio, it is possible to make a correction for detrital thorium. Post-depositional

Figure 2.8

The relationship between the activity ratios  $^{230}\text{Th}/^{234}\text{U}$  and  $^{234}\text{U}/^{238}\text{U}$  for systems with no initial thorium:

The near horizontal lines are the growth curves of the  $^{230}\text{Th}/^{234}\text{U}$  ratio vs. time for a fixed initial  $^{234}\text{U}/^{238}\text{U}$ , while the near vertical lines are isochrons (after Schwarcz, 1979).



contamination, although impossible to distinguish isotopically from initial contamination, can, on occasion be detected by microscopic examination.

The precise methodology and calculations will be described in the next chapter.

## THE U/Th DATING METHOD

In general, the U/Th dating method relies on chemical analyses, consisting in part, of dissolution, precipitation, etc., and  $\alpha$ -particle spectral analysis to measure the activities of the isotopes. First the traces of uranium and thorium are removed from the parent matrix by chemical procedures. Then, the activities of each isotope are measured. After the date has been computed from the spectral data, however, the method becomes very subjective: the geological decisions and archeological correlations which result are the product of experience, and are subject, therefore, to human error to a greater degree than the actual chemical procedures.

## 3.1 The Chemical Analysis

Although the actual chemical procedure is simple, it does require approximately three to six days to complete. As a consequence, several samples, usually five, are analyzed simultaneously. The procedure is as follows:

1. The sample to be dated is washed to remove the surface dirt, and then weighed. Normally, a sample weighs between 25 and 50 g, if it is expected to contain more than 0.1 ppm uranium. For less uraniferous samples, as much as 100 g may be used.
2. At this point, a "spike" solution containing  $^{232}\text{U}$ : $^{228}\text{Th}$  in

an activity ratio of 1.027, and  $\text{FeCl}_3$ , the carrier solution, are added. Normally, only 22.7  $\mu\text{g}$  of "spike" are added; however, for samples suspected to be more uraniferous, 45.4  $\mu\text{g}$  are used. Only 10.0  $\mu\text{g}$  of iron are added, because most natural speleothems already have iron present in trace amounts.

3. The sample is then dissolved in concentrated nitric acid,  $\text{HNO}_3(\text{aq})$ , of sufficient quantity to just dissolve the sample, and render the pH of the solution approximately 2.
4. The solution is centrifuged to remove any undissolved detrital material, providing there is visible detritus. Otherwise, this step is omitted. Any detritus is weighed and retained for possible further analysis.
5. The solution is boiled to remove carbon dioxide,  $\text{CO}_2$ .
6. In order to precipitate iron hydroxide,  $\text{Fe}(\text{OH})_3$ , which selectively absorbs both uranium and thorium on its surface, ammonium hydroxide is titrated into the hot solution until the red precipitate begins to form. The precipitation reaction is
 
$$\text{FeCl}_3 + 3\text{NH}_4\text{OH} \longrightarrow \text{Fe}(\text{OH})_3 + 3\text{NH}_4\text{Cl}$$
7. After the precipitate is collected by centrifuging the solution, it is redissolved in concentrated hydrochloric acid,  $\text{HCl}(\text{aq})$ .
8. In order to remove the  $\text{Fe}^{3+}$  ions but leave the uranium and thorium ions in solution, the aqueous solution is extracted with isopropyl ether,  $((\text{CH}_3)_2\text{HC})_2\text{O}$ , at a pH equivalent



to that of 9N HCl(aq).

9. The aqueous solution is then passed through an anion exchange column, of mesh size 100-200 filled with Dowex 1 x 8 anion resin at a pH equivalent to that of 8N HCl(aq). This acidic condition will allow the thorium ions to pass through and be collected for further processing (see 15), while the uranium ions are retained on the resin. The column is washed three times with approximately 10 ml 9N HCl(aq).
10. The uranium ions are eluted from the anion column with 0.1N HCl(aq). This aqueous solution is then evaporated to dryness, ready in most cases to be "plated out".
11. If iron is still present, another ether extraction will now be performed. For speleothems suspected of containing organic compounds, the uranium may be refluxed in aqua regia (concentrated  $\text{HNO}_3(\text{aq})$ :concentrated  $\text{HCl}(\text{aq})=1:1$ ).
12. The uranium is redissolved in 0.1M  $\text{HNO}_3$  and extracted with 0.25M thenoyltrifluoroacetone (4,4,4-trifluoro-1-(2-thienyl)-butane-1,3-dione,  $\text{C}_8\text{H}_5\text{F}_3\text{O}_2\text{S}$ ; also known as TTA) dissolved in benzene to extract any thorium which may have passed through the anion exchange column with the uranium.
13. The pH of the aqueous solution is adjusted to 3.5 using dilute  $\text{NH}_4\text{OH}$ , and again extracted with TTA in benzene, this time to extract the uranium from the aqueous solution. This is repeated two more times, discarding the final aqueous layer.
14. The organic layer, containing the uranium, is evaporated

down to approximately 0.1 ml which is then dripped onto a heated steel planchet, termed a "disc", and evaporated to dryness. This procedure is called "plating out the uranium".

15. The solution containing the thorium which dripped through the anion column is diluted to a pH equivalent to that of 3M HCl(aq) by adding twice the volume of deionized, distilled water to the 9N solution.
16. This solution is placed on a Dowex 50 cation exchange column of mesh size 100-200 which retains the thorium, but allows all the other ions to pass through. These will include the daughter ions of uranium and thorium, such as polonium and bismuth and any other ions which may have been adsorbed by the  $\text{Fe}(\text{OH})_3$ . The column is washed three times with 3M HCl(aq).
17. The column is eluted with 0.75M oxalic acid,  $\text{HO}_2\text{C}_2\text{O}_2\text{H}$ . To remove the organic compounds, including the oxalic acid, from the aqueous thorium-bearing solution, it is refluxed in aqua regia.
18. After the thorium has been dissolved in 0.1M  $\text{HNO}_3$ (aq) and extracted three times with TTA in benzene, the organic layer is plated out onto a disc, as the uranium was.
19. Before being counted, the discs are fired for ten seconds to remove any organic residue, including the TTA, or any ions which might still be present. Finally, the discs are counted for approximately two days on an  $\alpha$  counter.

Some of the equipment is shown in Figure 3.1, while Figure 3.2 gives a flowchart for the procedure. Figure 3.3 shows a typical spectrum for both uranium and thorium.

### 3.1.1 Detrital Contamination

Often an archeological sample will not have good yields of either uranium or thorium or both. Poor yields can result from any one of several factors, or a combination thereof. Some may be:

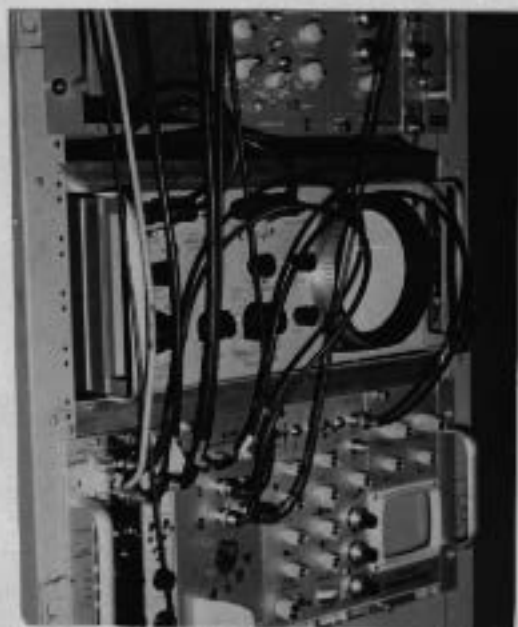
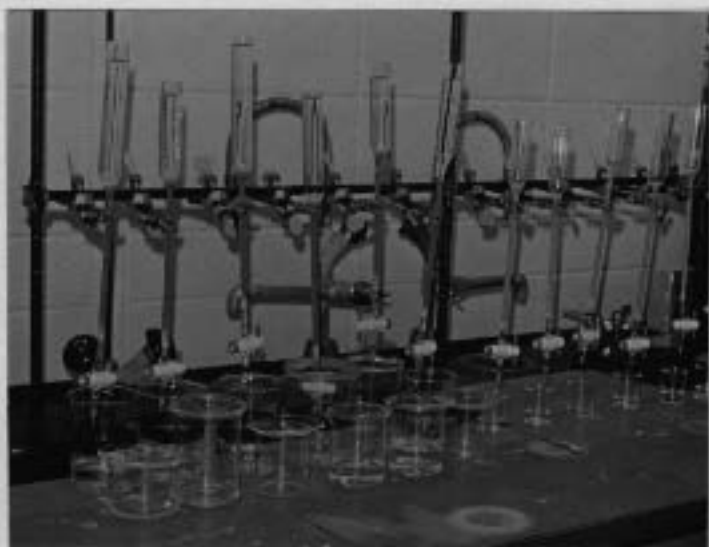
1. Organic contaminants: As a result of the presence of animal or vegetal matter in the cave sediments, excretia in the sediments or the percolating waters, or paleontological remains in the deposits, organic compounds can be incorporated into the calcite. These may adsorb uranium or thorium during the normal chemical procedure.
2. Phosphates: Phosphates in the calcite, as a result of the presence of bones or teeth in the cave, will interfere with the chemistry of the method, thereby resulting in poor yields.
3. Clays: These will adsorb thorium particularly, but also uranium, onto their surfaces. When the clays are removed in step 4, much or all of the uranium and thorium may also be lost.
4. Other trace elements or compounds: Because the chemistry of many trace elements and compounds is poorly understood, especially under the conditions used in the method, there may exist many which could adsorb uranium and thorium, or interfere with the chemistry.

Roasting the sample should destroy the organic material in it.

Figure 3.1

The chemical procedure: the equipment:

- a. The columns for uranium and thorium.  
Uranium and thorium are trapped on the surface of the resins, while other ions pass through. The thorium and uranium are later eluted by changing the conditions of the resin.
- b. The oscilloscope which shows the spectrum being accumulated in
- c. The counting chambers.



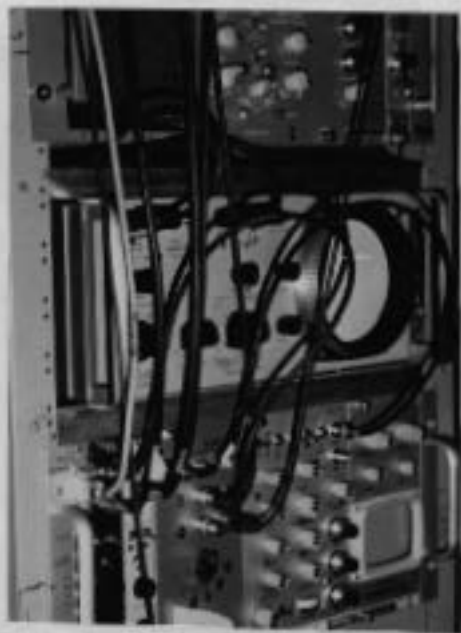
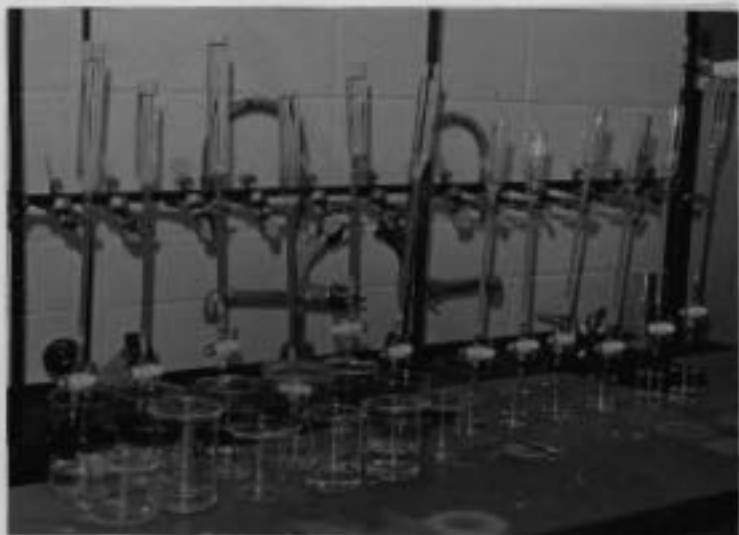
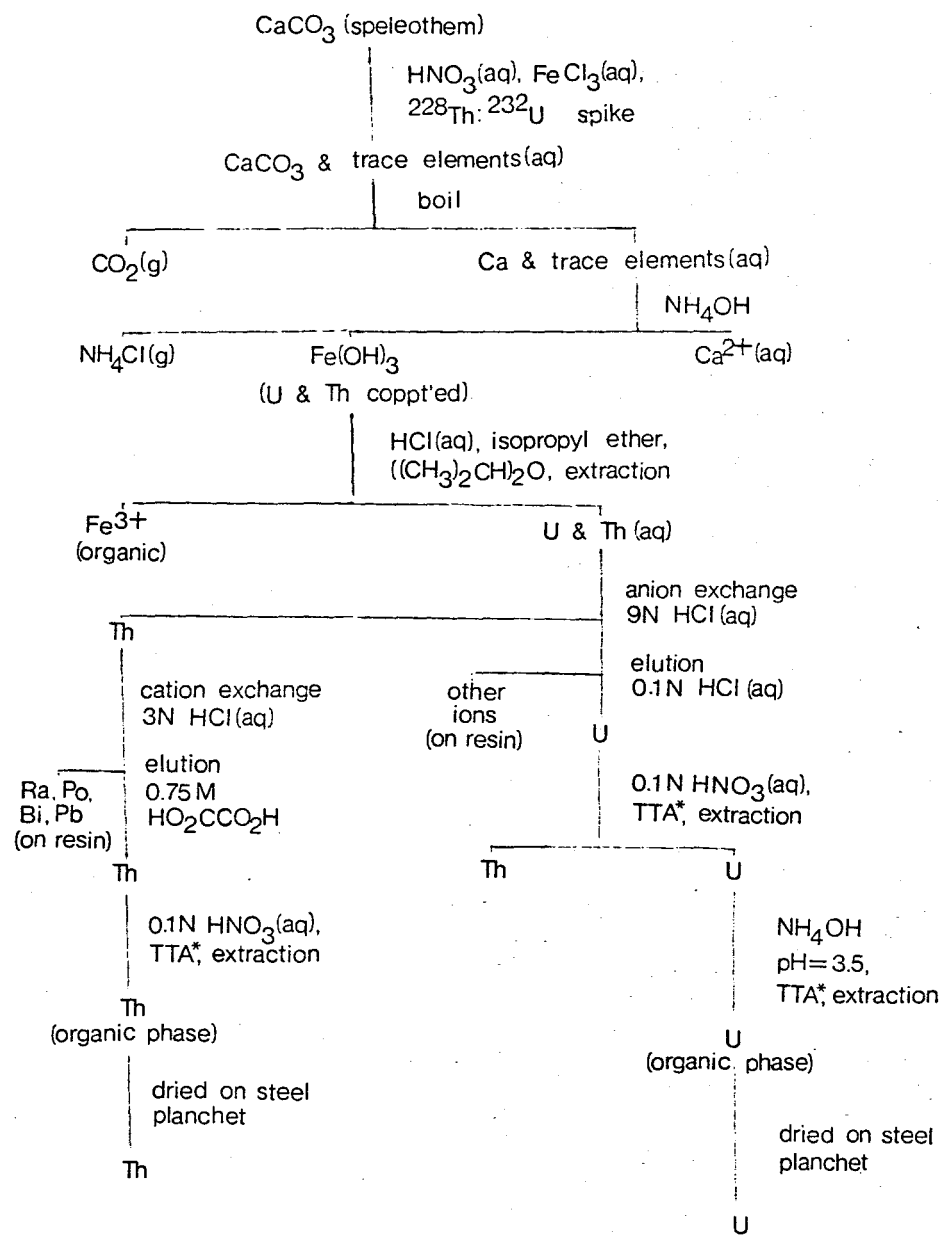


Figure 3.2

The chemical analysis for the separation of  
uranium and thorium from calcite



\* TTA = 0.25 M thenoyltrifluoroacetone (4,4,4-trifluoro-1-(2-thienyl)-butane-1,3-dione, C<sub>8</sub>H<sub>5</sub>F<sub>3</sub>O<sub>2</sub>S)



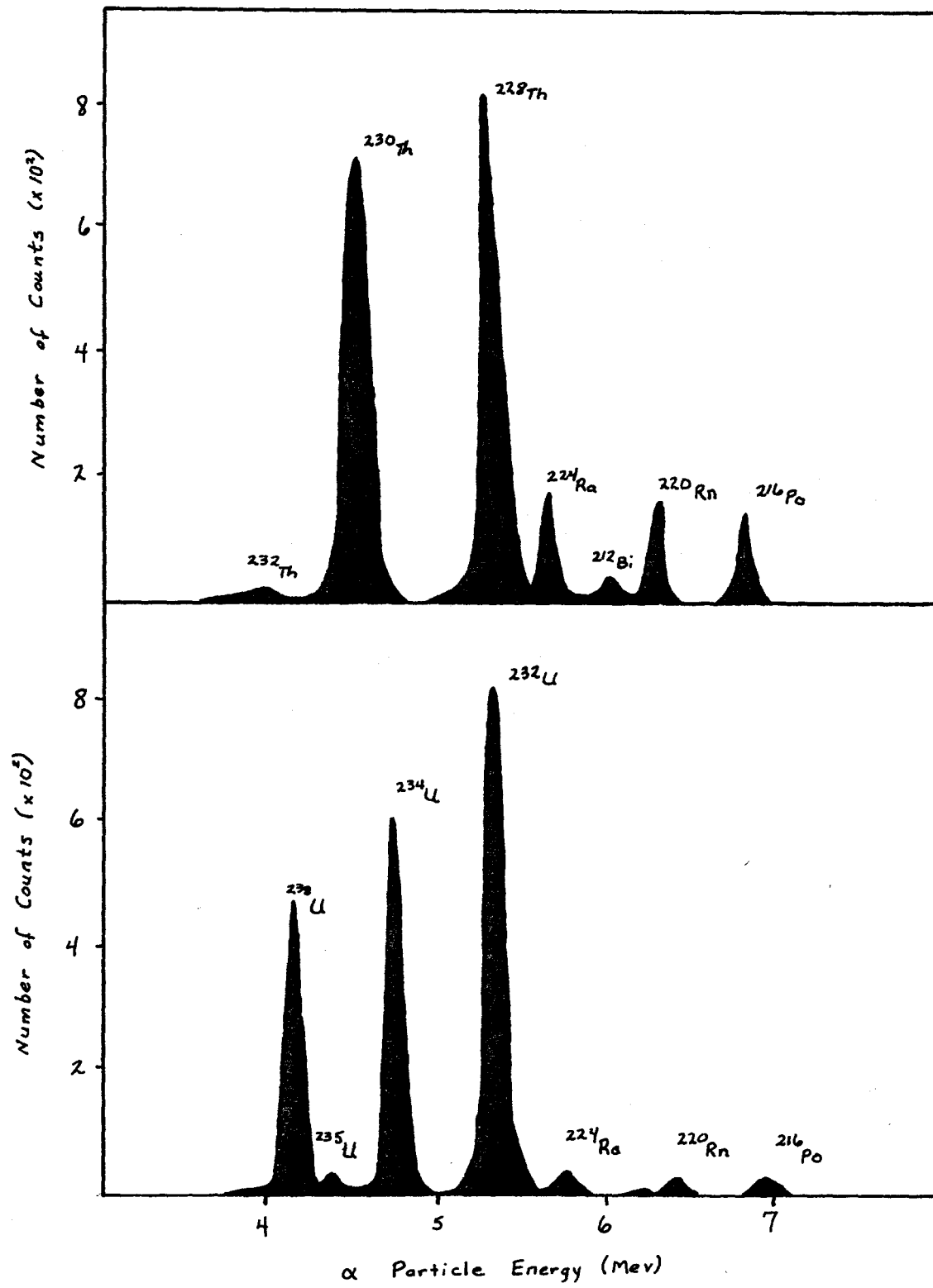
Figure 3.3

Typical emission spectra showing the energies  
and relative abundances:

A. Thorium

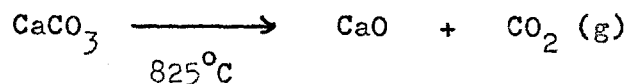
B. Uranium

(after Harmon, 1975)



### 3.1.2 The Roasting Technique

When the sample is roasted, the calcite is calcined to lime



Organic compounds are completely oxidized at approximately 600°C. Therefore, as the sample is heated to 900°C or more, the crystal lattice of the calcite breaks down, allowing any gases produced in the oxidation of the organics to be burned off.

The roasting procedure involves the following preliminary steps:

- A. The sample is crushed to be approximately 2  $\phi$  in size, and then weighed and placed in a silica or porcelain crucible for heating.
- B. It is then heated in a muffle furnace at a minimum temperature of 900°C for at least six hours. The temperature may be as high as 1100°C without causing problems.
- C. When removed from the furnace, the sample is stored in a dessicator to prevent absorption of water. Samples can be stored for several weeks in this state.
- D. When the sample is to be processed further, approximately 100 ml of water are added to the sample first, followed by sufficient concentrated nitric acid,  $\text{HNO}_3$  (aq) to dissolve the sample and render the pH of the solution approximately 2. The "spike" solution and the carrier  $\text{FeCl}_3$ , as described above are added at this point as well.

The sample is then treated as any ordinary sample would be, following the procedure discussed above, steps 4 through 19. Figure 3.4 gives the flowchart for the roasting technique, showing where it differs from that shown in Figure 3.2.

### 3.1.2.1 Problems with Roasted Samples

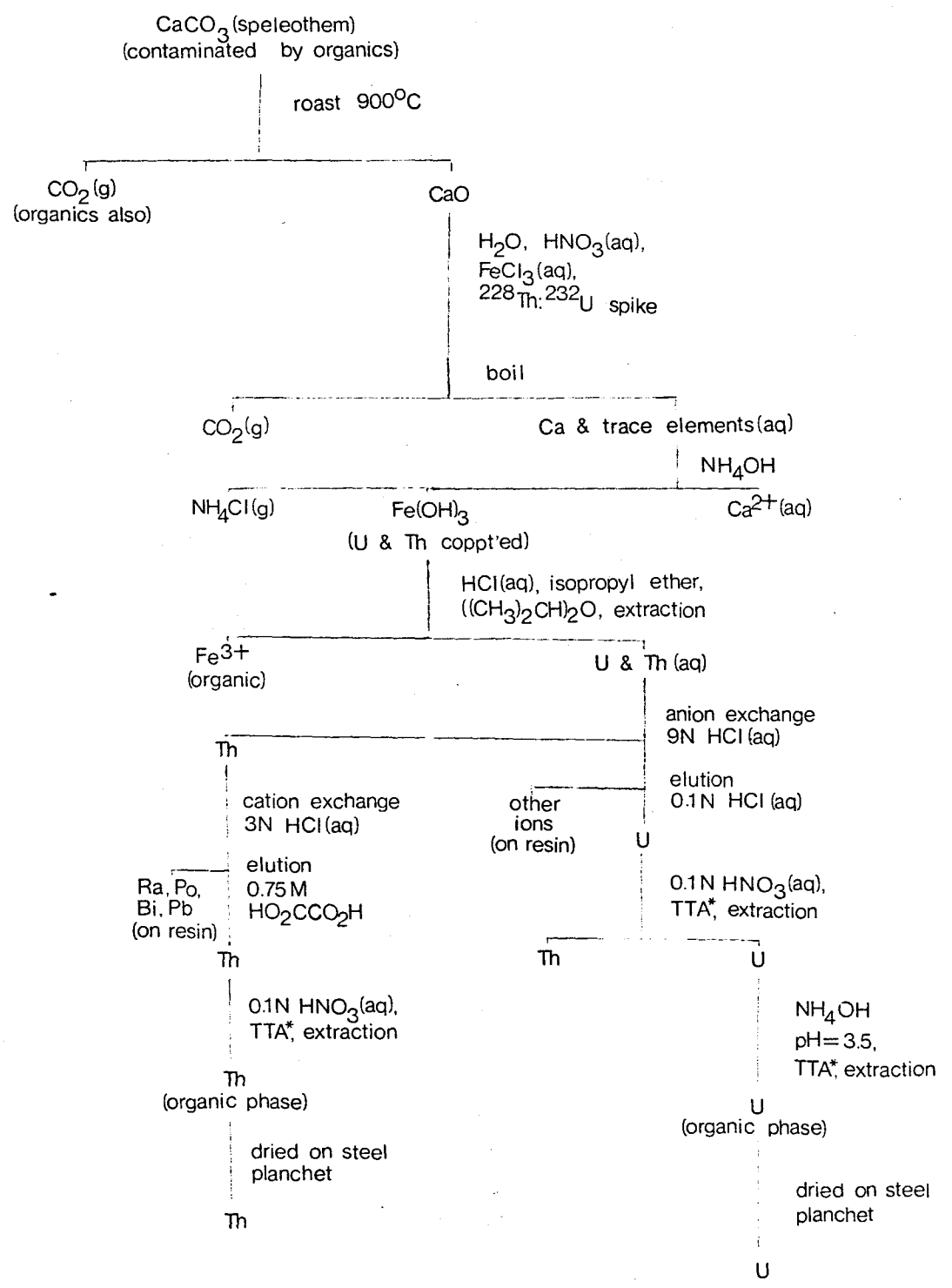
Although roasting may improve the yields, it can cause several problems which would not normally occur with an unroasted sample. Some of the major problems encountered include:

1. "Ether jelly" in the extraction: "Ether jelly", a yellow gelatin, can occur in a normal sample if the concentration of the acid, HCl, is too strong in step 8. Normally, this could be corrected by adding water (Gascoyne, 1979). With roasted samples, however, it is fairly common, but will not dissipate when water is added. Fortunately, its occurrence is not correlated with low yields in the roasted samples.

2. Slow dripping on the uranium columns: Often the uranium columns containing roasted samples will drip very slowly (a few drips per hour, as opposed to about one per minute). This can be complicated by the resin floating up to the surface, or the formation of a fluffy light yellow precipitate. Although the former can occur if the acid is too strong in normal samples, the latter never has occurred in unroasted samples. Furthermore, this situation can persist for up to nine days, before the column will begin to drip normally. Poking the top of the resin with a stirring rod or a long-nosed pipette will speed up the drip rate momentarily. The solution to this problem may be to dry out the precipitate before

Figure 3.4

The roasting procedure for organically contaminated samples



\* TTA = 0.25 M thenoyltrifluoroacetone (4,4,4-trifluoro-1-(2-thienyl)-butane-1,3-dione, C<sub>8</sub>H<sub>5</sub>F<sub>3</sub>O<sub>2</sub>S)

step 7. The final five roasted samples, all treated this way, dripped as do unroasted ones. Unfortunately, about half of the samples which suffer this result in no uranium yield, possibly because the resin degrades after long exposure to highly concentrated acid.

3. Iron in the uranium at step 12: Often, because of the formation of "ether jelly" which prevents complete extraction, or some other factor, the ether extractions at step 8, do not remove all the iron from the uranium. The iron will follow the uranium through the columns and even into the TTA, causing a disc which has more than a one atom thick plating on its surface, to be avoided because hitting other atoms slows the  $\alpha$ -particles as they are emitted, causing the peaks to be less resolved. requiring lengthy mathematical corrections. The problem is easily solved by extracting the uranium again with ether, followed by refluxing with aqua regia to remove all traces of the ether. This will not reduce the uranium yields.

4. Uranium which is insoluble in 0.1 N HCl at step 12: This can be easily corrected by adding a few drops of concentrated  $\text{HNO}_3$  to the beaker, then omitting step 12 (the extraction to remove thorium), and adding dilute  $\text{NH}_4\text{OH}$  until the pH is 3.5. Because step 12 has been shown by Gascoyne (1979) to remove no appreciable thorium, but has been retained in the method as a safety precaution, omitting this step is not detrimental to the results.

5. Loss of uranium: When samples are roasted, it is pos-

sible to reduce the uranium to the insoluble  $4+$  state. Only extremely strong acid will reoxidize it. Apparently, this has occurred in some roasted samples. Where it was possible to compare the uranium concentrations for samples which had been processed both with and without roasting, about 26% of the roasted samples showed significant losses of uranium which could not be attributed to leaching in all cases, suggesting that the uranium had been lost before the addition of the 'spike'. To prevent this, the 'spike' could be sprinkled on the ground sample before roasting, but this would not ensure that the 'spike' was homogenized with the sample uranium, thereby defeating the purpose. If the uranium is lost in such a manner, the date obtained is useless.

### 3.1.2.2 Results upon Roasting

From the preliminary results on 50 samples, 24 showed improved yields of uranium, 27 improved thorium yields. While approximately 34% of the samples resulted in useful dates, about 24% have been shown to be undatable with the present two methods. More work is needed to discover exactly what other problems exist with the method. Trace element and organic analysis of samples coupled with a study of how each particular trace element and organic compound found to be in the natural calcite actually reacts with the various reagents when combined with pure calcite and processed as an ordinary sample would be, is the only way problems with the method will be solved. Table 3.1 gives a comparison between the results on roasted and unroasted samples.

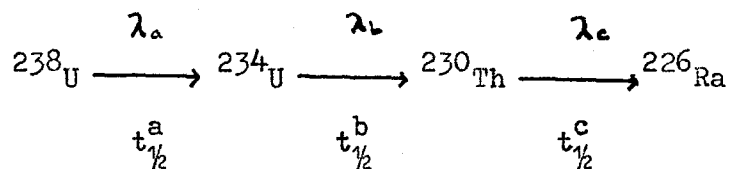


Table 3.1 Comparison of Roasted and Unroasted Results

Sample	Unroasted Yields (%) (U/Th)	Unroasted Results (Ka)	Roasted Yields (%) (U/Th)	Roasted Results (Ka)					
78GT1	0/0 5/0 7/80	- - 41 ± 4	7/41	98 ± 33 61 ± 15	78MG2	4/7 2/9 0/5	87 ± 65 - -	68/60	350
78GT3	0/0 1/9	- -	39/76	118 ± 8	78MG6	0/28 0/32	- -	17/24 40/64	122 ± 150 350
78GT4	0/5 0/4	- -	0/16	-	78MG4	0/1 0/4	- -	48/57	350
78GT5	2/12 15/37	- 14 ± 3	48/50	129 ± 31	78MG8	5/1 0/11 3/1	- - -	21/10 40/57	171 ± 17 39 ± 4
78AV1A	1/28 1/23	- -	1/28	-	78MG11	1/45 36/37 0/9 12/35 14/32	- 228 ± 121 - 202 ± 76 350	26/55	350
78AV1C	41/16 4/12	350 350	35/14 16/31 4/31 3/65	46 ± 19 350 114 ± 59 58 ± 41	78MG12	13/3 30/13 28/9	156 ± 109 350 273 ± 71	47/60	214 ± 26
78AV1B	9/0 1/8 1/29 1/24	- - - -	13/46 0/36 0/40	50 ± 8	78MG14	9/5	350	41/53	123 ± 23
78AV2	13/3 6/8	350 350	48/28	350	77PA5	6/19	37 ± 9	1/1	-
78AV3	20/7 27/4 2/37 2/27 13/36	219 ± 50 210 ± 128 - - 82 ± 19	47/44	350	77PA10	0/2	-	2/65	-
78AV5	8/0 2/13 9/56 1/43 1/8 1/8	- - 151 ± 43 - -	22/33	103 ± 69	77PA12	6/12	350	6/42	173 ± 61
78AV6	8/48 2/22	111 ± 23 -	36/11	63 ± 8	77PA13	0/2	-	22/1 23/36	- 103 ± 28
78AV8	2/9 1/4	- -	53/75	245 ± 90	77PA14A	40/63	350	28/40	350
78AV10	4/5 1/5	- -	6/30 0/0	22 ± 7	77PA14C	2/15	-	8/3	-
78AV11	14/1	-	74/26	350	77PA16B	15/14	75 ± 44	18/66	350
78AV12	11/66 0/6	187 ± 150 -	21/38	95 ± 14	77PA16A	13/10	236 ± 109	4/2	-
					77PA19	0/6	-	0/55	-
					77PA20	1/3	-	7/36 0/0	50 ± 13 -

### 3.2 Computing the Uranium-Thorium Relationship

After both the uranium and thorium from a sample have been counted on the  $\alpha$  counters for two days, or until the integrated "spike" peak is approximately 10,000 counts, the peaks of interest on both spectra,  $^{238}\text{U}$ ,  $^{234}\text{U}$ ,  $^{232}\text{U}$ ,  $^{232}\text{Th}$ ,  $^{230}\text{Th}$ , and  $^{228}\text{Th}$ , are integrated, and corrected for tail overlap, if necessary. In order to calculate an age for the sample from these data, it is necessary to understand the relationship between the various isotopes present and time. Let us consider the sequential decay of  $^{238}\text{U}$  to  $^{234}\text{U}$  to  $^{230}\text{Th}$ , assuming that there is no initial  $^{230}\text{Th}$  present in the sample,



where  $t_{1/2}^a$  = the halflife of  $^{238}\text{U}$ ,  $4.5 \times 10^9$  years

$t_{1/2}^b$  = the halflife of  $^{234}\text{U}$ ,  $2.47 \times 10^5$  years

$t_{1/2}^c$  = the halflife of  $^{230}\text{Th}$ ,  $7.42 \times 10^4$  years

Let  $N_a^0$  = the number of  $^{238}\text{U}$  atoms at time  $t = 0$

$N_b^0$  = the number of  $^{234}\text{U}$  atoms at time  $t = 0$

$N_c^0$  = the number of  $^{230}\text{Th}$  atoms at time  $t = 0$

$N_a$  = the number of  $^{238}\text{U}$  atoms at time  $t$

$N_b$  = the number of  $^{234}\text{U}$  atoms at time  $t$

$N_c$  = the number of  $^{230}\text{Th}$  atoms at time  $t$

then

$$\frac{dN_a}{dt} = -\lambda_a N_a \quad (3.1)$$

$$\frac{dN_b}{dt} = -\lambda_b N_b + \lambda_a N_a \quad (3.2)$$

$$\frac{dN_c}{dt} = -\lambda_c N_c + \lambda_b N_b \quad (3.3)$$

where

$$\lambda_a = \frac{\ln 2}{t_{\frac{1}{2}}^a}$$

$$\lambda_b = \frac{\ln 2}{t_{\frac{1}{2}}^b}$$

$$\lambda_c = \frac{\ln 2}{t_{\frac{1}{2}}^c}$$

Solving Equation 3.1 gives

$$N_a = N_a^0 e^{-\lambda_a t} \quad (3.4)$$

Substituting in Equation 3.2 for  $N_a$

$$\frac{dN_b}{dt} = -\lambda_b N_b + \lambda_a (N_a^0 e^{-\lambda_a t}) \quad (3.5)$$

Multiplying Equation 3.5 by  $e^{\lambda_b t}$  and rearranging

$$e^{+\lambda_b t} \left( \frac{dN_b}{dt} + \lambda_b N_b \right) = \lambda_a N_a^0 e^{-\lambda_a t + \lambda_b t} \quad (3.6)$$

Rearranging

$$\frac{d(N_b e^{\lambda_b t})}{dt} = \lambda_a N_a^0 e^{-(\lambda_a t - \lambda_b t)} \quad (3.7)$$

Integrating

$$N_b e^{\lambda_b t} = \frac{\lambda_a}{\lambda_b - \lambda_a} N_a^0 e^{-(\lambda_a - \lambda_b)t} + K \quad (3.8)$$

where

$$K = N_b^0 - N_a^0 \frac{\lambda_a}{\lambda_b - \lambda_a}$$

Multiplying Equation 3.8 by  $e^{-\lambda_b t}$

$$N_b = \frac{\lambda_a}{\lambda_b - \lambda_a} N_a^0 (e^{-\lambda_a t} - e^{-\lambda_b t}) + N_b^0 e^{-\lambda_b t} \quad (3.9)$$

Since the radioactivity is proportional to the derivative of  $N$  with respect to time,  $A \propto \frac{dN}{dt} \propto \lambda N$ , and at  $t < 10^6$  years,  $e^{-\lambda_a t} \approx 1$ , and  $\lambda_b - \lambda_a \approx \lambda_b$ , then Equation 3.9 becomes with rearrangement

$$\lambda_b N_b = \lambda_a N_a^0 (1 - e^{-\lambda_b t}) + \lambda_b N_b^0 e^{-\lambda_b t} \quad (3.10)$$

Rearranging further

$$\frac{\lambda_b N_b}{\lambda_a N_a^0} = \left( \frac{\lambda_b N_b^0}{\lambda_a N_a^0} - 1 \right) e^{-\lambda_b t} + 1 \quad (3.11)$$

where  $\frac{\lambda_b N_b}{\lambda_a N_a^0}$  = the activity ratio of  $^{234}\text{U} : ^{238}\text{U}$  at time  $t$

$\frac{\lambda_b N_b^0}{\lambda_a N_a^0}$  = the activity ratio of  $^{234}\text{U} : ^{238}\text{U}$  at time  $t = 0$

Substituting Equation 3.3 into 3.10

$$\frac{dN_c}{dt} + \lambda_c N_c = \lambda_a N_a^0 (1 - e^{-\lambda_b t}) + \lambda_b N_b^0 e^{-\lambda_b t} \quad (3.12)$$

Multiplying Equation 3.12 by  $e^{\lambda_c t}$  and simplifying

$$\frac{d(N_c e^{\lambda_c t})}{dt} = \lambda_a N_a^0 (e^{\lambda_c t} - e^{-(\lambda_b - \lambda_c)t}) + \lambda_b N_b^0 e^{-(\lambda_b - \lambda_c)t} \quad (3.13)$$

Integrating

$$N_c e^{\lambda_c t} = \frac{\lambda_a N_a^0}{\lambda_c} e^{\lambda_c t} + \frac{\lambda_a N_a^0}{\lambda_b - \lambda_c} e^{-(\lambda_b - \lambda_c)t} - \frac{\lambda_b N_b^0}{\lambda_b - \lambda_c} e^{-(\lambda_b - \lambda_c)t} + K \quad (3.14)$$

where

$$K = -\frac{\lambda_a}{\lambda_c} N_a^0 - \frac{\lambda_a N_a^0 - \lambda_b N_b^0}{\lambda_b - \lambda_c}$$

Multiplying Equation 3.14 by  $e^{-\lambda_c t}$  and simplifying

$$N_c = \frac{\lambda_a}{\lambda_c} N_a^0 (1 - e^{-\lambda_c t}) + \frac{\lambda_a N_a^0 - \lambda_b N_b^0}{\lambda_b - \lambda_c} (e^{-\lambda_b t} - e^{-\lambda_c t}) \quad (3.15)$$

Rearranging

$$\lambda_c N_c = \lambda_a N_a^0 \left\{ (1 - e^{-\lambda_c t}) + \frac{\lambda_c}{\lambda_b - \lambda_c} (e^{-\lambda_b t} - e^{-\lambda_c t}) \left( 1 - \frac{\lambda_b N_b^0}{\lambda_a N_a^0} \right) \right\} \quad (3.16)$$

From Equation 3.10

$$1 - \frac{\lambda_b N_b^0}{\lambda_a N_a^0} = \left(1 - \frac{\lambda_b N_b}{\lambda_a N_a}\right) e^{-\lambda_a t}$$

Substituting the above in Equation 3.16 gives

$$\frac{\lambda_c N_c}{\lambda_a N_a^0} = (1 - e^{-\lambda_c t}) + \frac{\lambda_c}{\lambda_b - \lambda_c} (1 - e^{-(\lambda_c - \lambda_b)t}) \left( \frac{\lambda_b N_b}{\lambda_a N_a^0} - 1 \right) \quad (3.17)$$

Since the radioactivity is proportional to the derivative of  $N$  with respect to time,  $A \propto \frac{dN}{dt} \propto \lambda N$ , and at time  $t < 10^6$  years,

$\frac{N_a}{N_a^0} \approx 1$ , then

$\frac{\lambda_c N_c}{\lambda_a N_a^0}$  = the activity ratio of  $^{230}\text{Th}$ : $^{238}\text{U}$  at time  $t$

$\frac{\lambda_b N_b}{\lambda_a N_a^0}$  = the activity ratio of  $^{234}\text{U}$ : $^{238}\text{U}$  at time  $t$

Since  $\lambda_a$  = the decay constant of  $^{238}\text{U}$

$\lambda_b$  = the decay constant of  $^{234}\text{U}$

$\lambda_c$  = the decay constant of  $^{230}\text{Th}$

then Equation 3.17 becomes

$$\frac{^{230}\text{Th}}{^{238}\text{U}} = (1 - e^{-\lambda_{230}t}) - \frac{\lambda_{230}}{\lambda_{230} - \lambda_{234}} (1 - e^{-(\lambda_{230} - \lambda_{234})t}) \left(1 - \frac{^{234}\text{U}}{^{238}\text{U}}\right)$$

Multiplying Equation 3.18 by  $\frac{238_{\text{U}}}{234_{\text{U}}}$

$$\frac{230_{\text{Th}}}{234_{\text{U}}} = \frac{234_{\text{U}}}{238_{\text{U}}} (1 - e^{-\lambda_{230}t}) + \frac{\lambda_{230}}{\lambda_{230} - \lambda_{234}} (1 - e^{-(\lambda_{230} - \lambda_{234})t}) \left(1 - \frac{238_{\text{U}}}{234_{\text{U}}}\right) \quad (3.19)$$

Hence the relationship between the various isotopes and time is Equation 3.19 assuming there is no nonradiogenic thorium present (Thompson 1973). If nonradiogenic thorium occurs, a correction factor must be introduced to compensate for the original thorium. To derive this, let us assume the same decay series, and further let

${}^{230}_{\text{r}}\text{Th}$  = the number of radiogenic thorium-230 atoms at time  $t$

${}^{230}_{\xi}\text{Th}$  = the number of all thorium-230 atoms at time  $t$

${}^{232}\text{Th}$  = the number of thorium-232 atoms at time  $t$

${}^{232}_{\circ}\text{Th}$  = the number of thorium-232 atoms at time  $t = 0$

${}^{230}_{\circ}\text{Th}$  = the number of thorium-230 atoms at time  $t = 0$ ,

or the number of nonradiogenic thorium-230 atoms

$\lambda_{230}$  = the decay constant of thorium-230

Therefore

$${}^{230}_{\text{r}}\text{Th} = {}^{230}_{\xi}\text{Th} - {}^{230}_{\circ}\text{Th} \quad (3.20)$$

and from Equation 3.1

$$\frac{{}^{230}\text{Th}_o}{{}^{232}\text{Th}_o} = \frac{{}^{230}\text{Th}_o}{{}^{232}\text{Th}_o} {}^{232}\text{Th} e^{-\lambda_{230}t} \quad (3.21)$$

Therefore

$$\frac{{}^{230}\text{Th}_r}{{}^{232}\text{Th}_r} = \frac{{}^{230}\text{Th}_o}{{}^{232}\text{Th}_o} - \frac{{}^{230}\text{Th}_o}{{}^{232}\text{Th}_o} {}^{232}\text{Th} e^{-\lambda_{230}t} \quad (3.22)$$

where  $\frac{{}^{230}\text{Th}_o}{{}^{232}\text{Th}_o}$  = the equilibrium activity ratio of  ${}^{230}\text{Th} : {}^{232}\text{Th}, \text{THR}$

Substituting Equation 3.22 into Equation 3.19 gives the equation for the correction

$$\frac{{}^{230}\text{Th}}{{}^{234}\text{U}} = \text{THR} \frac{{}^{232}\text{Th}}{{}^{234}\text{U}} e^{-230t} + \frac{{}^{234}\text{U}}{238\text{U}} (1 - e^{-230t}) + \frac{\lambda_{230}}{\lambda_{230} - \lambda_{234}} \times (1 - e^{-(230t - 234t)}) \left(1 - \frac{238\text{U}}{234\text{U}}\right) \quad (3.23)$$

There is no solution to either Equation 3.19 or equation 3.23, because both are transcendental. Therefore, a solution must be derived by either iteration using a computer, or graphic techniques. Figure 2.8 shows the relationship between the  ${}^{234}\text{U}/{}^{238}\text{U}$  and  ${}^{230}\text{Th}/{}^{234}\text{U}$  ratios over time. Using this graph, a graphic solution for the age can be determined, assuming there were insignificant amounts of detrital  ${}^{232}\text{Th}$ . If  ${}^{232}\text{Th}$  was present, the solution must be derived from iteration. When the date is computed by the dating program, the age will be corrected for  ${}^{232}\text{Th}$  if the  ${}^{230}\text{Th}/{}^{232}\text{Th}$



ratio is less than 25. Although this choice is somewhat arbitrary, for ratios greater than 25, the age is changed by less than its associated 1 $\sigma$  error. Below 25, the correction can become very large, particularly if the amount of uranium in the sample is small.

The error,  $\sigma$ , mentioned above is computed from Poisson statistics, i.e.  $\sigma = \sqrt{N}$ , where  $N$  is the number of counts; therefore, the larger the number of counts the smaller the error. The errors in the activity ratios are calculated from the count rate and the counting time for both the sample disc and a blank disc (background measurement). These errors are then used to calculate the upper and lower limits for the age in Equation 3.19 or 3.23. The upper error for the age is always slightly larger than the lower error, because the decay is exponential, not linear,

### 3.3 Calibration of the Method

In order to ensure the accuracy of the method, it is necessary to calibrate the equipment regularly. Because radioactive contamination is always possible, even when the utmost care is taken, analytical checks are also required.

Approximately once a month, a blank disc, i.e. one which has had neither uranium nor thorium plated on it, is counted on each of the  $\alpha$  counters for the normal counting period. Counting this disc gives an approximation of the background radiation on the detector which would be recording during any normal counting procedure in addition to that of the uranium- or thorium-bearing disc. background radiation is the result of stray recoiled nuclei

which have stuck to the detector and the housing chamber during normal counting. This amount, termed the "background", varies with the age of the detector, from as low as 0.01 for a new detector up to 0.1 counts/minute/35-channel-peak for a detector almost ready for retirement. For each of the isotope peaks, then, the background is subtracted to reflect the true count rates before any further calculations are performed.

Every six months to a year, a standard speleothem of known age is analyzed. Since this speleothem has been dated by the uranium-thorium method several times, and perhaps by other methods as well, this procedure acts as an indicator of the accuracy with which any given analyst is working.

Periodically a reagent blank is analyzed with and without spike to test for possible contamination. Although some contaminations from the reagents used is impossible to avoid, since all reagents contain minute traces of most elements including uranium and thorium, these analyses determine the level of contamination. The average level is then automatically subtracted from the isotopic count rates in the computer program.

All the numerical constants used in the calculations, such as the spike activity ratio and the counter calibration factor, are checked annually, unless it is suspected that there has been a change in these values. Under normal conditions, these are constants and will vary only if the spike's equilibrium or concentration has been changed, in the case of the spike constants, or if

the counter geometry has been changed, in the case of the counter-related constants. While the latter only affect the yields, a change in the spike constants can produce an erroneous age. If the spike activity ratio should change, the  $^{230}\text{Th}/^{234}\text{U}$  ratio will also change because

$$\frac{^{230}\text{Th}}{^{234}\text{U}} = \frac{^{230}\text{Th}}{^{228}\text{Th}} \times \frac{^{232}\text{U}}{^{234}\text{U}} \times \text{spike ratio} \quad (3.24)$$

A change of 10% in the spike ratio for a sample in the 250 Ka range could result in change of as much as 150 Ka in the age derived.

#### 3.4 The Application of the Method to Archeology

In order for an archeological site to be dated using the U/Th method, it must contain speleothem in stratigraphic context with the archeological material. Fortunately, since hominids invaded the northern latitudes, they have been predisposed to camp in caves, protected from the elements. Luckily, many of these caves contain speleothems.

Under ideal conditions, the artefacts are embedded in the calcite, ensuring the date obtained will be a minimum age for the artefacts. More frequently, however, the occupation levels are found interbedded with, or laterally related to the speleothem. Figure 3.5 shows several possible relationships between the speleothem and the artefacts. Planchers and stalagmites above or below the material may provide a post- or ante-quem date for the material. Pieces of stalagmites, stalactites and flowstone which are broken

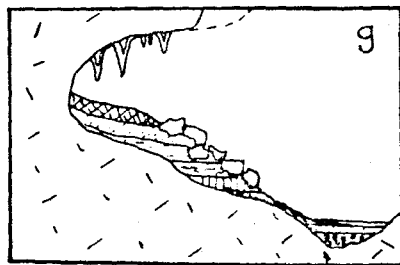
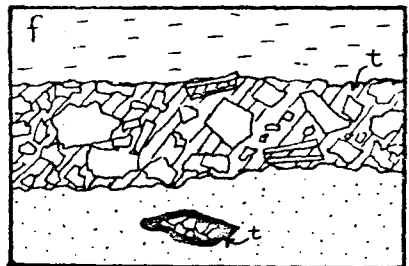
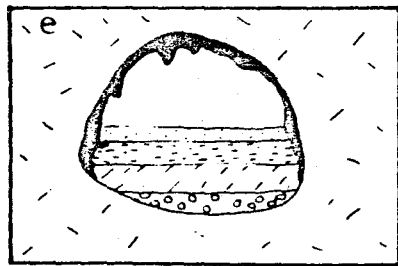
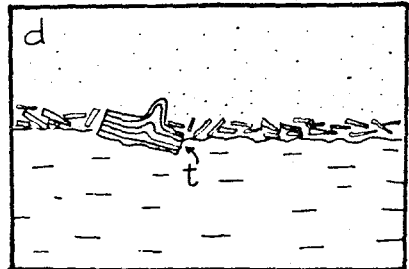
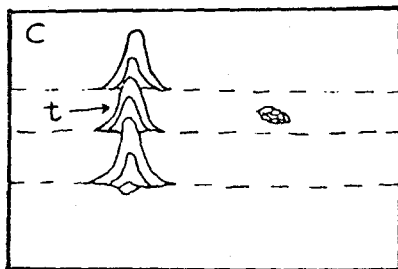
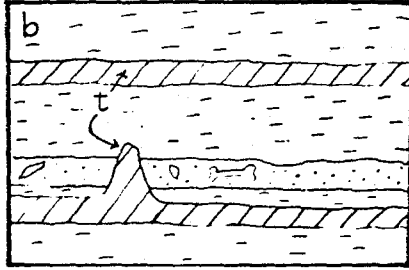
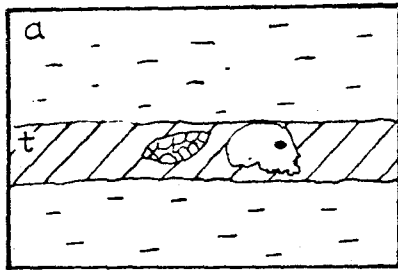
Figure 3.5

The relationship between travertine and sediments  
in archeological cave sites:

- a. Travertine enclosing artefacts or bones
- b. Artefacts intercalated with the travertine.
- c. Periodic deposition at one or more points  
on the cave floor.
- d. Broken fragments of travertine as coarse  
detritus in the sediment
- e. Wall and ceiling deposits or travertine  
partially interfingering with sediments
- f. Travertine filling interstices between coarse  
éboulis.
- g. Abri with collapse breccia from roof which may  
contain roof-deposited stalactites, etc.

t = travertine

(after Schwarcz, 1980).



in the sediment may provide a post-quem date. Soda straw stalactites will prove to be the most useful because they grew for so short a period before being broken off. Calcite concretions in the sediments, if not a result of water penetration, provide ante-quem dates for the sediments. Breccia, cemented calcite eboulis, may be datable if the cement can be separated from the allogenic component. The date would be an ante-quem date.

The speleothem collected for analysis must be of good quality, having undergone no secondary mineralization, particularly phosphatization. Nor should the calcite be near any phosphatic deposits, such as bone, since any phosphates present will cause problems with the method outlined in Chapter 3.1 (Ku, 1976). Also to be avoided is partially redissolved calcite, which may have had the uranium leached out. Finally the sample should be clean, i.e. free of detritus, and well crystalized, not the "chalky" or "muddy" deposits characteristic of cave entrances. Unfortunately, for sites of human occupation, such is rarely the state of any speleothem present. Because it is a human occupation site, phosphates will almost certainly be present, either in the form of bone, hydroxyapatite,  $\text{Ca}_3(\text{PO}_4)_2 \cdot \text{CaCO}_3$ , teeth, or other organically produced phosphates, along with large amounts of detritus, resulting from both the proximity of the occupation levels to the cave mouths, and human activity.

After removing the best sections possible for analysis, the speleothems are dated according to the method described in Chapter 3.1, unless previous analyses have indicated the method

may be unsuccessful, necessitating roasting the sample first as described in Chapter 3.1.1. Following counting of the sample, and computation of the data, including the age, chemical yields, various isotope ratios, and concentrations, a decision must be made as to the acceptability of the date. Figure 3.6 shows a typical computer printout. The age dating program is listed in the appendix, along with the program which averages dates for several samples from the same speleothem or plancher.

If the chemical yields are less than 10% for either uranium or thorium, the date obtained is suspect. Not only does the computed date have a large error associated with it, such low yields raise serious doubts about the veracity of the method under such conditions. In the archeological applications, however, yields are often low, as discussed above. Therefore, dates will be listed if the yields are less than 10% but must be regarded as highly questionable, until confirmed by other methods or better analyses. Furthermore, before any date is accepted as fact, the results must be consistent with other data obtained on the same or related material, in particular, the concentrations of uranium and thorium, the date, and the  $^{234}\text{U}/^{238}\text{U}$  activity ratio. Throughout any speleothem or plancher, these parameters should remain constant. In areas of active deposition, however, they may vary considerably, although for any one lamination, or growth horizon, they should not vary by more than one  $\sigma$ . Therefore, it is necessary to date one sample at least twice, or to date associated samples for confirmation. If, after several attempts,

Figure 3.6

A typical computer printout



SAMPLE 78MG9-3 , TR48A

DATE 7910.17

WEIGHT OF SAMPLE 78MG9-3 IS 38.6 G

SPIKE

VOLUME USED: U = 1.00 ML
SPIKE RATIO: U = 1.027
U-238 ACTIVITY: U = 22.7

DELAYS

FROM SEPARATION TO COUNTING OF THORIUM = 9. DAYS
FROM PLATING TO COUNTING OF THORIUM = 1904. MIN

COUNT TIMES AND COUNTER ACTIVITY OF 1 ML OF U-232 SPIKE

RAW DATA: U = 1402. MIN TH = 1253. MIN
BACKGROUND: U = 2317. MIN TH = 1417. MIN
ACTIVITY: U = 4.10 CPM TH = 5.00 CPM

\*\*\*\*\*

RAW DATA

U-238 = .541 CPM TH-232 = .090 CPM
U-234 = .576 CPM TH-230 = .943 CPM
U-232 = 1.369 CPM TH-228 = 2.249 CPM

BACKGROUND

U-238 = .004 CPM TH-232 = .048 CPM
U-234 = .005 CPM TH-230 = .054 CPM
U-232 = .049 CPM TH-228 = .073 CPM

CORRECTED DATA

U-238 = .535 .020 CPM TH-232 = .042 .010 CPM
U-234 = .557 .024 CPM TH-230 = .889 .028 CPM
U-232 = 1.320 .032 CPM TH-228 = 2.119 .042 CPM

URANIUM-238 CONCENTRATION = .24 PPM
THORIUM-232 CONCENTRATION = .04 PPM
CHEMICAL YIELD OF URANIUM = 32.20 PERCENT
CHEMICAL YIELD OF THORIUM = 41.26 PERCENT

ISOTOPE RATIO

U-234/U-238 = 1.042 ERROR .060
(U-234/U-238)0 = 1.071 .110
TH-230/U-234 = .837 .052
TH-230/TH-232 = 21.167 5.3

THORIUM AGE = 186600. + 39600. YEARS
- 29800.

AGE CALCULATED USING THORIUM CORRECTION
CORRECTED AT INITIAL THORIUM RATIO, R = 1.25000

UNCORRECTED = 191900. + 38200. YEARS
- 28400.

there is no agreement, then no age can be assigned.

After verifying the date statistically, correlations of the dates within the calcite body must be made, followed by correlation of these with the archeological material. Often, an entirely ridiculous age, which otherwise seems to be perfectly acceptable, must be abandoned at this juncture. For example, a date of 250,000 years for a plancher overlying Bronze Age materials would be ludicrous. On the other hand, some dates may require reinterpretations of the archeological precepts. What further correlations can be made at this juncture are entirely dependent upon the archeological material.

If there is sufficient material present, correlations between different sites, possibly even different regions may be possible. The entire process is diagrammed in Figure 3.7.

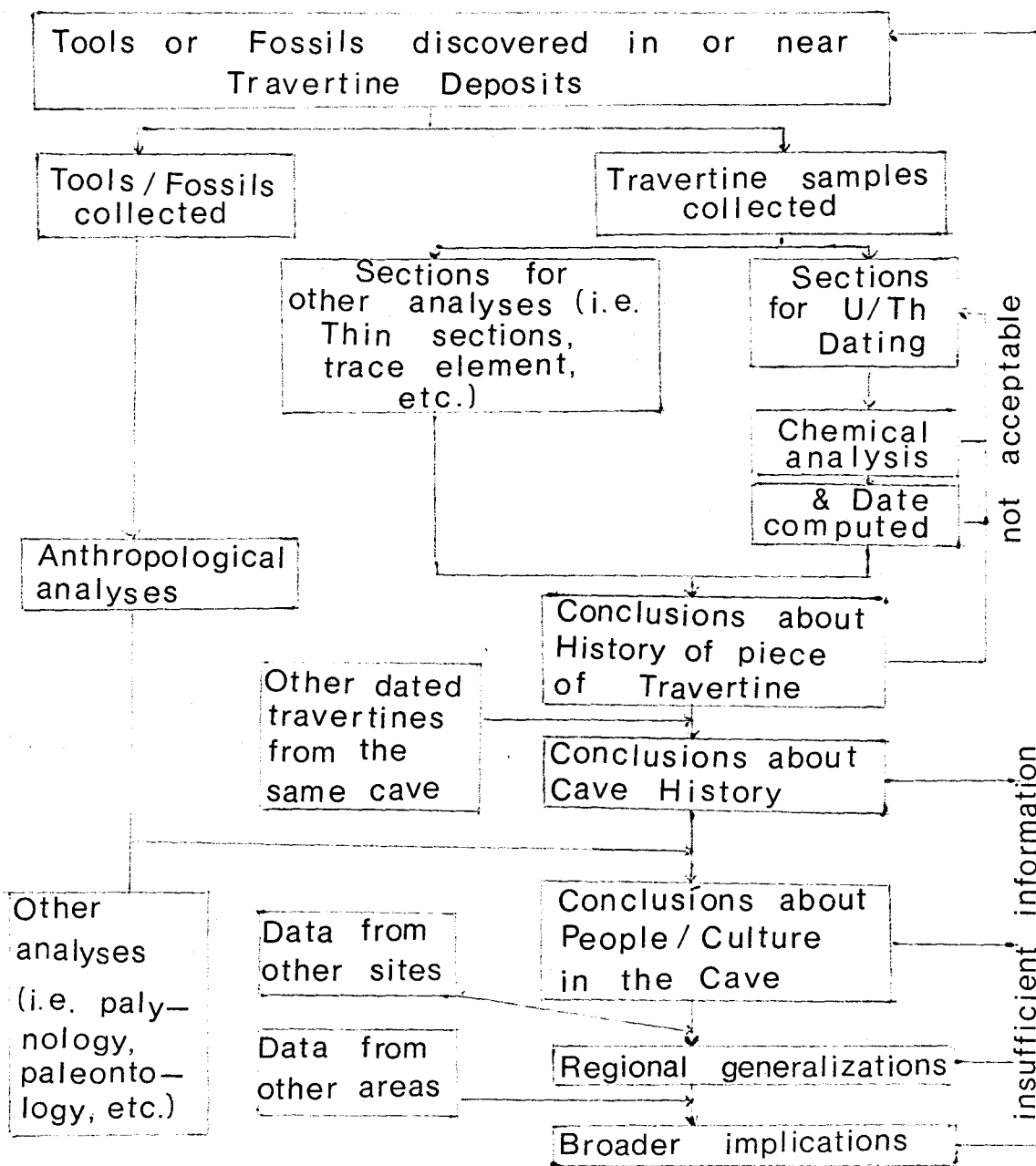
### 3.5 Limitations of the Method

In order to date actual samples, all of the radiometric dating methods require certain assumptions to be made, many of which assume, perhaps, too much when applied to the particular problems of archeological dating using the U/Th method. Some of the assumptions necessary are listed below.

1. The decay constants,  $\lambda_1$ , have not changed with time.
2. The system has been closed since deposition of the calcite, i.e. there has been neither addition or deletion of any uranium or thorium isotope or its daughters except due to radioactive decay.

Figure 3.7

A flowchart for the archeological application  
of U/Th dating



3. Uranium is present in sufficiently large amounts to make the method applicable with a short period of counting.
4. The initial  $^{230}\text{Th}/^{232}\text{Th}$  activity ratio, and hence the initial amount of nonradiogenic thorium, can be determined to allow the proper corrections to be made, if thorium was initially present in the calcite.
5. The time since deposition is less than 350 Ka.
6. Contamination of the sample by reagents, other samples, or other radiochemical impurities can be kept to a minimum.
7. The sample is pure, or almost pure, calcium carbonate, to ensure that proper chemical reactions can occur in the analysis.

There is one final assumption, which, although not integral to the method itself, is important when applying the method to archeological material.

8. The artefacts associated with the calcite are contemporaneous, or almost contemporaneous with the time of deposition.

While some of the above assumptions are easily verified, and therefore, present no problems with regard to the validity of the method as applied to archeological sites, others are less easily resolved.

The decay constant of any radioactive element depends, among other things, on the strength of the earth's gravitational field, which is proportional to the gravitational constant. If

this constant has varied with time, the equations given above must be altered to show the variable decay parameters. This, however, would affect all the radiometric methods.

If the concentration of uranium in the sample is greater than 1 ppm, then uncontaminated samples can be dated by the Pa/U method (Ku, 1976) to test for concordance of the dates obtained by the U/Th method. Contaminated samples, however, cannot be dated by Pa/U because the initial  $^{231}\text{Pa}$  activity can not be estimated like that of  $^{230}\text{Th}$ . Discordancy of the dates from the two methods, may indicate that the system has not been closed to radioisotopes. Thorium, however, is more immobile than protactinium; therefore, the U/Th date need not be incorrect. Unfortunately, the Pa/U method is limited to samples younger than 250 Ka. Similar concordancy tests for very young deposits can be made using  $^{14}\text{C}$ , although the travertine itself can not be dated by  $^{14}\text{C}$ , since its initial  $^{14}\text{C}$  activity is invariably less than modern atmospheric levels (see Chapter 4.6.1). Other indicators of open system behavior are:

1. Variation of the uranium concentration or  $^{234}\text{U}/^{238}\text{U}$  ratio within one layer.
2. A decrease in  $^{234}\text{U}$  correlated with the change in the concentration, due to preferential leaching of  $^{234}\text{U}$ . This can occur only in older calcites ( $t > 150$  Ka), where a significant number of the  $^{234}\text{U}$  atoms are in sites around which the crystal lattice has been damaged by  $\alpha$ -decay (i.e. the  $^{234}\text{U}$  is radiogenic, having decayed since the calcite was formed).

3. Gross variation in the  $^{230}\text{Th}/^{234}\text{U}$  ratio from layer to layer to layer, not correlated with the changes in  $^{230}\text{Th}/^{232}\text{Th}$ , which can not be attributed to changes in the age.
4. Visible changes in the crystal morphology as a result of secondary growth, recrystallization, or dissolution.
  - a. Secondary growth can be detected as small sparry crystals which grow radially into cavities and pores in the speleothem.
  - b. Recrystallization may be detected by the presence of relict grains or growth layers. These are marked by small linear inclusions of detritus, which surround the original grain, or are aligned along the original growth boundary (Kendall and Broughton, 1979).
  - c. Dissolution will produce rounded pores and possibly connected pores. Sharply angular pores are the product of normal speleothem growth.

None of these is a concern if the change occurred penecontemporaneously with the deposition of the speleothem. If, however, it occurred at some later time as the result of percolating solutions, the isotopes may have been mobilized.

Although none of these methods is perfect, the majority of open system behaviour should be detected using one or a combination.

Although it is rare for a speleothem not to contain some uranium, a preliminary chemical or neutron activation analysis will reveal if enough is present, at least 0.5 ppm, to allow a sufficiently short counting period.

In making the correction for initial nonradiogenic thorium, the initial ratio,  $^{230}\text{Th}/^{232}\text{Th}_i$ , must be assumed. Various authors have reported different values for this ratio, ranging from 0.5 to 1.7 (Thompson, 1974; Ku et al., 1979; Schwarcz et al., 1978; Schwarcz, 1979), but the most common ratio assumed is 1.5. In some instances where there have been sufficient analyses done for a given sample, or set of closely related samples, it is possible to plot the ratios of  $^{230}\text{Th}/^{234}\text{U}$  against  $^{232}\text{Th}/^{234}\text{U}$ , assuming the age to be constant, to produce the value of the initial  $^{230}\text{Th}/^{232}\text{Th}$  ratio, the slope of the line. This method could not be applied herein, because no sample had sufficient results.

Another method, proposed by Schwarcz (1979), assumes that only two components are present contributing isotopes to the sample, a detrital one, and a calcite one. Both components contribute all isotopes, except for  $^{232}\text{Th}$  which arises purely from the detrital component. Therefore,

$$i_c = k_d^w i_{d+} + (1 - k_d^w) i_c \quad (3.25)$$

where  $i$  = the isotope under consideration

$k$  = the number of the analysis

$C$  = the count rate (dpm/g)



$\Sigma$  = the total sample

$W$  = the weight fraction of either the detrital or  
or calcite component

$d$  = the detrital component

$c$  = the calcite component

From the assumption above,  $^{232}\text{C}_c = 0.0$  (3.26)

Therefore,  $k_d^W = \frac{^{232}\text{C}_\Sigma}{^{232}\text{C}_d}$  (3.27)

Substituting in Equation 3.25

$$\frac{i_{\text{C}_\Sigma}}{k_\Sigma} = i_a \frac{^{232}\text{C}_\Sigma}{k_\Sigma} + i_{\text{C}_c}, \quad i \neq 232$$

where  $a = \frac{i_{\text{C}_d} - i_{\text{C}_c}}{^{232}\text{C}_d}$

Plotting the values of the various count rates for the various isotopes in each analysis will result in a solution for  $i_{\text{C}_c}$ , following which the age can be computed as described in Chapter 3.2. The chemical method described in Chapter 3.1 does not liberate all the detrital isotopes from the detrital phase, as this correction must assume to have happened. Therefore, it was not applied herein.

If, in the calculation of the date, an age greater than 350,000 years is produced, the computer automatically rejects the date, although the lower age limit is computed, if it is less than 350,000 years. Should subsequent attempts give similar results, the sample is assigned the age ">350.0 ka".

Proper laboratory procedures, including cleaning all glassware with 9M HCl (aq), following prolonged immersion in a dilute aqua regia acid bath, in addition to using chemicals free from radioactive trace elements for preparation of stock solutions, should keep contamination to a minimum, as frequent reagent blank tests have shown to be the case.

The major problem encountered in the archeological samples is their impurity: many minerals, other than calcite, are present in the samples. With such samples, the problem of detrital thorium is compounded by the crystallographic behaviour of the contaminating minerals with regard to uranium and thorium. In particular, phosphates will cause serious difficulties with the chemical analysis, not to mention the theoretical problems of possible resolution, reprecipitation, etc, but phosphates, by the very nature of the study, are extremely likely within the sediments. Surficial detritus poses no great threat and is removed prior to the initial dissolution of the sample. Intercrystalline detritus, however, may be partially leached during the initial dissolution. Unfortunately, this is impossible to test. At present, intercrystalline detritus is collected by filtration, but is not analyzed in any manner, although many samples have totally lost either uranium or thorium or occasionally both, during the analysis, thereby resulting in no age being derivable for the sample. Presumably, the detritus is responsible for this loss. Roasting, as noted above did eliminate this problem for some samples.

When tools are embedded in a deposit, it is not absolute proof that the tools actually represent a cultural horizon. Included in the alternate possibilities for **their location are:**

1. transportation from its primary source by flood waters long after its original manufacture
2. human transportation through curiosity or secondary use by later cultural groups
3. transportation by slumping of the sediments into a puits or as a slump block (i.e. Montgaudier)
4. inclusion in an obviously older cultural level by human burial
5. disturbance of the sediments by cryo- or bioturbation

and many more. If the tool is not embedded in the actual deposit, but is found at what it is felt to be contemporaneous level elsewhere in the cave, often not traceable due to **poor** excavation techniques of **the past**, the argument for the applicability of the date becomes less convincing still. If, however, a complete occupation site is found in an **obviously uninterrupted depositional** sequence interbedded with speleothem deposits, as at Lachaise, the date should prove to be very accurate, providing the other seven conditions are met. Usually, this is not the case, as shown in Figure 53.5. Then the date may only be a post-quem or ante-quem estimate, as discussed above. If post-manufactural transport is apparent, then the date is that of the final movement which sets an upper limit on the date of their manufacture. Since few dating methods apply to the period, any date even one

with a large associated error, is better than none, given that the limitations of the application of the date are well known and understood by any who might subsequently use the date. Such is rarely the case among archeologists who often have a poor understanding of geochemistry.

## ARCHEOLOGICAL METHODS

Because there is no radiometric dating method, other than the U/Th method, which can be used in the French cave sites, archeologists have resorted to other methods in order to date the cave deposits. In France, where these methods are the most refined, an archeological investigation always includes a paleontologist, a palynologist, and a sedimentologist, in addition to the archeologists. With the data collected, these specialists attempt to reconstruct the paleoclimatology of the site, by studying the global granulometry, alteration and dissolution effects, porosity, concretions, pH, and calcimetry of the sediments, in addition to the pollen, faunal, and archeological analyses. After this is accomplished, relative dates are assigned using the climatic data.

#### 4.1 Sedimentology

Before the sedimentological analyses in the laboratory are begun, the stratigraphy must be carefully established using the criteria of colour, texture, sediment type, and sometimes the archeological contents. After the stratigraphy is defined, a diagram of the wall of the cut is profiled, carefully noting the position of the layers, the large éboulis, and the samples

for sedimentological and pollen analyses. Weighing from 500 grams to several kilograms, depending on the amount of éboulis contained therein, each sedimentological sample corresponds to at least one, if not several, pollen samples, all taken simultaneously. Figure 4.1 summarizes the sedimentological analysis.

#### 4.1.1 Global Granulometry

After removing the cobbles larger than 100 mm and the artefacts from the sediment sample, it is sieved into four fractions, sized 10 - 100 mm, 5 - 10 mm, 2 - 5 mm, and less than 2 mm. A global granulometry diagram for the section is then constructed by placing the cumulated weight percentages of each fraction on the abscissa and the position in the section on the ordinate. Usually, on this diagram, as shown in Figure 4.2, the two mid-range fractions are grouped together to form the fraction 2 - 10 mm.

In periods when frost action is a dominant climatic feature, the sediment will reflect this by containing a higher percentage of coarse elements detached from the roof and walls by the repeated freezing and thawing (Bordes, 1972).

#### 4.1.2 Element Separation

Both the large and medium fraction are separated by hand into five different types:

1. Calcareous elements: éboulis, calcite sand
2. Illuvial concretions
3. Pebbles with calcareous concretions
4. "P" concretions (wall concretions)

Figure 4.1

The analysis of cave sediments (translated from  
Debenath, 1974)

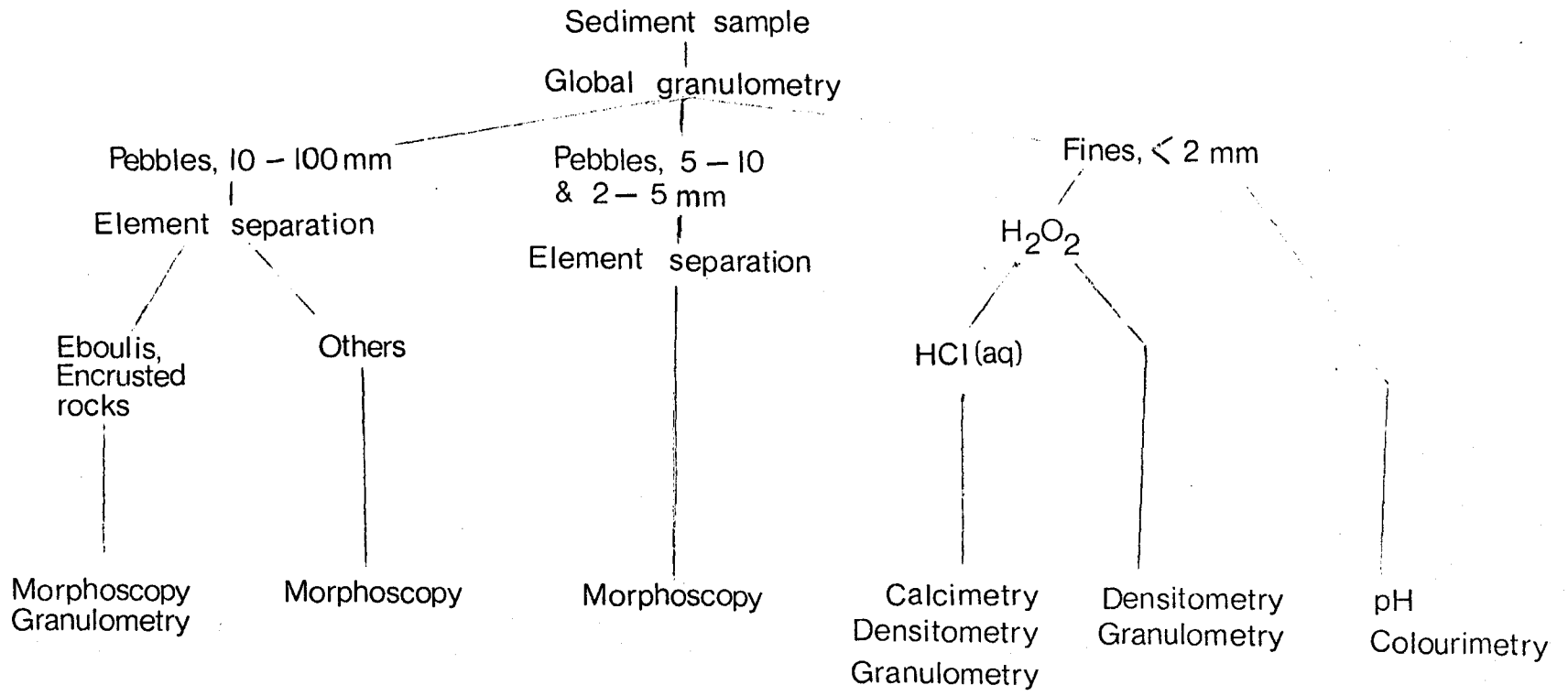
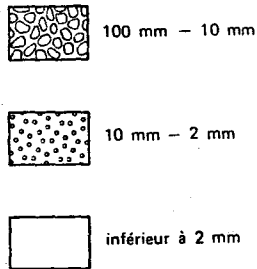




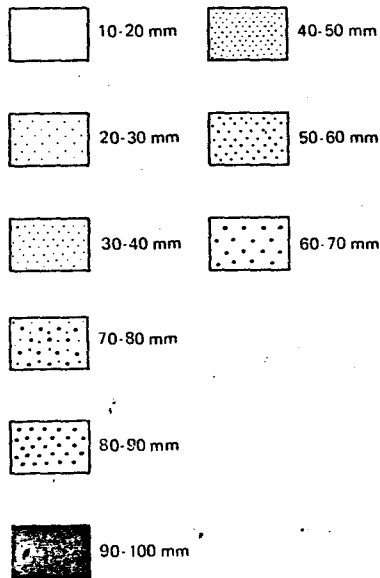
Figure 4.2

Granulometry of Poch de l'Azé I, upper levels:

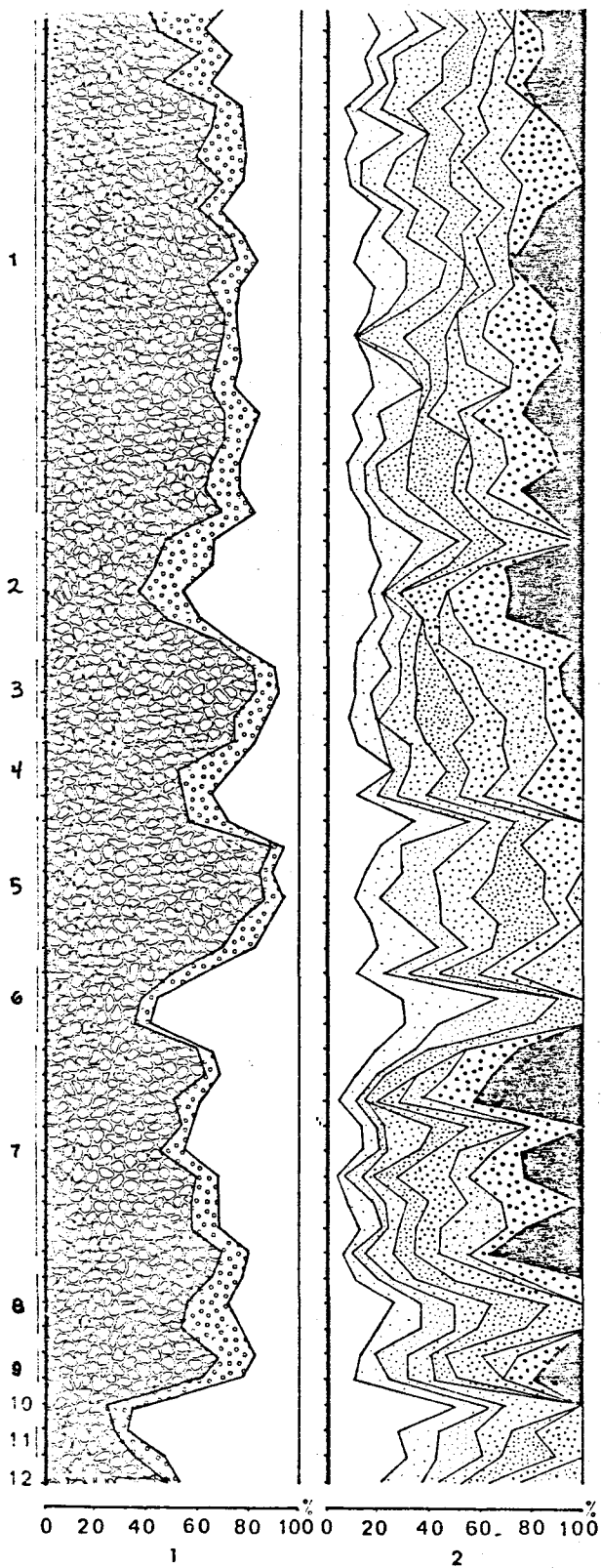
1. Global granulometry vs. depth in the section



2. Granulometry of the pebble fraction vs. depth in the section



(after Laville, 1975)



## 5. Other elements

As before, weight percentages of each type are compared with the weight of the total sample and the fraction under consideration in order to construct a graph similar to that constructed for the global granulometry above. The significance of these elements will be discussed below.

### 4.1.3 Granulometry of the Pebbles

All of the elements of types 1 to 4 above sized between 10 and 100 mm are divided into nine size classes according to the largest dimension, class 1 ranging 10 to 20 mm, and so on to class 9, 90 to 100 mm. As for the global granulometry, a cumulative graph is constructed, as shown in Figure 4.2. A higher percentage of the larger size classes implies more intensive frost action, as occurs during glacial maxima.

### 4.1.4 Morphoscopy

All the elements, except the fines, are analyzed morphoscopically to determine the importance of frost and humidity in the evolution of the sediments.

#### 4.1.4.1 The Effects of Frost

Plaquettes are frost-removed slabs, originally part of the wall rock, which have angular edges and one unweathered face, that was originally within the wall, as in Figure 4.3A. These are weighed and compared with the weight of the normal polyhedral éboulis. Although a higher percentage of plaquettes indicates intensive

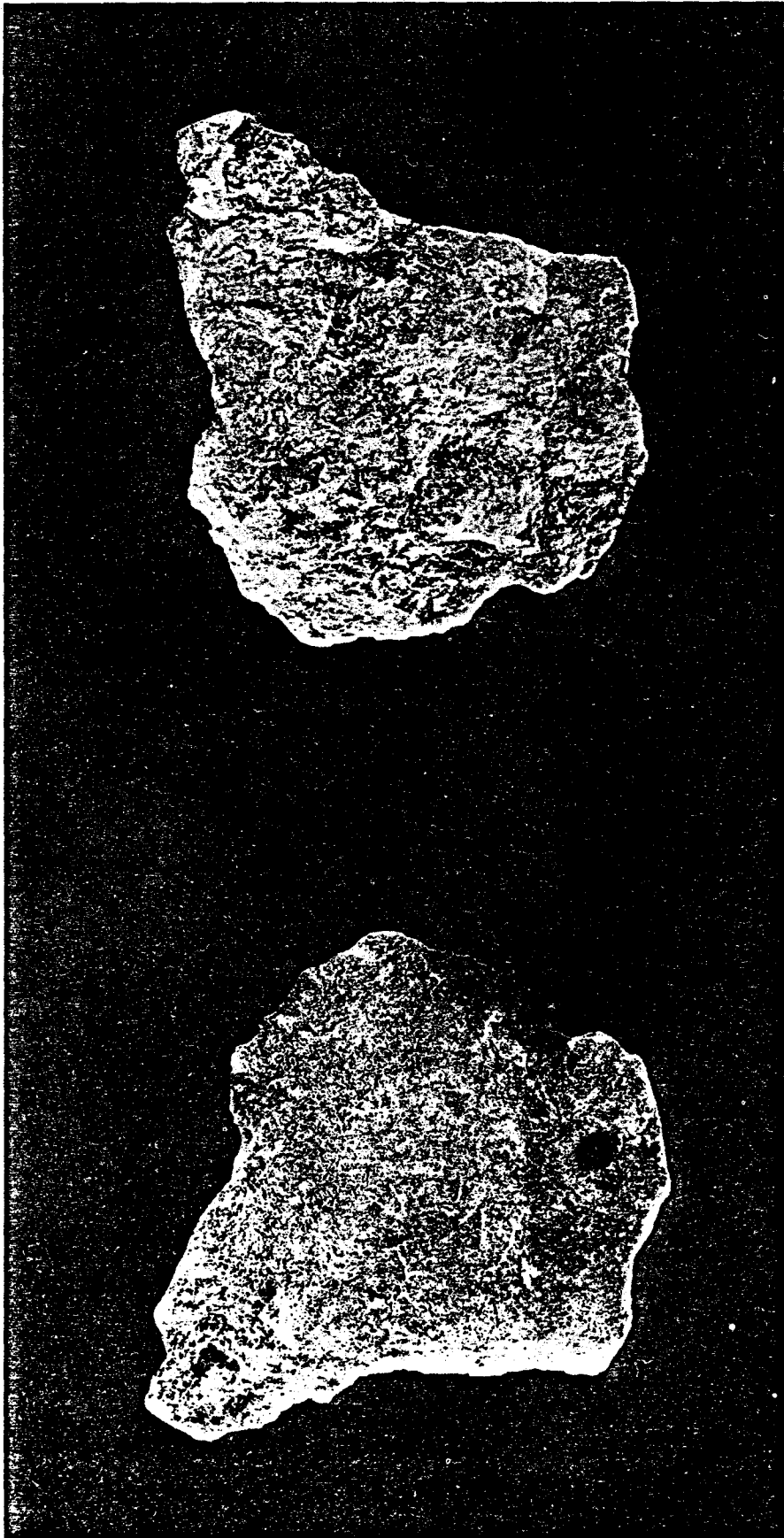
Figure 4.3

Plaquettes found in cave sediments:

- A. A plaquette showing the different faces:
  - 1. the face originally part of the interior of the wall
  - 2. the face originally forming part of the outside face of the wall
- B. Stalactites growing on a plaquette

(after Lavielle, 1975)

A



B

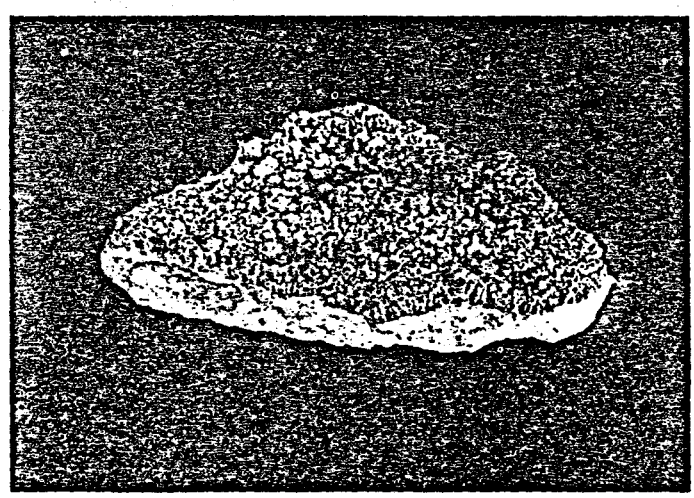
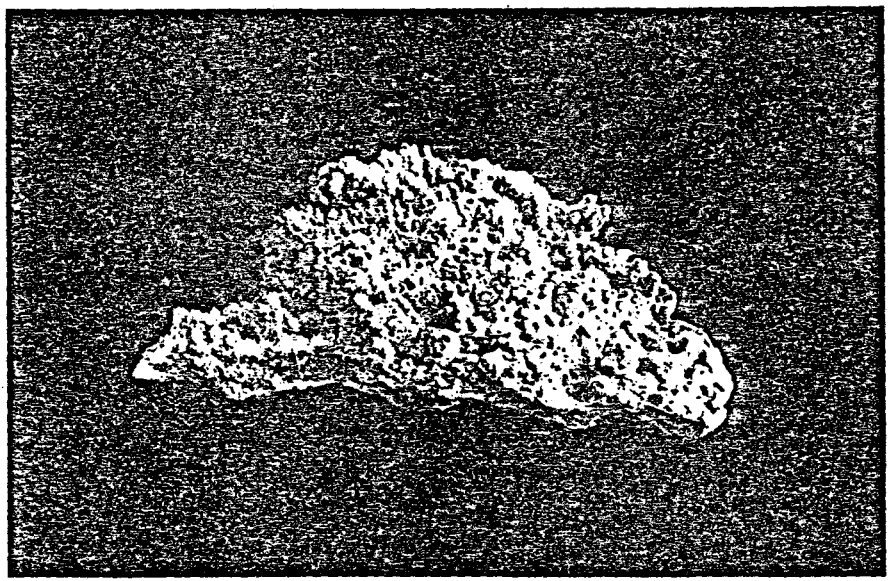
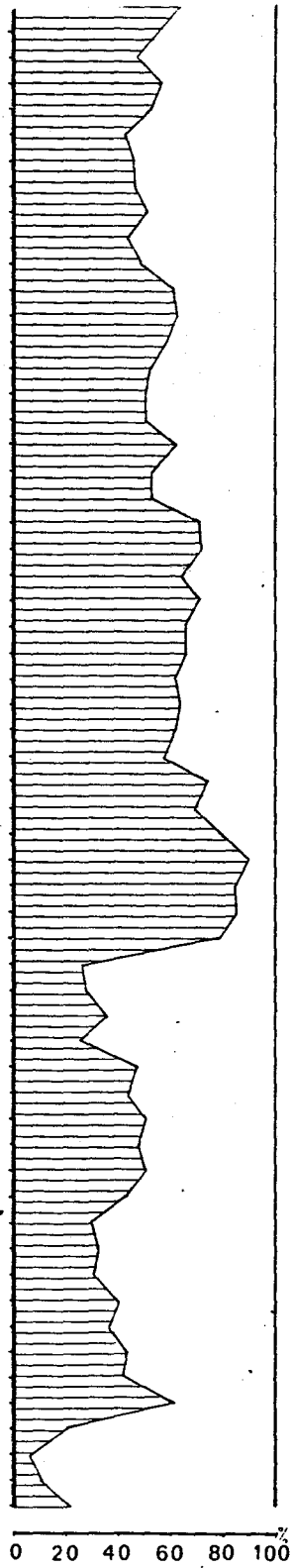


Figure 4.4

Percentage of plaquettes vs. Depth, Pech  
de l'Azé I, upper levels (after Laville,  
1975)





frost action, these may be modified by cryoturbation or altered chemically. Therefore, the sediments may appear to have been formed under mild conditions, rather than the harsh conditions (Bordes, 1972).

Frost-cracked and frost-fissured pebbles (Figure 4.5) form from frost action, resulting in a higher percentage of these types in sediments formed during colder periods (Bordes, 1972).

#### 4.1.4.2 The Effects of Humidity

Humidity in the cave can result in alteration of the elements, blunting of the edges, corrosion, or the formation of concretions on the pebbles.

To determine the degree of alteration which the sediments have undergone, the medium and large fractions are divided by hand into four groups:

1. Not altered
2. Slightly altered
3. Altered
4. Very altered

Each group is converted to a weight percentage of the total sediment size group under consideration, which is then used to calculate an alteration index, A.I., thus:

$$A = \text{Group 4} \times 1$$

$$B = \text{Group 3} \times \frac{1}{2}$$

$$C = \text{Group 2} \times \frac{1}{3}$$

$$D = \text{Group 1} \times 0$$

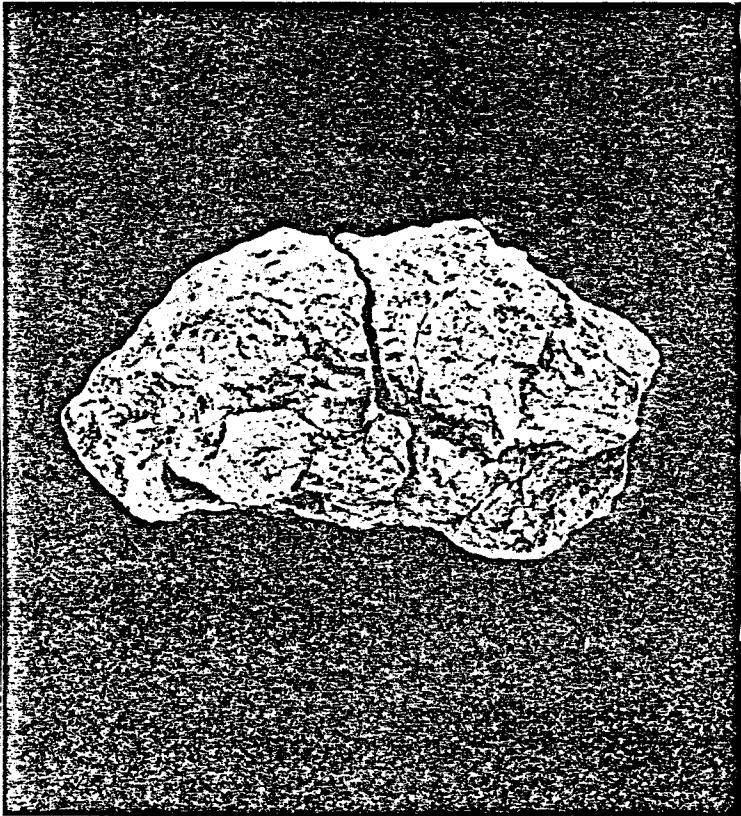
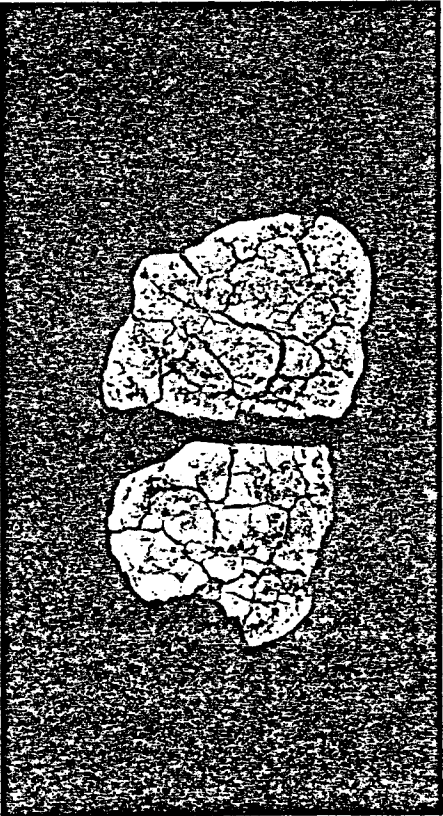
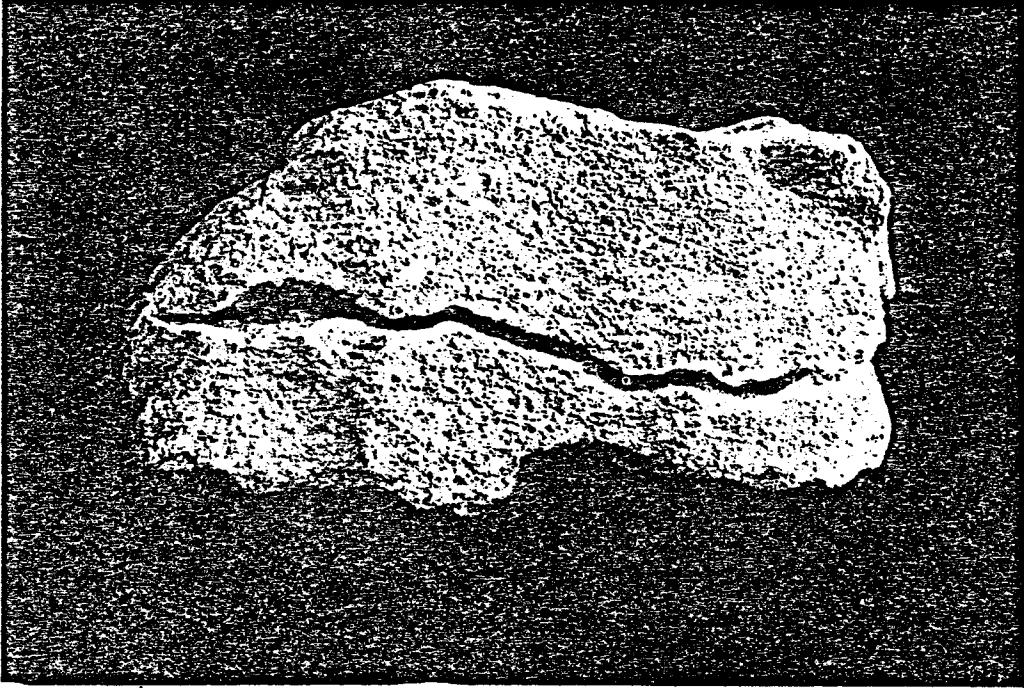
$$\text{A.I.} = A + B + C + D \quad (4.1)$$

Figure 4.5

Pebbles effected by frost action:

1. Frost cracked block, Pech de l'Azé  
I, couche 7 (2/3 natural size)
2. Frost cracked block, Combe-Cullier,  
couche 13, (2/3 natural size)
3. Frost fissured block, Flageolet II,  
couche V, (natural size)

(after Laville, 1975)



Varying from 0 to 100, the index indicates more humid conditions for the formation of the sediments if the index for those layers is relatively greater than for other layers.

Blunting of the pebble edges by humidity is determined in a similar manner to the alteration index above, with the sediments being grouped into the following groups:

1. Not blunted; all edges are fresh and sharp.
2. Slightly blunted; some edges are partially blunted or worn.
3. Blunted; all edges are worn but the original shape of the pebble is still discernable.
4. Very blunted; the pebble too rounded to allow recognition of the original shape.

Figure 4.6 shows the reference scale for these groups. Calculated using the same formula as that for the alteration index (4.1), the bluntness index, B.I. is difficult to interpret unless combined with the porosity measurements. Although both cryoturbation and humidity can cause an increase in the bluntness, only humidity will cause a concomitant increase in the porosity of the sediments.

In order to determine the porosity, a given standard weight of sediment is dried, weighed, and then placed in water for a standard time, usually one day, and reweighed. Porosity is defined as the difference in weight compared with the dry weight:

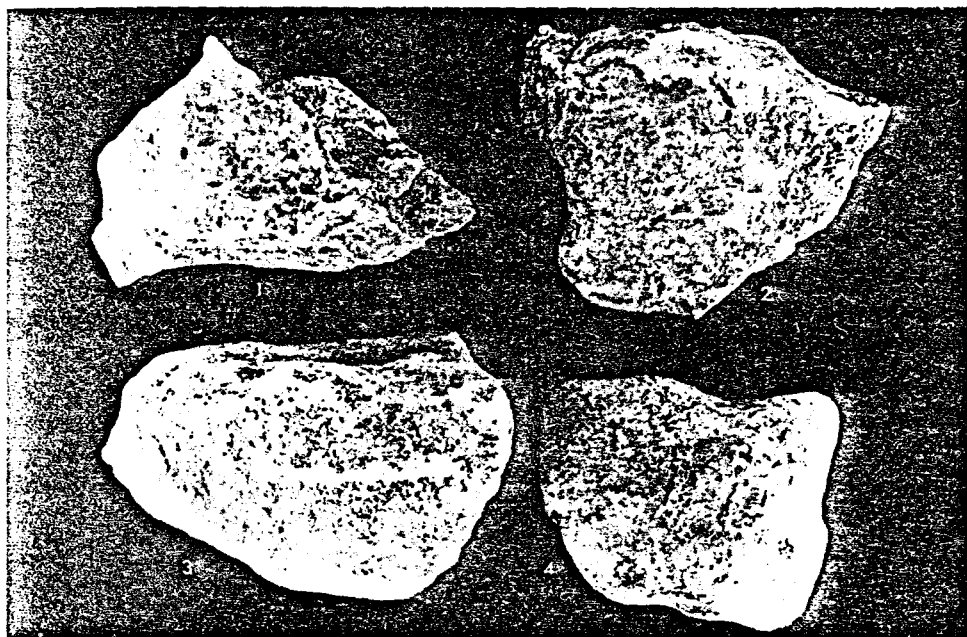
$$P = \frac{\Delta \text{ weight}}{\text{dry weight}} \quad (4.2)$$

Figure 4.6

The bluntness index references:

1. Not blunted
2. Slightly blunted
3. Blunted
4. Very blunted

(after Laville, 1975)



When both the porosity and the bluntness index are plotted vs. depth, as in Figure 4.7, parallel trends in the two indicate a damp climate for the formation of the sediment, while opposite trends indicate an increase in cryoturbation due to colder conditions (Debenath, 1974). Figure 4.8 shows pebbles blunted by both humidity and cryoturbation, in addition to corroded pebbles, those with pits, cavities, or alveoli on their surfaces.

When the cave is damp, "s" type, soil or illuvial concretions can be formed not in the uppermost layer, but in those at depth, where calcite is precipitated in cavities in the soil. Because some of the calcite was originally part of the walls that was dissolved by the dampness, these concretions are unsuitable for dating for several reasons:

1. They are not contemporaneous with the formation of the sediment, but post-date it.
2. Being formed within the soil, they may contain high concentrations of detrital thorium contaminants.
3. If sufficient water is moving through the soil, it may be transporting small bits of undissolved wallrock containing isotopes in equilibrium, thereby biasing any date obtained.

Soil breccias, common to many caves, form in this manner. Figure 4.9 shows different types of soil concretions, all easily distinguished from travertine deposits. Therefore, illuvial concretions in a layer, F, may be the result of a damp climate at the time of the

Figure 4.7

Effects of humidity on cave sediments

1. Bluntness index vs. Depth,  
pebbles 20 - 50 mm, Pech de l'Azé  
II, sector 1
2. Porosity vs. Depth, pebbles  
20 - 50 mm, Pech de l'Azé II,  
sector 1

(after Laville, 1975)



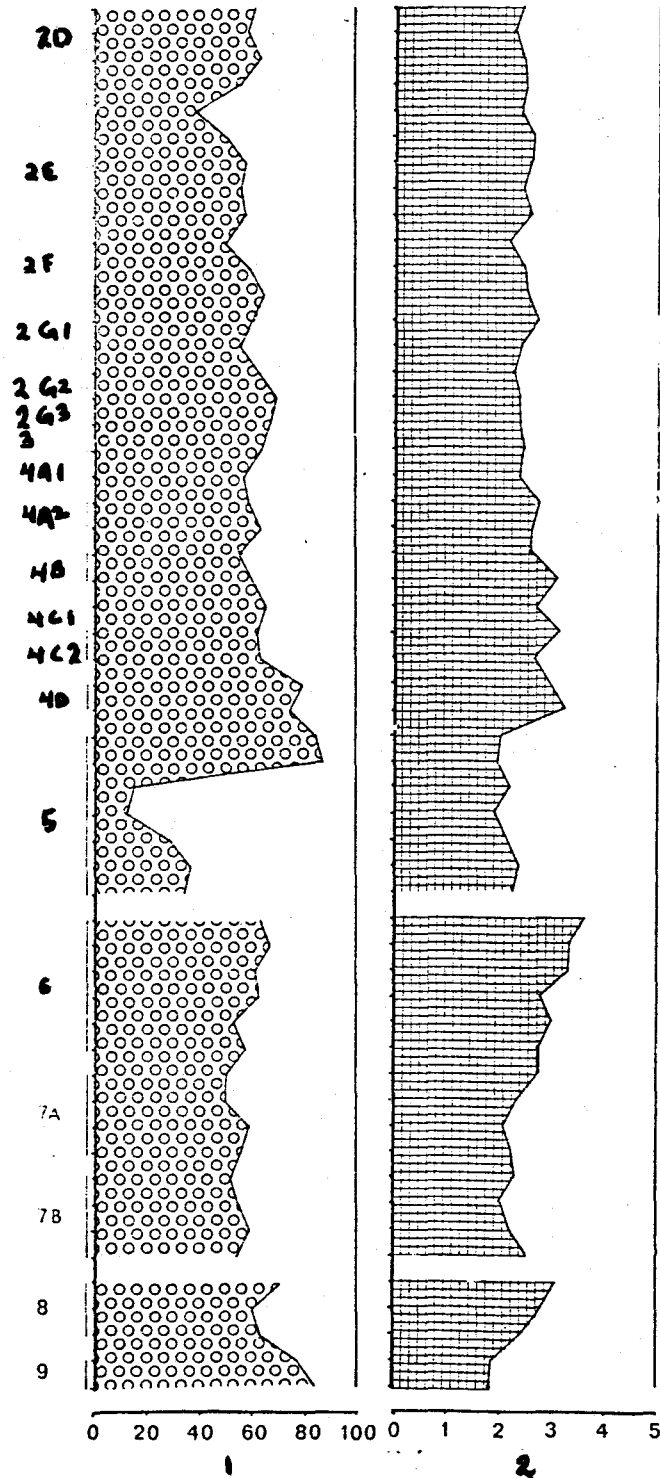
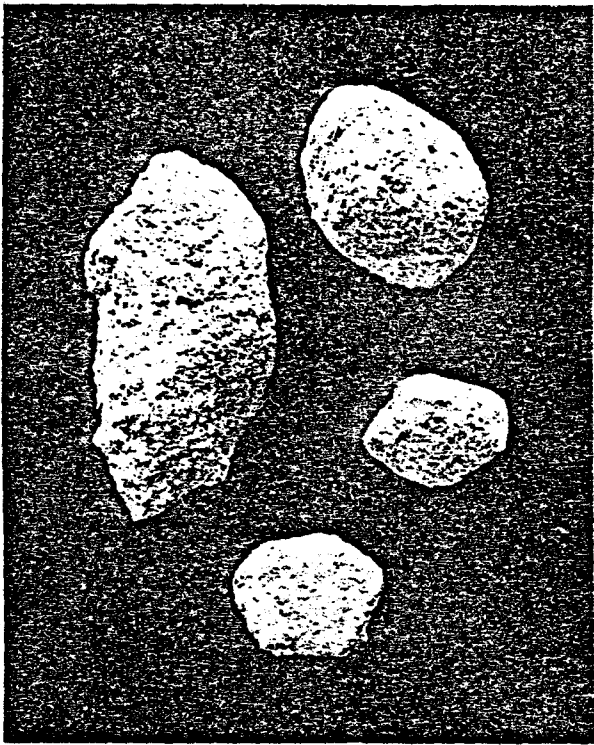


Figure 4.8

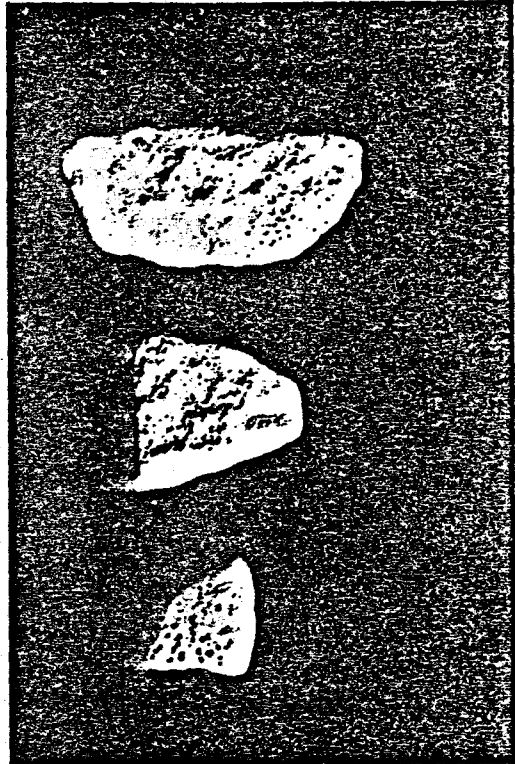
Pebbles affected by humidity and cryoturbation:

1. Pebbles blunted by dissolution,  
Pech de l'Azé II, couche 8, (2x  
natural size)
2. Pebbles blunted by cryoturbation,  
Combe-Grenal, couche 50, (natural  
size)
3. Pebbles broken by cryoturbation,  
showing pseudo-retouch, thick alternate  
type, le Moustier, abri supérieur  
(natural size)
4. Corroded pebbles, Combe-Grenal, couche  
50A, (natural size)

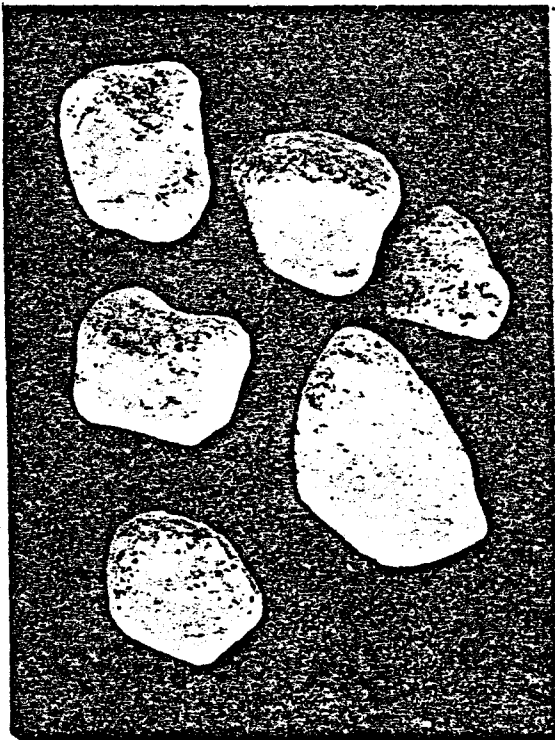
(after Laville, 1975)



1



2



3



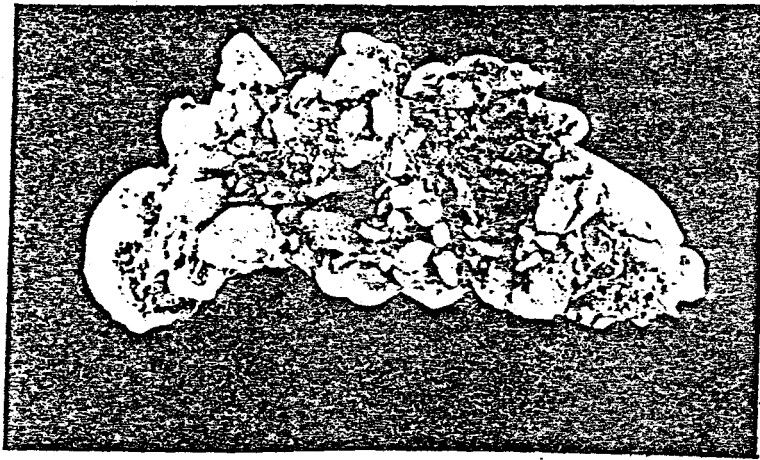
4

Figure 4.9

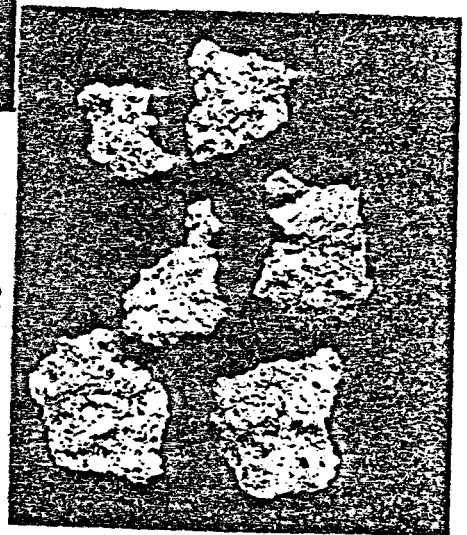
Illuvial concretions in cave sediments:

1. A pebble aggregate cemented with calcite, le Moustier, abri inferieur, couche D, (natural size)
2. Aggregates of gravel and sand cemented by calcite, Pech de l'Azé I, couche 11, (natural size)
3. Tubular concretions filling gaps in the sediments, Abri Caminade East (2x natural size)
4. "Cabbage Flowers", illuvial concretions, Combe-Cullier, couche 10 (natural size)

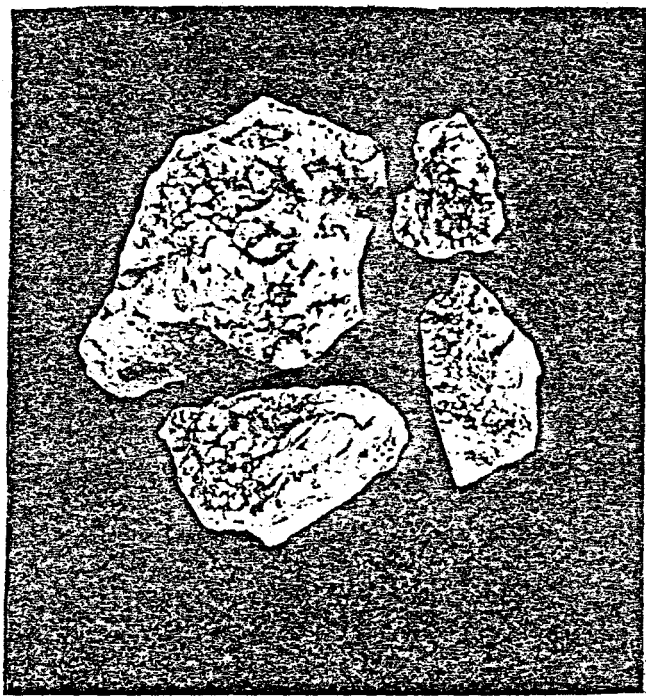
(after Laville, 1975)



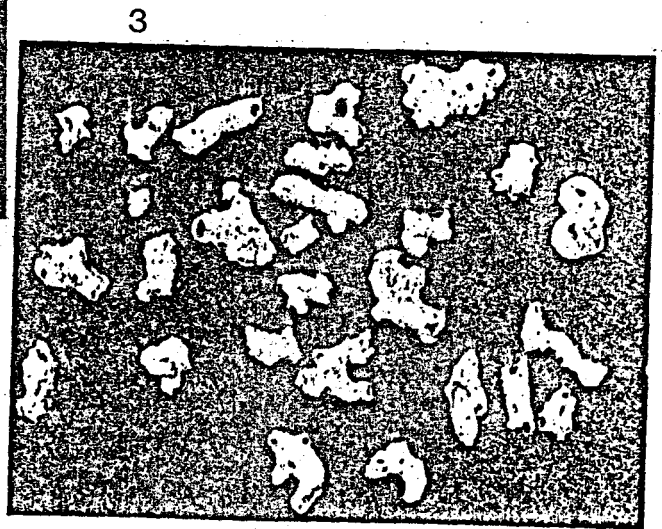
1



2



4



3

formation of couche C, three couches above, while when F was formed it was relatively dry.

"P" type, paroi or wall, concretions, on the other hand, are formed prior to the formation of the sediment in which they are found. Having formed on the walls, and ceiling of the cave, as stalactites for example, during damp periods, these will fall to the floor when frost occurs. Although this may occur penecontemporaneously, resulting in small concretions, including perhaps "soda straw" stalactites, more frequently, the concretions are much larger, often plaquettes, which predate the formation of the sediment. Therefore, wall concretions are also not suitable for use in U/Th dating, with the possible exception of "soda straws" (Schwarcz, pers. comm.), unless the purpose is only to establish a lower limit for the age of the sediment. Furthermore, wall concretions in the couche do not imply damp conditions at the time, but instead, relatively intense frost action. A stalagmitic plancher, however, does indicate a very damp period at the time of formation of the sediment: in fact, probably the floor was continually covered by a thin film of water.

#### 4.1.5 Fines Analysis

In order to determine the degree of weathering and the size distribution of the fines, this fraction is analyzed differently from the medium and large fractions. Before any other analysis is begun, all the organics in half the sample are destroyed by treatment with hot hydrogen peroxide,  $H_2O_2$ .

#### 4.1.5.1 Calcimetry

The difference in the weight of the fine fraction before and after treatment with cold hydrochloric acid, HCl (aq), equals weight of the calcite dissolved by the acid. As before, a comparison between several couches, as in Figure 4.10, reveals the degree of weathering which various couches have undergone, with the well-weathered layers having **relatively less** carbonate (Debenath, 1974).

#### 4.1.5.2 Granulometry and Densitometry

To determine the size distribution of the fines, both the decalcified and normal samples, the particles from 0.05 to 2 mm are sieved, while those less than 0.05 mm are sized by sedimentation techniques employing Stoke's Law. (See Blatt et al., 1980, 59-66, for an excellent discussion of the theory and methods involved.) From cumulative graphs, constructed as before (see Figure 4.11), weathered sediments are conspicuous, because both graphs will appear similar, whereas unweathered sediments show different size distributions (Debenath, 1974).

#### 4.1.5.3 pH of the Fines

After a sample of the fines has sat in distilled water for 24 hours, the pH is measured, while another sample, having sat in normal potassium chloride, KCl, for 24 hours also has its pH measured. The former measurement is referred to as the pH of the sediment, while the latter is called the  $\Delta$  pH, shown in Figure 4.10.

Figure 4.10

Analysis of the fines:

1. Calcimetry of the fines vs. Depth,  
Pech de l'Azé II, sector 2
2.  $\Delta$ pH vs. Depth, Pech de l'Azé II,  
sector 2

(after Laville, 1975)



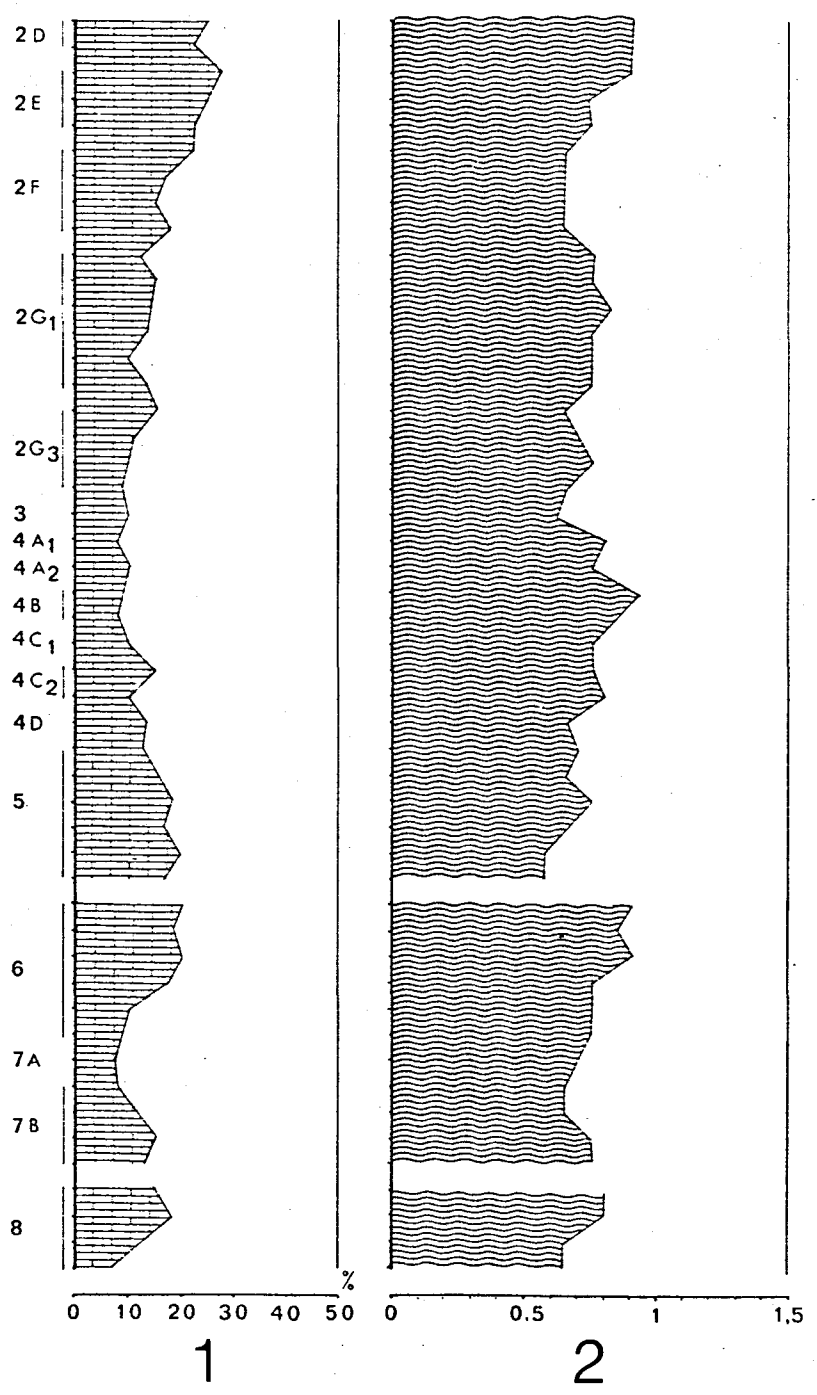
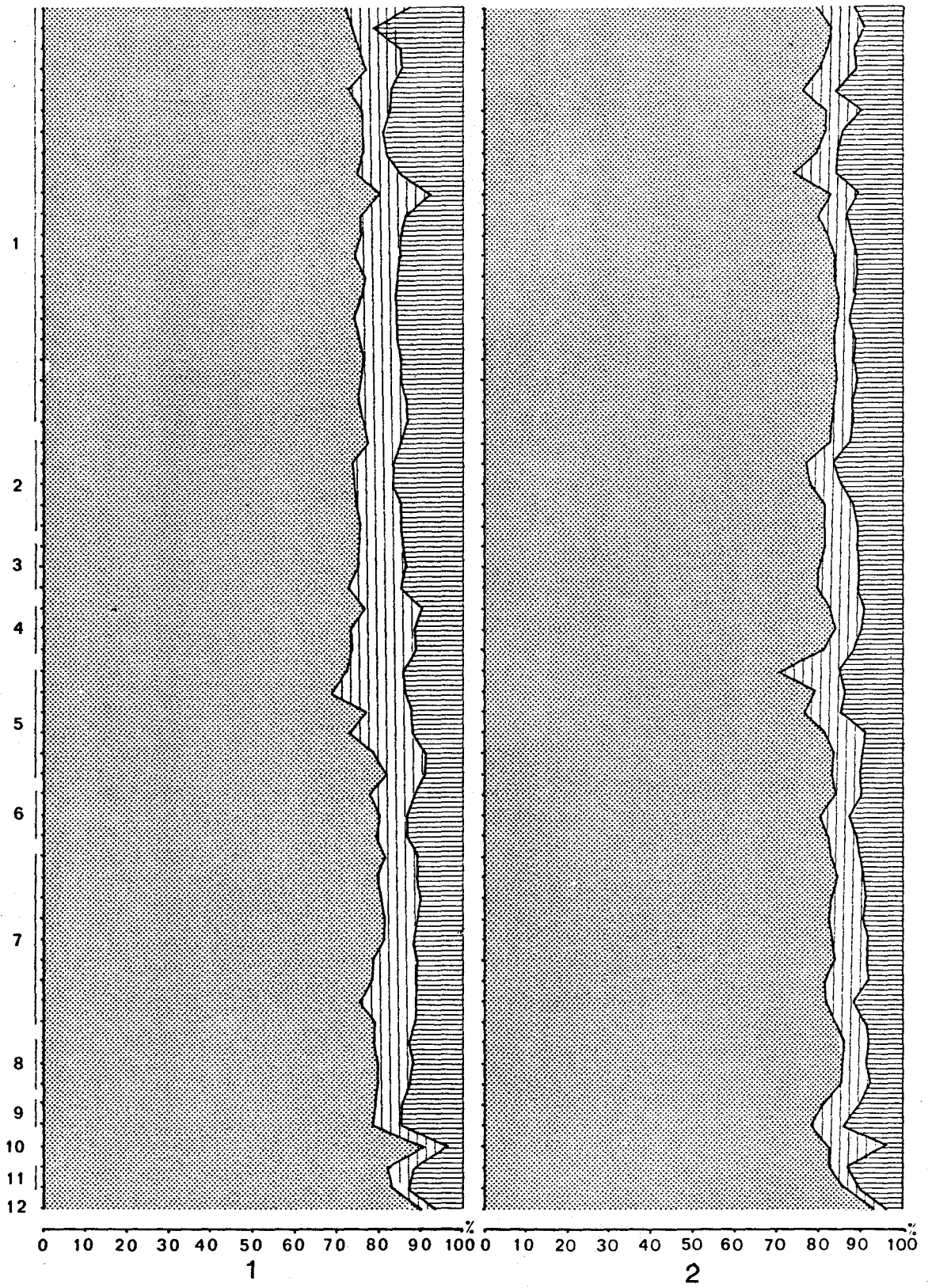


Figure 4.11

Granulometry and densitometry of the fines:

1. All fines
2. Decarbonated fines

Pech de l'Azé I, upper levels (after Laville,  
1975)



Weathering, particularly of the clays, can be detected by large values for the  $\Delta pH$ .

#### 4.1.5.4 Morphoscopy

Finally, the fines are examined under a binocular microscope to determine the origin of the sediments, especially the sands. Frosting of the grains indicates eolian transport, suggesting more desert-like conditions.

#### 4.1.5.5 Other Methods

Several other methods, not routinely performed, can be used, including X-ray diffractometry, standard chemical and organic analyses.

#### 4.1.6 Summary

No sedimentological analysis is complete, however, without the palynological, faunal, and archeological analyses. Although the sediments give many clues about the climate, these concomitant analyses can confirm many of the conclusions drawn from the sediments.

#### 4.2 Palynology

Because pollen and spores are resistant to decay in some sediments, they will be preserved for study after incorporation into the strata, providing the second clue to the paleoclimatology of the cave. Occasionally, it may be possible to identify an extinct pollen species which can set a lower limit on the age of the

deposit, but this is rare. Most of the relative dating is done after the paleoclimate has been established, rather than with fossils or pollen.

To prepare the pollen samples, several of which correspond to one sediment sample, it is washed, and treated with hydrochloric acid, HCl (aq), to remove the carbonates. After sieving at 200  $\mu\text{m}$ , the decarbonated sediment is suspended in Thoulet's solution, centrifuged, and filtered to remove the siliceous material which is heavier than the pollen. Hydrofluoric acid, HF (aq), is used to remove all traces of silica, following which the pollen is washed, neutralized, and mounted for counting.

To determine the paleoclimate, the percentages of various pollen types are computed. A higher percentage of tree or shrub pollens implies damper conditions than a sample with a high percentage of grass pollens. Among the arboreal pollens, pines, spruce, and firs indicate cold conditions, while elm, linden (basswood), oak, maple, and ash require a warm temperate climate. Oak and elm, in particular, suggest very mild temperature, but Pinus sylvestris, Scotch pine, hints at subarctic conditions. Furthermore, as the climate gets colder, there will be fewer trees, compared with the percentage of grasses (Figure 4.12).

Unfortunately, contamination of the pollen samples is always possible as a result of several factors, including:

1. Bioturbation of the sediment layers causing mixing of two different pollen suites.
2. Mixing of suites by cryoturbation, or other natural

Figure 4.12

The palynology of Combe-Grenal, couches

36 - 55 (after Bordes, 1972)



processes.

Unfortunately, there is often no control over these problems. Although a given site's pollen suite is largely a function of random variables, such as wind directions, and microenvironment, when uncontaminated palynology is a most reliable paleoclimate indicator.

#### 4.3 Faunal Analysis

As with the pollen suites, the fauna of Europe experienced relatively few extinctions during the middle and late Pleistocene, although many did occur at the end of the Lower Pleistocene, the Villefranchian. Unfortunately, there are few mammal lineages sufficiently well-understood to act as index fossils for this time, the exceptions being the bears, rodents, and mammoths (Figure 4.16). Figure 4.13 through 4.15 show some of the typical Pleistocene fauna in Europe, while Table 4.1 lists the first appearances and extinctions of many of the mammals.

Of all the Pleistocene faunal extinctions, most occurred in the northerly latitudes as the climate grew colder. Certain of these extinctions in Europe can be used to date the stratigraphic levels in which species are found. For example, during the Mindel, Dicerorhinus kirchbergensis (Merck's rhinoceros) appeared, but Ursus deningeri became extinct, while in the Mindel/Riss, Ursus speleus (cave bear) and U. arctos (brown bear) appear, but Mammuthus (Mammonteus) trogontherii (mammoth) became extinct (Kurtén, 1968). Therefore, if one is lucky enough to find the right fossils in the sediments, it may be possible to set limits on the age of



Figure 4.13

European mammal fauna during the Villefranchian;  
scale preserves the relative size (after Flint,  
1971)

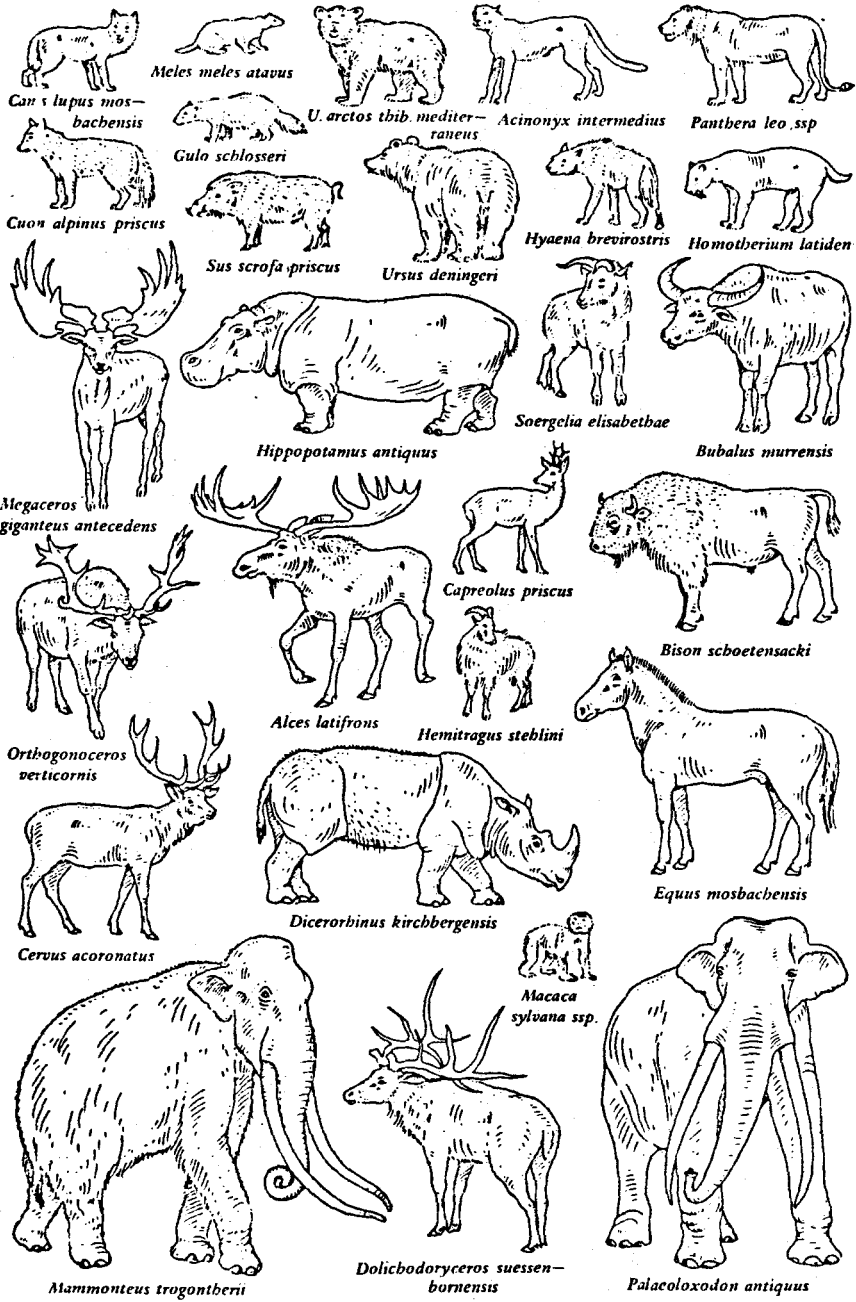


Figure 4.14

European mammal fauna from the Middle Pleistocene;  
scale preserves the relative size (after Flint,  
1971)

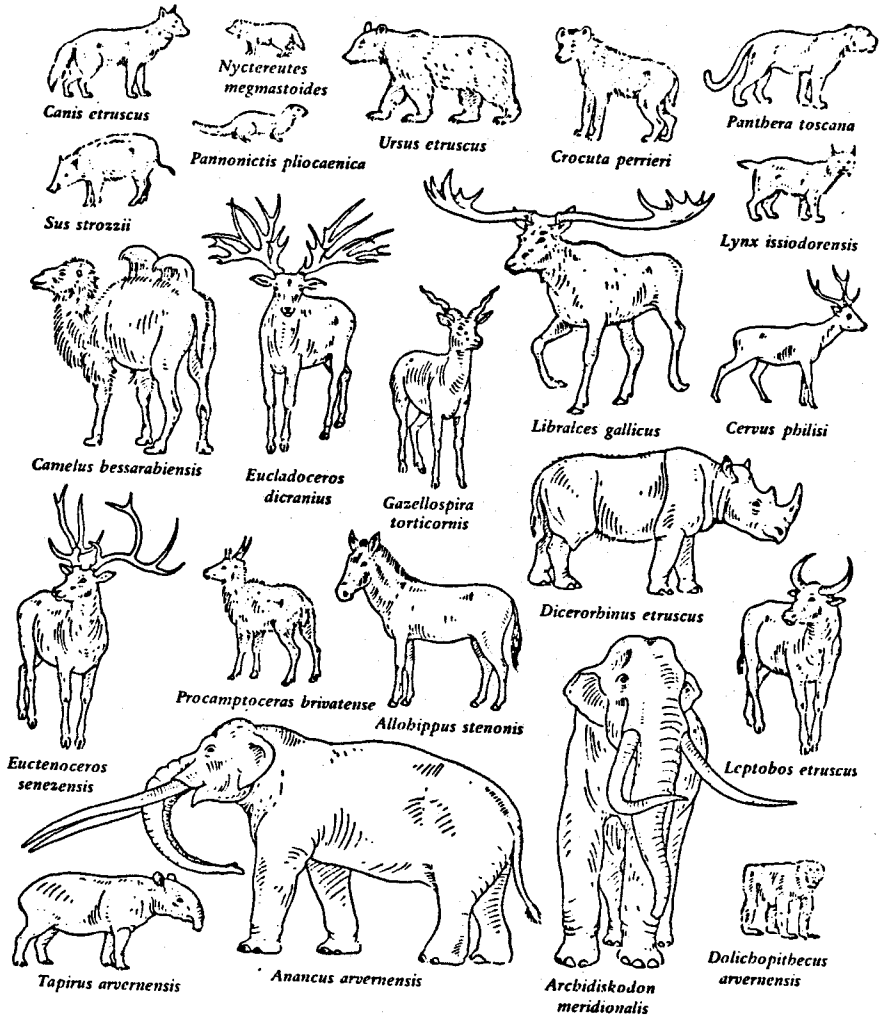


Figure 4.15

European mammal fauna from the Upper Pleistocene;  
scale preserves the relative size (after Flint,  
1971)

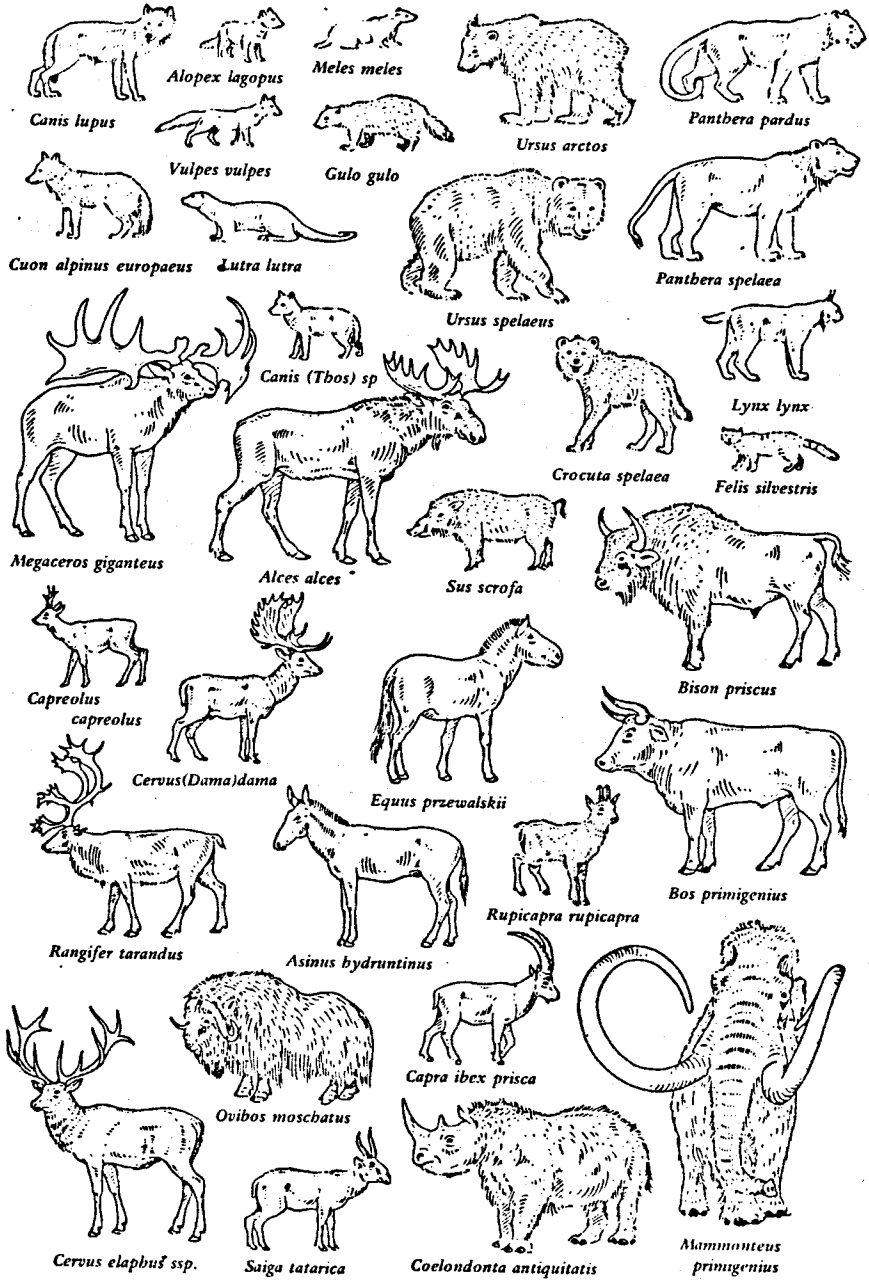


Figure 4.16

Evolution of the elephants and bears during the  
Quaternary (after Flint, 1971)

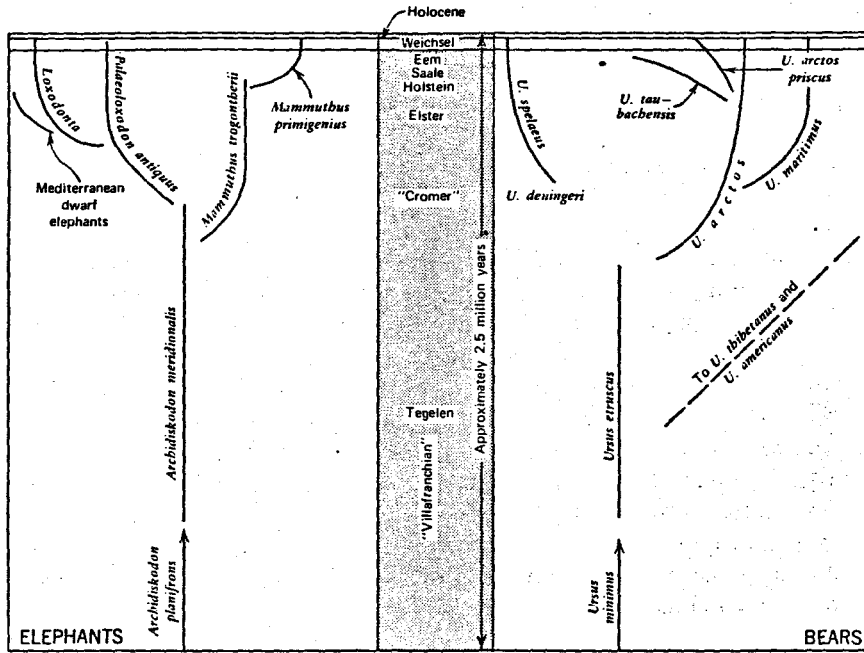




Table 4.1 Chronology of the Pleistocene Mammals

Stratigraphic Units		Fauna (Chief Elements Only)	Most significant localities of occurrence	
PLEISTOCENE	Middle	Menap	<p>First appearance of arctic mammals: <i>Gulo schlosseri</i>, <i>Rangifer tarandus</i>, <i>Præovibos priscus</i>, <i>Ovibos moschatus</i>, <i>Lemmus lemmus</i> and also of: <i>Mammuthus trogontherii</i>, <i>Equus sussenbornensis</i>, <i>Sus scrofa</i>, <i>Megaloceros savini</i>, <i>Capreolus capreolus</i>, <i>Alces latifrons</i>, <i>Soergelia elisabethae</i>, <i>Bison priscus</i>, <i>Crocota crocata</i>, <i>Homotherium latidens</i>, <i>Felis pardina</i>, <i>Meles meles</i>, <i>Aonyx bravardi</i>, <i>Lutra simplicidens</i>, <i>Canis lupus</i>, <i>Lycan lycanoides</i>, <i>Ursus deningeri</i>, <i>Ursus thibetanus</i>, <i>Hystrix vinogradovi</i>, <i>Allophaiomyis pliocenicus</i>, <i>Arvicola terrestris</i>.</p> <p>Last appearance: <i>Anancus arvernensis</i>, <i>Equus sussenbornensis</i>, <i>Hyaena brevirostris</i>, <i>Homotherium sanzelli</i>, <i>Acinonyx pardineus</i>, <i>Baranogale antiqua</i>, <i>Enhydrictis ardea</i>, <i>Cuon majori</i>, <i>Lycan lycanoides</i>, <i>Vulpes alopecoides</i>, <i>Vulpes praecorsae</i>, <i>Citellus primigenius</i>, <i>Lepus terraerubrae</i>.</p>	<p>Germany: Mustlach (lower layers) Süssenborn France: Valerots Czechoslovakia: Chlum 6 Hungary: Nagyhaszanyhegy 2 Poland: Kamyk Romania: Bettia Soviet Union: Nogaisk, Kair, Chortkov</p>
	Villfranchian (Lower)	Upper	<p>First appearance: <i>Archidiskodon meridionalis</i>, <i>Equus stenonis</i>, <i>Equus hydruntinus</i>, <i>Hippopotamus amphibius</i>, <i>Dama nesti</i>, <i>Leptobos etruscus</i>, <i>Felis lunensis</i>, <i>Canis arvernensis</i>, <i>Cuon majori</i>, <i>Citellus primigenius</i>, <i>Trogontherium cuvieri</i>, <i>Lagurus panonicus</i>, <i>Lepus terraerubrae</i>.</p> <p>Last appearance: <i>Tapirus arvernensis</i>, <i>Equus stenonis</i>, <i>Equus bressanus</i>, <i>Sus strozzii</i>, <i>Cervus perrieri</i>, <i>Cervus etieriarius</i>, <i>Alces gallicus</i>, <i>Gazella borbonica</i>, <i>Deperetia ardea</i>, <i>Leptobos elatus</i>, <i>Leptobos etruscus</i>, <i>Dulichopithecus arvernensis</i>, <i>Eurybosc lunensis</i>, <i>Megantereon megartereon</i>, <i>Felis issiodorensis</i>, <i>Canis etruscus</i>, <i>Nyctereutes megaristoides</i>, <i>Ursus etruscus</i>, <i>Hystrix refossa</i>, <i>Dolomys nillieri</i>, <i>Oryctolagus lacosti</i>.</p>	<p>Spain: Olivola Italy: Val d'Arno Superiore, Luffe France: Saint Vallier, Senèze Holland: Togelen Hungary: Beremend 1, Villany 5 Poland: Kadzielnia Soviet Union: Chapry, Sinaia Balka</p>
		Lower	<p>First appearance: <i>Dicerorhinus etruscus</i>, <i>Hipparion crusafonti</i>, <i>Equus bressanus</i>, <i>Cervus perrieri</i>, <i>Alces gallicus</i>, <i>Leptobos elatus</i>, <i>Gazella borbonica</i>, <i>Deperetia ardea</i>, <i>Macaca florentina</i>, <i>Dulichopithecus arvernensis</i>, <i>Hyaena perrieri</i>, <i>Eurybosc lunensis</i>, <i>Ursus etruscus</i>, <i>Megantereon megartereon</i>, <i>Homotherium sanzelli</i>, <i>Felis issiodorensis</i>, <i>Felis toscana</i>, <i>Acinonyx pardineus</i>, <i>Enhydrictis ardea</i>, <i>Aonyx bravardi</i>, <i>Canis etruscus</i>, <i>Nyctereutes megaristoides</i>, <i>Castor fiber</i>, <i>Hystrix refossa</i>, <i>Mimomys pliocenicus</i>, <i>Oryctolagus lacosti</i>.</p> <p>Last appearance: <i>Zygodon borsoni</i>, <i>Dicerorhinus megarhinus</i>, <i>Sus arvernensis</i>, <i>Parailurus anglicus</i>, <i>Agriotherium insigne</i>.</p>	<p>Spain: Villaroya Italy: Villafranca d'Asti France: Violette, Mt. Perrier, Chagny England: Red Crag Czechoslovakia: Hájnačka Romania: Mălusesti, Berești, Căpeni Soviet Union: Stavropol</p>
		Astian	<p><i>Anancus arvernensis</i>, <i>Zygodon borsoni</i>, <i>Dicerorhinus megarhinus</i>, <i>Hipparion crassum</i>, <i>Tapirus arvernensis</i>, <i>Pliolynx occidentalis</i>, <i>Parailurus anglicus</i>, <i>Agriotherium insigne</i>, <i>Ursus rusciniensis</i>, <i>Nyctereutes sinensis</i>, <i>Trilophomys pyrenaeus</i>, <i>Stachomys trifidodon</i>, <i>Mimomys stehlini</i>.</p>	<p>France: Montpellier, Roussillon, Sète, Nîmes Czechoslovakia: Ivanovce Poland: Weze, Rebelice Hungary: Gödöllő, Csarnota</p>

Stratigraphic Units	Fauna (Chief Elements Only)	Most significant localities of occurrence
PLEISTOCENE	<p>First appearance: <i>Mammuthus primigenius</i>, <i>Coelodonta antiquitatis</i>, <i>Equus hemionus</i>, <i>Alces alces</i>, <i>Capra ibex</i>, <i>Marmota marmota</i>, <i>Lagurus lagurus</i>.</p> <p>Last appearance: <i>Dama clactoniana</i>, <i>Ursus thibetanus</i></p> <p>In Middle and Western Europe, arctic fauna with: <i>Mammuthus primigenius</i>, <i>Coelodonta antiquitatis</i>, <i>Rangifer tarandus</i>, <i>Alopec lagopus</i>, <i>Gulo gulo</i>, <i>Lemmus lemmus</i>, <i>Dicrostonyx torquatus</i>, <i>Microtus nivalis</i>, <i>Microtus gregalis</i>, <i>Lagurus lagurus</i>, <i>Ochotona pusilla</i>.</p>	<p>Italy: San Agostino France: La Fage, Lazaret, Grimaldi England: Glutton Stratum in the Tornewton Cave Hungary: Ujonyony 1 Poland: lowest layers in Nieto-perzowa and other caves</p>
	<p>First appearance: <i>Dicerorhinus hemitoechus</i>, <i>Equus germanicus</i>, <i>Megaloceros giganteus</i>, <i>Dama clactoniana</i>, <i>Bos primigenius</i>, <i>Macaca sylvana</i>, <i>Hyaena hyaena</i>, <i>Felis silvestris</i>, <i>Martes martes</i>, <i>Aonyx antiqua</i>, <i>Vulpes vulpes</i>, <i>Ursus spelaeus</i>, <i>Ursus arctos</i>, <i>Oryctolagus cuniculus</i></p> <p>Last appearance: <i>Mammuthus trogontherii</i>, <i>Trogontherium cuvieri</i>, <i>Mimomys cantianus</i>.</p> <p>In Middle and Western Europe, forest fauna with: <i>Palaeoloxodon antiquus</i>, <i>Dicerorhinus kirchbergensis</i>, <i>Dama clactoniana</i>, <i>Bubalus murensis</i>.</p>	<p>Italy: Spessa II France: Lunel-Viel England: Swanscombe, Gray's Thurrock, Clacton, Hoxne Germany: Heppenloch</p>
	<p>First appearance: <i>Dicerorhinus kirchbergensis</i>, <i>Gulo gulo</i>, <i>Mustela nivalis</i>, <i>Dicrostonyx torquatus</i>.</p> <p>Last appearance: <i>Dicerorhinus etruscus</i>, <i>Equus mosbachensis</i>, <i>Megaloceros savini</i>, <i>Alces latifrons</i>, <i>Præovibos priscus</i>, <i>Soergelia elisabethae</i>, <i>Macaca florentina</i>, <i>Felis toscana</i>, <i>Ursus deningeri</i>.</p> <p>Arctic mammals appear in Middle and Western Europe (<i>Rangifer</i>, <i>Ovibos</i>, <i>Gulo</i>, <i>Lemmus</i>, <i>Dicrostonyx</i>).</p>	<p>Germany: Mosbach upper layers France: Cagny, Estève Janson Hungary: Tarkó, Vertesszöllös Czechoslovakia: Koneprusy</p>
	<p>First Appearance: <i>Palaeoloxodon antiquus</i>, <i>Equus mosbachensis</i>, <i>Felis leo</i>, <i>Felis pardus</i>, <i>Pitymys gregaloides</i>, <i>Microtus arvaloides</i>.</p> <p>Last appearance: <i>Archidiskodon meridionalis</i>, <i>Dama nestii</i>, <i>Hyaena perrieri</i>, <i>Felis lunensis</i>, <i>Gulo schlosseri</i>, <i>Panonicus pliocenicus</i>, <i>Lutra simplicidens</i>, <i>Mimomys savini</i>, <i>Hypolagus brachygnathus</i>.</p> <p>In Middle and Western Europe, forest fauna with <i>Hippopotamus amphibius</i>, <i>Macaca florentina</i>, numerous <i>Cervids</i>, etc.</p>	<p>England: Cromer Forest Bed Germany: Voigstedt, Mauern Austria: Hundsheim Czechoslovakia: Stranska Skala</p>
	<p>In Middle and Western Europe, forest fauna with <i>Hippopotamus amphibius</i>, <i>Macaca florentina</i>, numerous <i>Cervids</i>, etc.</p>	

Stratigraphic Units		Fauna (Chief elements only)	Most significant localities of occurrence
HOLOCENE		<p><u>First appearance:</u> <i>Bison bonasus</i>, <i>Apodemus agrarius</i> and numerous synanthropic and introduced mammals, e.g. <i>Rattus rattus</i>, <i>Rattus norvegicus</i>, <i>Mus musculus</i>, <i>Fiber zibethicus</i>, <i>Nyctereutes procyonoides</i>, <i>Dama dama</i>.</p> <p><u>Last appearance:</u> <i>Megaloceros giganteus</i>, <i>Bos primigenius</i>, <i>Equus gmelini</i>, <i>Myotragus balearicus</i>, <i>Prolagus sardus</i>.</p> <p>Arctic mammals (e.g. <i>Rangifer tarandus</i>) successively disappear from Middle Europe replaced by forest species. In the period of climatic optimum <i>Bison bonasus</i> appears in Middle Europe and many other species (e.g. <i>Myotis bechsteini</i>, <i>Felis silvestris</i>, <i>Eliomys quercinus</i>) extend their ranges beyond their present northern limits. With the replacement of forest by arable fields steppe mammals (e.g. <i>Apodemus agrarius</i>, <i>Cricetus cricetus</i>) spread to the West. Many synanthropic and introduced mammals appear in Europe.</p>	
PLEISTOCENE	Upper	<p><u>First appearance:</u> <i>Saiga tatarica</i>, <i>Felis manul</i>, <i>Allactaga jaculus</i>.</p> <p><u>Last appearance:</u> <i>Palaeoloxodon antiquus</i>, <i>Mammuthus primigenius</i>, <i>Dicerorhinus kirchbergensis</i>, <i>Coelodonta antiquitatis</i>, <i>Equus germanicus</i>, <i>Equus hemionus</i>, <i>Hippopotamus amphibius</i>, <i>Dama dama</i>, <i>Ovibos moschatus</i>, <i>Bison priscus</i>, <i>Crocota crocata</i>, <i>Homotherium latidens</i>, <i>Felis leo</i>, <i>Felis pardus</i>, <i>Aonyx antiqua</i>, <i>Cuon alpinus</i>, <i>Ursus spelaeus</i>, <i>Microtus gregalis</i>, <i>Lagurus lagurus</i>, <i>Dicrostonyx torquatus</i>, <i>Ochotona pusilla</i>.</p> <p>In Middle and Western Europe arctic and steppe mammals prevail: <i>Mammuthus primigenius</i>, <i>Coelodonta antiquitatis</i>, <i>Ovibos moschatus</i>, <i>Bison priscus</i>, <i>Rangifer tarandus</i>, <i>Felis leo</i>, <i>Crocota crocata</i>, <i>Ursus spelaeus</i>, <i>Mustela nivalis</i>, <i>Dicrostonyx torquatus</i>, <i>Lemmus lemmus</i>, <i>Microtus gregalis</i>, <i>Microtus oeconomus</i>, <i>Ochotona pusilla</i>, <i>Lepus timidus</i>. In the time of the interstadials forest mammals regain part of their areas in Middle Europe. For particular places the succession of many tundra-, steppe- and forest stages can be stated in the composition of the mammalian fauna.</p>	Cave sediments, loess, peat bogs, river and glacial sediments throughout Europe, too numerous for a general list
	Eem	<p><u>First appearance:</u> <i>Dama dama</i>, <i>Rupicapra rupicapra</i>, <i>Felis lynx</i>, <i>Lutra lutra</i>, <i>Vulpes corsac</i>, <i>Ursus maritimus</i>, <i>Hystrix cristata</i>, <i>Lepus europaeus</i>, <i>Lepus timidus</i>.</p> <p><u>Last appearance:</u> <i>Dicerorhinus hemitoechus</i>, <i>Hyaena hyaena</i></p> <p>In Middle and Western Europe, forest fauna with: <i>Palaeoloxodon antiquus</i>, <i>Dicerorhinus kirchbergensis</i>, <i>Hippopotamus amphibius</i>, <i>Cervus elaphus</i>, <i>Capreolus capreolus</i>, <i>Felis chaus</i>, <i>Hystrix cristata</i> etc.</p>	<p>England: <i>Hyaena Stratum</i> in Tornewton Cave</p> <p>Germany: travertines of Cannstatt and Taubach</p> <p>Czechoslovakia: travertines of Ganocve</p> <p>Deep layers of cave sediments throughout Europe</p>
	Weichsel		

(after Flint, 1971)

a level.

As before, however, the main purpose of the faunal analysis is to determine the paleoclimatology for the sequence. During the mid and upper Pleistocene in Europe, there existed several faunal associations from different climatic and floral biomes (see Figure 4.17). As the climate fluctuated, so did the ranges of the animals. While the arctic fauna was primarily a newly evolved one adapted to the new climate, the others were groups of Pliocene types, some of which had evolved (Flint, 1971). First recognized in Europe in the Mindel, the arctic fauna comprised Rangifer (reindeer), Ovibus (muskox), Gulo (wolverine), Lemmus (lemmings), and Dicrostonyx (a rodent) which recurred in the Riss, having added Mammuthus primigenius (woolly mammoth), Coelodonta antiquitatis (woolly rhino), and Alopex (arctic fox), and recurred again in the Wurm. Diceros rhinus, Dama (elk), Cervus (deer), Macaca (macaque monkeys), Bison, Hippopotamus, Paleoloxodon (straight-tusked elephant), and Lynx could be found among the forest (interglacial) fauna. During the Wurm, the faunal changes can be noted during the shift from glacial to interstadial as the arctic fauna was slowly replaced by the steppic fauna, including Capra ibex, Equus (horse), Leptobos (cattle), Bubalus (oxen), Felis (lion, panther), Hyaena, and Crocota (hyena), to be followed by the true forest species. From the faunal assemblage, it should be possible to assign the couche to a paleoclimatic type, which then must be given a relative date.

Figure 4.17

European bioherms during the Upper Pleistocene  
As the weather became warmer the tundra would  
be replaced gradually by boreal forest and then  
temperate forest, near the coasts, and by cold  
steppe and then warm steppe inland. As the  
weather became cooler the process was reversed  
(after Flint, 1971).

(Cold summer temperatures)

TUNDRA

Woolly mammoth, woolly rhinoceros, muskox, wolverine, tundra reindeer, hares, lemming

O  
c  
c  
e  
a  
n  
i  
c  
  
c  
l  
i  
m  
a  
t  
e

BOREAL FOREST

Brown bear, lynx, elk, deer, moose, forest reindeer, wolverine, cattle

COLD STEPPE

Woolly mammoth, woolly rhinoceros, tundra reindeer, muskox, wolf, hares

C  
o  
n  
t  
i  
n  
e  
n  
t  
a  
l  
  
c  
l  
i  
m  
a  
t  
e

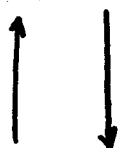
TEMPERATE FOREST

Elephant, rhinoceros, elk, hippopotamus, moose, deer, bison, cattle, lynx

WARM STEPPE

Horse, antelope, marmot, rodents, cattle

(Warm summer temperatures)



#### 4.4 Interpreting the Paleoclimatological Data

In order to relatively date the sediments, the paleoclimatological data must be interpreted carefully. Although the process seems something akin to divination, until recently, this was the only method by which many of the **sites** could be dated.

Using such index fossils as there may be in the site, i.e. Ursus deningeri, limits are set for the possible age of the deposits. This, however, is often a circular argument, because the age ranges of many such "index Fossils" was originally determined using the same methods. Often the human cultures are used to set such limits, as well. By this formula, if Mousterian is present, it must be no older than the Würm, or possibly late Riss/Würm, while Upper Paleolithic tools indicate Würm II/III or younger. Although the ages of many of the Upper Paleolithic cultures have been corroborated with  $^{14}\text{C}$  dates, the argument is still circular, because the age ranges for all the cultures was established using paleoclimatologically derived relative dates.

From the climatological pattern and the limits set at certain levels by the fossils, the relative dates are assigned. First the climatic curve is fitted to the global pattern of climate change. Each cold period is matched to a stadial, and each warm period to an interstadial or interglacial. But if the fit is not quite perfect, then a stadial may be skipped, or a cold or warm oscillation added to make the pattern fit. The difference between the Würm I and Würm II is understood with a bit more precision.

A higher percentage of roe deer and red deer are more likely to represent the Würm I, whereas reindeer in great numbers suggest Würm II, unless the Magdalenian culture is present to determine a Würm IV (Bordes, 1972).

Perhaps not the most scientific method, this was the sole method by which archeologists could date the sites until the development of radiometric methods, which even now will not provide dates for all sites.

#### 4.5 Archeological Techniques

Although the French may be criticized for their dating, they can not be criticized for their excavation techniques or archeology which are the most sophisticated in the world.

##### 4.5.1 Excavation

In excavating a site it is crucial to maintain strict control over the stratigraphy. Often during the excavation this will not be possible, because minute changes in the sediments are often indistinguishable until the laboratory analysis is completed. Therefore, all objects when found, whether rocks, tools, teeth, bones, or anything, are located within the grid square in all three directions, numbered and noted in a book. All measurements are to within a half centimetre as referenced to the grid pattern of the site which is established before any digging begins (see Figure 4.18). Each piece found is also noted on a map constructed for each couche of each square. In this way, any areal associations

Figure 4.18

The grid system in Abri Vaufrey:

The string at the rear of the picture is the base line, with coordinate zero for the numerical portion of the bicharacter system. That with the other strings suspended from it parallel to the side wall is the zero line for the alphabetic portion. Therefore, the log in the picture is in squares A-E 6. Each suspended string marks the corners of a square (courtesy of C. Pierce).





can be seen at a glance. It is also possible to construct profiles, using the record books, either parallel to the square boundaries or diagonally, at any interval to determine stratigraphic relations. Often subdivisions for the cultural layers hitherto unrecognized can be distinguished using these techniques. This, however, is only the start of the archeological treatment of the artefacts.

#### 4.5.2 Typological Analysis

In order to characterize an assemblage of artefacts, it is necessary to compute certain statistics. When confronted by the total assemblage, it is first essential to organize the material into classes of artefacts. For example, in a Mousterian kit, the artefacts are grouped into the following classes:

1. Primary elements: Pieces showing portions of the original cortex, namely pieces removed in the core preparation
2. Cores: Pieces from which specially prepared flakes, blades, and points have been struck
3. Debitage: Both Levallois and non-Levallois types, including tools, flakes, blades and points, which have been shaped by core preparation, rather than by simply flaking the nodule until it is the desired shape. Debitage technique allows several flakes to be removed from a core, all of which have the same shape.
4. Tools: Debitage which has been retouched by secondary flaking to produce special features in the tool.
5. Waste and Debris: Any material which does not appear to

have been utilized, but was produced during the tool manufacturing process.

All these classes are then statistically described in greater detail, especially for such features as size relationships, retouch for tools, scar patterns, etc. Some classes are further subdivided for descriptive purposes.

#### 4.5.2.1 Cores or Nuclei

Cores are further subdivided into several subtypes dependent upon the type of debitage removed from the core, including discoidal, pyramidal, Levallois flake, Levallois blade; some are shown in Figures 4.19 (hypothetical) and 4.20 (actual). The Levallois technique was a special flaking technique developed in the Mousterian in which the sides of the nodule were reduced to the desired shape. Using these flake scars as a striking platform, the upper surface was removed, and a special striking platform prepared at one end from which was struck the desired flake, the shape of which was predetermined by the original flaking (Bordes, 1961, 1968). Although some experts prefer a more restricted definition of Levallois requiring centripetal dorsal flaking, this is too restrictive a definition when applied to the early Mousterian (Bordes, 1961; Crew, 1976).

#### 4.5.2.2 Debitage

Like the cores, the debitage is further subdivided into Levallois and non-Levallois types, which are then categorized as blades, flakes, points, and occasionally other minor types, such

Figure 4.19

Core typology

1. Normal single platform
2. Angled single platform
3. Pyrimadal
4. Opposed double platform
5. Orthogonal double platform
6. Double platform in different planes
7. Double platform with opposed parallel planes
8. Bipolar
9. Irregular
10. Proto-biconcial
11. Biconical
12. Levallois flake, flat
13. Levallois flake, high-backed
14. Levallois blade
15. Levallois point
16. Discoidal, flat
17. Discoidal, high-backed

(source unknown)

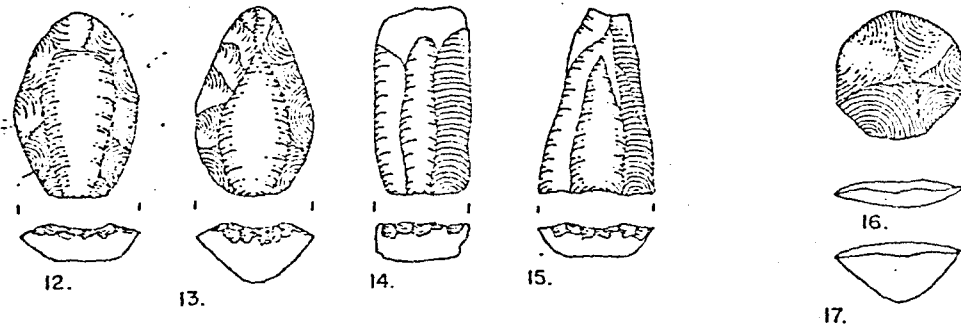
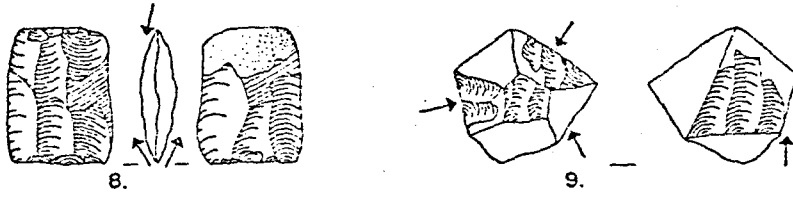
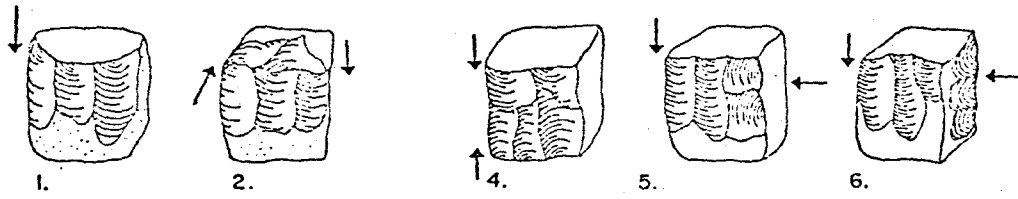
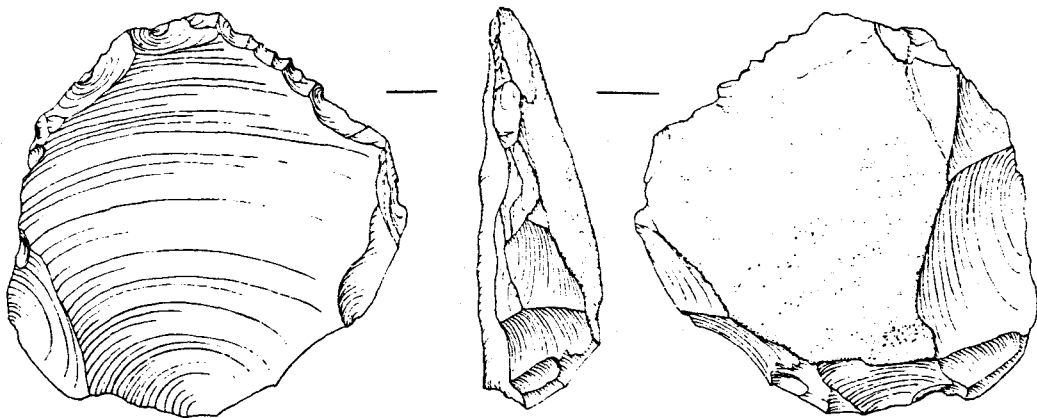


Figure 4.20

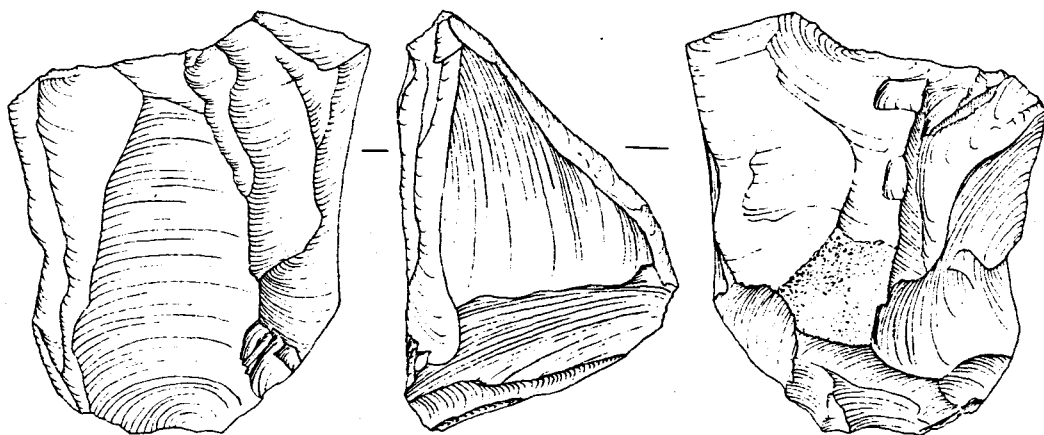
Mousterian cores

- a. Typical Levallois flake
- b. Bidirectional Levallois blade
- c. Single platform blade (pyramidal)
- d. Discoidal

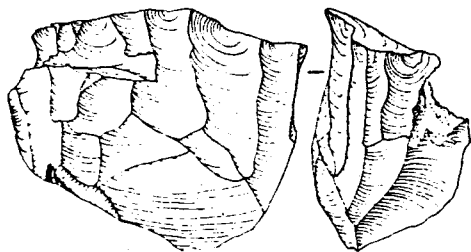
(after Crew, 1976)



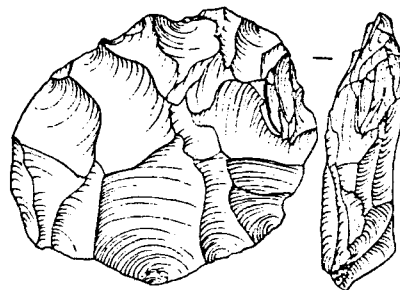
a



b



c



d

0 1 2 cm.

as naturally backed pieces. Usually, the debitage is described in terms of plan form, striking platform, dorsal scar patterns, and the type of hammer used to remove the piece, all shown in Figure 4.21 along with the reference points.

#### 4.5.2.3 Retouched Tools

The restricted typology is the list of actual tool types recognized in the retouched tool category. Bordes (1961, 1968, 1974) lists 62 such types, but occasionally a few more types might be added, such as handaxes (blattspitzen), or foliated pieces (see Table 4.2).

Statistically, the retouched tools are described in several ways. In addition to the descriptive classes applied to all debitage noted above, the retouched tools are described in terms of retouch type, edge plan, edge category, retouch class, profile form, and cross sectional form, as shown in Figure 4.22.

Sidescrapers, as the name implies, have a retouched edge which has been prepared, probably to use for scraping things. In Bordes' (1961b) list 22 types of sidescrapers are defined, depending on shape and type of retouch. Most common in la Quina and la Ferrassie Mousterians, la Quina sidescrapers are made on thicker than normal flakes, and have scalariform retouch (Bordes, 1972).

Endscrapers have a retouched edge at the distal end of the flake. Several types are common, including nosed, shouldered and carinated versions. Both endscrapers and burins are more common in the Upper Paleolithic kits than the Mousterian. Burins possess



Figure 4.21

Debitage description

- A. Reference points
  - 1. Plan view
  - 2. Profile
  - 3. Cross section
- B. Striking platforms
- C. Plan forms
  - 1. Irregular
  - 2. Short quadrilateral
  - 3. Long (blade) quadrilateral
  - 4. Shrot triangular
  - 5. Long triangular
- D. Hammer technique
  - 1. Hard
  - 2. Soft
- E. Dorsal scar patterns
  - 1. Parallel unidirectional
  - 2. Convergent unidirectional
  - 3. Irregular unidirectional
  - 4. Irregular bidirectional
  - 5. Opposed bidirectional
  - 6. Radial

(source unknown)

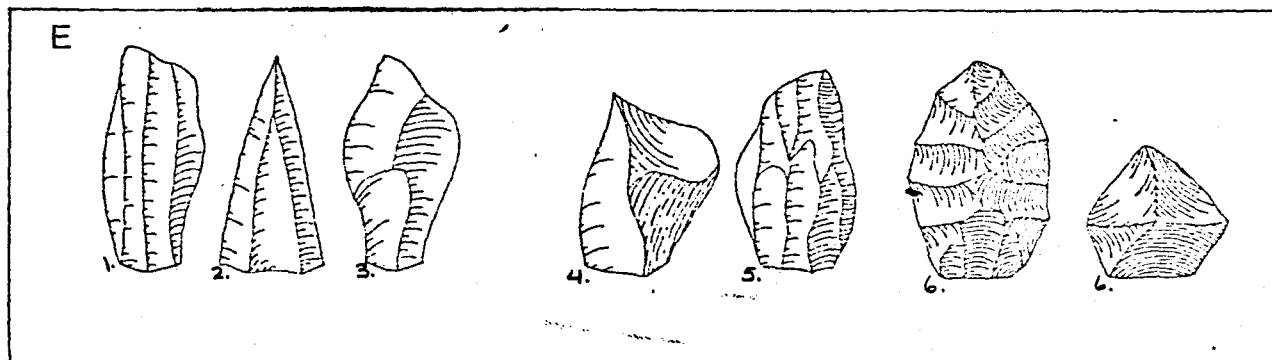
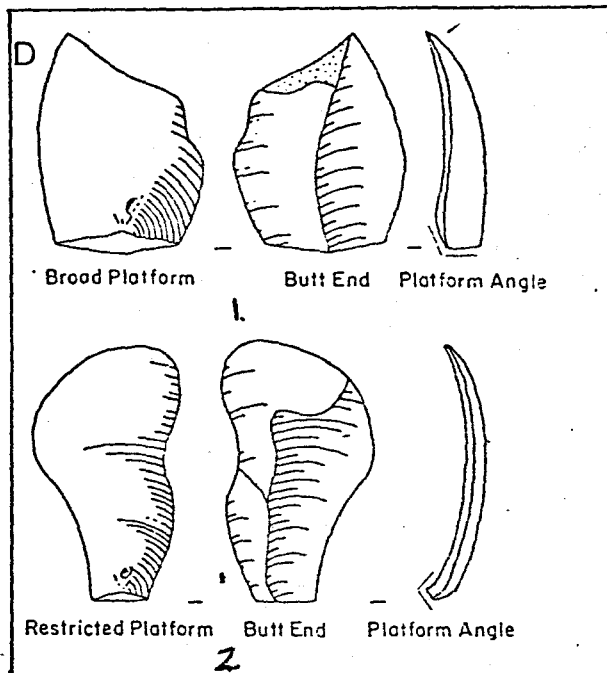
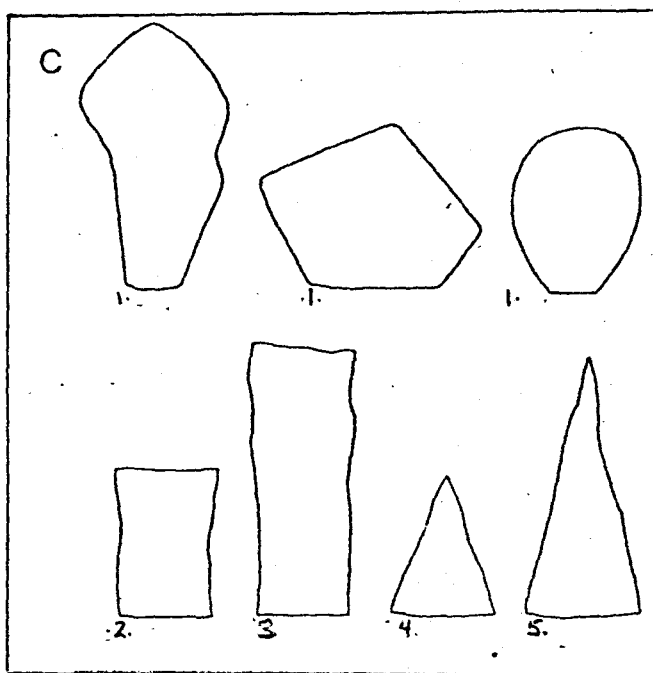
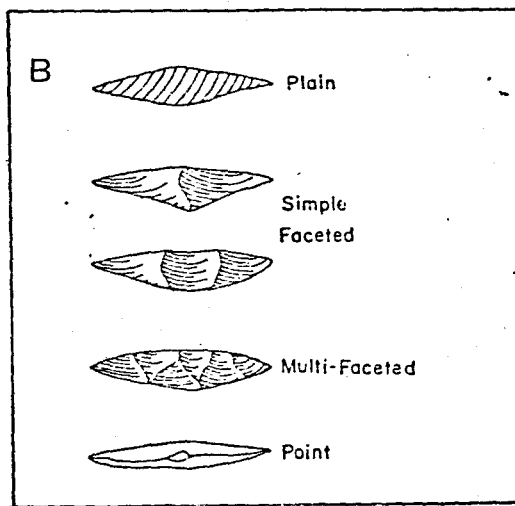
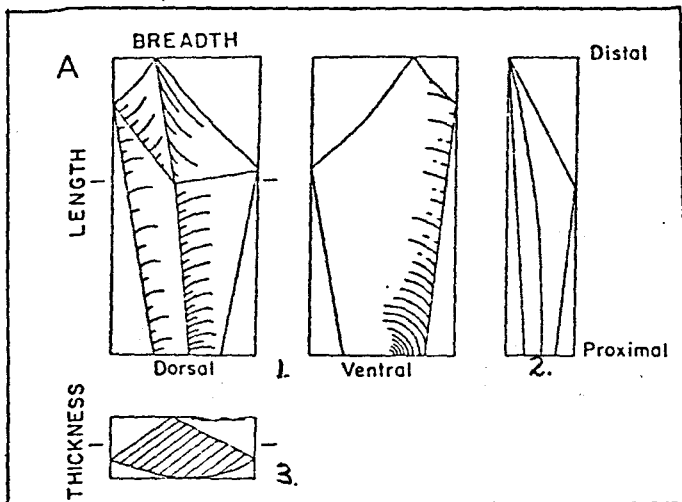


Figure 4.22

Modification and retouch categories for retouched tools:

- A. Modification type
- B. Retouch angle
- C. Retouch category
- D. Edge plan
- E. Edge category
- F. Retouch class
- G. Profile form
- H. Cross sectional form

(source unknown)

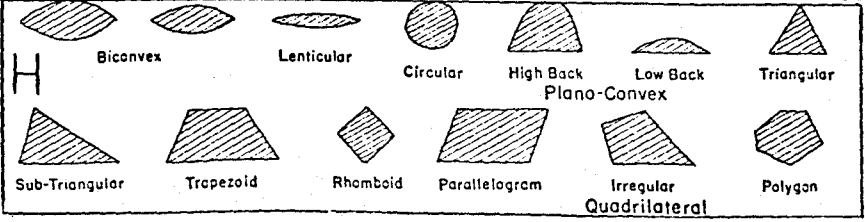
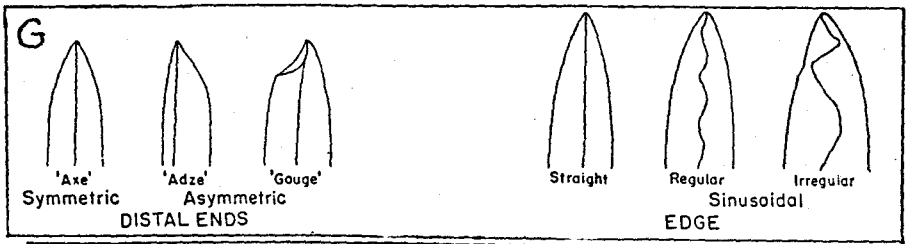
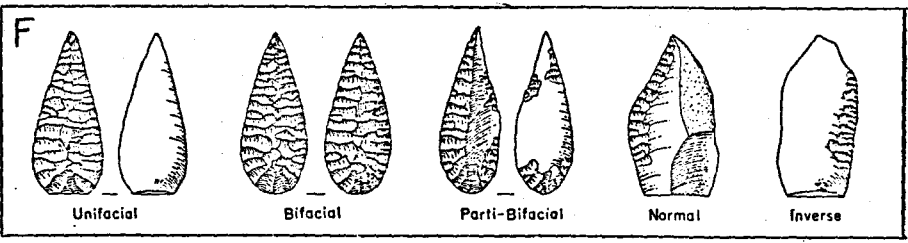
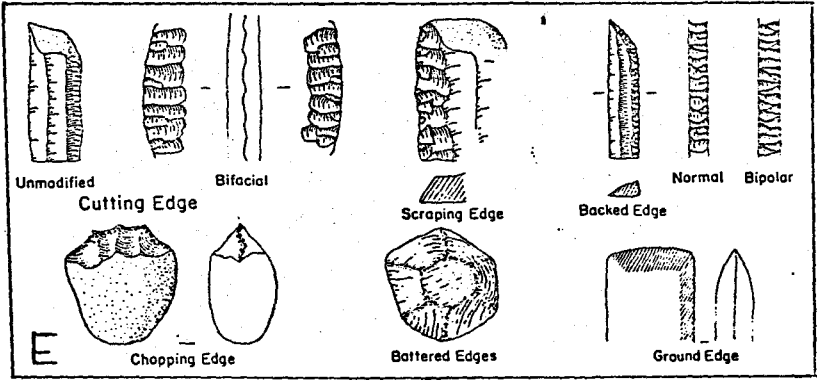
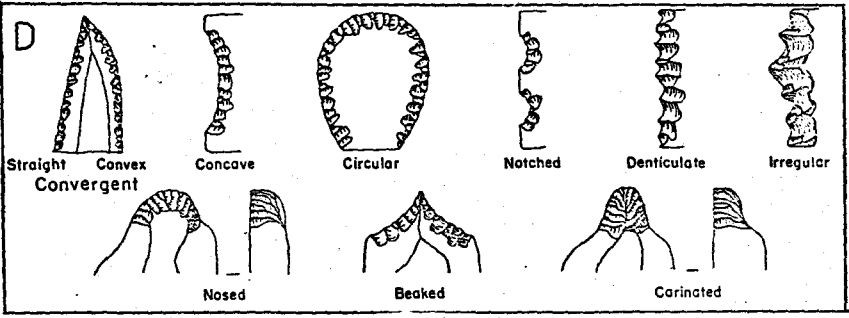
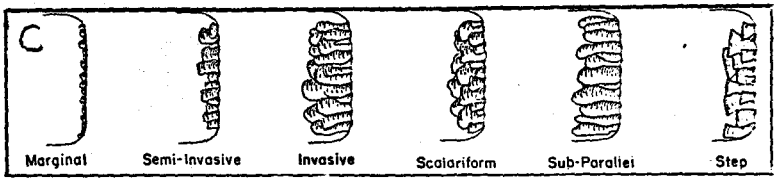
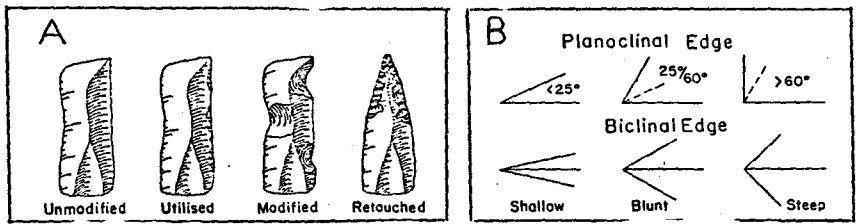


Table 4.2 Bordes' List of Mousterian Tool Types

Tool		
	21. Sidescraper, asymmetrical	43. Denticulate
	22. Sidescraper, transverse straight	44. Bec burinante alterne
1. Typical Levallois flake	23. Sidescraper, transverse convex	45. Flake, retouched on the ventral surface
2. Atypical Levallois flake	24. Sidescraper, transverse concave	46. Miscellaneous retouched flake, abrupt thick retouch
3. Levallois point	25. Sidescraper, retouched on the ventral surface	47. Miscellaneous retouched flake, alternate thick retouch
4. Retouched Levallois point	26. Sidescraper, with abrupt retouch	48. Miscellaneous retouched flake, abrupt thin retouch
5. Pseudo-Levallois point	27. Sidescraper, with thin back	49. Miscellaneous retouched flake, alternate thin retouch
6. Mousterian point	28. Sidescraper, bifacial retouch	50. Flake, bifacial retouch
7. Elongated Mousterian point	29. Sidescraper, with alternate retouch	51. Tayac point
8. Linace	30. Typical endscraper	52. Notched triangle
9. Sidescraper, single straight	31. Atypical endscraper	53. Pseudo-microburin
10. Sidescraper, single convex	32. Typical burin	54. Flake, notched end
11. Sidescraper, single concave	33. Atypical burin	55. Cleavers
12. Sidescraper, double straight	34. Typical borer	56. Rabot (plane)
13. Sidescraper, double straight convex	35. Atypical borer	57. Aterian tanged point
14. Sidescraper, double straight concave	36. Typical backed knife	58. Tanged piece
15. Sidescraper, double biconvex	37. Atypical backed knife	59. Chopper
16. Sidescraper, double biconcave	38. Naturally backed knife	60. Inverse chopper
17. Sidescraper, double convex concave	39. Mousterian raclette	61. Chopping tool
18. Sidescraper, convergent straight	40. Truncated piece	62. Miscellaneous piece
19. Sidescraper, convergent convex	41. Mousterian tranchet	63. Blattspitzen
20. Sidescraper, convergent concave	42. Notched pieces	

at least one graver facet, a facet which has been struck against and truncates the working edge previously prepared by retouch. Several different types are defined based upon the number and location of the graver facets, and the manner in which the edge was prepared. A bec (or bec-burin) is a special nosed burin formed from several graver facets oriented in different directions. Another typical Upper Paleolithic tool, the borer or awl, has point which was produced by retouch either through  $360^{\circ}$  or  $180^{\circ}$  appearing in cross section as circular or D-shaped (Burkitt, 1963).

A tool is classified as a denticulate if it possesses three or more contiguous notches. This is further subdivided by the number of notches along a standard 5 cm length of edge as microdenticulation having more than  $10/5$  cm, normal 6 to  $10/5$  cm, and macrodenticulation less than  $6/5$  cm (Crew, 1976). In order to produce a notched piece, the notch must have been removed by retouch rather than natural breakage. A Clactonian notch is formed by the removal of a single flake larger than 1 cm (Crew, 1976).

#### 4.5.2.4 Other Tools

Handaxes are core tools both the ventral and dorsal faces of which have been retouched to produce a shape edge except for the butt. As can be seen in Figure 4.23, shape may vary from ovate to triangular. If the distal end is removed from a handax, a cleaver is formed, also shown in Figure 4,23.

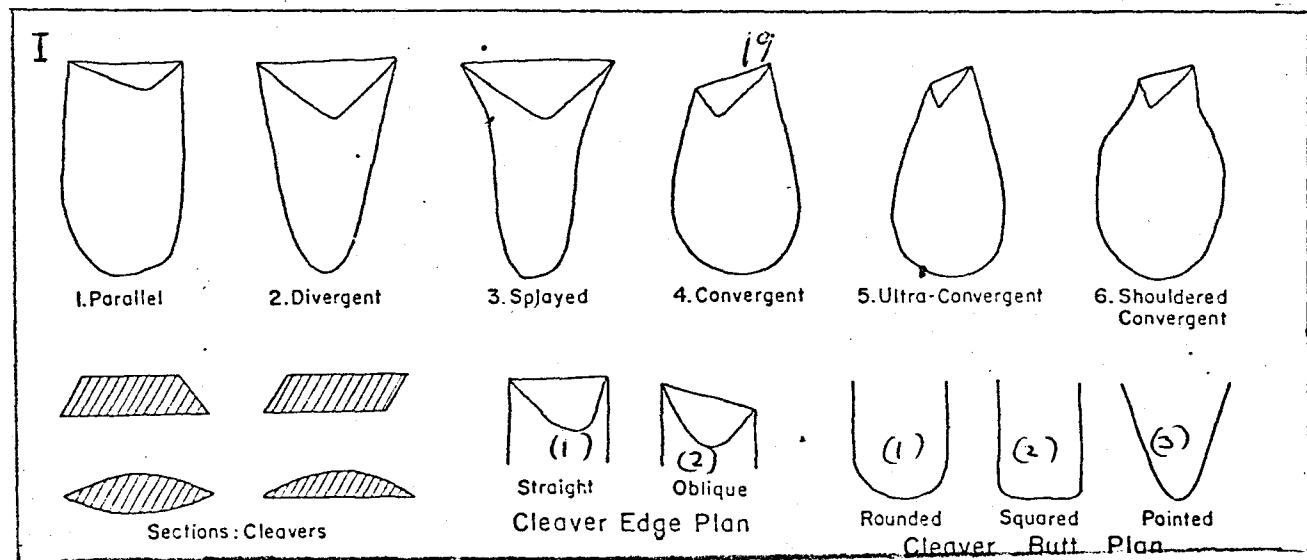
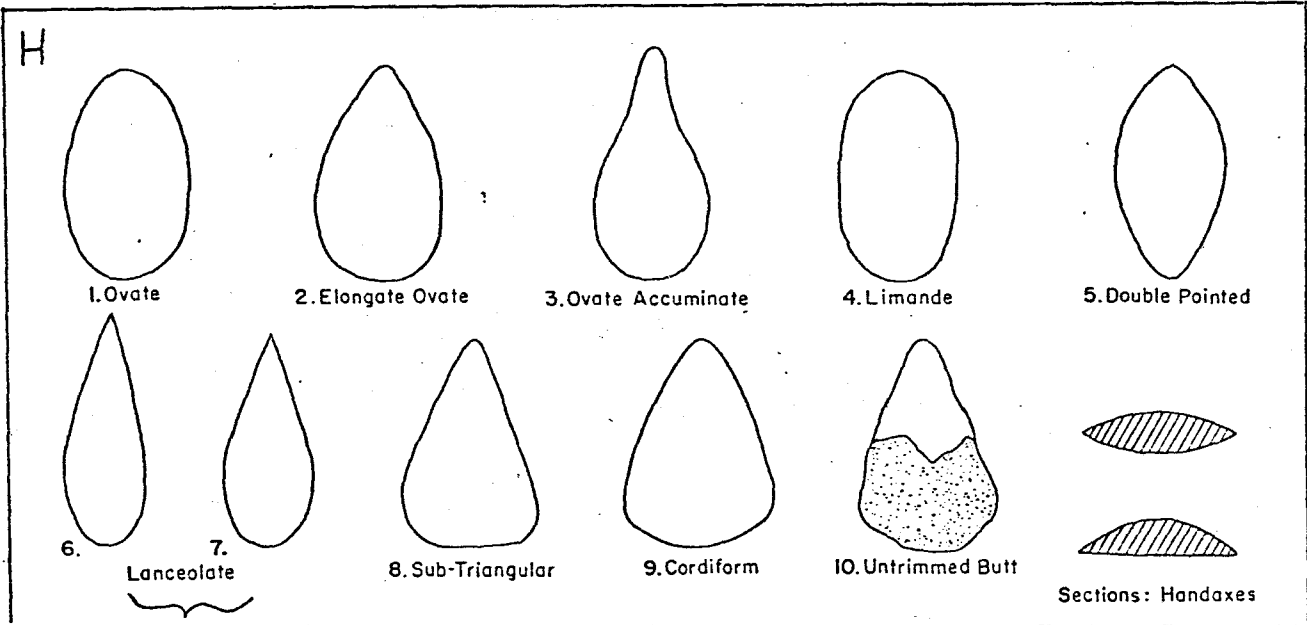
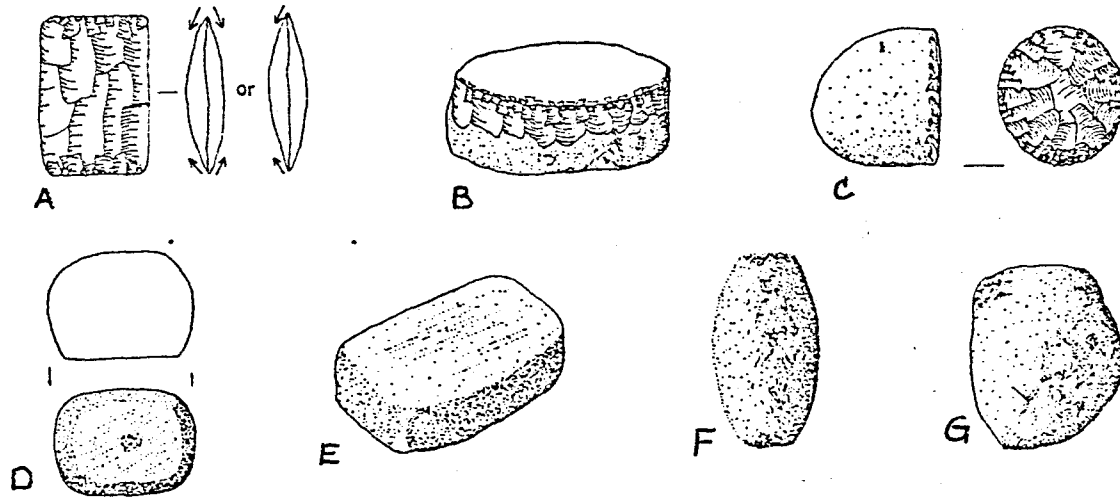
A rather crude round or oval shaped tool with very irregular edges which are formed by irregular working on both surfaces is known as a chopper. Much of the chopper is not worked at all.

Figure 4.23

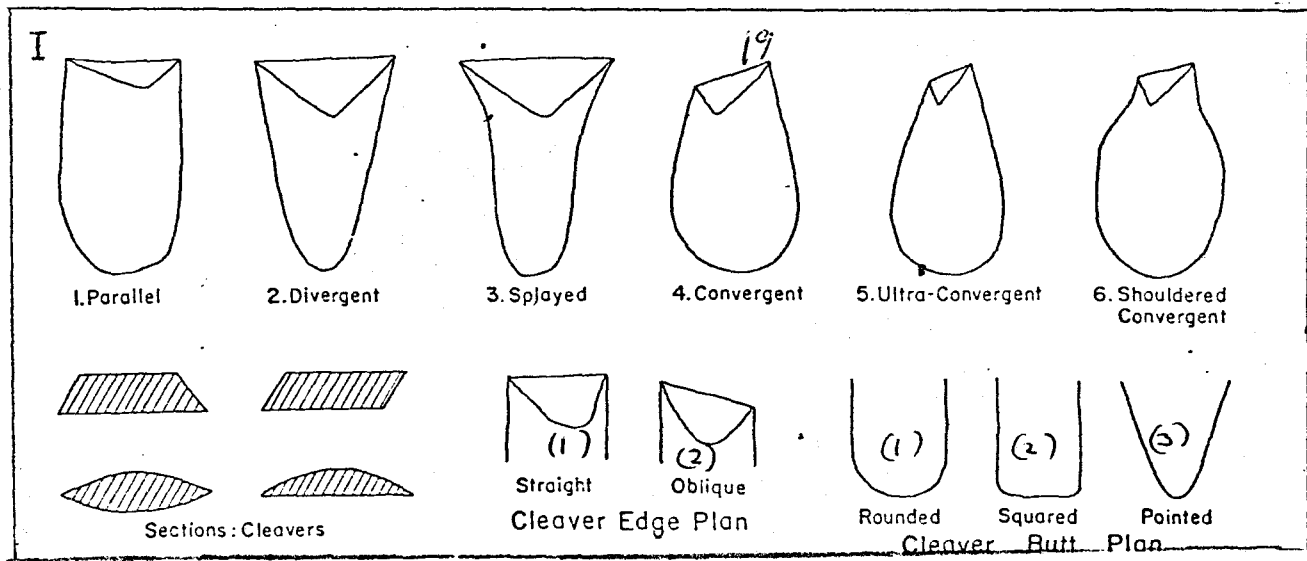
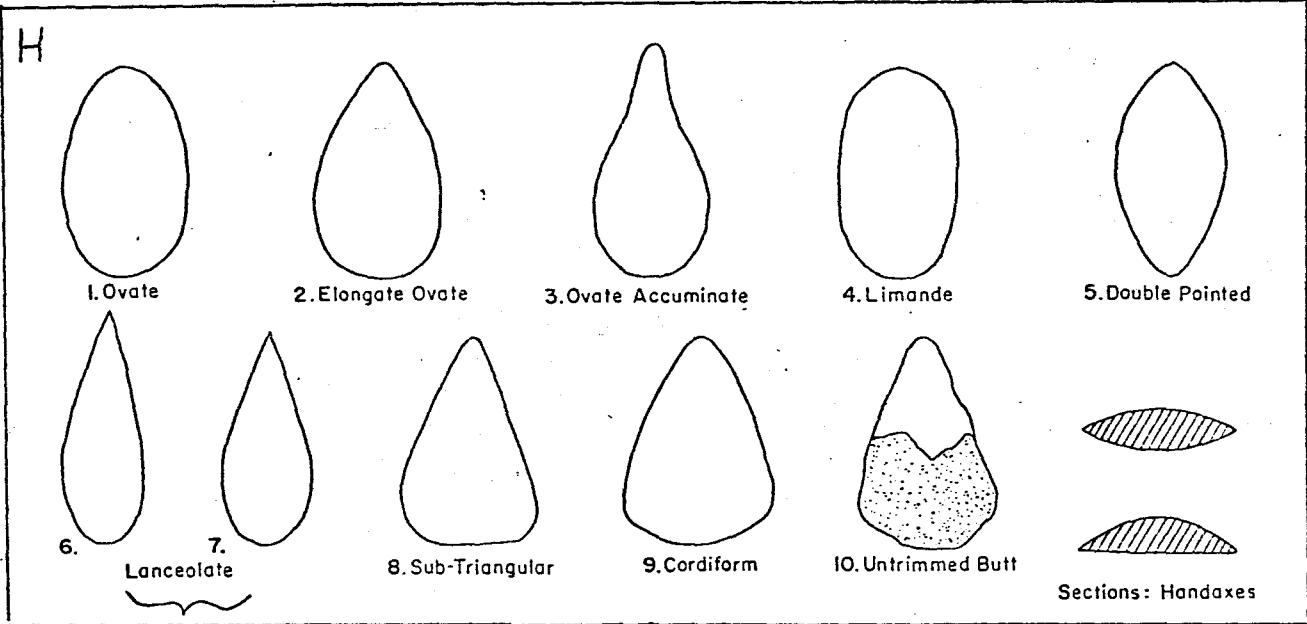
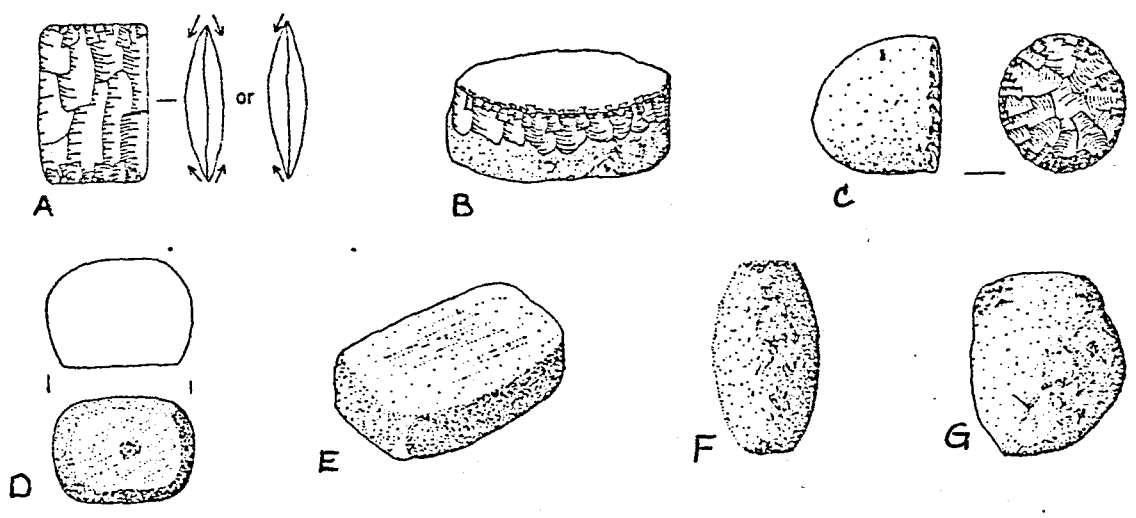
Other artefacts often found in tool assemblages:

- A. Outil esquillé
- B. Block anvil
- C. Split cobble anvil
- D. Dimple scarred rubbing tool
- E. Lower grindstone
- F. Pestle
- G. Hammerstone
- H. Handaxe types
- I. Cleaver shapes

(source unknown)







Other utilized artefacts which may be found at a site can include anvils, hammerstones, pestles, rubbing tools, and grindstones.

#### 4.5.2.5 Typological Indices

Table 4.3 lists the typological indices usually calculated for a Mousterian assemblage. These indices help to differentiate between the different types of Mousterian, discussed later. Characteristic group indices are also calculated using percentages of each group, of either the whole of the retouched tools (nos. 1 to 63) or of the restricted list (nos. 4 to 45 and 51 to 63). Because types 1 to 3 and 46 to 50 are easily produced by natural action (Bordes, 1972), eliminating these types facilitates comparisons of assemblages in which one has been cryoturbated badly but the other has not.

#### 4.5.3 Technical Indices

Technical indices are calculated for both the total and restricted tool lists. The Levallois index (LI) indicates the relative importance of the Levallois technique compared with non-Levallois techniques for the total industry. The faceting index indicates the type of striking platforms most common to an industry, while the restricted faceting index shows how important multifaceted striking platforms were when compared to the normal faceting index. The blade index suggests the degree to which the industry has progressed toward the Upper Paleolithic where blade techniques are dominant.

Table 4.3 Index Definitions

A. Technical Indices

Levallois, IL =  $\frac{(\text{Levallois flakes, blades, and points}) \times 100}{(\text{All flakes, blades, and points})}$

Faceting, IF =  $\frac{(\text{Convex, dihedral and flat faceted platforms}) \times 100}{(\text{All recognizable striking platforms})}$

Faceting, IFs (restricted) =  $\frac{(\text{Convex and dihedral faceted platforms}) \times 100}{(\text{All recognizable striking platforms})}$

Blade, Blade =  $\frac{\text{Blades} \times 100}{(\text{All blades, points and flakes})}$

B. Typological Indices \*

Typological Levallois ILty =  $\frac{\text{Tool types 1 - 4 (nonworked Levallois pieces)} \times 100}{\text{Tool types 1 - 63 (all tools)}}$

Racloir, IR =  $\frac{\text{Tool types 9 - 29 (sidescrapers)} \times 100}{\text{Tool types 1 - 63}}$

Unifacial Acheulian IAU =  $\frac{\text{Tool types 36, 37 (backed knives)} \times 100}{\text{Tool types 1 - 63}}$

Biface,\*\* IB =  $\frac{\text{Tool types 50, 55, 63} \times 100}{\text{Tool types 1 - 63}}$

Total\*\* Acheulian, IA =  $\frac{\text{Tool types 36, 37, 50, 55, 63} \times 100}{\text{Tool types 1 - 63}}$

Charentian IC =  $\frac{\text{Tool types 8, 10, 22 - 24} \times 100}{\text{Tool types 1 - 63}}$

Quina, IQ =  $\frac{\text{All Quina sidescrapers} \times 100}{\text{Tool types 1 - 63}}$

C. Characteristic Groups \*

I Levallois = ILty

II Mousterian =  $\frac{\text{Tool types 5 - 29} \times 100}{\text{Tool types 1 - 63}}$

III Upper Palcolithic =  $\frac{\text{Tool types 30 - 37, 40} \times 100}{\text{Tool types 1 - 63}}$

IV Denticulate =  $\frac{\text{Tool type 43} \times 100}{\text{Tool types 1 - 63}}$

\* All the typological and characteristic group indices can be calculated for the restricted typology by dividing the numerators listed above by the denominator (Tool types 4 - 45, 51-63).

\*\* Some archeologists prefer to use types 1 - 62 rather than 1 - 63 for the denominator of the unrestricted indices for both the typology and characteristic groups. Therefore, when the biface and total Acheulian indices are calculated, types 1 - 63 must be used. Under this system it is not possible to simply add the unifacial Acheulian and the biface indices as would normally be the case.

#### 4.5.4 Representing the Archeological Data

In addition to the tables of tool typologies, indices, raw materials, piece typologies, nuclei forms and characteristic techniques, it is common for the French to draw a cumulative graph for the tool typologies, as shown in Figure 4.24. There are many problems associated with such graphs.

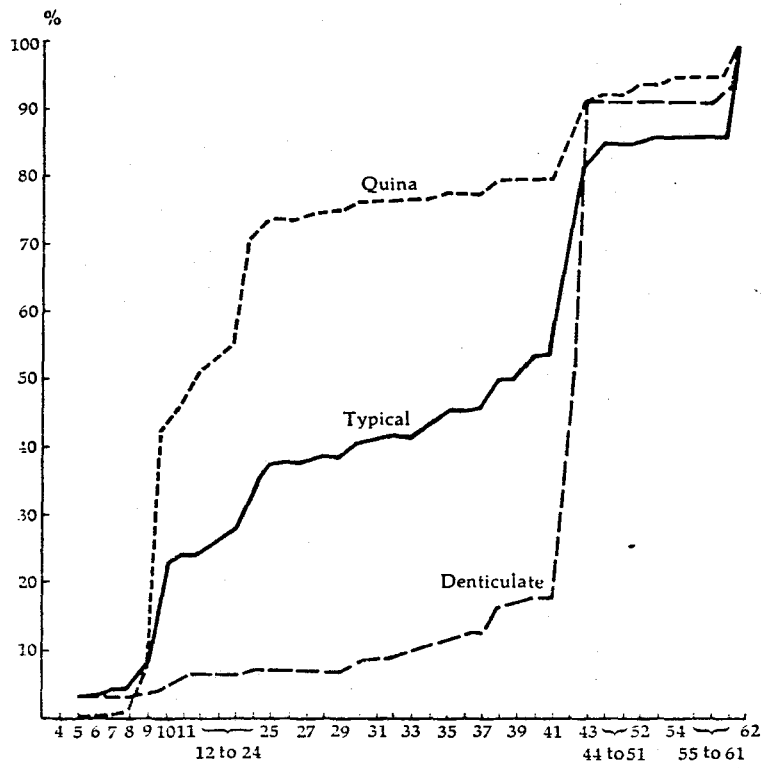
Although there is no reason for the cumulative graph to follow the same order as the type list, it does invariably, and because this order produces the differences seen and expected between different types of assemblages, it has become tautological to require it always be done that way (Webb, 1978). Furthermore, the graph treats the data as ordinal data rather than nominal (Thomas, 1971), implying that the order given has some inherent meaning. Although it may make archeological sense to order the sidescrapers, for example, from least to most complex, the order of the groups is arbitrary. Intragroup distinctions are susceptible to Q-mode statistics only, but the cumulative graph measures R-mode variations (Webb, 1978).

The fact the graph is based upon percentages creates another problem: percentages are interdependent variables. A change in one of the tool types frequencies will result in changes in all percentages. Therefore, a high frequency of any one tool, a denticulate, for example, will result in an extreme dissimilarity for two otherwise similar assemblages. Furthermore, it is difficult to compare two assemblages using percentages, because even though the total number of artefacts is known, it is hard to determine

Figure 4.24

Cumulative graphs of tool typologies:

These graphs show three of the Mousterian assemblages from Southern France as defined by Bordes. Each shows the restricted tool list (after Bordes, 1972).



exactly what significance a difference in percentages really has.

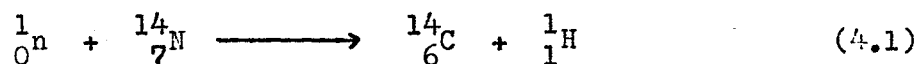
Finally, there are many problems with the visual aspects of the graph. Not only is it difficult to distinguish between artefacts whose percentages are 0, 1, and 2, it difficult to compare any two graphs if they overlap, or cross each other. Furthermore, such comparison invites value judgments, rather than statistical inference. When an archeologist claims there is a similarity between two assemblages, is he saying the overall shape is the same, or that the minute **step** pattern is the same, or that the percentage jump differences is the same? A better approach would be to calculate some coefficient of difference (Webb, 1978). Therefore, no cumulative graphs will be shown for assemblages described herein.

#### 4.6 Absolute Dating Methods Used by Archeologists

Other than the U/Th method, which has only recently been applied to sites,  $^{14}\text{C}$  and K/Ar methods have been used extensively to date sites.

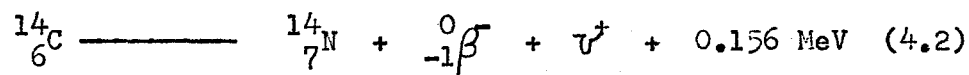
##### 4.6.1 $^{14}\text{C}$ Dating

In the upper atmosphere, neutrons produced by cosmic rays interact with nitrogen to produce a radioactive form of carbon



which then forms  $\text{CO}_2$   $\text{CO}$ . Mixing of the radioactive gases with normal gases is rapid, resulting in a constant level of radioactive gases. All living organisms assimilate the radioactive molecules

into their tissues. Because the process is in dynamic equilibrium due to the balance between decay and production, while the organism is alive, its concentration of radioactive  $^{14}\text{C}$  in the tissue will be constant. When the organism dies, however, the  $^{14}\text{C}$  is not replenished but decays to  $^{14}\text{N}$



Therefore, the age of the tissue is a function of the decay of the  $^{14}\text{C}$ . At present, the activity of  $^{14}\text{C}$  in the atmosphere is  $13.56 \pm 0.07$  dpm/g, while the half-life of  $^{14}\text{C}$  is best estimated at 5.730 Ka.

Therefore, the age,  $t$ , is

$$t = 1.209 \times 10^{-4} \ln \left( \frac{A_0}{A} \right) \quad (4.3)$$

where  $A_0$  = the present activity of  $^{14}\text{C}$  in the atmosphere

$A$  = the observed activity of  $^{14}\text{C}$  in the sample.

This, however, assumes that the activity  $^{14}\text{C}$  in the atmosphere has remained constant, which assumes the cosmic ray flux has been constant. Because the cosmic ray flux is a function of the activity within the sun and the earth magnetic intensity, it has varied significantly in the past. Therefore, the accuracy of the method has been calibrated for the past 7 Ka using dendochronology, and for the past 30 Ka using glacial varved clays (Faure, 1977).

At present, the method is only effective on samples less about 50 Ka old. Older samples contain too little  $^{14}\text{C}$  to be detected by normal methods, but a new modification using an accelerator to count the atoms (Burke, pers. comm), which may eventually make



it possible to date samples as old as 100 Ka, although the costs are prohibitive (\$ 300/sample estimated in 1979). This method, however, is the most widely used and believed of the radiometric methods, because almost all sites contain some form of carbon, either tissue or charcoal to which the method can be applied.

#### 4.6.2 K/Ar Dating

$^{40}\text{K}$ , representing  $1.18 \times 10^{-3}\%$  of all K atoms, decays by a branched pattern to either  $^{40}\text{Ca}$ , or in 11.2% of the cases, to  $^{40}\text{Ar}$  by electron capture. In minerals containing potassium, such as feldspars, feldspathoids, clays, and some evaporites, the radioactive  $^{40}\text{K}$  will decay from the time of the formation of the mineral. Argon, however, will be retained by the mineral only when it has cooled below the blocking temperature for the given crystal. In order to successfully compute a date, there should have been no initial Ar present. Therefore, the minerals usually chosen are feldspars from volcanic basalts, which have not been reheated. Given that the rock cooled rapidly, its age,  $t$ , is

$$t = \frac{1}{\lambda} \ln \frac{{}^{40}\text{Ar}^*}{{}^0\text{Ar}} \frac{\lambda}{\lambda_e} + 1 \quad (4.4)$$

where  ${}^{40}\text{Ar}^*$  = the activity of radiogenic  ${}^{40}\text{Ar}$

${}^{40}\text{K}$  = the activity of  ${}^{40}\text{K}$  present in the rock

$\lambda$  = the total decay constant for  ${}^{40}\text{K}$

$\lambda_e$  = the decay constant for the electron capture branch for  ${}^{40}\text{K}$ .

The most widely used values for  $\lambda$  and  $\lambda_e$  are  $5.305 \times 10^{-10}$  and

Samples which are younger than approximately 400 Ka do not possess sufficient radiogenic argon to be detected, and hence, are undatable by this method. In a modification of the method, using an incremental heating technique on samples irradiated with thermal and fast neutrons, heating the samples releases the argon gas which is then analyzed for  $^{39}\text{Ar}/^{40}\text{Ar}$ . This method can be used on samples very low in argon, but is very expensive.

#### 4.6.3 Thermoluminescence

Several other methods have been used in archeological sites including Thermoluminescence. This method measures the amount of radiation which a sample has absorbed since it was heated at some time in its history. When the radiation in the sample is compared to the flux in the sediments in which it was buried, a date can be established. Although this method is most often used to date pottery, it can also be used to date rocks from hearths, burnt artefacts, etc.

PEOPLES AND CULTURES  
OF THE  
MIDDLE AND UPPER PLEISTOCENE

Although the K/Ar method effectively dates sites older than 400 Ka, and the  $^{14}\text{C}$  method has been extended back to date some pieces as old as 80 Ka, there still remains a gap in the Pleistocene which can not be effectively dated by the usual radiometric methods. Unfortunately, many of the significant changes in human cultures, and the humans themselves, occurred within this period, which can only be dated with U/Th methods, or amino acid racemization. Therefore, before proceeding to discuss the sites which have been dated by the U/Th method herein, it is essential to briefly summarize the changes of the Middle and Upper Pleistocene, in terms of the climate, physical anthropology, and archeology.

#### 5.1 Terminology for the Pleistocene

Before discussing the occurrences in the Pleistocene, it is instructive to define the epoch and its subdivisions in more detail. The Pleistocene epoch is the latest of the geologic epochs, excepting the Recent, having begun between 1.5 and 2.0 million years ago (Brace, 1978; Bowen, 1978). Although the preceding epoch, the Pliocene, is now known to have had glacial advances

as well, the Pleistocene was thought to have the only Tertiary glacial advances. Lyell, who originally defined the Pleistocene, defined it to be the sequence of Tertiary rocks, with the type site in Italy, the Calabrian Formation, in which at least 90% of the fossils are living species, prior to the appearance of humans (Mintz, 1977). Although the upper boundary is now invalid, because hominids appeared in the early Pleistocene, while Homo sapiens appeared in the late Pleistocene, the lower boundary definition, based on fossil abundances, is still the strict definition. Therefore, it should not be surprising that most of the species found in Pleistocene sites are modern species, most still extant today.

Because each of the glaciations was studied in at least four different geologic regions, there is a proliferation of stage names for the various advances and retreats. Because of the proximity of southern France to the Alps, the alpine system is the one archeologists applied to refer to the various periods. Table 5.1 lists the different systems now in use, while Table 5.2 gives approximate dates for each advance, and the anthropologically important events occurring therein. Unfortunately, it is extremely difficult to correlate the different areas, thereby correlating the names, although the deep sea core record appears to show the same major fluctuations, indicating that the advances were indeed global trends (Shakleton and Opdyke, 1973), as shown in Figure 5.1. Until this problem is resolved, satisfactorily, the alpine system will be the one used archeologically, because most of the archeological literature contains this system.

Table 5.1 Terminology for the Pleistocene

		Climate	Alps	North America	Europe	Britain	
HOLOCENE		Interglacial	Holocene	Recent	Holocene	Flandrian	
PLEISTOCENE	UPPER	Glacial	Würm	Wisconsin	Weichel	Devensian	
		Interglacial	Riss/Würm	Sangamon	Eemian	Ipswichian	
	MIDDLE	Glacial	Riss	Illinoian	Saale	Wolstonian	
		Interglacial	Mindel/Riss	Yarmouth	Holstein	Hoxnian	
		Glacial	Mindel	Kansan	Elster	Anglian	
		Interglacial	Günz/Mindel	Aftonian	Cromer	Cromer	
		Glacial	Günz	Nebraskan	Menap	Baventian	
		LOWER (VILLEFRANCHIAN)	Upper	Interglacial	Donau/Günz		Waal
	Glacial			Donau		Eburon	Thurnian
	Lower		Interglacial	"Pre-Donau"		Tegelen	Ludhamian
Glacial?			Biber?		Brüggen	Waltonian	

(adapted from Flint, 1971)

Table 5.2 Chronology of the Pleistocene

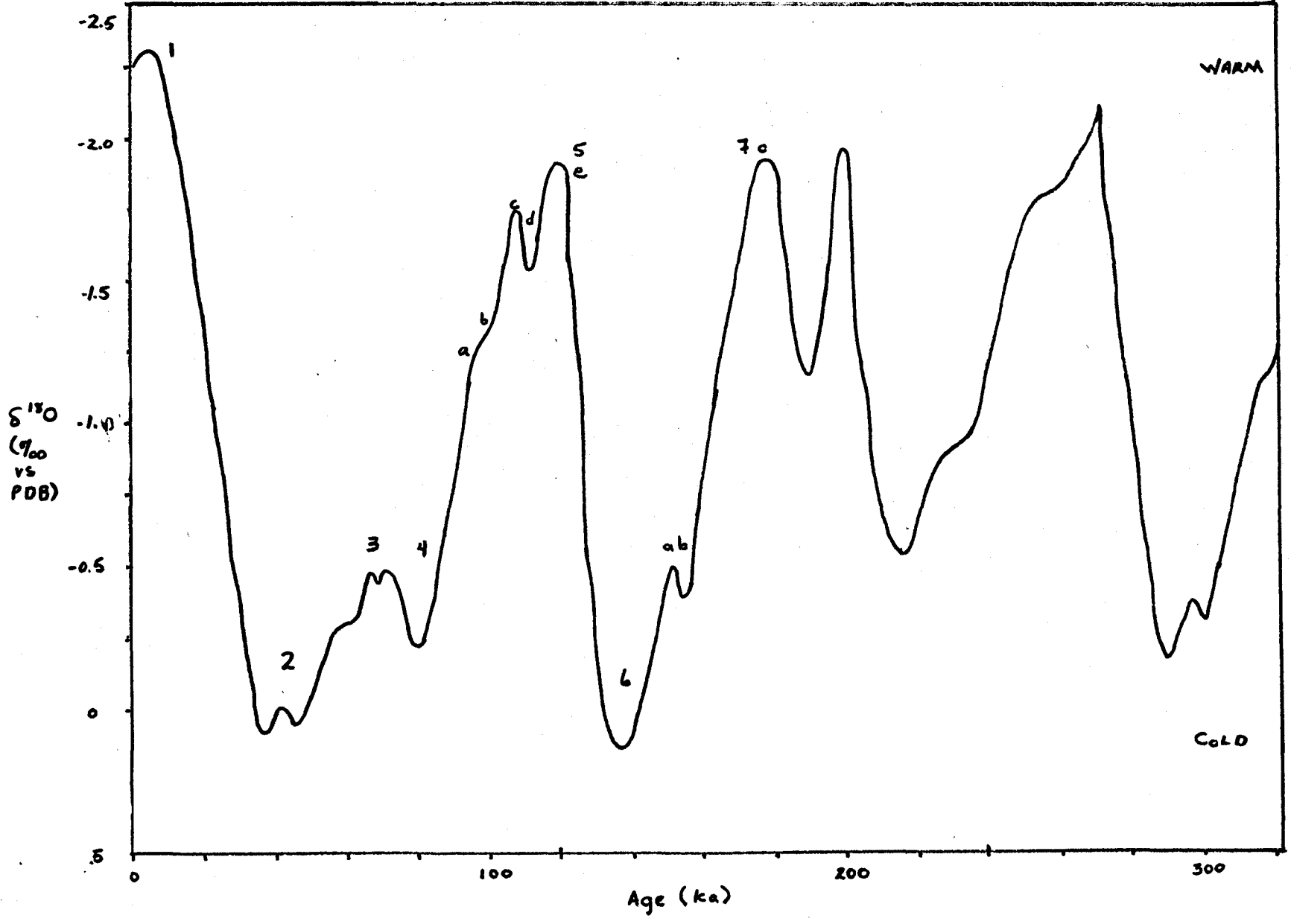
Absolute Time	Geologic Time	Glacial Period	Cultural Period	Tool Complexes	Hominid Forms
$1 \times 10^4$ y	Recent	Würm	Mesolithic		<u>Homo sapiens sapiens</u>
$2 \times 10^4$ y	Upper Pleistocene		Upper Paleolithic	Perigordian	<u>Homo sapiens neanderthalensis</u>
$4 \times 10^4$ y			Middle Paleolithic	Mousterian	
$8 \times 10^4$ y	Middle Pleistocene	Riss	Lower Paleolithic	Acheulean	<u>Homo erectus</u>
$1.6 \times 10^5$ y		Mindel		Abbevillian	
$3.2 \times 10^5$ y				Günz	
$6.4 \times 10^5$ y	Lower Pleistocene	Villefranchian	<u>Australopithecus africanus</u>		
$1.3 \times 10^6$ y	Pliocene				
$2.6 \times 10^6$ y					
$5.2 \times 10^6$ y					

(adapted from Brace et al., 1971)

Figure 5.1

Deep Sea core record for temperature change during  
the late Pleistocene (redrawn from Broecker and van  
Donk, 1970).

175





Within each of the major glaciations, there were minor periods of ameliorated climates, referred to as interstadials. For the Würm, the French archeologists recognize four stadials and three interstadials, although others would agree to only two stadials (Bordes, 1961). Since the caves under study are French, the French system will be used here. Although these may correlate with the oxygen isotope record, such that the Würm I is stage 5d, Würm II, 5b, Würm III, 4 and Würm IV, 2, it is generally agreed that stage 5 a-e represents the Riss/Würm, in which case the full four fluctuations may indeed be present on the continent, but not represented in the ocean cores. Within the Riss, there were three stadials. Of the three, the second was the coldest corresponding to stage 6.

## 5.2 Climate

During the Pleistocene, the climate fluctuated wildly, causing shifts in the ranges of animals, and flora, and in the climatic patterns of Europe. Furthermore, with each glacial advance, the sea level dropped as much as 90 m, causing the coastlines to prograde. During the glaciations, western Europe experienced a damp cold maritime climate, with associated tundra, or sparse coniferous vegetation (Howell, 1952), while in the interglacials and warmer of the interstadials, the climate was much as today, a warm maritime to Mediterranean with deciduous and parkland vegetation. Regardless of the climate, however, abundant game inhabited the region, as described in Chapter 4.3. Western

Europe, however, was separated from Russia and Asia by a periglacial climatic intrusion, as shown in Figure 5.2, extending from the Bradenburg Lobe of the Fennoscadian Sheet to the Alpine Sheet. Although this region was never completely glaciated, as a highland region it apparently made an effective climatic and topographic barrier, greatly restricting the movement of game and hominids between Eastern and Western Europe.

If the positions of the terminal moraines of the major advances are any indication of the severity of the glaciation, the Mindel was the most severe in Europe, but the Riss was more extensive in Russia. In terms of length, however, the Mindel appears to be far longer than the younger two, having had apparently four major advances over some 150 ka. No one, however, will date the Mindel for certain: estimates range from 0.3 to 1.2 Ma (Flint, 1971; Bowen, 1978; Mintz, 1977). The Riss is more accurately dated, with most agreeing that it began about 190 ka and ended about 120 ka, while the best estimates for the beginning of the Wurm are about 80 ka. With such disagreement among the experts for the correlation of the glacial advances and the dating thereof, it gives one pause as to how the archeologists can say with such certainty which cold snap in the cave is related to which stadial.

### 5.3 Pleistocene Hominids

Within the context of the Pleistocene, Homo sapiens sapiens evolved from the Australopithecines of the Pliocene.

Figure 5.2

Climatic zones during the Würm glaciation:

1. Glacial maritime
2. Maritime tundra
3. Maritime forest (including the Charente and Dordogne)
4. Permafrost tundra
5. Continental glacial
6. Permafrost forest
7. Cool steppe
8. Warm steppe

-x-x- Maximum limit of permafrost

-|-|- Northern limit of forest

— Maximum limit of glacial advance

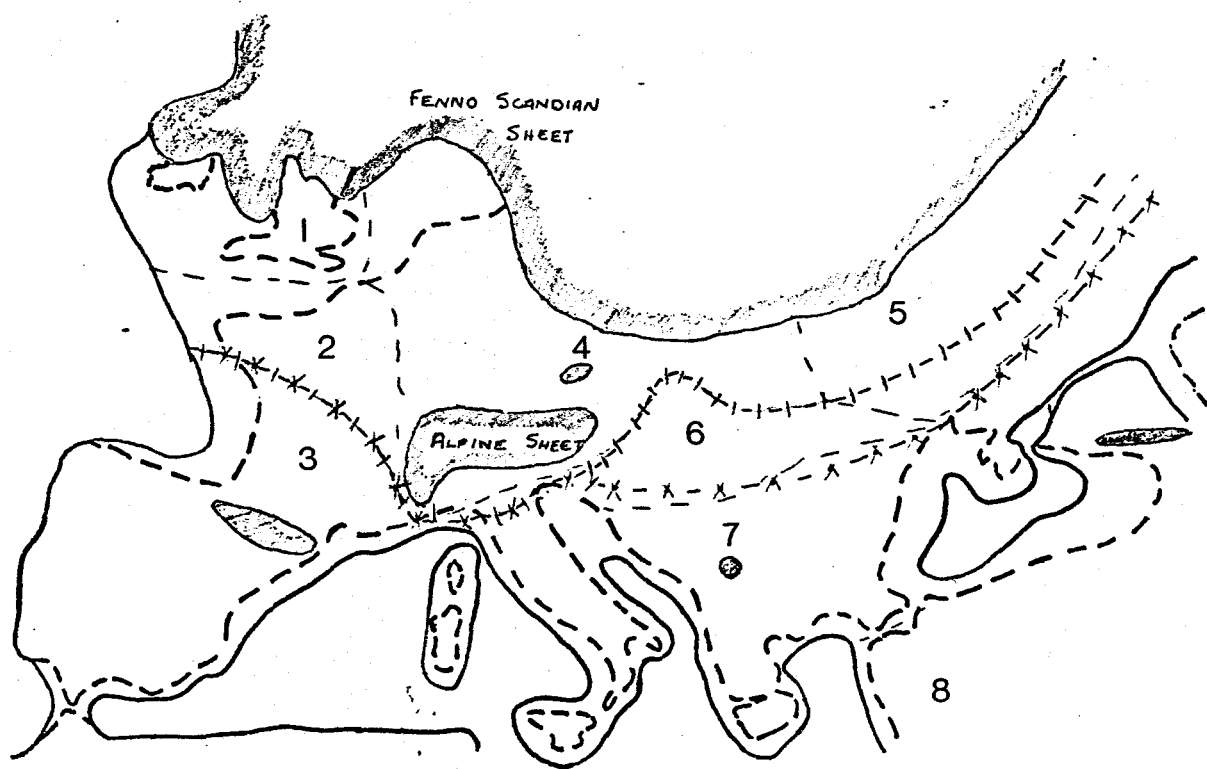
- - - Climatic zone boundaries

— Present coastline

— Coastline during maximum advance

(90 m isobath)

(adapted from Howell, 1952)



### 5.3.1 Homo erectus

Prior to the development of Homo sapiens, the dominant hominid in the world was H. erectus, known to have ranged over much of the temperate and tropical Old World. Extant from approximately 1.7 Ma (Brace et al., 1979; Leakey and Lewin, 1977) to 150 Ka, French finds are restricted to post-Mindel times comprising, among others, three individuals from Arago in the Pyrenees, and two partial calottes from Fontchevade, across the river from Lachaise (Brace et al., 1971, 1979). Although the cranial capacity of H. erectus averages from 750 to 1050 cc, as compared to 1150 for H. sapiens, H. erectus finds are associated with the use of fire at Choukoutien and Torralba, organized hunting by bands at several sites, and the use of shelters at Terra Amata (Fagan, 1974).

Anatomically, the skull of H. erectus looks very primitive with massive suprorbital tori, a post-orbital constriction, a sagittal keel, an occipital bun complementing the angulated but platycephalic thick boned vault, a large robust mandible with no chin but slightly prognathic face, while the post-cranial skeleton is almost identical to that of modern humans, Figure 5.3 is the classic "Pekin Man", while 5.4 shows Arago and Fontchevade.

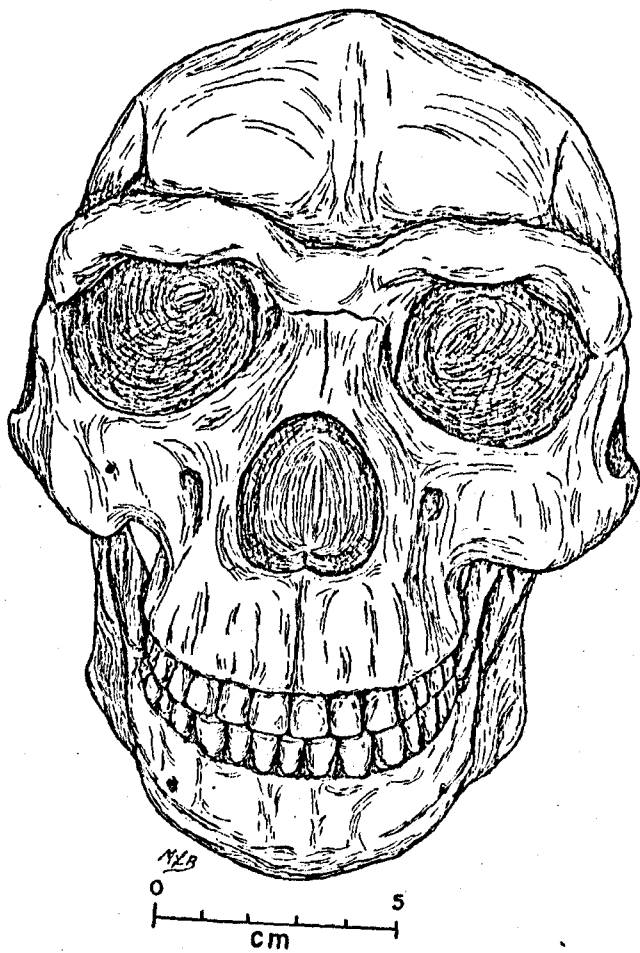
Some of the late forms in Europe are often considered to be transitional from H. erectus to H. sapiens. Because the finds are often fragmentary, the exact species is often difficult to determine. Fontchevade is one such find dated relatively to the late Riss. It may possibly be a "classic" Neanderthal. Two individuals from nearby Lachaise also pose similar problems to be

Figure 5.3

Homo erectus:

One of the classic examples of H. erectus, "Pekin Man", found at Choukoutien, near Peking, in 1929. This female is one of more than forty individuals found at the site, all of which were lost during the Japanese invasion in 1936. This specimen is guessed to be about 700 Ka old (after Brace et al., 1979).

"Pekin Man"



"Pekin Man"

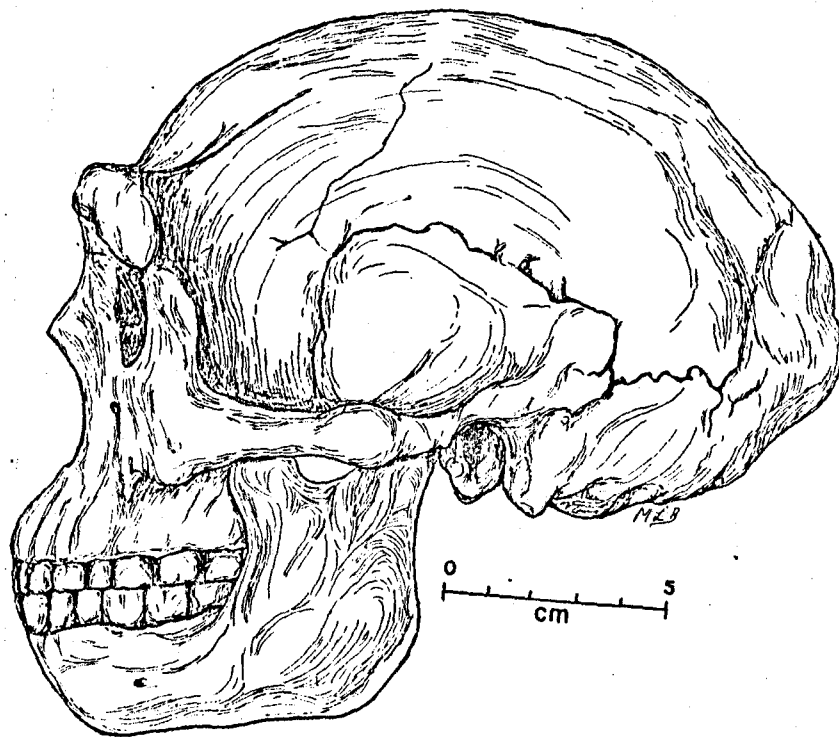


Figure 5.4

Homo erectus in Europe:

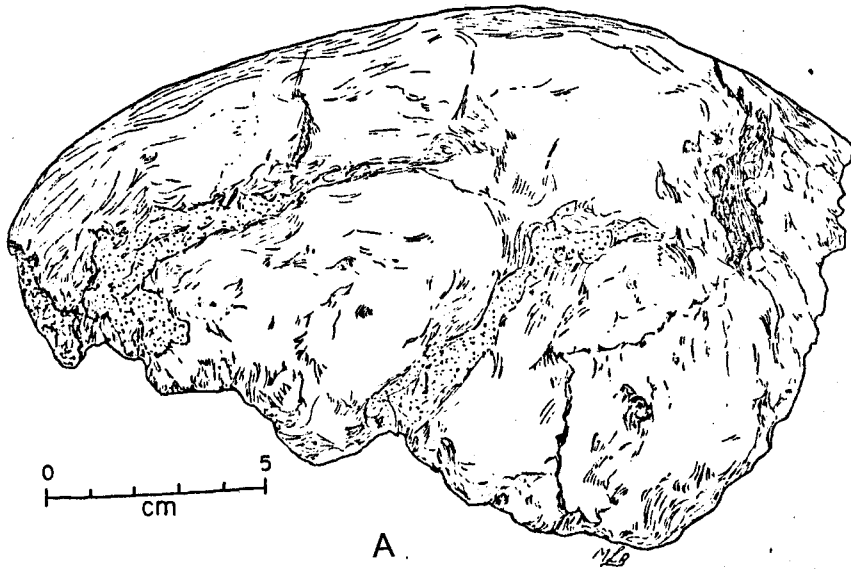
- A. Fontchevade: Partial cal tte, one of two individuals found in Fontchevade, Charente by Mlle. Henri-Martin in 1947. Because it lacks teeth and facial skeleton, it is of uncertain afinities. It is guessed to be about 115 Ka.
- B. Arago XXI: One of many individuals found in la Caune de l'Arago in the French Pyrenees by de Lumley in 1971. This is the first certain H. erectus in Europe, dated at about 200 Ka.

(after Brace et al., 1979)

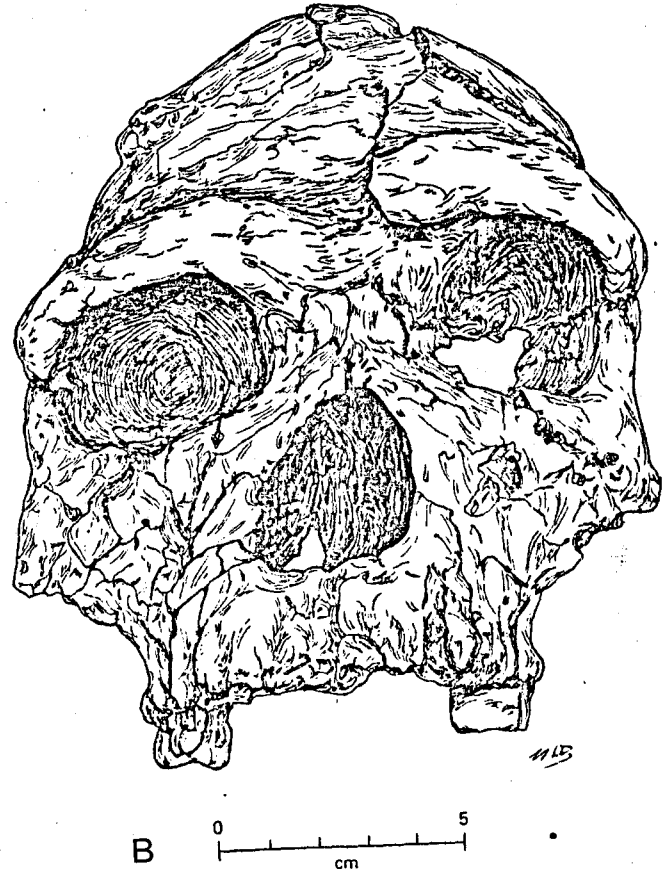


H 81

"Fontéchevade"



"Arago XXI"



discussed later.

### 5.3.2 Neanderthals

Although there are many conflicting definitions of "Neanderthal" and "Neanderthaloid" (Brace et al., 1977; LeGros Clark, 1965, Howells, 1974; Howell, 1957; Trinkaus and Howells, 1979; Brace, 1978), all of which are confusing, some of which have inherent errors in the application of evolutionary theory, some of which are extremely misleading, and none of which the experts can agree upon, the best definition seems to result if "Neanderthal" is considered as a morphological grade, similar to, and temporally preceeding H. sapiens sapiens.

Therefore, in general, a Neanderthal possessed a brain whose cranial capacity was within, but often averaged more than that of modern human populations, but whose frontal and occipital bones were more rounded than those of H. erectus. Surmounted by massive supraorbital tori, the facial skeleton is usually large with rounded orbits, separated by a great interorbital distance, housing large anterior teeth. As a population, they had a high frequency of taurodont molars, but a low frequency of well-developed mastoid processes, and mental eminences. Using this definition, it is possible that Neanderthals existed contemporaneously with the so-called "pre-sapiens" forms in the Riss, and with H. sapiens sapiens in the mid-Würm, as Jelinek (1969) states may have occurred in several places. Moreover, this allows for the **contemporaneous existence** of several Neanderthal populations, partially isolated

by the Würm glaciers. Therefore, the Neanderthals, while they were extant as a subspecies, H. sapiens neanderthalensis, were polytypic, but achieved nearly worldwide distribution (see Figure 5.5).

#### 5.3.2.1 "Classic" Neanderthal Morphology


When the majority of people hear "Neanderthal", they envision the "classic" Neanderthal crouching in his cave with his club. With a short but powerful build, these "classic" forms inhabited southwestern Europe during the late Riss/Würm, and Würm I and II. Specifically, they possessed a broad upper thorax supported by a vertebral column with low-bodied vertebrae, marked by large spinous and transverse processes. In the pectoral girdle, the scapula had a well-developed sulcus and auxiliary crest supporting the robust arm. In addition to massive bones, especially in the articular regions, the radius and ulna curve noticeably, unlike those of modern humans. As in the arms, the bones of the legs are massive with enlarged articular surfaces, while both the tibia and femur also curve. The radiohumeral index is 70 - 79 on average, while the tibiofemoral index is low, 74 - 79. The femur is platymeric, while the tibia is eurymeric (Bass, 1971). Squatting facets appear on both the tibia and fibula. With a long heel, the calcaneum is massive. In both extremities, the metacarpals, or -tarsals, are long and massive, while the phalanges are short in comparison (Howell, 1957). (See Figure 5.6)


The major differences, between Neanderthals and moderns, however, occur in the cranium. Perhaps the most noticeable feature

Figure 5.5

Neanderthal sites:

1. Neanderthal
2. Spy
3. Ehringsdorf
4. La Chapelle-aux-Saints
5. Le Moustier
6. La Ferrassie
7. La Quina
8. Gibraltar
9. Saccopastore
10. Monte Circeo
11. Krapina
12. Teshik Tash
13. Shanidar
14. Mount Carmel
15. Haua Fteah
16. Jebel Irhoud
17. Dire Dawa
18. Cave of the Hearths
19. Mapa

 Cold-adapted Mousterian

 Unspecialized Mousterian-like

(after Brace et al., 1979)

Figure 5.6

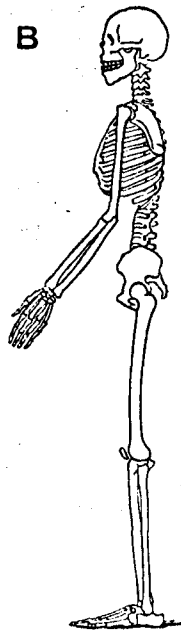
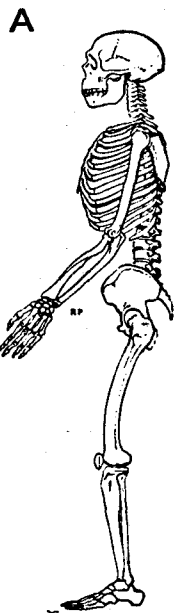
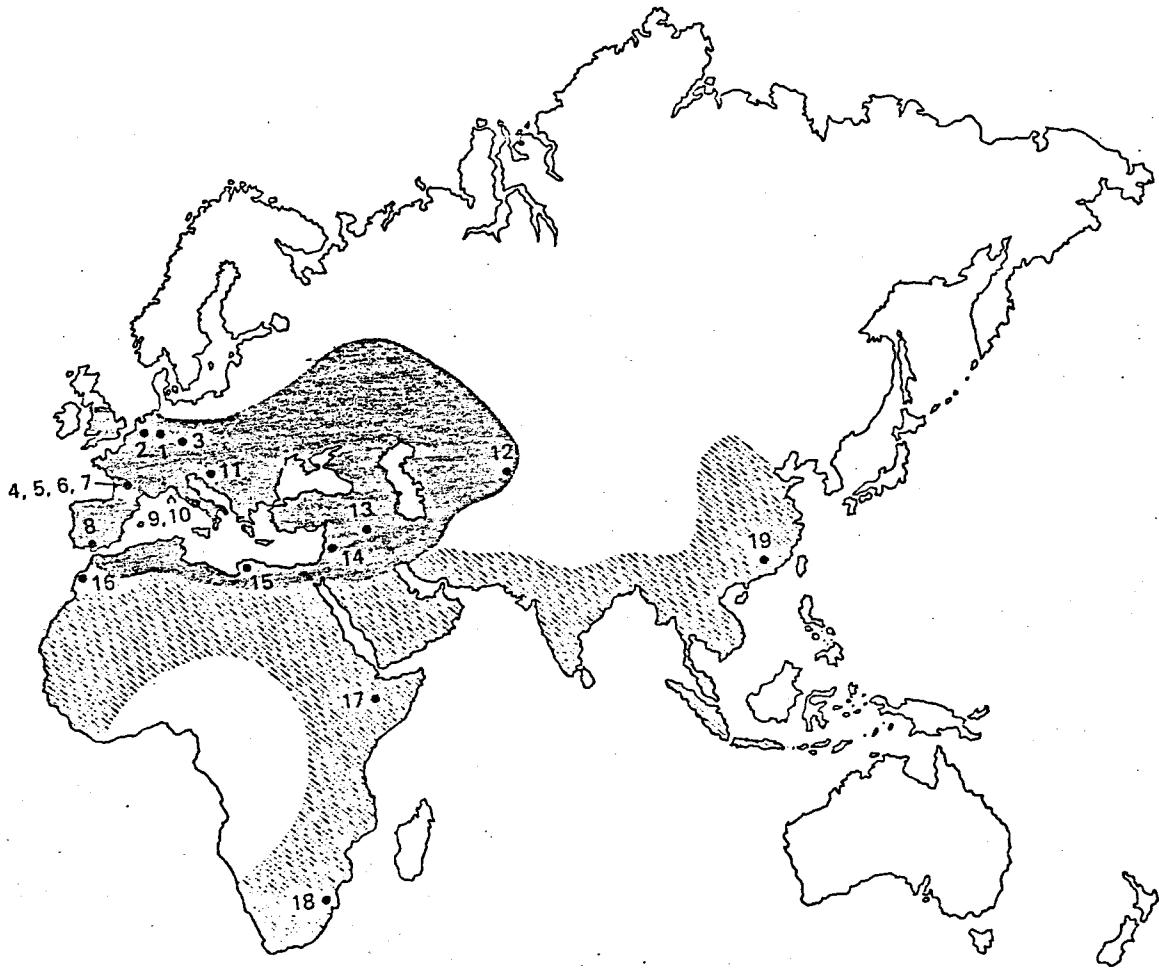
Comparative anatomy for Homo sapiens subspecies

A. H. sapiens neanderthalensis, classic

form

B. H. sapiens sapiens

(after le Gros Clark, 1965)



is the large facial skeleton, particularly the large nasal aperture, great interorbital distance, and the large rounded orbits, topped by a massive supraorbital torus composed of fused medial and lateral elements. Compared to modern humans, the "classic" forms have longer, lower, wider vaults, with a high frequency of postlambdaoidal flattening, a more sharply angled occipital with the occipital bun, and a less flexed basiocranial angle (Howell, 1957). In most forms, the mastoid process is small, the external auditory meatus ellipsoidal, the molars torodont, and the anterior teeth large. Usually, no mental eminence is present. Generally, the bones are thick and robust.

Yet this description is not indicative of the whole Neanderthal population, but only a small percentage which was isolated in southwestern Europe, subject to the vagaries of genetic drift during the early Würm.

#### 5.3.2.2 Other Neanderthals

Unlike the "classic" forms, the Neanderthals of Eastern Europe and the Middle East were not isolated as a small population, but remained as a widely distributed group experiencing constant gene exchange. As a population, these forms present a great deal of morphological variability. Although most individuals possessed some of the classic features, none of them have the full complement, as the "classic" forms do.

Compared to the "classic" forms, the Eastern Neanderthals are significantly different in several aspects. Using discriminant analysis and intergroup distances,  $D^2$ , based upon Gower's Q

mode analysis, Bilsborough (1972) found that the eastern forms differ from the "classic" forms in the upper face and cranial vault at the 0.001 level, and overall at the 0.001 level. Table 5.2 lists the significant points. Between the eastern forms and H. sapiens sapiens, there is an overall significant difference, but it is larger than that between the two Neanderthal populations. Similarly, the "classic" forms differ significantly from modern humans. Therefore, it seems consistent to consider the two Neanderthal groups as partially isolated populations of the same subspecies, which is, in turn, different from the modern subspecies.

The Eastern Neanderthal population conforms to the pattern expected of a population undergoing gradual evolutionary modification. As the genetic pattern of the population is modified, any individual may or may not possess one of the old traits, or the new trait. Because the rate of change of any gene will proceed at different speed the population will appear as a mosaic of traits, both old and new. Therefore, the eastern forms were probably evolving constantly throughout the Wurm.

Yet the classic forms apparently evolved into a highly specialized group. Because they were isolated during the critical period of the change, genetic drift acted to eliminate many of more modern-appearing alleles. Because the isolation was of short duration, when the populations were reunited, they were still capable of interbreeding, with the result that in a few generations, the two populations were indistinguishable. Figure 5.7 shows two "classic" Neanderthals from Monte Circeo and Shanidar, while 5.8

Table 5.3 Differences between "Classic" and Eastern Neanderthals and Homo sapiens sapiens.

Functional Complex	"Classic" vs Eastern Neanderthals	"Classic" Neanderthals vs <u>H. sapiens sapiens</u>	Eastern Neanderthals vs <u>H. sapiens sapiens</u>
Upper face	8.5**	5.1**	7.1**
Upper jaw (sic)	2.4	1.9	3.4
Mandible	3.0	5.4**	5.6**
Cheeks & masticatory muscles	3.5	3.5*	7.7**
Articular region	1.2	0.8	0.9
Balance	1.9	4.3**	4.4**
Vault	8.5**	8.9**	5.4**
Basicranium	4.8*	4.5**	1.3
Overall	5.2**	8.4**	8.7**

\*  $D^2$  significant at 0.01 level

\*\*  $D^2$  significant at 0.001 level

(after Bilsborough 1972)



Figure 5.7

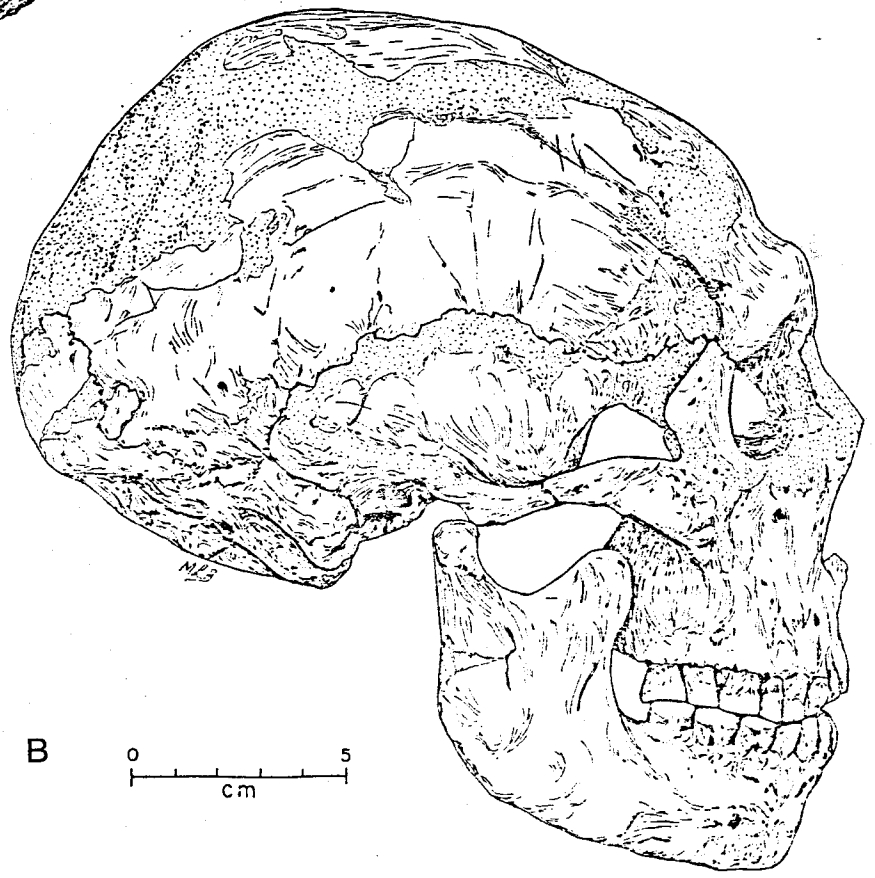
Homo sapiens neanderthalensis, "classic" form:

- A. Monte Circeo: An adult male skull, one of three individuals found south of Rome, Italy in 1939. It is thought to be from the early Wurm.
- B. Shanidar I: One of eight or more skeletons associated with Mousterian artefacts found in Shanidar Cave, Iraq, by Ralph Solecki. It is dated by  $^{14}\text{C}$  to just less than 50 Ka. This adult suffered from a deformed right arm which was amputated and may have been blind in the left eye.

(after Brace et al., 1979)



A



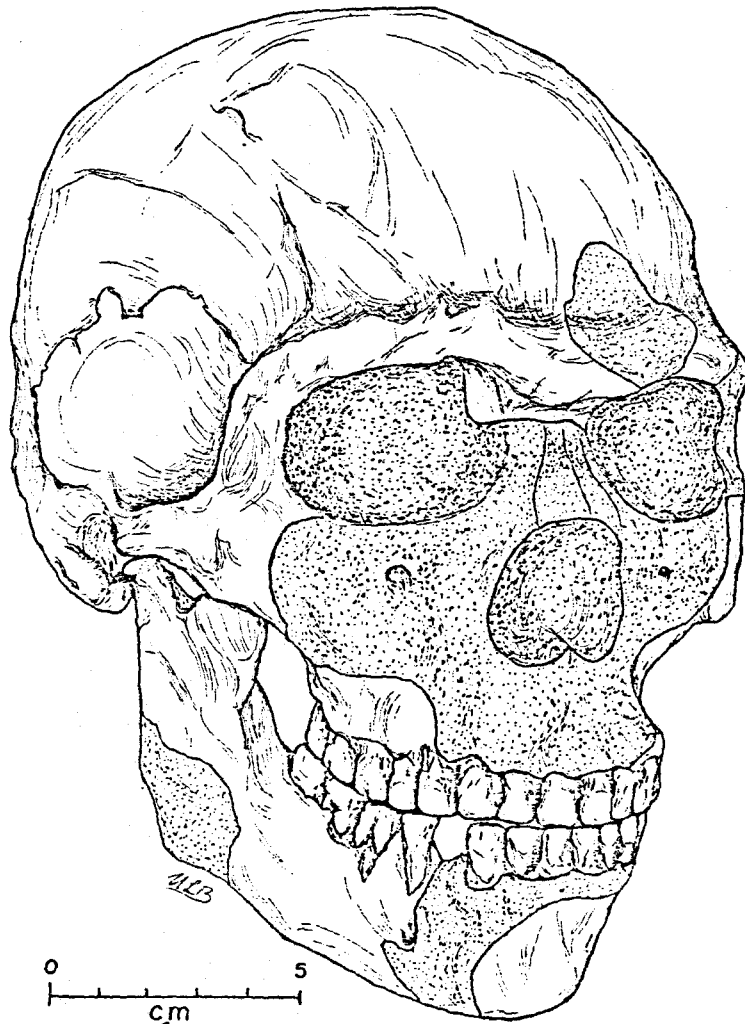
B

Figure 5.8

An Eastern Neanderthal:

Skhul V: An adult male skull with complete post-cranial skeleton, one of ten individuals associated with Mousterian cultural remains at Mugharet es-Skhul, Isreal. This more unspecialized Neanderthal is estimated to be about 40 Ka old (after Brace et al., 1979).

"Skhül V"



shows an eastern form from Skhūl, along with the distribution of the entire Neanderthal population.

### 5.3.3 Homo sapiens sapiens

The earliest true H. sapiens sapiens appeared in Europe about 30 to 35 Ka BP, perhaps slightly earlier in the Middle East. Although the skulls are still robust, a definite chin (mental eminence) is present, while the majority of the Neanderthal characteristics listed above have disappeared. The Cro-Magnon skull, found in 1868 at Tayac near les Eyzies, is still often considered to be the classic example of the earliest true man, although its date, stratigraphy, and exact original location are in doubt. (see Figure 5.9).

## 5.4 Pleistocene Cultures

During the Pleistocene, hominids learned to control fire, build shelters, shape stone into a variety of sophisticated tools, use wood and bone as tools, and create art.

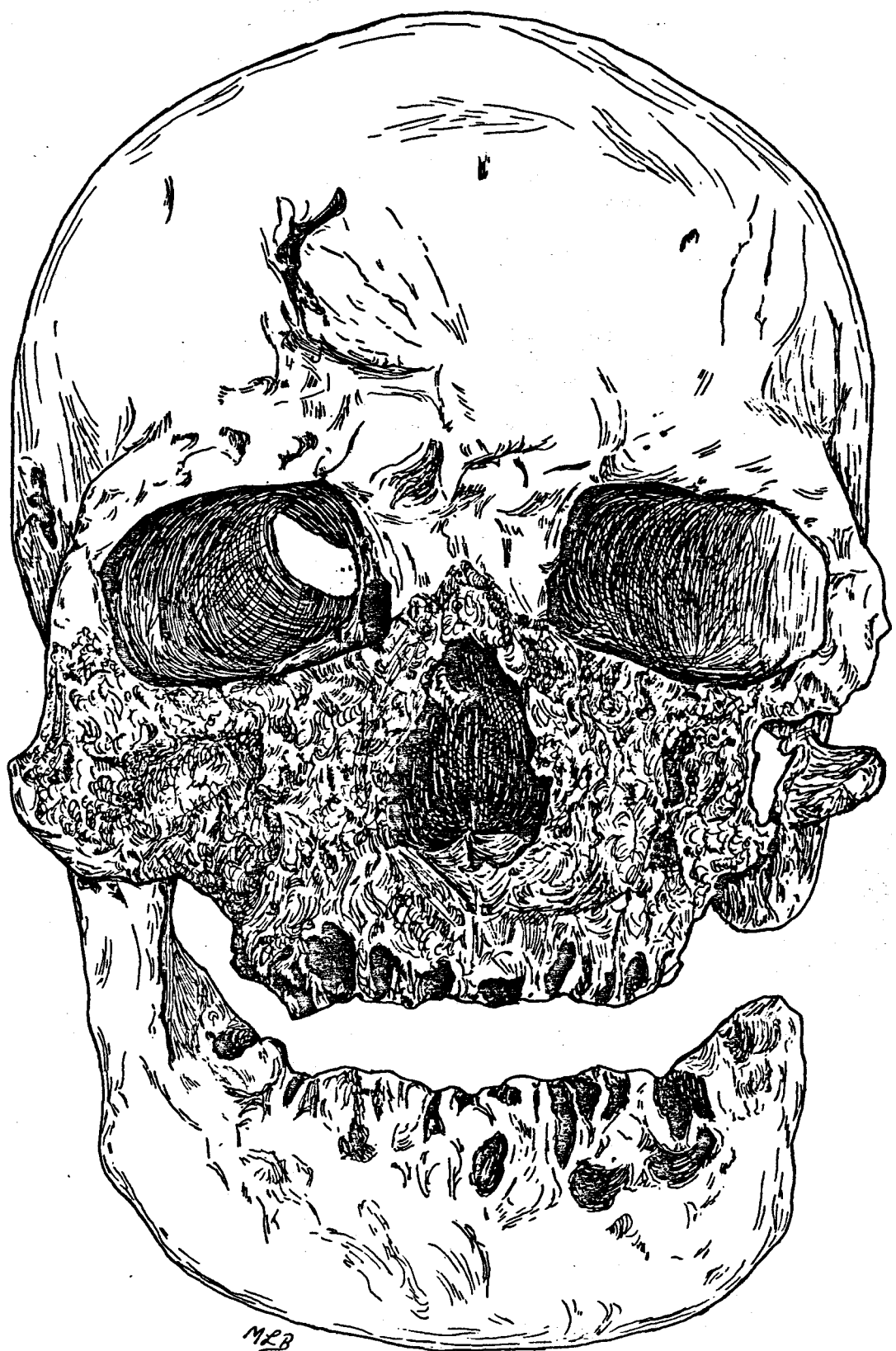
### 5.4.1 The Acheulian

Appearing first in Africa about 1.5 Ma, then appearing later in Europe during the late Gunz/Mindel, the Acheulian tool kit comprised mostly handaxes and cleavers, as shown in Figure 4.23. In addition, choppers and spheres, which may have been used in food preparation, can be found in most Acheulian sites. The first known example of the use of wood is an Acheulian spear from Clacton, England. Bone or wood may have been used to rework the final

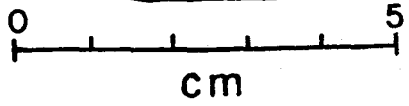
Figure 5.9

The Cro-Magnon Skull, H. sapiens sapiens:

Discovered by Lartet in an abri near les Eyzies, this skull, along with five skeletons and Upper Paleolithic tools, is thought to be about 30 Ka. It is uncertain, however, because the skull was found out of stratigraphic context. Although the teeth, and parts of the face are missing, the skull is still very robust, although it does lack the prominent brow ridges and sports a true chin. This is the specimen most people remember when talking about early modern men (after Brace et al., 1979).



MRB



tools, in some of the later kits. With time, the culture gradually evolved to include flakes of either proto- or true Levallois technique, cores, and a variety of tools more typical of the Mousterian. Eventually, more tools were made using flakes, with continually more advanced techniques for flake production (Bordes, 1968). More detailed descriptions of the typical Acheulian tool kit can be found in works by Clark and Kleindienst (1974), Kleindienst (1961), Leakey (1971), and Roe (1964).

Containing no handaxes, the Clactonian flake tradition used an anvil in the production of the flakes, which was derived from the chopping tool traditions of the East, rather than the handax traditions of the West. Most of the tools in the Clactonian are worked flint or quartzite nodules. Of the flake tools, many are scrapers, notched pieces, denticulates, or truncations. According to Bordes (1968), the Tayacian tradition is a late development of the Clactonian.

Named for the type site of la Micoque, the Micoquian is classified as a Mousterian kit purely on the basis of chronology, although it is an Acheulian tradition found in the Wurm 1. Differing from the Mousterian of Acheulian Tradition only by the presence of the typical Micoquian handax, a lanceolate form with concave edges, this assemblage uses the Levallois technique occasionally. In some sites, la Quina sidescrapers can be found (Bordes, 1968).

As can be seen in Figure 5.10, the varieties of the Acheulian were widely distributed throughout the world. Because it is

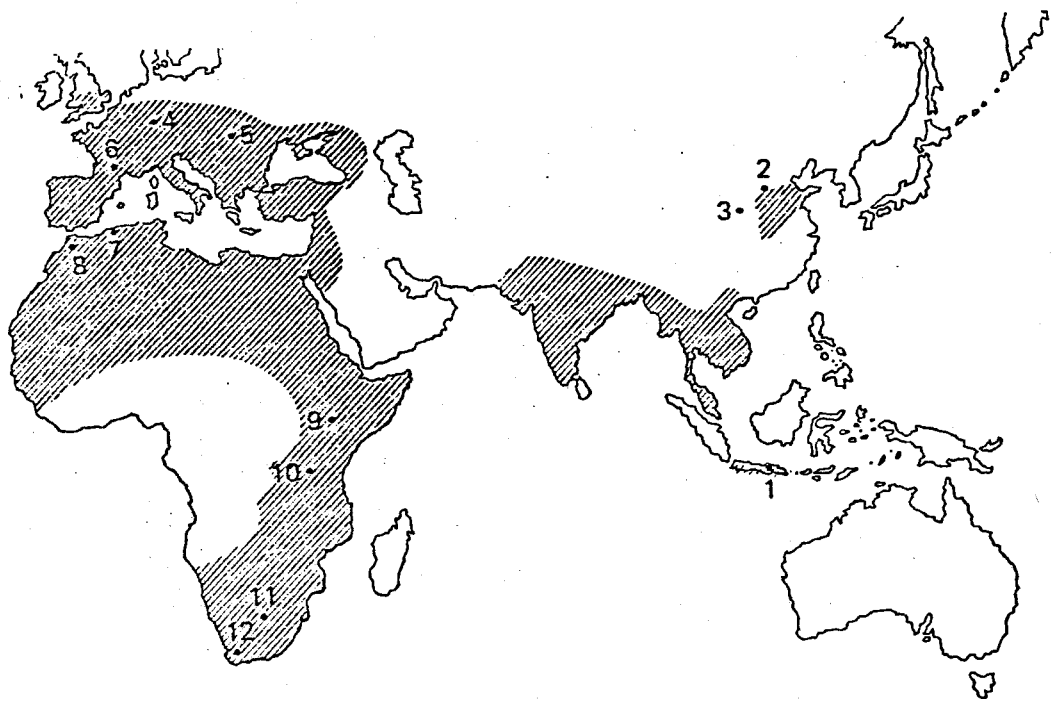


Figure 5.10

Distribution of Lower Paleolithic industries  
associated with H. erectus:

1. Java
2. Choukoutien
3. Lan-t'ien
4. Heidelberg
5. Vertesszöllös
6. Arago
7. Ternifine
8. Rabat
9. Koobi Fora
10. Olduvai Gorge
11. Swartkrans
12. Saldanha

(after Brace et al., 1979)



the tradition ancestral to the Mousterian, its tools, are less sophisticated technologically, while the variety of tool types is more restricted.

#### 5.4.2 The Mousterian

Having its roots in the Acheulian, the Mousterian is usually thought to have begun at approximately the same time as the Würm, circa 80 Ka BP, lasting until the appearance of the Perigordian during the Würm II/III, 35 Ka. In France, where the Mousterian was first defined, there are several tool kits recognized, along with at least as many theories for their coexistence.

Probably related to the industry at la Micoque, the Typical Mousterian assemblage employs the Levallois technique, shown in Figure 5.11, to varying extents. Very rarely does it contain limaces, handaxes, or backed knives, but sidescrapers comprise between 25 and 55% of the total tool kit, with la Quina types contributing 1% at most. Well-developed points are present, but notched pieces and denticulates add only a few percent to the total. According to Bordes (1961, 1968), this assemblage is found in sites dated from the earliest Würm I to the upper Würm II. There may be two subtypes of this assemblage with varying percentages of sidescrapers (Bordes, 1972). Le Moustier is the type site.

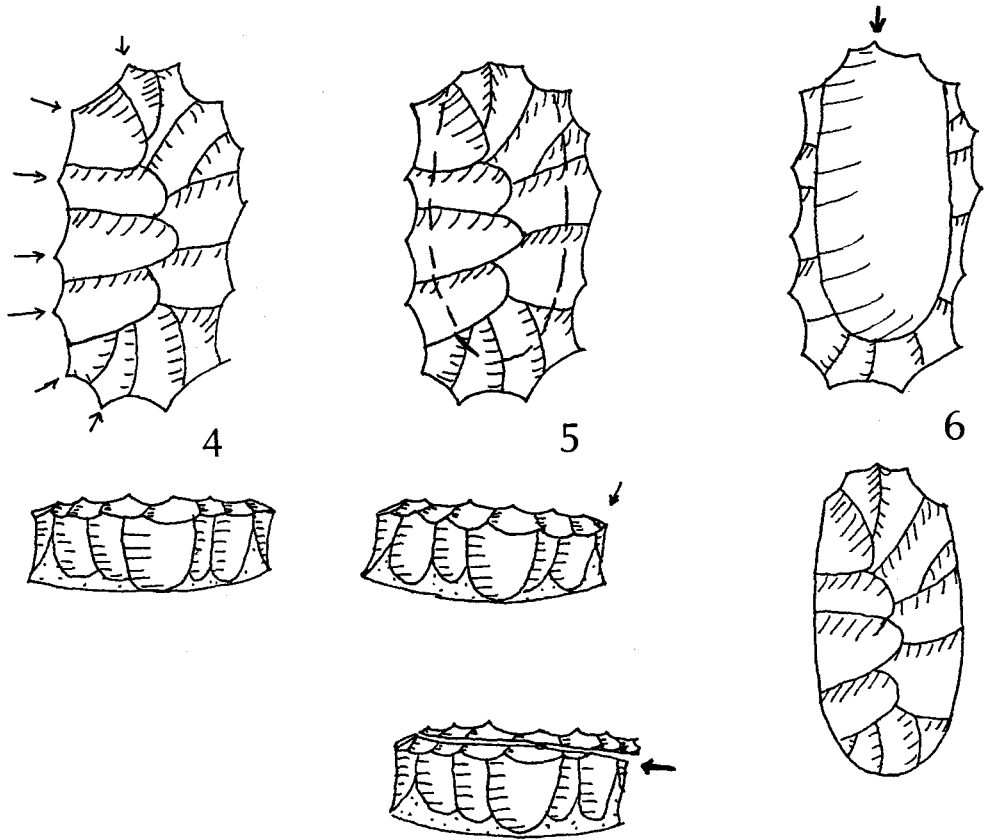
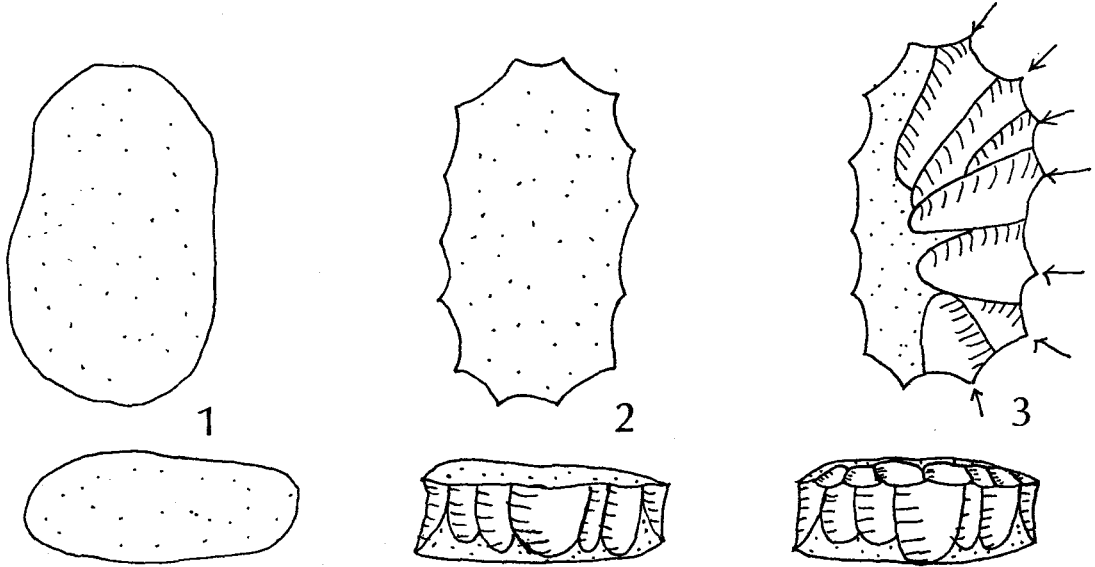
Named after the site of la Quina, la Quina Mousterian is also found from the lower Würm I to upper Würm II. Of the total kit, scrapers comprise 50 to 80%. Most of these, sidescrapers

Figure 5.11

The production of Levallois flakes

1. The original core
2. Flaking off the lateral edges
3. Flaking off the dorsal surface
4. Continued dorsal flaking
5. Preparation of the final striking platform
6. Removal of the Levallois flake

(adapted from Bordes 1961).



tranchoirs, and limaces included, have resoled or thick scleriform retouch (Quina retouch). Sidescrapers may contribute up to 75% and la Quina types up to 25% of the total. Other types include denticulates, notched pieces, burins, borers, and endscrapers, including nosed and carinated types. Among the tools rarely found in this kit are backed knives and handaxes. The Levallois technique is not used as frequently to produce the tools of la Quina Mousterian as in the Typical Mousterian. Bordes (1961) feels la Quina Mousterian may have its origins in the Tayacian or the Clactonian Acheulian.

Both la Quina and la Ferrassie type Mousterians have their type sites in the Charente, where they are most common. Like la Quina, la Ferrassie has a very high percentage of sidescrapers, but few of these are the transverse types (numbers 22 to 24 on Bordes' list, Table 4.1) unlike la Quina. Again backed knives and handaxes are rare. Although there are fewer Quina-retouched tools, the Levallois technique is more often utilized than in la Quina. (Bordes, 1972).

Very few of the typical Mousterian tools, sidescrapers, are present in the Denticulate Mousterian, but as the name implies there is a great development of denticulate and notched pieces, comprising from 35 to 80% of the total. While there are no handaxes or backed knives, points and scrapers only contribute 3 to 7%. Quina-type retouch is extremely rare, but the use of the Levallois technique can vary greatly. With its type site at Combe-Grenal, the Denticulate Mousterian ranges from the lower Würm I

to the upper Würm II (Bordes, 1961, 1968, 1972).

The Mousterian of Acheulian Tradition, as might be guessed, arises from the tool kits of the late Acheulian in the lower Würm I. As its history implies, handaxes form a major portion of these kits, especially in the earlier form. Essentially, there are two different kits, one from the Würm I (A), and one from the Würm II (B). In the former, handaxes contribute 8 to 40%, sidescrapers 20 to 40%, denticulates 10 to 15%, while there are a few backed knives, awls, burins, notched pieces, points, and Abri Audi knives. Rather than the Levallois technique, many of the tools are made on the flakes removed during handax production. Type A gradually evolves into type B, in which handaxes comprise less than 5%, and sidescrapers only 4 to 10%, but backed knives contribute up to 20%, and denticulates more than 25%. Intermediates between the two types are found particularly during the transition in the Würm I/II. Type B finally disappears in the mid Würm II/III, where it is very similar to Perigordian I (Bordes, 1961, 1968).

#### 5.4.2.1 Significance of the Mousterian Assemblages

Because the different Mousterian assemblages are often found interstratified in the same cave site, or in neighbouring caves, the question of what type of man was using the different kits has been one over which archeologists have debated for several years. Because there seems to be no relationship between the fauna and the type of tool kit found in a site, Bordes (1961) contends there is not a seasonal relationship between the various kits. He does, however, claim there is a one-to-one correspondence

between a given tool kit and a tribe of Neanderthals. Although this is reasonable, the appearance of several kits in one cave indicates the tribes must have migrated several times during their history, yet never exchanged any ideas with the other tribes who obviously lived in the same area at least some of the time.

If, however, an assemblage of tools from several sites is analyzed statistically for its associations of tool, called factor analysis, a different picture is painted. The Binfords (1966) analyzed assemblages from three sites, Shubbabiq and Jabrud in the Middle East, and Houpeville in France. The tools clustered well into several factors, each representing a different specialized kit, possibly used for such activities as butchering, wood and bone working, food processing, and tool production. If such was the case, then all the Neanderthals used essentially the same basic kit but left different tool assemblages behind at sites, because of the manner in which the site was used. This analysis, however, is not statistically valid, because, for the number of tool types considered, the number of sites or even levels within the sites was insufficient to establish valid factors. To be valid, the study would have had to have included many more sites. Other similar more extensive studies have lead to less conclusive results (Kurashina, pers. comm., 1979). Therefore, at present, neither solution to the problem is conclusive, but more research into the uses to which each tool can be put may solve it in future.



### 5.4.3 The Upper Paleolithic

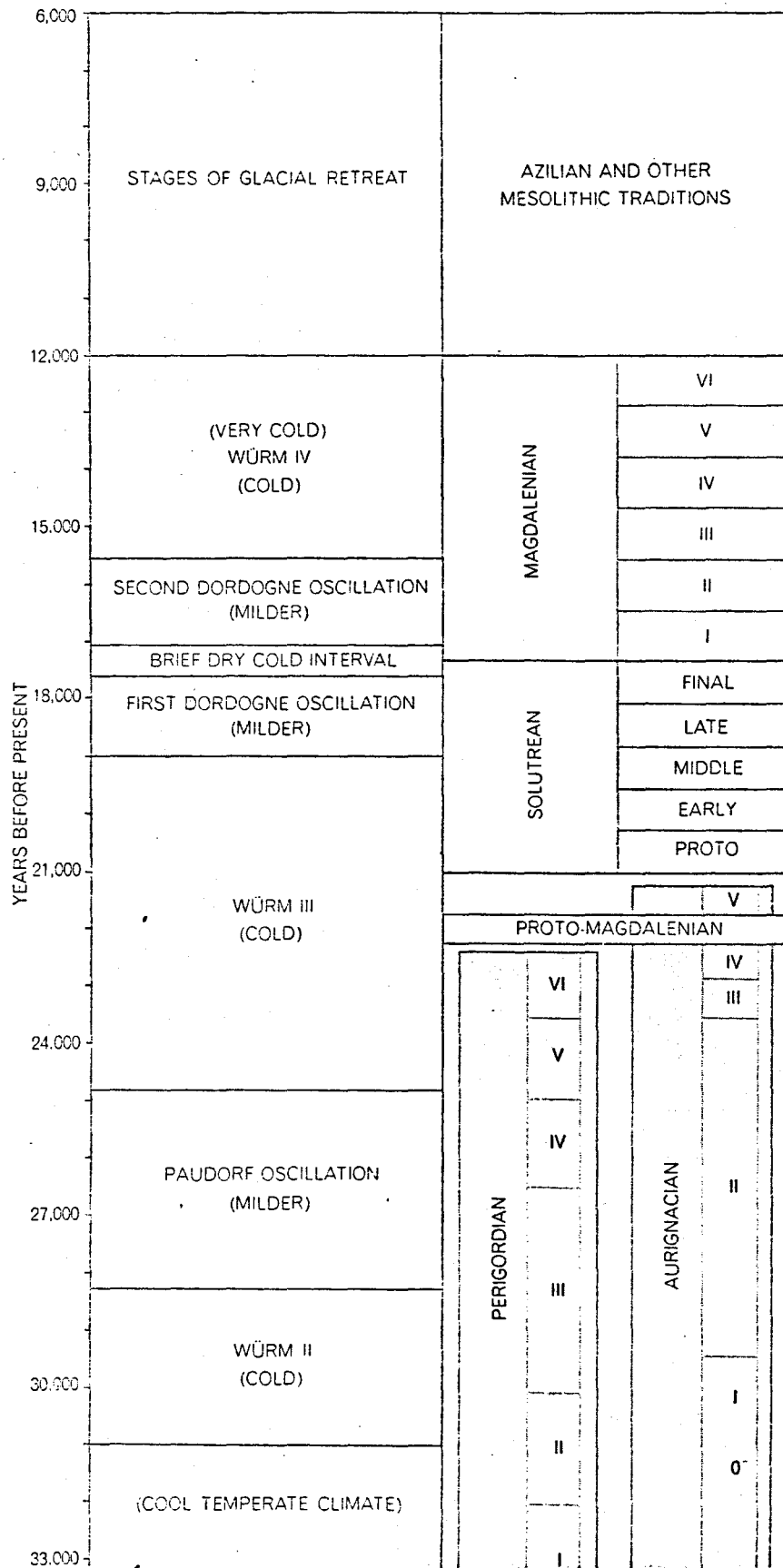
Following the disappearance of the Mousterian about 35 ka BP, there arose several different cultures comprising the Upper Paleolithic which lasted until approximately 10 to 12 Ka BP. Unlike the Mousterian tools, those of the Upper Paleolithic are made predominantly on blades struck from specially prepared cores by bone or wooden punches. Consequently, the tools appear more delicate. Retouch was often very finely done because of the thinness of the blades. Common Upper Paleolithic tools include end-scrapers, burins, awls, backed knives and points, and truncated pieces. A more complete discussion of the Upper Paleolithic tool types can be found in de Sonneville-Bordes and Perrot (1956).

Named for the site of Châtelperron, en Périgord, the Périgordian first appears in the Würm II/III, lasting until the early Würm III/IV. At least six different phases of Périgordian are known, listed in Table 5.4. The first recognized art, small portable forms, are associated with these sites, notably Venus statues.

Found originally at Aurignac, the Aurignacian began slightly later than the Périgordian, but also lasted a few thousand years longer. Having at least five stages, the Aurignacian is noted for its specialized scrapers and burins, the latter of which may have been used to engrave bones found with the sites. The first of the cave paintings, the primitive style, are also Aurignacian (Leroi-Gourhan, 1968).

Perhaps the most famous the Upper Paleolithic cultures is

Table 5.4 Chronology of the Upper Paleolithic Cultures



(after Smith, 1964)

the Solutrean, lasting only a few thousand years in the early Würm III/IV. The laurel leaf points and blades of the Solutrean are one of the major distinctions between it and the Perigordian or Aurignacian. By using a small piece of wood or bone, extremely fine flakes could be removed from flints held in the hand to produce points many of which are too delicate to have been utilized, and perhaps constituted art forms. Painting during the Solutrean reached a highly sophisticated form, stressing naturalism.

In the late Würm III/IV, the Solutrean was displaced by the Magdalenian, a culture having six stages. Named for the type site of le Madaleine, its tools include scrapers and burins, in addition to engraved bone and antler harpoon heads, spear points with beveled and forked bases, needles, thong softeners, and spear-throwers. Magdalenian art is classic, utilizing the features of the rock faces to enhance the drawings, many of which overly one another. Colour was used to highlight the engravings. Finally, in the late Magdalenian, the bow and arrow were included in the tool kit.

When the Magdalenian, died with it died the Paleolithic, and most of the traditions it had fostered, including cave painting, and the Pleistocene also was over.

## THE SITES IN THE CHARENTE

Some of the archeological sites which were first excavated by professionals exist along the Charente River and its tributaries. Along the Tardoire, in Figure 6.1, are two sites, Lachaise and Montgaudier which contain artefacts, hominid remains, and travertines datable by the U/Th method. Although the latter **site is only** partially excavated, Lachaise not only is well-studied archeologically, the speleothems therein have provided some of the most reliable U/Th dates yet obtained on archeologically-related calcite.

### 6.1 Geography

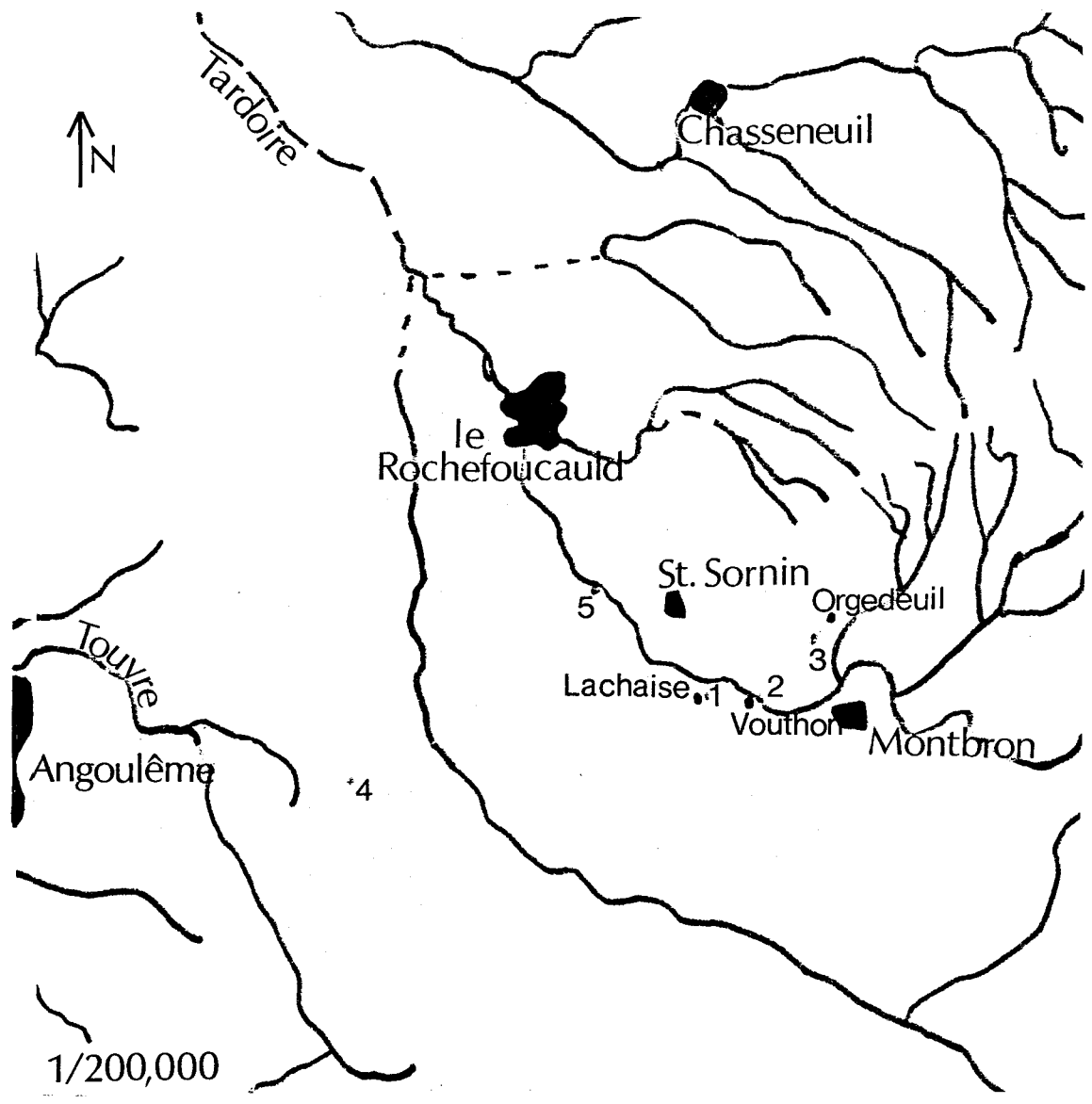
Climatologically, the Charente, although slightly farther north, is very similar to the Dordogne (Chapter 7.1). The Charente River, from which the region derives its name, rises at Limousin in the Massif Central; flowing 361 km westerly to the Bay of Biscay, with an average slope of  $0.75 \times 10^{-3}$ . Near Montbron and Angoulême, the countryside is composed of rolling hills, probably originally forested by deciduous trees before agriculture began. Occasionally, the ground is broken by escarpments of limestone riddled with caves and abris. Because the region is karstic most of the surface water exists in the armoured rivers. Agriculture in the region is mainly forage crops, cattle, sheep, and goats.

Figure 6.1

The Charente, France

Caves and archeological sites in the area:

1. Lachaise
2. Montgaudier
3. Fontechevade
4. Grottes du Quéroy
5. Abri du Chasseur, etc.



## 6.2 Geology

In the northern part of the Charente, the basement is a garnet-bearing mica schist covered by a post-Paleozoic salt layer. This southern part, acting as a stable craton was eroded during the late Paleozoic, and subsequently covered by up to 800 m of Jurassic sediments, much of it limestones. The late Jurassic saw a lake or epeiric seas which deposited shales, the marly Rochefoucauld limestone, and locally, gypsum. Some of the region has not been emerged since the Jurassic seas departed. The Cretaceous strata, where present, are pyritiferous coals, shales, and limestones (Debenath, 1974).

In the early Tertiary, the area was deformed slightly to cause several NW-SE trending anticlines and synclines. In the Eocene, much of the Jurassic limestone was eroded into typical karst landforms, especially noticeable near la Rochefoucauld. Primarily, the softest layers were attacked resulting in abris and overhangs. Between Jonzac and the Charente River, the region was covered by detrital sediments, forming acidic soils, called le Pays de Bois. Between les Bois and the ridges near Angoulême is the Charentais region, marked by dolines and bell-shaped depressions, filled by calcareous soils intermixed with the red Bois soils. Finally, the Plio-Quaternary deformation forming the Alps affected the area. The whole pattern is further complicated by the drainage system and its interaction with the karst.

### 6.2.1 The Charente Karst

Because of the extensive karst development near la Rochefoucauld, many caves and abris have been formed which were used by Paleolithic **hominids**. The Charente Karst occupies approximately 400 km<sup>2</sup>, bordered by the **Limousin Plateau** (Massif Central) to the east. A joint system trends NW-SE through the area, particularly well-marked between Montbron and la Rochefoucauld (Figure 6.2).

The karst system strongly influences the drainage pattern, especially of the Tardoire and Bandiat. Between Vouthon and la Rochefoucauld, the Tardoire has seven sinkholes, while the Bandiat has thirteen near Agris, some reaching 10 m in diameter. None of these dolines allow access to the subterranean system, but much of the water must flow generally SW to the edge of the karst to resurge as a spring flowing into the Touvre River. La Font de Lussac, however, has been explored to a depth of 70 m. Lachaise Cave is active as a conduit, and probably has been active through much of its history.

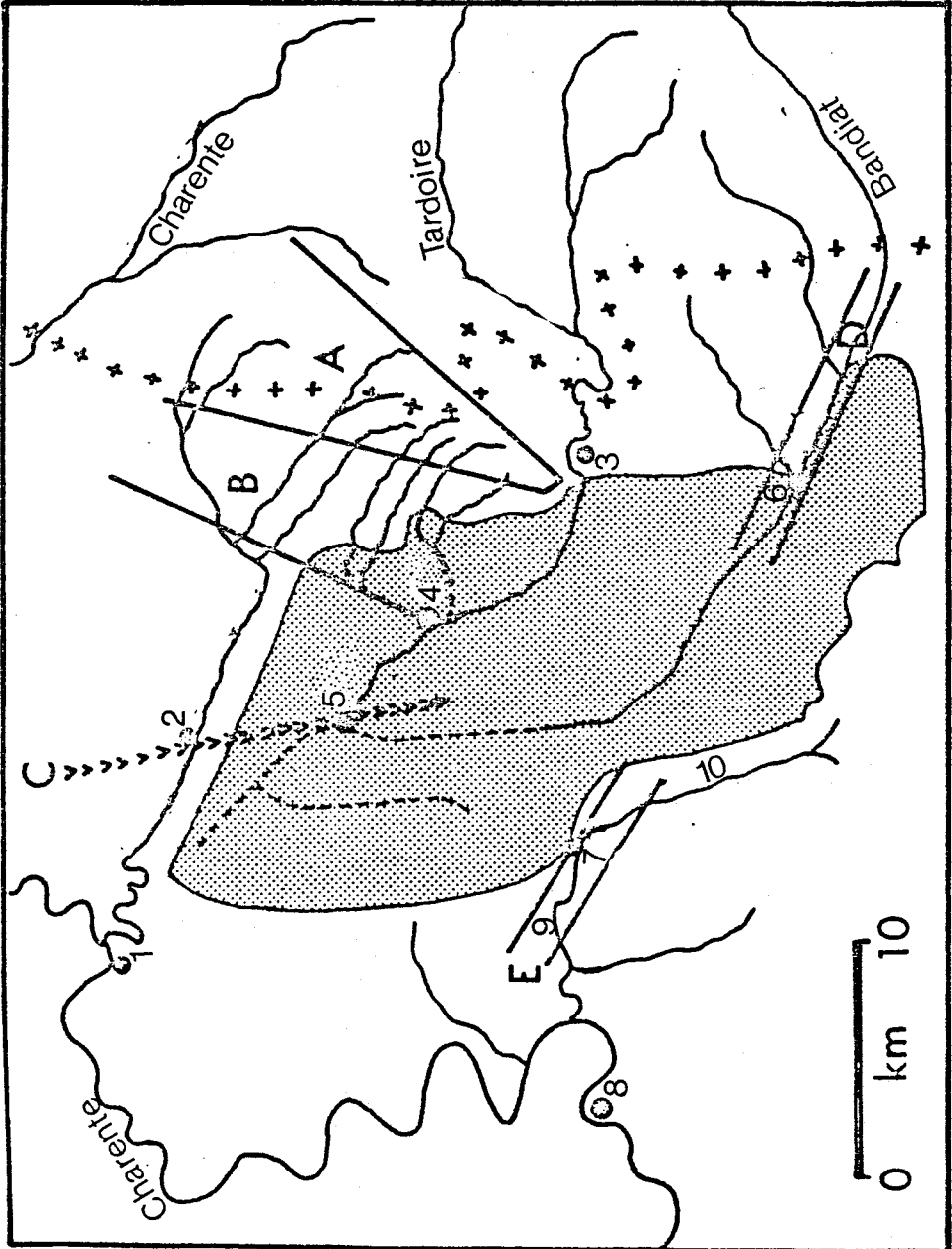
In the Tardoire Valley, the Jurassic limestone bluffs reach up to 50 m in height, riddled by caves and abris. These limestones are almost pure or slightly dolomitic, porous, fine-grained rocks which contain larger, more well-developed cave systems than the Cretaceous limestones. Some caves have developed on several levels, connected by puits, while others are horizontal and of uniform width. Both Lachaise and Montgaudier are found in Jurassic limestones, although they differ radically in appearance.



Figure 6.2

The Charente Karst

1. Mansle
  2. Puy-Bouc
  3. Montbron
  4. La Rochefoucauld
  5. Agris
  6. Marathon
  7. The source of the Trouvre River
  8. Angouleme
  9. The Touvre River
  10. The Echelle River
- A. The Horst of l'Arbre
  - B. The tectonic depression of La Rochefoucauld-Chasseneuil
  - C. The Puy-Bouc Syncline
  - D. The fosse of the Bandiat
  - E. The fosse of the Touvre
- Dry valleys
- +++ Eastern edge of Massif Central
- >>>> Synclinal axis



The Charente Karst

### 6.3 Lachaise

Lachaise Cave, a complex of three **caves**, contains two enigmatic skulls, many rich archeological layers, and a rich faunal **suite** interbedded with several stalagmitic planchers of pure calcite. Although the cave has been excavated since the mid-nineteenth century, there are still problems in interpreting the archeological data. All the data given below regarding the sedimentology and archeology is taken from Debénath (1974), Debénath (1977), and Schwarcz and Debénath (1978), where not otherwise noted.

#### 6.3.1 The History of Excavation at Lachaise

L'abri Bourgeois-Delaunay at Lachaise was first discovered by Fermond, who began excavating there about 1850. In 1865, the Abbés Bourgeois and Delaunay, for whom the abri is named, began a more extensive investigation. Fermond returned, and in 1894, published a paper discussing the Upper Paleolithic industries. In 1910, Chauvet worked the site. Probably Lartet, Vibraye, and Tremeau de Rochebrune also excavated there.

About 1870, Abbé Suard opened up Abri Suard, which had been completely filled with sediments until then. Subsequently, many amateur collectors destroyed much of the material in Suard. In 1936, David began a systematic excavation in Suard. In 1954, he discovered Duport Cave, named for his partner.

David excavated both Suard and Bourgeois-Delaunay from about 1950 until his death in 1963. His techniques, however, often left something to be desired. Because of the extremely well-cemented

sediments in Suard, he often resorted to dynamiting the material, a technique not conducive to great stratigraphic control. When Debénath began to excavate in 1967, the owner of the chateau which sits atop the caves was reluctant to give his permission, because part of his chateau had collapsed due to the blasting (Figure 6.3). Debenath, who agreed not to dynamite the caves, has excavated there since 1967, but only recently has done any work in Duport Cave, having concentrated on Suard and Bourgeois-Delaunay.

### 6.3.2 General Description

Midway between Montbrcon and Vilhonneur on the banks of the Tardoire sits the hamlet of Lachaise, beneath which is the cave system. A promontory of mid-Jurassic limestone emerges from the Tertiary cover at Lachaise. Because the limestone comprises an upper hard crystalline limestone and a lower more easily-eroded, soft horizon, many small abris and a complex of caves open to the northeast along the course of the Tardoire near Lachaise.

Of the many caves and abris, only four have been extensively excavated: abris Suard, and Bourgeois-Delaunay, Duport Cave, and one other north of these three excavated by Pintaud. Figure 6.4 depicts the first three, which form a network of caves, abris, and passageways. Duport, the smallest of the three, is a true cave measuring about 10 m in depth and 8 m wide. A small passage at the rear connects it with Bourgeois-Delaunay, a cave some 20 m deep, 15 m wide, and more than 10 m in height. To the northwest in Bourgeois-Delaunay is a passage to Suard, which measure 40 m deep, but

Figure 6.3

Lachaise Chateau.

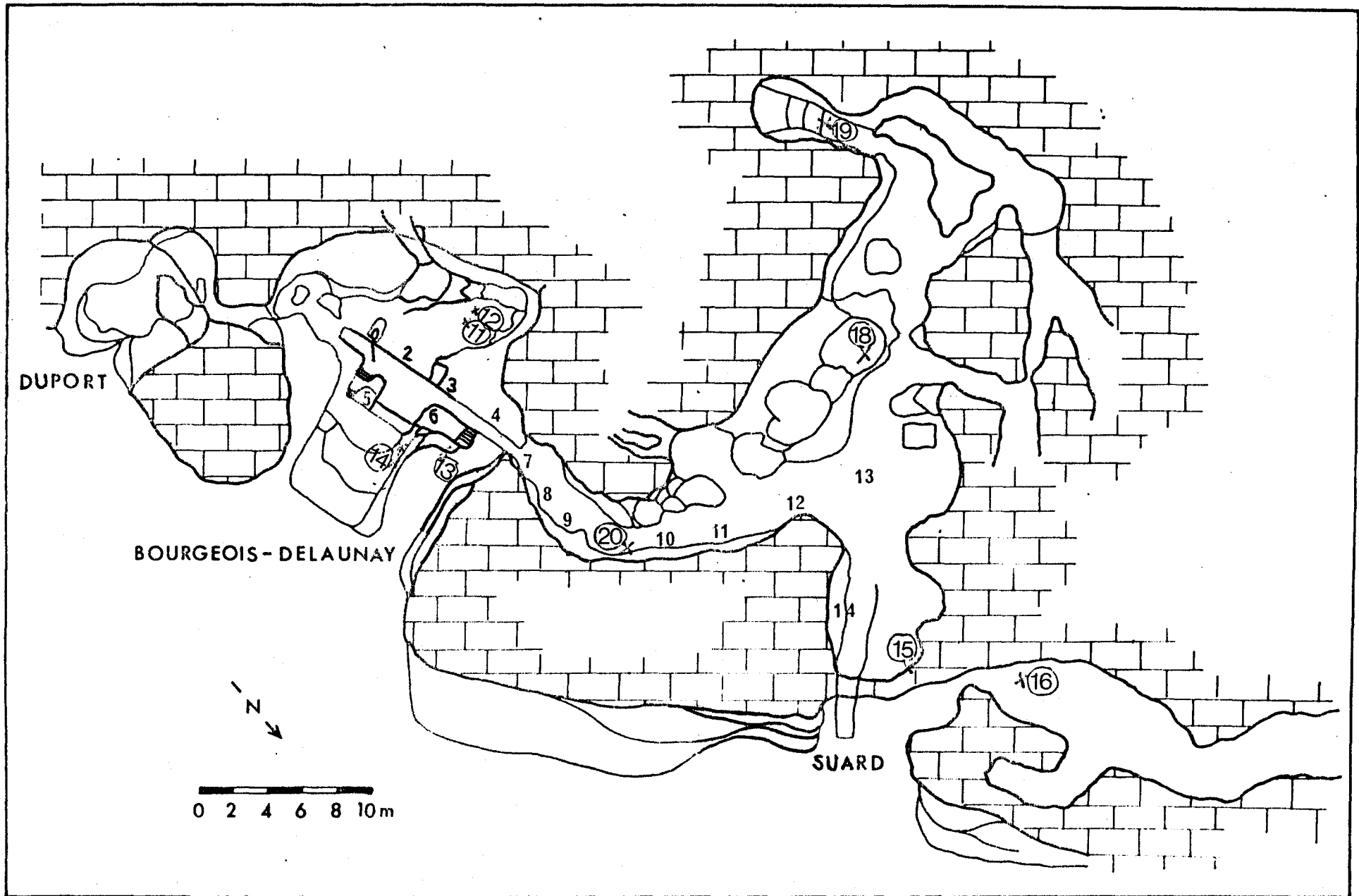
During David's excavations in Abri Suard, he used dynamite to removed the indurated sediments. After several years of blasting the southeast tower of the chateau collapsed, the tower closest to the girl in the picture, which starts at the second storey unlike the other three. When Débenath came to begin his excavations in 1967, the chateau owner did not want him to work there for fear of losing another tower to science. Fortunately, work proceeded because Débenath agreed to use no dynamite (Débenath, pers. comm. 1979).



Figure 6.4

Plan view of Lachaise.

Uncircled numbers refer to the series of sedimentological samples studied by Débenath, while circled numbers represent travertine samples within Lachaise collected in 1979 for dating. If (13) is the number, then the sample number is actually 79LC13 (adapted from Débenath, 1974).





averages 10 m wide and 2 to 3 m high. Within Suard are many small grottos, passages, and leads. At the back of Suard, active deposition is occurring, as shown in Figure 6.5, while at a lower level, erosion is occurring. The levels are connected by a shaft.

Because no recent excavations have occurred at Duport and no samples were collected there, it will be ignored from here.

### 6.3.3 Stratigraphy

Because both Suard and Bourgeois-Delaunay were extensively excavated by David before Debénath worked the sites, there are two sets of stratigraphy for each. David did not give thickness!

#### 6.3.3.1 Bourgeois-Delaunay

According to David (in Debénath, 1974), the upper part of the stratigraphy in Bourgeois-Delaunay, the witness section for which is shown in Figure 6.6a, was from the top:

1. Relict soil.
- 2a. An Aurignacian level with many types of fauna and two living floors.
- 2b. Locally, blocks of éboulis.
- 2c. Locally, worked bones.
3. Sterile red sandy silt.
4. An archeologically sterile layer with many faunal remains.
5. Sterile red sand.
6. A Mousterian layer with fauna.
7. Stalagmitic plancher averaging less than 0.1 m thick, not continuous throughout the abri, well fractured.

Figure 6.5

Active speleothem deposition in Lachaise.

In Abri Suard, some 35 m from the opening, active speleothem deposition is occurring. Similar deposition occurs throughout the back of the cave (photo courtesy of H. Schwarcz).



Figure 6.6

Stratigraphy in Bourgeois-Delaunay:

- A. David's witness section in the rear of Bourgeois-Delaunay, couches 1 - 7.
- B. Débénath's witness section in Bourgeois-Delaunay, couches 7 - 11.
- C. Couches 7 - 11, in cut number 5, Bourgeois Delaunay east side.
- D. A remnant of couche 7 (also in C far right middle).
- E. Couche 11.
- F. Close-up of the structure in couch 11.
- G. The section along the west side of squares I - K 5, around the corner to the north side of squares I5 & 6; cuts 2 and 3.

(photos courtesy of H. Schwarcz; diagram adapted from Débénath, 1974)



A



B



C



D



E



F

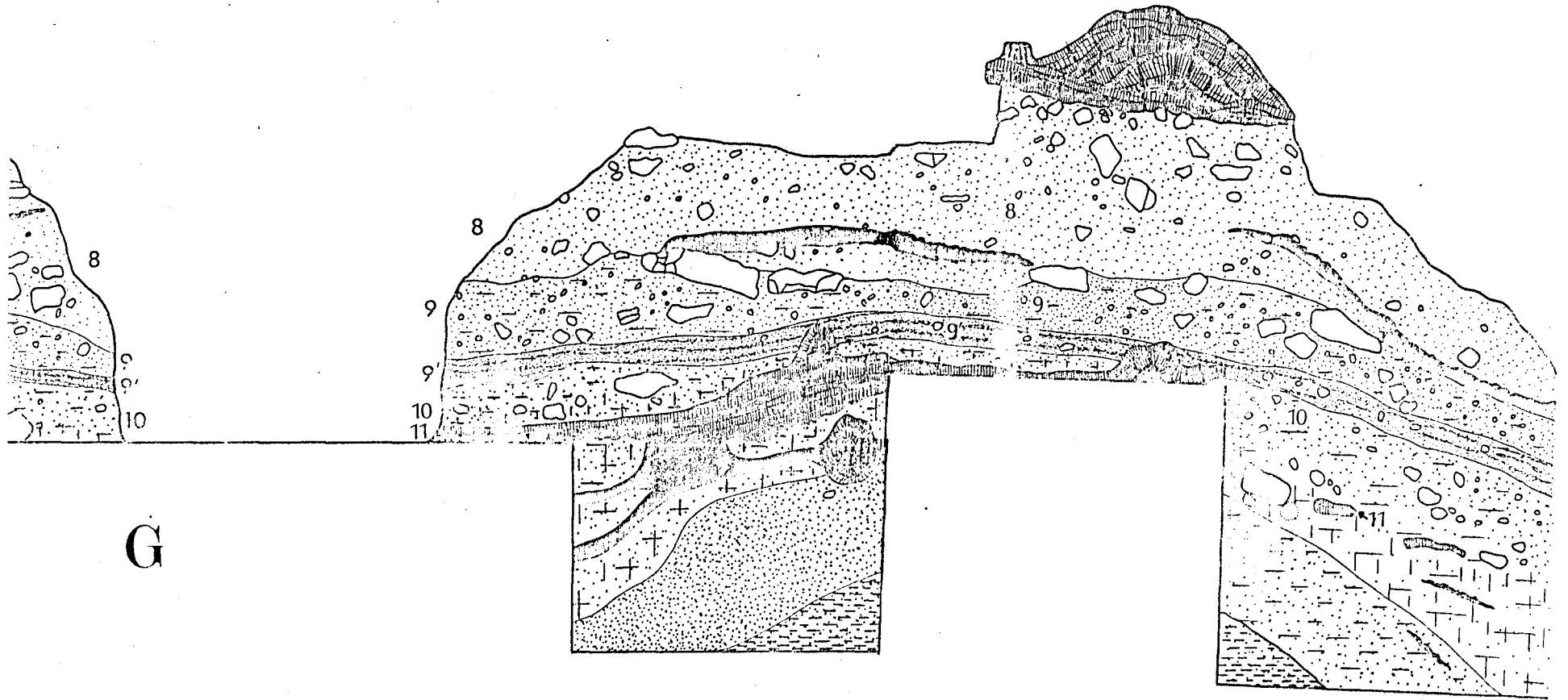
K5

J5

I5

i5

i6



G



Debenath's excavations resulted in the following stratigraphy, continuing from layer 7 down, as shown in Figure 6.6e,f:

8. Total thickness 0.45 m (a-d only).
  - 8a. A zone of alteration immediately below the stalagmitic plancher.
  - 8b. Layer with rounded calcareous elements, very altered.
  - 8c. Yellow sandy silt
  - 8d. Red sandy silt.
  - 8e (8') Oxides of manganese, Mousterian assemblage, 0.15 m thick (David's layer 9).
9. Total thickness from 0.2 to 0.4 m (a,b only).
  - 9a. Silty sand with some rounded calcareous elements, very altered, encrusted with manganese.
  - 9b. Very similar to 9a, but contain a higher percentage of silt.
  - 9c (9') Thin, white, powdery layer with rare tools, 0.15 m maximum, divisible into two layers in the west (cut 5).
    - 9c1. very rich in manganese, otherwise similar to 9c.
    - 9c2. As described in 9c, varved.
10. Brown silt with rare calcareous elements, very altered with abundant fauna, Mousterian culture, 0.30 m thick.
11. Stalagmitic plancher averaging 0.15 m thick.
12. Large éboulis and roof debris, altered and encrusted with manganese.
13. Beds of sand and silt with rare gravel (maximum diameter 3 cm) interbedded with manganese-rich layers.

This stratigraphy is fairly constant throughout the western and northern portions of the abri, but in cut 5 (Figure 6.7), the stratigraphy was different (no thicknesses given):

1. Relict soil.
- AO. Thin layer of pebbles.
- A1. Thermoclastic éboulis enclosing frost-cracked pebbles in a sandy matrix.
- B1. Small rounded éboulis, very altered.
- B2. Gravel in a sandy matrix.
- C1. Rounded calcareous elements, very altered.
- C2. Sandy silt with rare éboulis.
- D1. Small pebbles.
- D2. Very silty with almost no calcareous elements.
- E. Manganese nodules.
- F. Brown silt with very altered calcareous elements.

The relationship between the two stratigraphies given is listed in Table 6.1. Layer 13 lies on limestone, but whether it is the basement or a debris fall of massive proportions is impossible to say.

At the front of Bourgeois-Delaunay, what is now outside the dripline, but was inside the cave at one time, the stratigraphy is different again (no thickness given):

- $\alpha$ . Small angular, calcareous elements in a yellow sand matrix.
- $\beta$ . Red soil with an Upper Paleolithic industry.
- $\gamma$  1. Small éboulis with sharp edges cemented in place.

**Figure 6.7**

**Stratigraphic section of cut 5, Abri Bourgeois-Delaunay,  
Lachaise (after Débenath, 1974)**

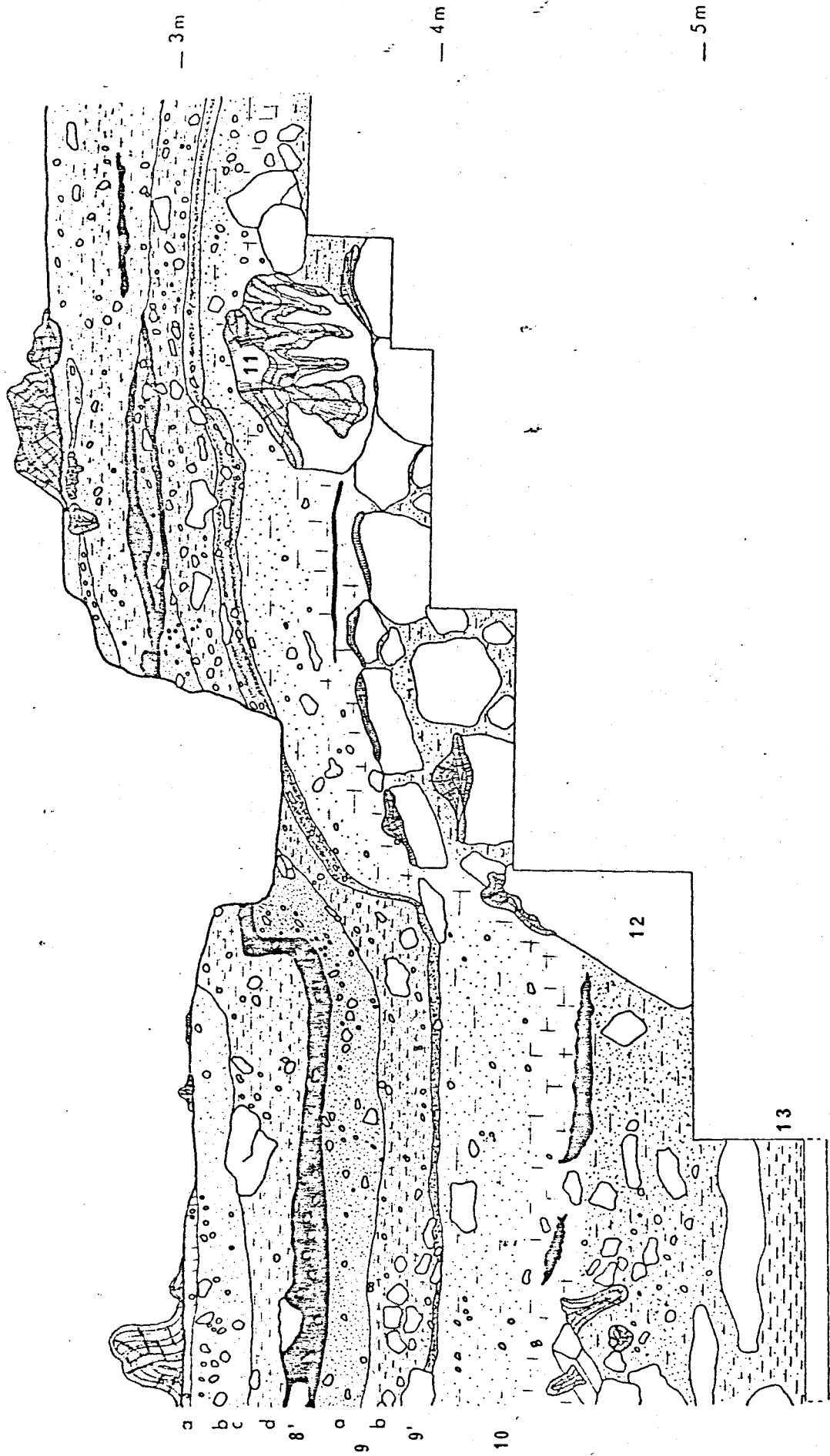


Table 6.1 Correspondence Between the Excavations  
of David and Débénath in Abri Bourgeois-  
Delaunay

David's Excavations	Débénath's Excavations		
	Frontal Cut	Sagittal Cut	
		West	East
			AO
			A1
			B1
			B2
8	8a	8a	
	8b	8b	C1
	8c	8c	C2
	?	?	D1
	8d	8d	D2
9	8e	8e	E
	9a	9	F?
	9b		
	9c	9c1	
9c2			
10	10		
11	11		
	12	12	
	13	13	

(after Débénath, 1974)

- γ. Large blocks of roof rock.
- δ. Small rounded éboulis, very altered.
- ε. Silty matrix enclosing a lens of manganese oxides.
- ζ. Small rounded éboulis in a silty matrix.
- η. Silt with altered éboulis.

The manner in which this stratigraphy matches the others is not fully understood.

#### 6.3.3.2 Suard

Suard, originally blasted apart by David, has its stratigraphy numbered from 50, because Debénath's section did not correspond to anything described by David. Therefore, to prevent confusion, new numbers were assigned. Debénath's layer 50 probably corresponds to David's VIII. Figure 6.8 shows the witness section. Debénath's stratigraphy from the top is:

- 48. Small cryoclastic éboulis, cemented, with numerous cryoturbated lesions.
- 49. Eboulis similar to those in 48, sandy matrix, not cemented.
- 50. Large blocks of fallen roof rock.
- 50a. Blocks.
- 50b. Fine éboulis in a sandy matrix with cryoturbated lesions.
- 50c. Blocks.

The blocks in 50 a-c have fallen as flagstones, then been cemented in place by calcareous concretions beneath the blocks.

**Figure 6.8**

**Stratigraphy of Abri Suard, Lachaise:**

A. Witness section in Abri Suard, couches I  
- VIII

B. Couche 53' (53c), near where 79LC17 was  
collected.

C. Diagramatic section of couches 48 to 54.

D. Diagramatic section of couches 2 to 10.

(photos courtesy of H. Schwarcz; diagrams from  
Débénath, 1974)

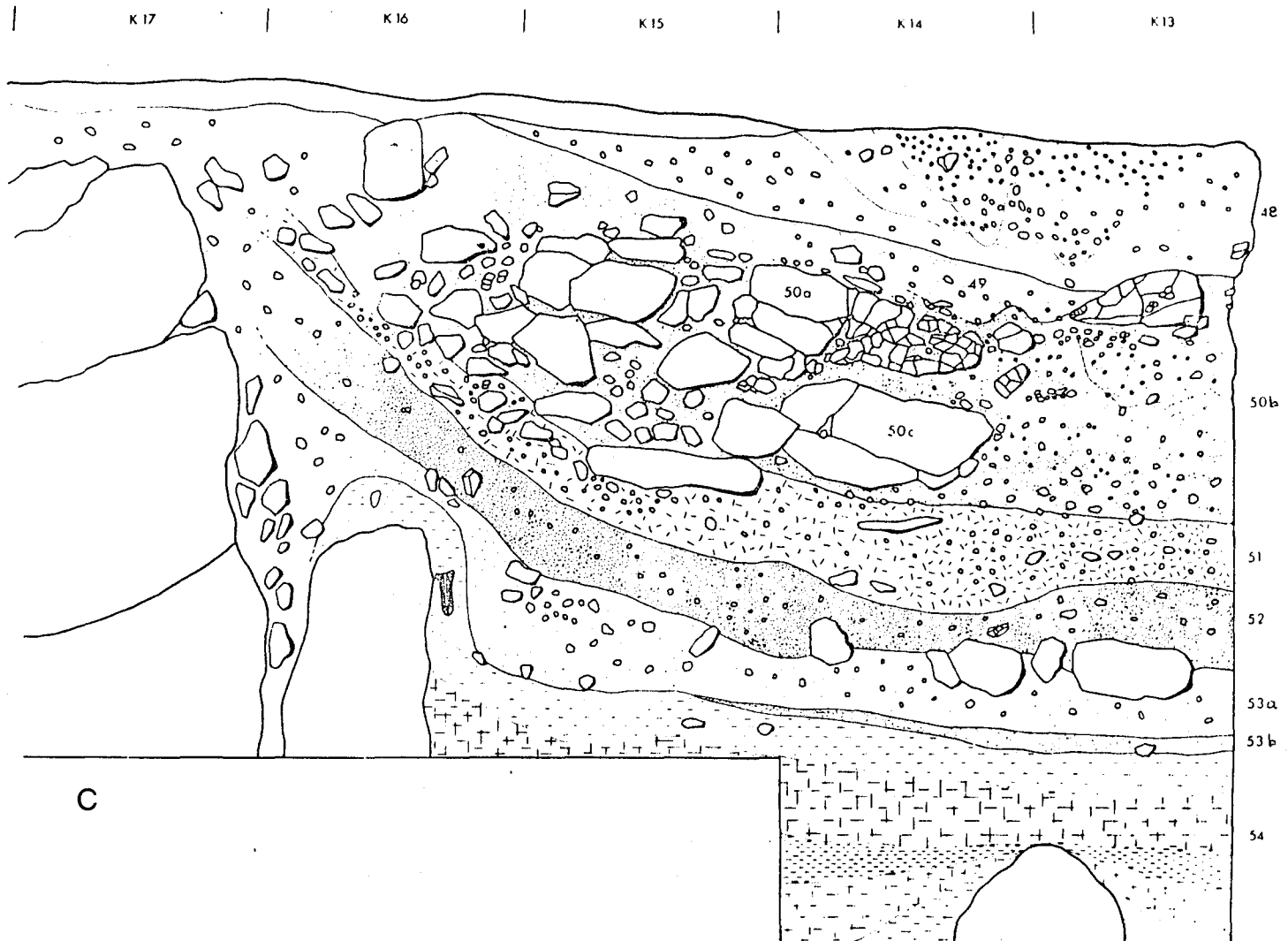


A

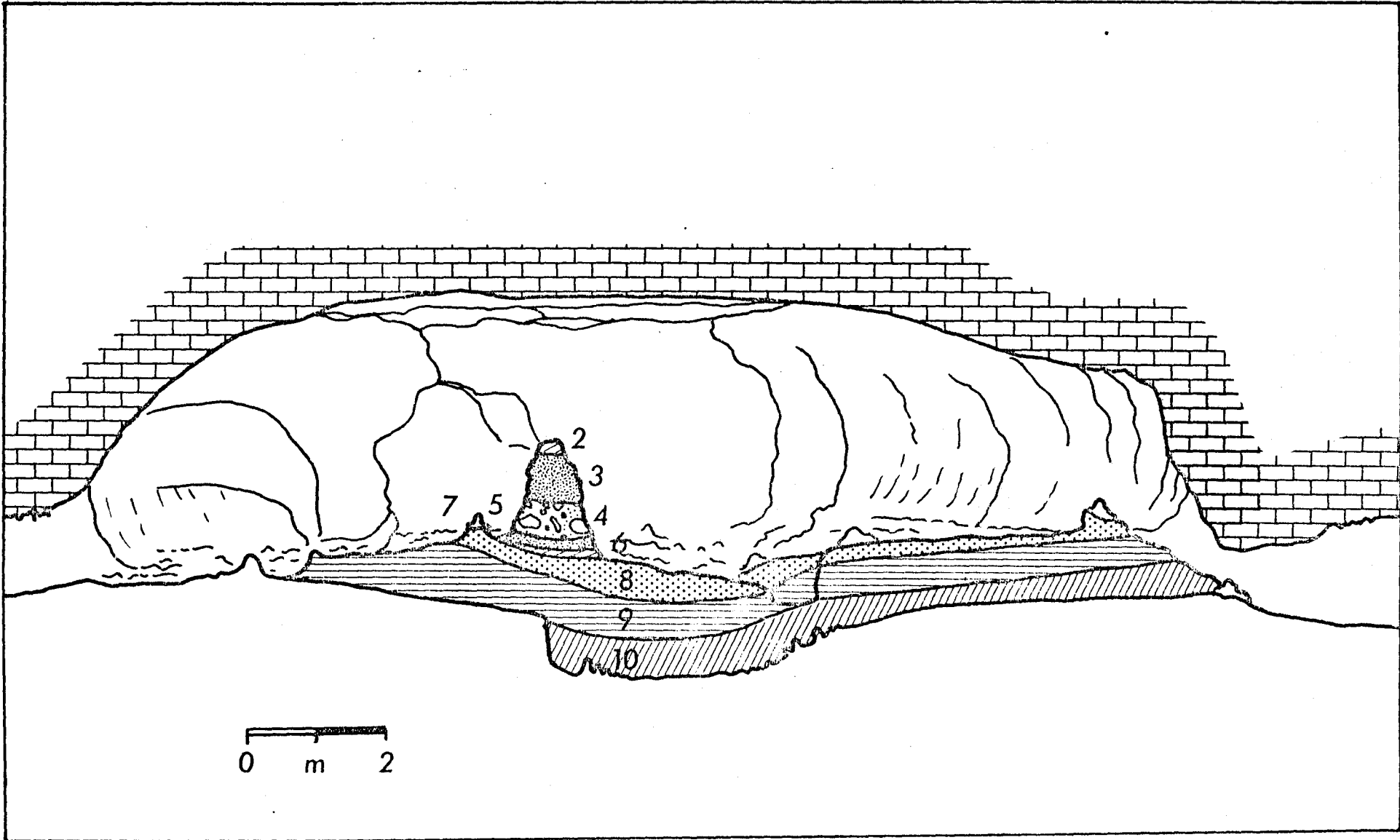


B





D



me

- 51. Small calcareous blocks, cemented in some places in a yellow sand matrix.
- 52. A red silty matrix, otherwise as 51.
- 53a. Brown silty matrix containing large calcareous blocks.
- 53b. Yellow sand matrix with blocks similar to those in 53a.
- 53c (53') Stalagmitic plancher about 10 cm thick, often referred to as the Plancher Inférieur.
- 54. An assemblage of sandy silty layers resembling layer 13 in Bourgeois-Delaunay in some respects. This layer is up to 2 m thick, sterile, and overlies limestone, either native rock or collapsed roof rock. The limestone is 1.5 m thick at the minimum.

Layers 48 to 53b measure about 2.5 m outside the front of the present cave entrance, but thin down to 1.5 m inside in squares Q20 and Q21, beyond which it is very difficult to distinguish them due to the intense alteration. Inside, these layers are overlain by a stalagmitic plancher, known as the Plancher Supérieur, averaging about 0.50 m thick.

#### 6.3.3.3 Comparison between Bourgeois-Delaunay and Suard

Although Bourgeois-Delaunay is an assemblage of solutionally altered sediments, Suard contains calcite-cemented éboulis. How two caves so close to one another could have experienced such different styles of sedimentation, especially as many of the levels are supposed contemporaneous, is a problem. Furthermore, although both caves contain stalagmitic planchers, layer 11 in Bourgeois-Delaunay apparently corresponds to the plancher supérieur in Suard.

This correlation, however is not absolutely certain, because, although the sediments can be traced into the couloir into Suard, the correlation within Suard is uncertain because much of the intervening material was removed by David, whose descriptions match none of the sediments seen. Table 6.2 gives the correspondence.

#### 6.3.4 Archeology

Several levels of human occupation have been found in Lachaise ranging from the upper Acheulian to the Upper Paleolithic.

##### 6.3.4.1 Suard

Tables 6.3 to 6.5 describe in detail the archeological material found in Suard, layers I and II excavated by David. These have been grouped by Debénath into Facies C, a composite industry having a low index for both blades and Levallois technique, but a high facetting index. This facies, an early form of Mousterian is thought to be an in situ development from Facies B, localized in the Tardoire region.

Facies B, like C, has a low Levallois index, but a high facetting index. This facies comprises layers III to VIII (David) Tables 6.6 to 6.16 and layer 50 (Debénath) table: 6.17. Facies A again has a low Levallois index, but a high facetting index, as represented by layers 51 to 53 (Debénath) Tables 6.18 to 6.22.

In general, the industry is unique, although it is a bifacially based one. Generally, the tools are very small for Acheulian or early Mousterian, in addition to being irregular in form. Cobbles form a significant portion of the raw material used for

Table 6.2 Débénath's Chronology for Lachaise Sediments

Age	Abri Bourgeois-Delaunay	Abri Suard	
		Débénath's Excavations	David's Excavations
Wurm III	2		
Wurm II/III	3?		
Wurm II	4		
	5		
	6		
Wurm I/II	7 (plancher)		
Wurm I	8a		
	8b		
	9a		I
	9b		
	10		
Riss/Wurm	11 (plancher)	(plancher)	II (breccia)
Riss III			III-IV
			V-VI
		48	VII
		49	VIII
		50	
		51	
	52		
	53		
Riss II/III	13	(plancher)	
Riss II	13?	54	

(after Débénath, 1974)

Table 6.3 Tool Typology, Couche I,

Abri Suard, Lachaise

Tool	Number	Total Percentage	Restricted Percentage
1. Typical Levallois flake	6	6.0	
2. Atypical Levallois flake	12	12.0	
3. Levallois point	0	0	
4. Retouched Levallois point	0	0	0
5. Pseudo-Levallois point	0	0	0
6. Mousterian point	0	0	0
7. Elongated Mousterian point	0	0	0
8. Limace	0	0	0
9. Sidescraper, single straight	5	5.0	9.3
10. Sidescraper, single convex	13	13.0	24.1
11. Sidescraper, single concave	1	1.0	1.9
12. Sidescraper, double straight	0	0	0
13. Sidescraper, double straight convex	0	0	0
14. Sidescraper, double straight concave	1	1.0	1.9
15. Sidescraper, double biconvex	1	1.0	1.9
16. Sidescraper, double biconcave	0	0	0
17. Sidescraper, double convex concave	0	0	0
18. Sidescraper, convergent straight	0	0	0
19. Sidescraper, convergent convex	1	1.0	1.9
20. Sidescraper, convergent concave	0	0	0

Tool	Number	Total Percentage	Restricted Percentage
21. Sidescraper, asymmetrical	0	0	0
22. Sidescraper, transverse straight	0	0	0
23. Sidescraper, transverse convex	3	3.0	5.5
24. Sidescraper, transverse concave	0	0	0
25. Sidescraper, retouched on the ventral surface	0	0	0
26. Sidescraper, with abrupt retouch	0	0	0
27. Sidescraper, with thin back	0	0	0
28. Sidescraper, bifacial retouch	0	0	0
29. Sidescraper, with alternate retouch	0	0	0
30. Typical endscraper	0	0	0
31. Atypical endscraper	0	0	0
32. Typical burin	0	0	0
33. Atypical burin	0	0	0
34. Typical borer	1	1.0	1.9
35. Atypical borer	1	1.0	1.9
36. Typical backed knife	0	0	0
37. Atypical backed knife	0	0	0
38. Naturally backed knife	0	0	0
39. Mousterian raclette	1	1.0	1.9
40. Truncated piece	0	0	0
41. Mousterian tranchet	0	0	0
42. Notched pieces	6	6.0	11.1

Table 6.4

Tool	Number	Total Percentage	Restricted Percentage	Tool	Number	Total Percentage	Restricted Percentage
21. Sidescraper, asymmetrical	9	1.1	2.7	43. Denticulate	51	9.9	15.5
22. Sidescraper, transverse straight	3	0.4	0.9	44. Bec burinante alterne	1	0.1	0.3
23. Sidescraper, transverse convex	11	1.4	3.3	45. Flake, retouched on the ventral surface	8	1.0	
24. Sidescraper, transverse concave	1	0.1	0.3	46. Miscellaneous retouched flake, abrupt thick retouch	311	38.6	
25. Sidescraper, retouched on the ventral surface	7	0.9	2.1	47. Miscellaneous retouched flake, alternate thick retouch			
26. Sidescraper, with abrupt retouch	2	0.2	0.6	48. Miscellaneous retouched flake, abrupt thin retouch	68	8.4	
27. Sidescraper, with thin back	5	0.6	1.5	49. Miscellaneous retouched flake, alternate thin retouch			
28. Sidescraper, bifacial retouch	6	0.7	1.8	50. Flake, bifacial retouch	10	1.2	
29. Sidescraper, with alternate retouch	0	0	0	51. Tanged point	0	0	0
30. Typical endscraper	2	0.2	0.6	52. Notched triangle	0	0	0
31. Atypical endscraper	5	0.6	1.5	53. Pseudo-microburin	0	0	0
32. Typical burin	3	0.4	0.9	54. Flake, notched end	0	0	0
33. Atypical burin	6	0.7	1.8	55. Cleavers	0	0	0
34. Typical borer	2	0.2	0.6	56. Bobot (plane)	0	0	0
35. Atypical borer	2	0.2	0.6	57. Aterian tanged point	0	0	0
36. Typical backed knife	0	0	0	58. Tanged piece	0	0	0
37. Atypical backed knife	1	0.1	0.3	59. Chopper	0	0	0
38. Naturally backed knife	12	1.5	3.6	60. Inverse chopper	0	0	0
39. Neanderian raclette	2	0.2	0.6	61. Chopping tool	5	0.6	1.5
40. Truncated piece	3	0.4	0.9	62. Miscellaneous piece	29	3.6	8.8
41. Neanderian tranchet	0	0	0	63. Blattspitzen	0	0	0
42. Notched pieces	31	3.9	9.4				
				Total	805	103.0	99.2
					(328)		

246

Table 6.5 Technical and Typological Indices and Characteristic Groups, Couche II, Abri Suard, Lachaise

Index	Total	Restricted
Levallois	10.47	
Facetting	50.43	
Restricted Facetting	40.10	
Blade (laminar)	5.31	
Typological Levallois	10.0	0.3
Sidescraper (Group II)	20.4	49.3
Total Acheulian	1.4	3.3
Unifacial Acheulian	0.1	0.3
Bifacial	1.3	3.0
Charentien	11.9	29.3
Quina	1.8	
Group I: tools # 1 - 4	10.0	0.3
Group III: tools # 30 - 37, 40	3.0	7.3
Group IV: denticulates	9.9	15.5

Table 6.6 Tool Typology, Couche III, Abri Suard, Lachaise

Tool	Number	Total Percentage	Restricted Percentage
1. Typical Levallois flake	18	3.7	
2. Atypical Levallois flake	58	12.1	
3. Levallois point	0	0	
4. Retouched Levallois point	0	0	0
5. Pseudo-Levallois point	4	0.8	1.4
6. Mousterian point	4	0.8	1.4
7. Elongated Mousterian point	2	0.4	0.7
8. Limace	0	0	0
9. Sidescraper, single straight	18	3.7	6.3
10. Sidescraper, single convex	40	8.3	14.1
11. Sidescraper, single concave	7	1.5	2.5
12. Sidescraper, double straight	1	0.2	0.4
13. Sidescraper, double straight convex	4	0.8	1.4
14. Sidescraper, double straight concave	0	0	0
15. Sidescraper, double biconvex	8	1.7	2.8
16. Sidescraper, double biconcave	0	0	0
17. Sidescraper, double convex concave	0	0	0
18. Sidescraper, convergent straight	2	0.4	0.7
19. Sidescraper, convergent convex	4	0.8	1.4
20. Sidescraper, convergent concave	0	0	0

247



Tool	Number	Total Percentage	Restricted Percentage
21. Sidescraper, asymmetrical	0	0	0
22. Sidescraper, transverse straight	1	0.6	1.0
23. Sidescraper, transverse convex	2	1.1	2.0
24. Sidescraper, transverse concave	1	0.6	1.0
25. Sidescraper, retouched on the ventral surface	2	1.1	2.0
26. Sidescraper, with abrupt retouch	1	0.6	1.0
27. Sidescraper, with thin back	0	0	0
28. Sidescraper, bifacial retouch	1	0.6	1.0
29. Sidescraper, with alternate retouch	0	0	0
30. Typical endscraper	1	0.6	1.0
31. Atypical endscraper	0	0	0
32. Typical burin	0	0	0
33. Atypical burin	2	1.1	2.0
34. Typical borer	0	0	0
35. Atypical borer	1	0.6	1.0
36. Typical backed knife	3	1.7	3.0
37. Atypical backed knife	4	2.2	4.0
38. Naturally backed knife	3	1.7	3.0
39. Mousterian raclette	2	1.1	2.0
40. Truncated piece	2	1.1	2.0
41. Mousterian tranchet	0	0	0
42. Notched pieces	12	6.8	12.1

Tool	Number	Total Percentage	Restricted Percentage
43. Denticulate	34	19.1	34.3
44. Ecc burinante alterne	1	0.6	1.0
45. Flake, retouched on the ventral surface	4	2.2	4.0
46. Miscellaneous retouched flake, abrupt thick retouch	0	0	
47. Miscellaneous retouched flake, alternate thick retouch	0	0	
48. Miscellaneous retouched flake, abrupt thin retouch			
49. Miscellaneous retouched flake, alternate thin retouch	39	21.3	
50. Flake, bifacial retouch	5	2.8	
51. Tayac point	1	0.6	1.0
52. Notched triangle	0	0	0
53. Pseudo-microburin	0	0	0
54. Flake, notched end	0	0	0
55. Cleavers	0	0	0
56. Rabot (plane)	0	0	0
57. Aterian tanged point	0	0	0
58. Tanged piece	0	0	0
59. Chopper	1	0.6	1.0
60. Inverse chopper	0	0	0
61. Chopping tool	0	0	0
62. Miscellaneous piece	5	2.8	5.1
63. Blattspitzen	0	0	0
	<hr/>	<hr/>	<hr/>
	178	99.5	99.7
	(99)		

Table 6.8 Tool Typology, Couche IV,  
Abri Suard, Lachaise

Table 6.7 Technical and Typological Indices and Characteristic  
Groups, Couche III, Abri Suard, Lachaise

Index	Total	Restricted
Levallois	13.60	
Facetting	56.13	
Restricted Facetting	48.87	
Blade (lamellar)	9.43	
Typological Levallois	15.8	0
Sidescraper (Group II)	22.2	37.6
Total Acheulian	6.5	10.7
Unifacial Acheulian	1.7	2.8
Bifacial	4.9	8.1
Charentien	10.0	16.9
Quina	0	
Group I: tools # 1 - 4	15.8	0
Group III: tools # 30 - 37, 40	6.6	11.2
Group IV: denticulates	9.4	15.8

Tool	Number	Total Percentage	Restricted Percentage
1. Typical Levallois flake	55	4.9	
2. Atypical Levallois flake	117	10.3	
3. Levallois point	2	0.2	
4. Retouched Levallois point	2	0.2	0.3
5. Pseudo-Levallois point	1	0.1	0.2
6. Mousterian point	2	0.2	0.3
7. Elongated Mousterian point	1	0.1	0.2
8. Limace	3	0.3	0.5
9. Sidescraper, single straight	35	3.1	5.3
10. Sidescraper, single convex	120	10.6	16.2
11. Sidescraper, single concave	18	1.6	2.7
12. Sidescraper, double straight	2	0.2	0.3
13. Sidescraper, double straight convex	12	1.1	1.8
14. Sidescraper, double straight concave	0	0	0
15. Sidescraper, double biconvex	7	0.6	1.1
16. Sidescraper, double biconcave	2	0.2	0.3
17. Sidescraper, double convex concave	6	0.5	0.9
18. Sidescraper, convergent straight	1	0.1	0.2
19. Sidescraper, convergent convex	14	1.2	2.1
20. Sidescraper, convergent concave	0	0	0

642

Tool	Number	Total Percentage	Restricted Percentage	Tool	Number	Total Percentage	Restricted Percentage
21. Sidescraper, asymmetrical	11	1.0	1.7	43. Denticulate	150	13.3	23.8
22. Sidescraper, transverse straight	1	0.1	0.2	44. Rec burinante alterne	10	0.9	1.5
23. Sidescraper, transverse convex	7	0.6	1.1	45. Flake, retouched on the ventral surface	13	1.1	
24. Sidescraper, transverse concave	0	0	0	46. Miscellaneous retouched flake, abrupt thick retouch			
25. Sidescraper, retouched on the ventral surface	11	1.0	1.7	47. Miscellaneous retouched flake, alternate thick retouch	120	10.6	
26. Sidescraper, with abrupt retouch	8	0.7	1.2	48. Miscellaneous retouched flake, abrupt thin retouch	154	13.6	
27. Sidescraper, with thin back	2	0.2	0.3	49. Miscellaneous retouched flake, alternate thin retouch			
28. Sidescraper, bifacial retouch	4	0.4	0.6	50. Flake, bifacial retouch	13	1.1	
29. Sidescraper, with alternate retouch	4	0.4	0.6	51. Tazac point	0	0	0
30. Typical endscraper	11	1.0	1.7	52. Notched triangle	0	0	0
31. Atypical endscraper	6	0.5	0.9	53. Pseudo-microburin	0	0	0
32. Typical burin	3	0.3	0.5	54. Flake, notched end	6	0.5	0.9
33. Atypical burin	7	0.6	1.1	55. Cleavers	0	0	0
34. Typical borer	3	0.3	0.5	56. Rabot (plane)	0	0	0
35. Atypical borer	3	0.3	0.5	57. Aterian tanged point	0	0	0
36. Typical backed knife	5	0.4	0.8	58. Tanged piece	0	0	0
37. Atypical backed knife	9	0.8	1.4	59. Chopper	1	0.1	0.2
38. Naturally backed knife	10	0.9	1.5	60. Inverse chopper	0	0	0
39. Mousterian raclette	21	1.9	3.2	61. Chopping tool	2	0.2	0.3
40. Truncated piece	16	1.4	2.4	62. Miscellaneous piece	53	5.1	8.8
41. Mousterian tranchet	0	0	0	63. Blattspitzen	0	0	0
42. Notched pieces	63	5.6	9.6	Total	1132	101.4	101.9

(658)

Table 6.9 Technical and Typological Indices and Characteristic Groups, Couche IV, Abri Suard, Lachaise

Index	Total	Restricted
Levallois	15.64	
Facetting	58.64	
Restricted Facetting	52.42	
Blade (lamellar)	11.20	
Typological Levallois	15.5	0.3
Sidescraper (Group II)	23.4	40.2
Total Acheulian	3.2	5.3
Unifacial Acheulian	0.7	2.1
Bifacial	2.0	3.4
Charentien	12.3	21.1
Quina	1.5	
Group I: tools # 1 - 4	19.5	0.3
Group III: tools # 30 - 37, 40	9.5	9.5
Group IV: denticulates	13.3	22.8

Table 6.10 Tool Typology, Couche V, Abri Suard, Lachaise

Tool	Number	Total Percentage	Restricted Percentage
1. Typical Levallois flake	18	3.6	
2. Atypical Levallois flake	68	13.5	
3. Levallois point	1	0.2	
4. Retouched Levallois point	0	0	
5. Pseudo-Levallois point	1	0.2	0.4
6. Mousterian point	2	0.4	0.8
7. Elongated Mousterian point	0	0	0
8. Limace	0	0	0
9. Sidescraper, single straight	8	1.6	3.2
10. Sidescraper, single convex	26	5.2	10.3
11. Sidescraper, single concave	5	1.0	2.0
12. Sidescraper, double straight	0	0	0
13. Sidescraper, double straight convex	2	0.4	0.8
14. Sidescraper, double straight concave	0	0	0
15. Sidescraper, double biconvex	1	0.2	0.4
16. Sidescraper, double biconcave	0	0	0
17. Sidescraper, double convex concave	2	0.4	0.8
18. Sidescraper, convergent straight	0	0	0
19. Sidescraper, convergent convex	2	0.4	0.8
20. Sidescraper, convergent concave	0		

Tool	Number	Total Percentage	Restricted Percentage
21. Sidescraper, asymmetrical	2	0.4	0.8
22. Sidescraper, transverse straight	0	0	0
23. Sidescraper, transverse convex	0	0	0
24. Sidescraper, transverse concave	0	0	0
25. Sidescraper, retouched on the ventral surface	15	3.0	5.9
26. Sidescraper, with abrupt retouch	0	0	0
27. Sidescraper, with thin back	0	0	0
28. Sidescraper, bifacial retouch	5	1.0	2.0
29. Sidescraper, with alternate retouch	1	0.2	0.4
30. Typical endscraper	2	0.4	0.8
31. Atypical endscraper	3	0.6	1.2
32. Typical burin	1	0.2	0.4
33. Atypical burin	5	1.0	2.0
34. Typical borer	3	0.6	1.2
35. Atypical borer	0	0	0
36. Typical backed knife	2	0.4	0.8
37. Atypical backed knife	6	1.2	2.4
38. Naturally backed knife	12	2.4	4.7
39. Mousterian scalotte	2	0.4	0.8
40. Truncated piece	3	0.6	1.2
41. Mousterian tranchet	0	0	0
42. Notched pieces	31	6.2	12.3

Tool	Number	Total Percentage	Restricted Percentage
43. Denticulate	83	16.5	32.8
44. Sec burinante alterne	1	0.2	0.4
45. Flake, retouched on the ventral surface	15	3.0	
46. Miscellaneous retouched flake, abrupt thick retouch	23	4.6	
47. Miscellaneous retouched flake, alternate thick retouch			
48. Miscellaneous retouched flake, abrupt thin retouch			
49. Miscellaneous retouched flake, alternate thin retouch	119	23.7	
50. Flake, bifacial retouch	6	1.2	
51. Tanged point	1	0.2	0.4
52. Notched triangle	0	0	0
53. Pseudo-microburin	0	0	0
54. Flake, notched end	0	0	0
55. Cleavers	0	0	0
56. Rabet (plane)	0	0	0
57. Aterian tanged point	0	0	0
58. Tanged piece	0	0	0
59. Chopper	0	0	0
60. Inverse chopper	0	0	0
61. Chopping tool	0	0	0
62. Miscellaneous piece	27	5.4	10.7
63. Blattspitzen	0	0	0
Total	503	100.5	100.3

(253)

252

Table 6.11 Technical and Typological Indices and Characteristic Groups, Couche V, Abri Suard, Lachaise

Index	Total	Restricted
Levallois	17.90	
Facotting	65.02	
Restricted Facotting	58.96	
Blade (lamellar)	13.23	
Aypological Levallois	17.3	0
Sidescraper (Group II)	13.5	26.5
Total Acheulian	1.9	3.8
Unifacial Acheulian	1.6	3.2
Bifacial	0.4	0.8
Charentien	5.3	10.7
Quina	1.5	
Group I: tools # 1 - 4	17.3	0
Group III: tools # 30 - 37, 40	4.9	9.9
Group IV: denticulates	16.5	32.8

Table 6.12 Tool Typology, Couche VI, Abri Suard, Lachaise

Tool	Number	Total Percentage	Restricted Percentage
1. Typical Levallois flake	5	2.8	
2. Atypical Levallois flake	26	14.9	
3. Levallois point	0	0	
4. Retouched Levallois point	1	0.6	1.0
5. Pseudo-Levallois point	0	0	0
6. Mousterian point	0	0	0
7. Elongated Mousterian point	0	0	0
8. Limace	0	0	0
9. Sidescraper, single straight	5	2.8	5.1
10. Sidescraper, single convex	6	3.4	6.1
11. Sidescraper, single concave	2	1.1	2.0
12. Sidescraper, double straight	1	0.6	1.0
13. Sidescraper, double straight convex	0	0	1.0
14. Sidescraper, double straight concave	1	0.6	1.0
15. Sidescraper, double biconvex	1	0.6	1.0
16. Sidescraper, double biconcave	0	0	0
17. Sidescraper, double convex concave	0	0	0
18. Sidescraper, convergent straight	1	0.6	1.0
19. Sidescraper, convergent convex	0	0	0
20. Sidescraper, convergent concave	0	0	0

453

Tool	Number	Total Percentage	Restricted Percentage
21. Sidescraper, asymmetrical	4	0.8	1.4
22. Sidescraper, transverse straight	0	0	0
23. Sidescraper, transverse convex	4	0.8	1.4
24. Sidescraper, transverse concave	1	0.2	0.4
25. Sidescraper, retouched on the ventral surface	11	2.3	3.9
26. Sidescraper, with abrupt retouch	0	0	0
27. Sidescraper, with thin back	0	0	0
28. Sidescraper, bifacial retouch	2	0.4	0.7
29. Sidescraper, with alternate retouch	1	0.2	0.4
30. Typical endscraper	2	0.4	0.7
31. Atypical endscraper	3	0.6	1.1
32. Typical burin	3	0.6	1.1
33. Atypical burin	6	1.2	2.1
34. Typical borer	1	0.2	0.4
35. Atypical borer	8	1.7	2.8
36. Typical backed knife	2	0.4	0.7
37. Atypical backed knife	6	1.2	2.1
38. Naturally backed knife	7	1.5	2.5
39. Mousterian raclette	10	2.1	3.5
40. Truncated piece	1	0.2	0.4
41. Mousterian tranchet	0	0	0
42. Notched pieces	36	7.5	12.7

Tool	Number	Total Percentage	Restricted Percentage
43. Denticulate	45	9.4	15.8
44. Bec burinante alterne	3	0.6	1.1
45. Flake, retouched on the ventral surface	13	2.7	
46. Miscellaneous retouched flake, abrupt thick retouch			
47. Miscellaneous retouched flake, alternate thick retouch	29	6.0	
48. Miscellaneous retouched flake, abrupt thin retouch			
49. Miscellaneous retouched flake, alternate thin retouch	70	14.6	
50. Flake, bifacial retouch	9	1.9	
51. Tanged point	1	0.2	0.4
52. Notched triangle	0	0	0
53. Pseudo-microburin	0	0	0
54. Flake, notched end	0	0	0
55. Cleavers	0	0	0
56. Rabot (plane)	0	0	0
57. Aterian tanged point	0	0	0
58. Tanged piece	0	0	0
59. Chopper	1	0.2	0.4
60. Inverse chopper	0	0	0
61. Chopping tool	2	0.4	0.7
62. Miscellaneous piece	30	6.2	10.6
63. Elbttspitzen	0	0	0
Total	461	99.7	163.9

(284)

254

Table 6.14 Tool Typology, Couche V-VI (mixed),  
Abri Suard, Lachaise

Table 6.13 Technical and Typological Indices and Characteristic  
Groups, Couche VI, Abri Suard, Lachaise

Index	Total	Restricted
Levallois	18.58	
Facetting	63.52	
Restricted Facetting	61.71	
Blade (lamellar)	10.91	
Typological Levallois	18.2	1.0
Sidescraper (Group II)	14.0	25.3
Total Acheulian	4.5	7.5
Unifacial Acheulian	3.9	7.1
Bifacial	0.6	1.0
Charentien	5.1	9.1
Quina	0	
Group I: tools # 1 - 4	18.2	1.0
Group III: tools # 30 - 37, 40	7.8	14.1
Group IV: denticulates	19.1	34.3

Tool	Number	Total Percentage	Restricted Percentage
1. Typical Levallois flake	69	4.6	
2. Atypical Levallois flake	243	16.8	
3. Levallois point	1	0.1	
4. Retouched Levallois point	1	0.1	0.1
5. Pseudo-Levallois point	3	0.2	0.4
6. Mousterian point	5	0.3	0.6
7. Elongated Mousterian point	3	0.2	0.4
8. Limace	1	0.1	0.1
9. Sidescraper, single straight	30	2.0	3.7
10. Sidescraper, single convex	95	6.3	11.6
11. Sidescraper, single concave	28	1.9	3.4
12. Sidescraper, double straight	3	0.2	0.4
13. Sidescraper, double straight, convex	4	0.3	0.5
14. Sidescraper, double straight concave	1	0.1	0.1
15. Sidescraper, double biconvex	4	0.3	0.5
16. Sidescraper, double biconcave	1	0.1	0.1
17. Sidescraper, double convex concave	2	0.1	0.2
18. Sidescraper, convergent straight	1	0.1	0.1
19. Sidescraper, convergent convex	8	0.5	1.0
20. Sidescraper, convergent concave	0	0	0

where is the rest of 6.38



Tool	Number	Total Percentage	Restricted Percentage
21. Sidescraper, asymmetrical	12	0.8	1.5
22. Sidescraper, transverse straight	1	0.1	0.1
23. Sidescraper, transverse convex	3	0.2	0.4
24. Sidescraper, transverse concave	1	0.1	0.1
25. Sidescraper, retouched on the ventral surface	43	2.9	5.2
26. Sidescraper, with abrupt retouch	1	0.1	0.1
27. Sidescraper, with thin back	8	0.5	1.0
28. Sidescraper, bifacial retouch	17	1.1	2.1
29. Sidescraper, with alternate retouch	9	0.6	1.1
30. Typical endscraper	10	0.7	1.2
31. Atypical endscraper	8	0.5	1.0
32. Typical burin	7	0.5	0.9
33. Atypical burin	15	1.0	1.8
34. Typical borer	6	0.4	0.7
35. Atypical borer	5	0.4	0.6
36. Typical backed knife	7	0.5	0.9
37. Atypical backed knife	9	0.6	1.1
38. Naturally backed knife	31	2.0	3.8
39. Mousterian raclette	14	0.9	1.7
40. Truncated piece	13	0.9	1.6
41. Mousterian tranchet	0	0	0
42. Notched pieces	86	5.7	10.5

Tool	Number	Total Percentage	Restricted Percentage
43. Denticulate	209	13.9	25.5
44. Bec burinante alterne	5	0.4	0.6
45. Flake, retouched on the ventral surface	41	2.7	
46. Miscellaneous retouched flake, abrupt thick retouch	44	2.9	
47. Miscellaneous retouched flake, alternate thick retouch			
48. Miscellaneous retouched flake, abrupt thin retouch			
49. Miscellaneous retouched flake, alternate thin retouch	269	17.9	
50. Flake, bifacial retouch	16	1.1	
51. Tayac point	1	0.1	0.1
52. Notched triangle	2	0.1	0.2
53. Pseudo-microburin	2	0.1	0.2
54. Flake, notched end	1	0.1	0.1
55. Cleavers	0	0	0
56. Rabot (plane)	0	0	0
57. Aterian tanged point	0	0	0
58. Tanged piece	0	0	0
59. Chopper	0	0	0
60. Inverse chopper	0	0	0
61. Chopping tool	1	0.1	0.1
62. Miscellaneous piece	104	6.9	12.7
63. Blattspitzen	0	0	0
Total	1504	101.6	100.1
	(821)		

Table 6.45 Technical and Typological Indices and Characteristic Groups, Couche V-VI (mixed), Abri Suard, Lachaise

Index	Total	Restricted
Levallois	14.54	
Facetting	63.37	
Restricted Facetting	58.67	
Blade (lame)llar)	12.78	
Typological Levallois	21.5	0.1
Sidescraper (Group II)	18.1	34.4
Total Acheulian	1.5	2.8
Unifacial Acheulian	0.8	1.9
Bifacial	0.5	0.8
Charentien	7.4	18.7
Quina	1.5	
Group I: tools # 1 - 4	21.5	0.1
Group III: tools # 30 - 37, 40	5.3	9.7
Group IV: denticulates	13.9	16.5

Table 6.46 Tool Typology, Couche VIII, Abri Suard, Lachaise

Tool	Number	Total Percentage	Restricted Percentage
1. Typical Levallois flake	4	4.0	
2. Atypical Levallois flake	14	14.0	
3. Levallois point	1	1.0	
4. Retouched Levallois point	0	0	0
5. Pseudo-Levallois point	0	0	0
6. Mousterian point	0	0	0
7. Elongated Mousterian point	0	0	0
8. Limace	0	0	0
9. Sidescraper, single straight	4	4.0	6.6
10. Sidescraper, single convex	7	7.0	11.5
11. Sidescraper, single concave	1	1.0	1.6
12. Sidescraper, double straight	1	1.0	1.6
13. Sidescraper, double straight convex	0	0	0
14. Sidescraper, double straight concave	0	0	0
15. Sidescraper, double biconvex	3	3.0	4.9
16. Sidescraper, double biconcave	0	0	0
17. Sidescraper, double convex concave	0	0	0
18. Sidescraper, convergent straight	0	0	0
19. Sidescraper, convergent convex	0	0	0
20. Sidescraper, convergent concave	0	0	0

257

Tool	Number	Total Percentage	Restricted Percentage
21. Sidescraper, asymmetrical	1	1.0	1.6
22. Sidescraper, transverse straight	1	1.0	1.6
23. Sidescraper, transverse convex	1	1.0	1.6
24. Sidescraper, transverse concave	0	0	0
25. Sidescraper, retouched on the ventral surface	1	1.0	1.6
26. Sidescraper, with abrupt retouch	0	0	0
27. Sidescraper, with thin back	0	0	0
28. Sidescraper, bifacial retouch	0	0	0
29. Sidescraper, with alternate retouch	0	0	0
30. Typical endscraper	0	0	0
31. Atypical endscraper	0	0	0
32. Typical burin	1	1.0	1.6
33. Atypical burin	0	0	0
34. Typical borer	0	0	0
35. Atypical borer	2	2.0	3.3
36. Typical backed knife	0	0	0
37. Atypical backed knife	2	2.0	3.3
38. Naturally backed knife	2	2.0	3.3
39. Mousterian raclette	0	0	0
40. Truncated piece	0	0	0
41. Mousterian tranchet	0	0	0
42. Notched pieces	9	9.0	14.8

Tool	Number	Total Percentage	Restricted Percentage
43. Denticulate	16	16.0	26.2
44. Bec burinante alterne	0	0	
45. Flake, retouched on the ventral surface	0	0	
46. Miscellaneous retouched flake, abrupt thick retouch	0	0	
47. Miscellaneous retouched flake, alternate thick retouch	0	0	
48. Miscellaneous retouched flake, abrupt thin retouch			
49. Miscellaneous retouched flake, alternate thin retouch	18	18.0	
50. Flake, bifacial retouch	2	2.0	
51. Tayac point	0	0	0
52. Notched triangle	0	0	0
53. Pseudo-microburin	0	0	0
54. Flake, notched end	0	0	0
55. Cleavers	1	1.0	1.6
56. Rabot (plane)	0	0	0
57. Aterian tanged point	0	0	0
58. Tanged piece	0	0	0
59. Chopper	0	0	0
60. Inverse chopper	0	0	0
61. Chopping tool	0	0	0
62. Miscellaneous piece	5	5.0	8.2
63. Blattspitzen	0	0	0
Total	100	100.0	95.4

Table 6.17 Tool Typology, Couche 51,  
Abri Suard, Lachaise

Tool	Number	Total Percentage	Restricted Percentage	Tool	Number	Total Percentage	Restricted Percentage
1. Typical Levallois flake	33	10.5		21. Sidescraper, asymmetrical	2	0.6	0.9
2. Atypical Levallois flake	26	8.3		22. Sidescraper, transverse straight	2	0.6	0.9
3. Levallois point	3	1.0		23. Sidescraper, transverse convex	2	0.6	0.9
4. Retouched Levallois point	4	1.3	1.9	24. Sidescraper, transverse concave	0	0	0
5. Pseudo-Levallois point	1	0.3	0.5	25. Sidescraper, retouched on the ventral surface	1	0.3	0.5
6. Mousterian point	4	1.3	1.9	26. Sidescraper, with abrupt retouch	3	1.0	1.4
7. Elongated Mousterian point	1	0.3	0.5	27. Sidescraper, with thin back	1	0.3	0.5
8. Limace	0	0	0	28. Sidescraper, bifacial retouch	2	0.6	0.9
9. Sidescraper, single straight	26	8.3	12.0	29. Sidescraper, with alternate retouch	0	0	0
10. Sidescraper, single convex	45	13.7	19.9	30. Typical endscraper	2	0.6	0.9
11. Sidescraper, single concave	7	2.2	3.2	31. Atypical endscraper	1	0.3	0.5
12. Sidescraper, double straight	3	1.0	1.4	32. Typical burin	2	0.6	0.9
13. Sidescraper, double straight convex	8	2.5	3.7	33. Atypical burin	3	1.0	1.4
14. Sidescraper, double straight concave	0	0	0	34. Typical borer	1	0.3	0.5
15. Sidescraper, double biconvex	11	3.5	5.1	35. Atypical borer	1	0.3	0.5
16. Sidescraper, double biconcave	0	0	0	36. Typical backed knife	0	0	0
17. Sidescraper, double convex concave	2	0.6	0.9	37. Atypical backed knife	2	0.6	0.9
18. Sidescraper, convergent straight	0	0	0	38. Naturally backed knife	16	5.1	7.4
19. Sidescraper, convergent convex	1	0.3	0.5	39. Mousterian raclette	1	0.3	0.5
20. Sidescraper, convergent concave	1	0.3	0.5	40. Truncated piece	6	1.9	2.8
				41. Mousterian tranchet	0	0	0
				42. Notched pieces	16	5.1	7.4

Table 6.19 Tool Typology, Couche 52,  
Abri Suard, Lachaise

Tool	Number	Total Percentage	Restricted Percentage
1. Typical Levallois flake	17	10.8	
2. Atypical Levallois flake	15	9.6	
3. Levallois point	0	0	
4. Retouched Levallois point	3	1.9	2.8
5. Pseudo-Levallois point	0	0	0
6. Mousterian point	1	0.6	0.9
7. Elongated Mousterian point	2	1.3	1.9
8. Limace	0	0	0
9. Sidescraper, single straight	12	7.6	11.3
10. Sidescraper, single convex	20	12.7	18.9
11. Sidescraper, single concave	5	3.2	4.7
12. Sidescraper, double straight	0	0	
13. Sidescraper, double straight convex	6	3.8	5.7
14. Sidescraper, double straight concave	1	0.6	0.9
15. Sidescraper, double biconvex	6	3.8	5.7
16. Sidescraper, double biconcave	0	0	0
17. Sidescraper, double convex concave	0	0	0
18. Sidescraper, convergent straight	1	0.6	0.9
19. Sidescraper, convergent convex	4	2.5	3.8
20. Sidescraper, convergent concave	0	0	0

Table 6.18 Technical and Typological Indices and Characteristic Groups, Couche 51, Abri Suard, Lachaise

Index	Total	Restricted
Levallois	20.81	
Facetting	60.60	
Restricted Facetting	52.81	
Blade (lamellar)	8.12	
Typological Levallois	20.9	1.9
Sidescraper (Group II)	36.4	53.2
Total Acheulian	1.8	2.7
Unifacial Acheulian	0.6	0.9
Bifacial	1.3	1.8
Charentien	14.6	22.7
Quina	0.9	
Group I: tools # 1 - 4	20.9	1.9
Group III: tools # 30 - 37, 40	5.7	8.3
Group IV: denticulates	4.4	6.5

260

Tool	Number	Total Percentage	Restricted Percentage
21. Sidescraper, asymmetrical	0	0	0
22. Sidescraper, transverse straight	0	0	0
23. Sidescraper, transverse convex	2	1.3	1.9
24. Sidescraper, transverse concave	0	0	0
25. Sidescraper, retouched on the ventral surface	0	0	0
26. Sidescraper, with abrupt retouch	1	0.6	0.9
27. Sidescraper, with thin back	1	0.6	0.9
28. Sidescraper, bifacial retouch	0	0	0
29. Sidescraper, with alternate retouch	0	0	0
30. Typical endscraper	2	1.3	1.9
31. Atypical endscraper	0	0	0
32. Typical burin	2	1.3	1.9
33. Atypical burin	0	0	0
34. Typical borer	0	0	0
35. Atypical borer	0	0	0
36. Typical backed knife	1	0.6	0.9
37. Atypical backed knife	1	0.6	0.9
38. Naturally backed knife	5	3.2	4.7
39. Mousterian raclette	0	0	0
40. Truncated piece	5	3.2	4.7
41. Mousterian tranchet	0	0	0
42. Notched pieces	7	4.5	6.5

Tool	Number	Total Percentage	Restricted Percentage
43. Denticulate	9	5.7	8.5
44. Eec burinante alterne	1	0.6	0.9
45. Flake, retouched on the ventral surface	0	0	0
46. Miscellaneous retouched flake, abrupt thick retouch	0	0	0
47. Miscellaneous retouched flake, alternate thick retouch	0	0	0
48. Miscellaneous retouched flake, abrupt thin retouch	0	0	0
49. Miscellaneous retouched flake, alternate thin retouch	19	12.1	
50. Flake, bifacial retouch	0	0	0
51. Tazac point	0	0	0
52. Notched triangle	0	0	0
53. Pseudo-microburin	0	0	0
54. Flake, notched end	0	0	0
55. Cleavers	0	0	0
56. Rabet (plane)	0	0	0
57. Aterian tanged point	0	0	0
58. Tanged piece	0	0	0
59. Chopper	3	1.9	2.8
60. Inverse chopper	0	0	0
61. Chopping tool	2	1.3	1.9
62. Miscellaneous piece	3	1.9	2.8
63. Blattspitzen	0	0	0
Total	157	99.7	99.6

Table 6.21 Tool Typology, Couche 53,  
Abri Suard, Lachaise

Table 6.20 Technical and Typological Indices and Characteristic  
Groups, Couche 52, Abri Suard, Lachaise,

Index	Total	Restricted	Tool	Number	Total Percentage	Restricted Percentage
Levallois	19.52		1. Typical Levallois flake	11	15.9	
Facetting	49.63		2. Atypical Levallois flake	5	7.2	
Restricted Facetting	40.14		3. Levallois point	0	0	
Blade (lamellar)	7.14		4. Retouched Levallois point	0	0	
Atypological Levallois	22.3	2.8	5. Pseudo-Levallois point	0	0	0
Sidescraper (Group II)	37.5	58.4	6. Mousterian point	0	0	0
Total Acheulian	1.3	2.0	7. Elongated Mousterian point	0	0	0
Unifacial Acheulian	1.3	2.0	8. Limace	0	0	0
Bifacial	0	0	9. Sidescraper, single straight	6	8.7	14.0
Charentien	7.0	10.4	10. Sidescraper, single convex	5	7.2	11.6
Quina	6.7		11. Sidescraper, single concave	0	0	0
Group I: tools # 1 - 4	22.3	2.8	12. Sidescraper, double straight	0	0	0
Group III: tools # 30 - 37, 40	7.0	10.4	13. Sidescraper, double straight convex	1	1.4	2.3
Group IV: denticulates	6.8	8.5	14. Sidescraper, double straight concave	0	0	0
			15. Sidescraper, double biconvex	1	1.4	2.3
			16. Sidescraper, double biconcave	0	0	0
			17. Sidescraper, double convex concave	1	1.4	2.3
			18. Sidescraper, convergent straight	0	0	0
			19. Sidescraper, convergent convex	1	1.4	2.3
			20. Sidescraper, convergent concave	0	0	0

26

Tool	Number	Total Percentage	Restricted Percentage	Tool	Number	Total Percentage	Restricted Percentage
21. Sidescraper, asymmetrical	2	2.9	4.7	43. Denticulate	5	7.2	11.6
22. Sidescraper, transverse straight	0	0	0	44. Bec burinante alterne	0	0	0
23. Sidescraper, transverse convex	1	1.4	2.3	45. Flake, retouched on the ventral surface	0	0	
24. Sidescraper, transverse concave	0	0	0	46. Miscellaneous retouched flake, abrupt thick retouch	0	0	
25. Sidescraper, retouched on the ventral surface	1	1.4	2.3	47. Miscellaneous retouched flake, alternate thick retouch	0	0	
26. Sidescraper, with abrupt retouch	0	0	0	48. Miscellaneous retouched flake, abrupt thin retouch			
27. Sidescraper, with thin back	1	1.4	2.3	49. Miscellaneous retouched flake, alternate thin retouch	10	14.5	
28. Sidescraper, bifacial retouch	0	0	0	50. Flake, bifacial retouch	0	0	
29. Sidescraper, with alternate retouch	0	0	0	51. Tagac point	0	0	0
30. Typical endscraper	2	2.9	4.7	52. Notched triangle	0	0	0
31. Atypical endscraper	0	0	0	53. Pseudo-microburin	0	0	0
32. Typical burin	0	0	0	54. Flake, notched end	0	0	0
33. Atypical burin	0	0	0	55. Cleavers	0	0	0
34. Typical borer	0	0	0	56. Rabot (plane)	0	0	0
35. Atypical borer	0	0	0	57. Aterian tanged point	0	0	0
36. Typical backed knife	0	0	0	58. Tanged piece	0	0	0
37. Atypical backed knife	1	1.4	2.9	59. Chopper	1	1.4	2.3
38. Naturally backed knife	5	7.2	11.6	60. Inverse chopper	0	0	0
39. Mousterian raclette	0	0	0	61. Chopping tool	3	4.3	7.0
40. Truncated piece	1	1.4	2.3	62. Miscellaneous piece	1	1.4	2.3
41. Mousterian tranchet	0	0	0	63. Blattspitzen	0	0	0
42. Notched pieces	4	5.6	9.3				
				Total	63	99.0	99.5

263



Table 6.22 Technical and Typological Indices and Characteristic Groups, Couche 53, Abri Suard, Lachaise

Index	Total	Restricted
Levallois	19.35	
Facetting	47.45	
Restricted Facetting	44.06	
Blade (lamellar)	10.74	
Atypological Levallois	23.2	0
Sidescraper (Group II)	28.9	46.5
Total Acheulian	1.4	2.3
Unifacial Acheulian	1.4	2.3
Bifacial	0	0
Charentien	11.6	18.6
Quina	5.0	
Group I: tools # 1 - 4	23.2	0
Group III: tools # 30 - 37, 40	5.8	9.3
Group IV: denticulates	7.2	11.6

Table 6.23 Tool Typology, Couche 5, Abri Bourgeois-Delaunay, Lachaise

Tool	Number	Total Percentage	Restricted Percentage
1. Typical Levallois flake	5	3.5	
2. Atypical Levallois flake	8	5.6	
3. Levallois point	0	0	
4. Retouched Levallois point	0	0	0
5. Pseudo-Levallois point	4	2.8	3.7
6. Mousterian point	0	0	0
7. Elongated Mousterian point	1	0.7	0.9
8. Limace	0	0	0
9. Sidescraper, single straight	7	4.9	6.4
10. Sidescraper, single convex	34	23.9	31.2
11. Sidescraper, single concave	2	1.4	1.8
12. Sidescraper, double straight	2	1.4	1.8
13. Sidescraper, double straight convex	1	0.7	0.9
14. Sidescraper, double straight concave	0	0	0
15. Sidescraper, double biconvex	2	1.4	1.8
16. Sidescraper, double biconcave	0	0	0
17. Sidescraper, double convex concave	0	0	0
18. Sidescraper, convergent straight	1	0.7	0.9

264

Tool	Number	Total Percentage	Restricted Percentage	Tool	Number	Total Percentage	Restricted Percentage
21. Sidescraper, asymmetrical	1	0.7	0.9	43. Denticulate	5	3.5	4.6
22. Sidescraper, transverse straight	1	0.7	0.9	44. Bec burinante alterne	2	1.4	1.8
23. Sidescraper, transverse convex	5	3.5	4.6	45. Flake, retouched on the ventral surface	2	1.4	
24. Sidescraper, transverse concave	0	0	0	46. Miscellaneous retouched flake, abrupt thick retouch	0	0	
25. Sidescraper, retouched on the ventral surface	0	0	0	47. Miscellaneous retouched flake, alternate thick retouch	0	0	
26. Sidescraper, with abrupt retouch	0	0	0	48. Miscellaneous retouched flake, abrupt thin retouch	18	12.7	
27. Sidescraper, with thin back	0	0	0	49. Miscellaneous retouched flake, alternate thin retouch			
28. Sidescraper, bifacial retouch	0	0	0	50. Flake, bifacial retouch	2	1.4	
29. Sidescraper, with alternate retouch	0	0	0	51. Tayac point	1	0.7	0.9
30. Typical endscraper	0	0	0	52. Notched triangle	0	0	0
31. Atypical endscraper	1	0.7	0.9	53. Pseudo-microburin	0	0	0
32. Typical burin	2	1.4	1.8	54. Flake, notched end	2	1.4	1.8
33. Atypical burin	2	1.4	1.8	55. Cleavers	0	0	0
34. Typical borer	0	0	0	56. Rabot (plane)	0	0	0
35. Atypical borer	0	0	0	57. Aterian tanged point	0	0	0
36. Typical backed knife	1	0.7	0.9	58. Tanged piece	0	0	0
37. Atypical backed knife	0	0	0	59. Chopper	1	0.7	0.9
38. Naturally backed knife	4	2.8	3.7	60. Inverse chopper	0	0	0
39. Mousterian raclette	2	1.4	1.8	61. Chopping tool	2	1.4	1.8
40. Truncated piece	0	0	0	62. Miscellaneous piece	10	7.0	9.2
41. Mousterian tranchet	0	0	0	63. Blattspitzen	0	0	0
42. Notched pieces	6	4.2	5.5				
				Total	142	98.2	96.0

all facies. Debenath (1974) feels the Tardoire acted as a frontier separated from the traditional regions of Acheulian to the north and south, in which the Acheulian had evolved further toward the Mousterian than in contemporaneous, neighbouring regions. Figures 6.9 to 6.11 show the three facies' typical tools.

In layer 51, occupying 4.5 m<sup>2</sup> in squares K-M 13,14, a collection of reindeer antlers forms a semi-circle, within which were many artefacts. The exact purpose of the collection is not known, but the antlers were whole at the time of their introduction into the cave. Possibly they were used to dry skins, to ward off animals like a fence, or to support skins used as part of a tent or weather guard. Found nearby was an incised bone. Two other incised bones were found in layers 50 and 52. These are among the earliest incised bones ever found. Figure 6.12 shows the reindeer antler assemblage, while Figure 6.13 shows the incised bones.

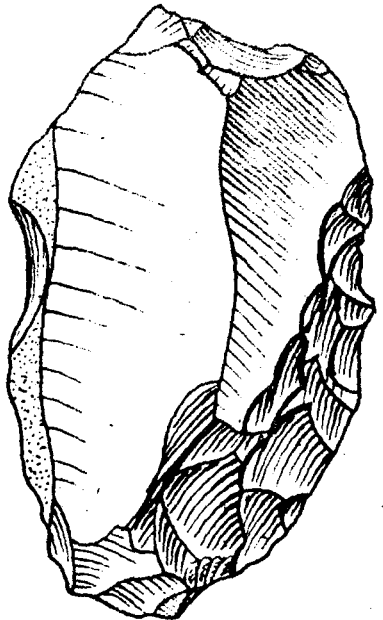
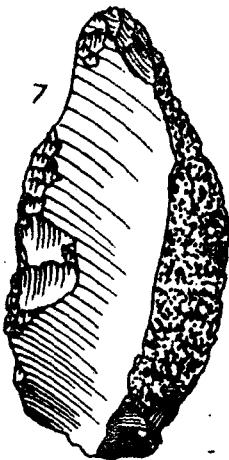
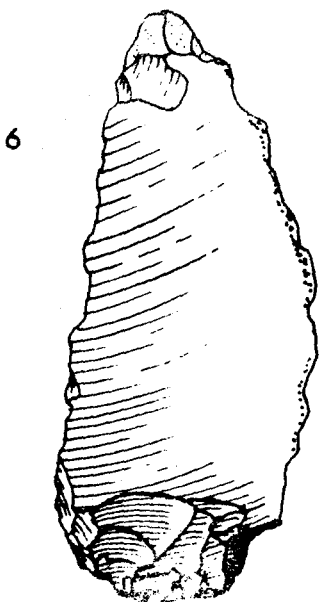
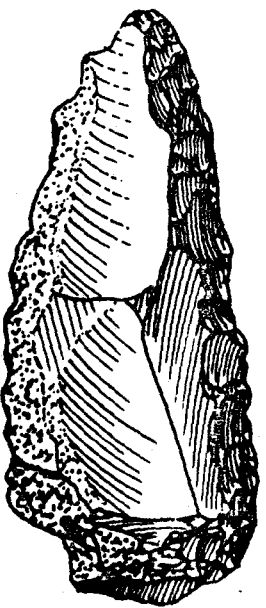
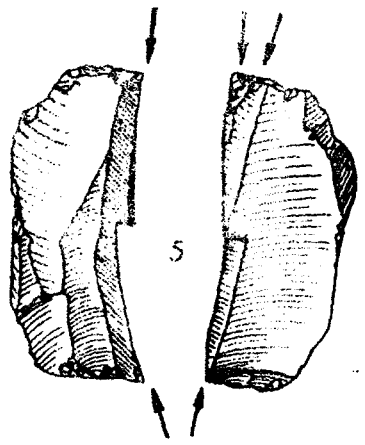
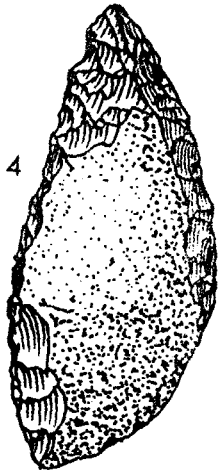
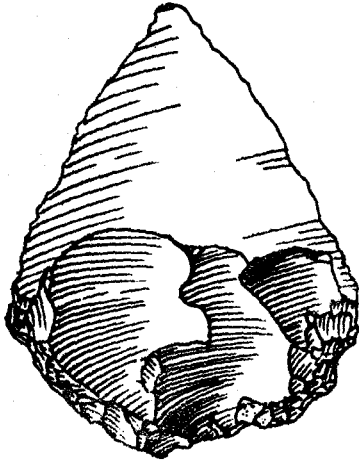
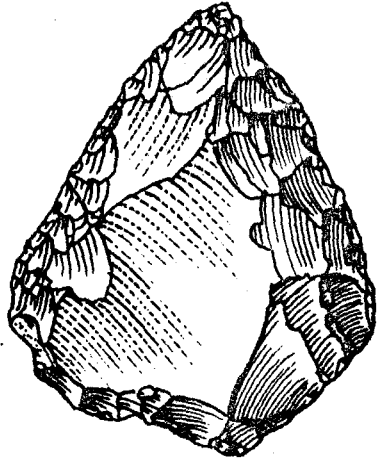
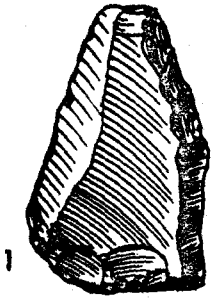
#### 6.3.4.2 Bourgeois-Delaunay

The archeological material above layer 7 in Bourgeois-Delaunay is poorly described by David: that in 2 is an Aurignacian, while that in 5 appears to a poor Mousterian, as is 6. Tables 6.23 to 6.26 describe the latter two.

Layer 8 is also extremely poor, but layer 9 is intermediate between a Mousterian and an Upper Acheulian. It appears very similar to the industry of Facies A in Suard. Layers 8 through 10 are described in Tables 6.27 to 6.37.

Figure 6.9

Tools from Facies A (after Debenath, 1974).



**Figure 6.10**

**Tools from Facies B (after Debenath, 1974).**

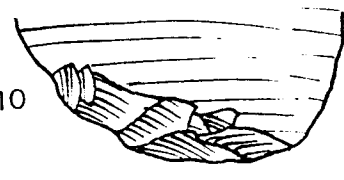
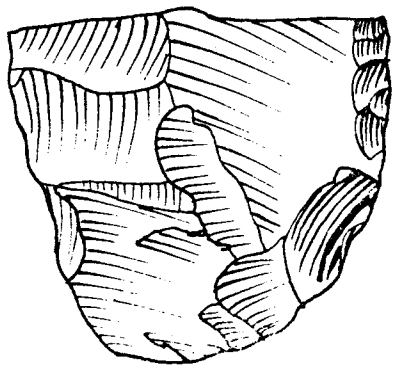
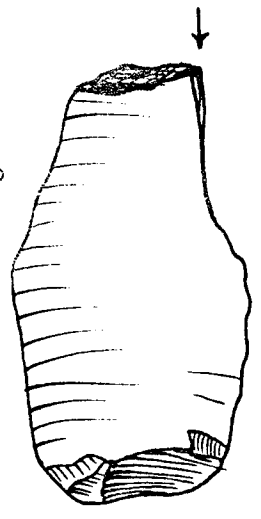
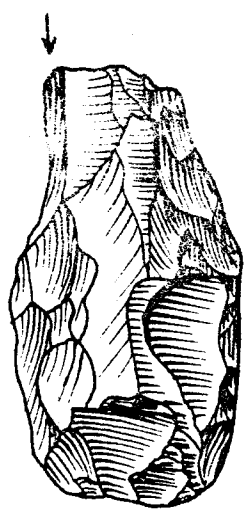
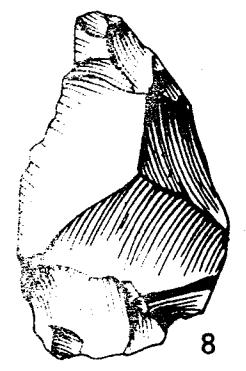
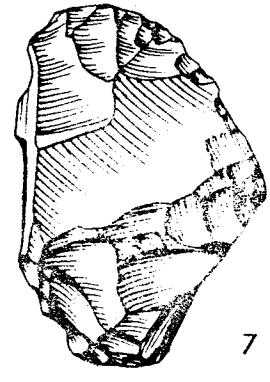
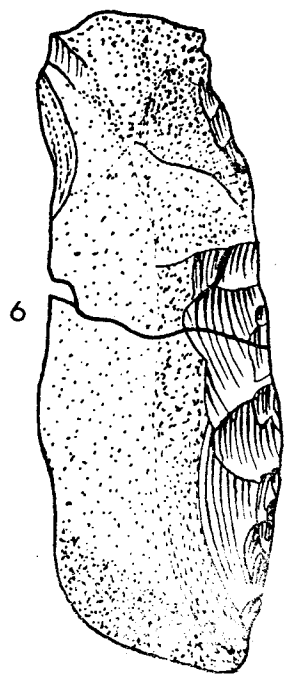
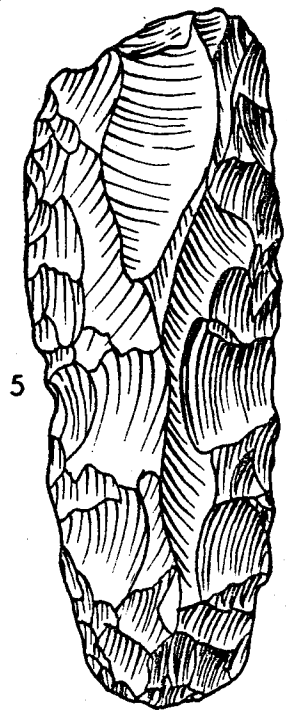
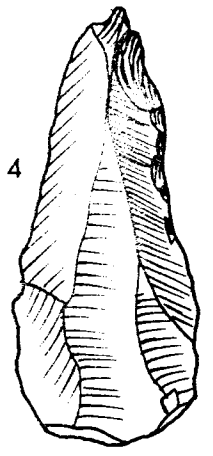
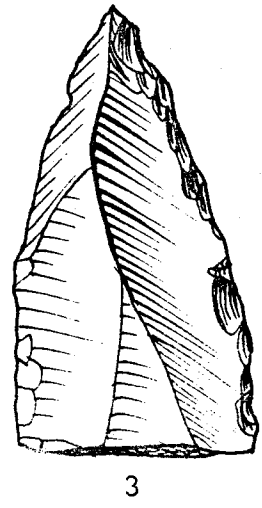
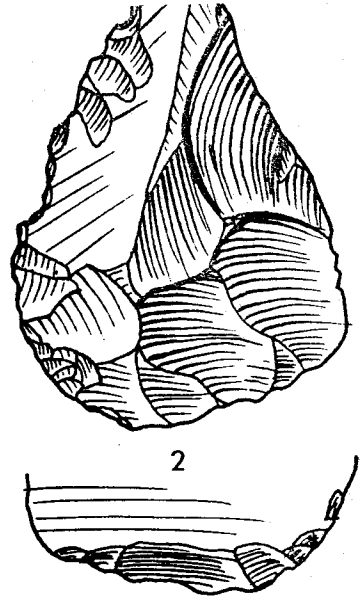
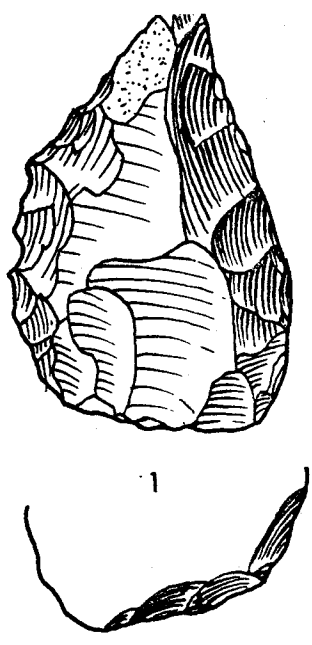
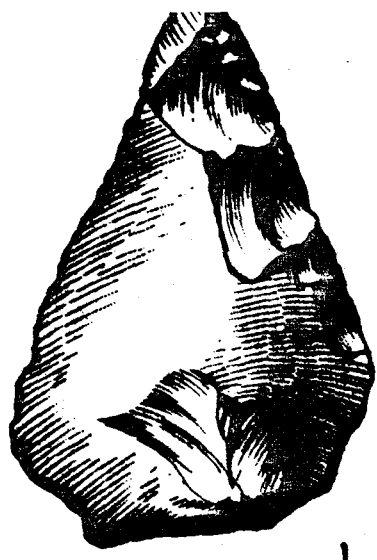


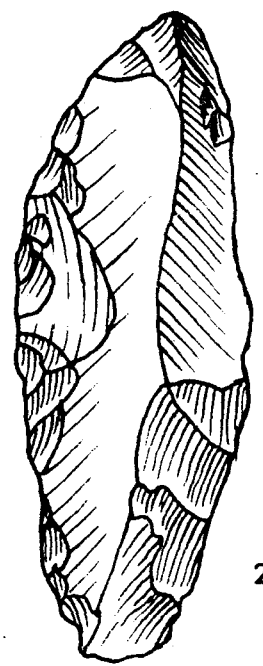
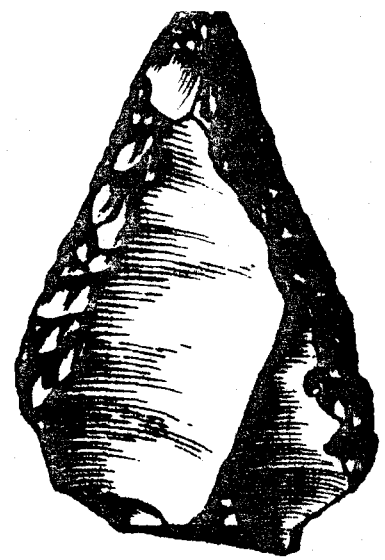
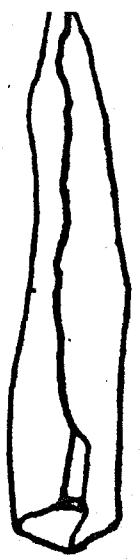
Figure 6.11

Tools from Facies C (after Debenath, 1974)

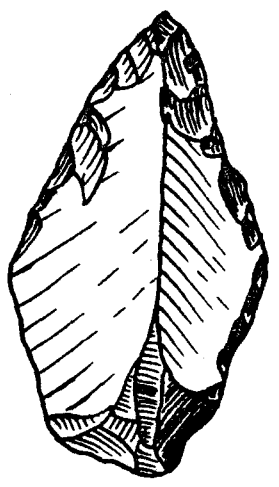




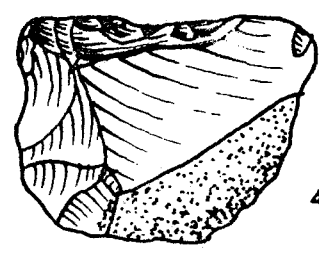
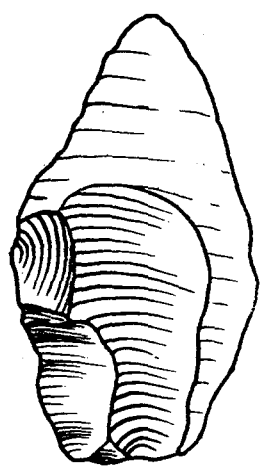
1



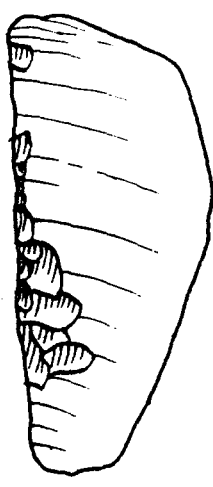
2



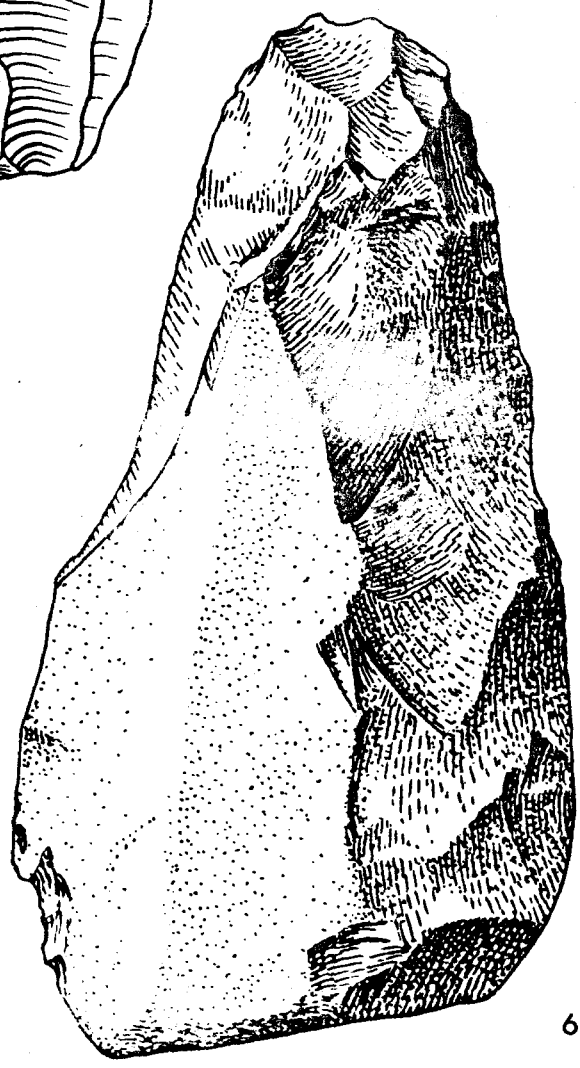
3



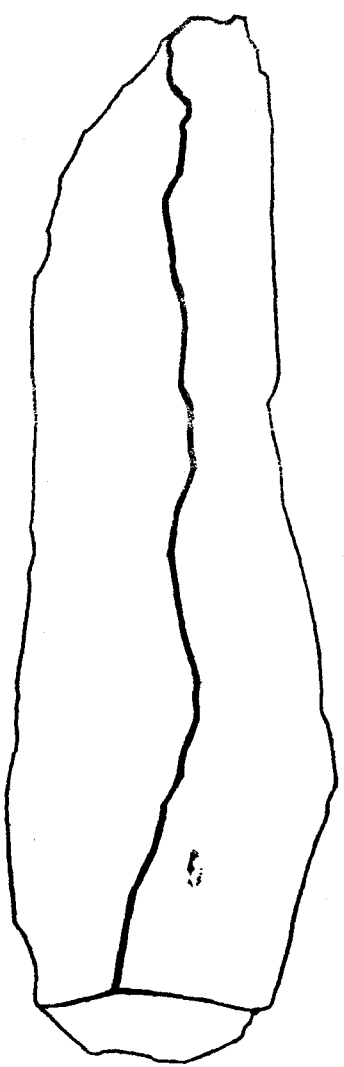
4



5



6



7

**Figure 6.12**

**The structure made of reindeer antlers in Couche  
51, Abri Suard.**

**Black dots are tools found within the structure, while  
the shaded region is a large cobble.**

**X marks the position of the incised bone shown in Figure  
6.13 A (after Débenath, 1974).**

13



14

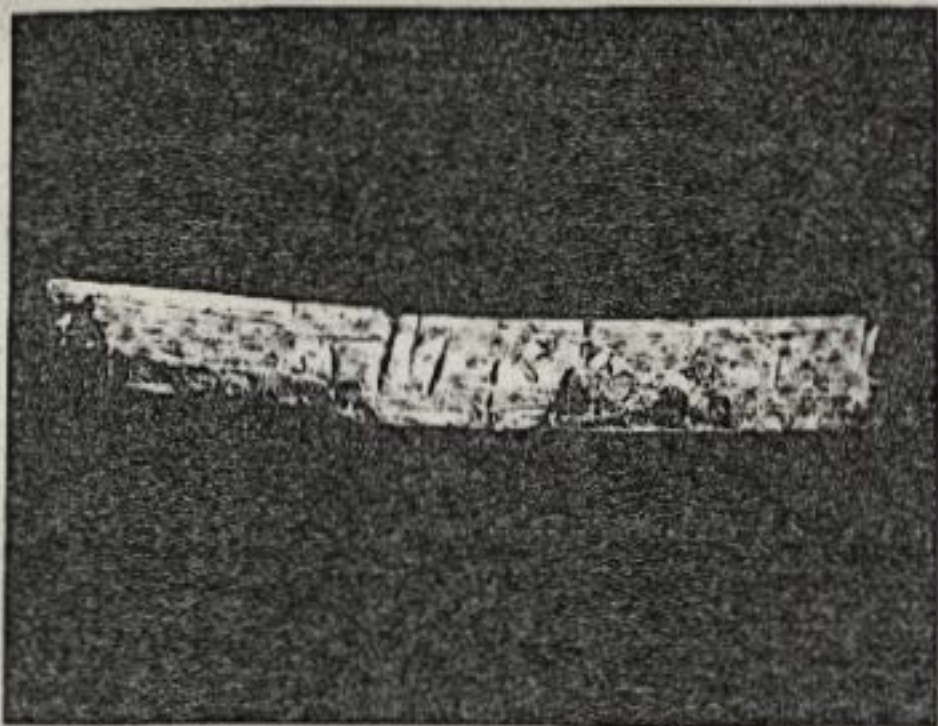


**Figure 6.13**

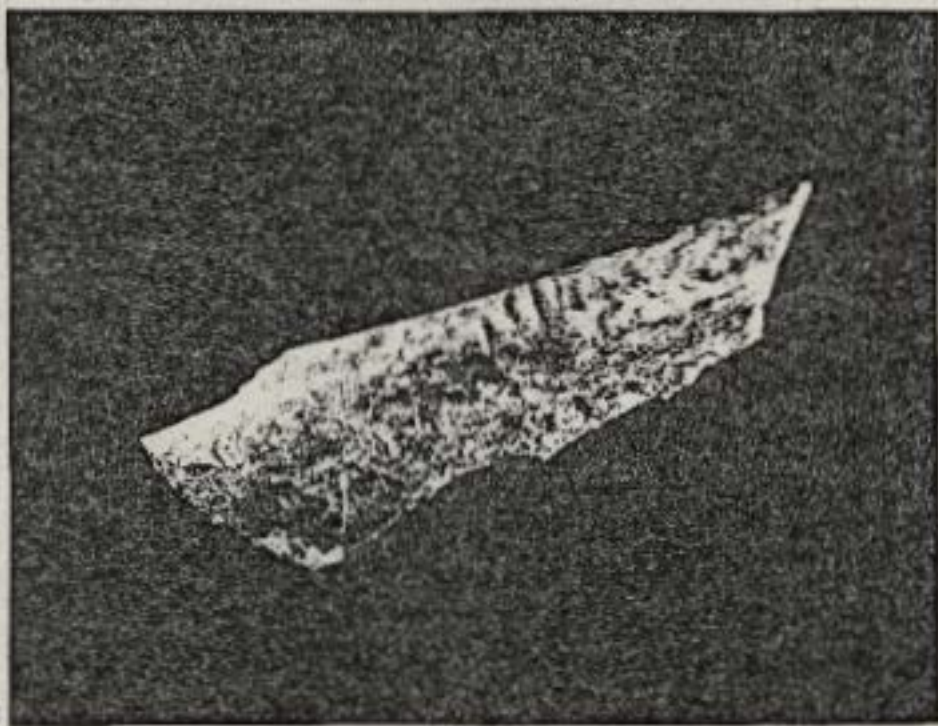
**Incised bones from Abri Suard.**

- A. Incised bone found in couche 51 within  
the circle of reindeer antlers (Figure 6.12)
- B. Incised bone found in couche 52.

(after Débenath, 1974)



A



B

Table 6.25 Tool Typology, Couche 6,  
Abri Bourgeois-Delaunay, Lachaise

Tool	Number	Total Percentage	Restricted Percentage
1. Typical Levallois flake	8	2.5	
2. Atypical Levallois flake	27	8.5	
3. Levallois point	0	0	
4. Retouched Levallois point	0	0	0
5. Pseudo-Levallois point	4	1.3	1.9
6. Mousterian point	1	0.3	0.5
7. Elongated Mousterian point	1	0.3	0.5
8. Limace	0	0	0
9. Sidescraper, single straight	15	4.7	7.2
10. Sidescraper, single convex	62	19.6	29.8
11. Sidescraper, single concave	4	1.3	1.9
12. Sidescraper, double straight	3	0.9	1.4
13. Sidescraper, double straight convex	0	0	0
14. Sidescraper, double straight concave	0	0	0
15. Sidescraper, double biconvex	5	1.6	2.4
16. Sidescraper, double biconcave	0	0	0
17. Sidescraper, double convex concave	0	0	0
18. Sidescraper, convergent straight	3	0.9	1.4
19. Sidescraper, convergent convex	8	2.5	3.8
20. Sidescraper, convergent concave	0	0	0

Table 6.24 Technical and Typological Indices and Characteristic Groups, Couche 5, Abri Bourgeois-Delaunay, Lachaise

Index	Total	Restricted
Levallois	13.50	
Facetting	66.16	
Restricted Facetting	53.38	
Blade (lamellar)	7.50	
Typological Levallois	9.2	0
Sidescraper (Group II)	42.9	55.8
Total Acheulian	0.7	0.9
Unifacial Acheulian	0.7	0.9
Bifacial	0	0
Charentien	28.2	37.7
Quina	4.9	
Group I: tools # 1 - 4	9.2	0
Group III: tools # 30 - 37, 40	4.2	5.5
Group IV: denticulates	3.5	4.5

Table 6.26 Technical and Typological Indices and Characteristic Groups, Couche 6, Abri Bourgeois-Delaunay, Lachaise

Index	Total	Restricted
Levallois	15.10	
Facetting	55.67	
Restricted Facetting	47.87	
Blade (lamellar)	8.03	
Typological Levallois	11.1	0
Sidescraper (Group II)	38.2	58.1
Total Acheulian	1.6	2.3
Unifacial Acheulian	0.9	1.4
Bifacial	0.6	1.0
Charentian	26.7	36.0
Quina	4.1	
Group I: tools # 1 - 4	11.1	0
Group III: tools # 30 - 37, 40	7.5	11.5
Group IV: denticulates	4.4	6.7

Table 6.27 Tool Typology, Couche 8 (a-d), Abri Bourgeois-Delaunay, Lachaise

Tool	Number	Total Percentage	Restricted Percentage
1. Typical Levallois flake	11	7.6	
2. Atypical Levallois flake	10	6.9	
3. Levallois point	0	0	
4. Retouched Levallois point	0	0	0
5. Pseudo-Levallois point	0	0	0
6. Mousterian point	1	0.7	1.7
7. Elongated Mousterian point	0	0	0
8. Limbe	0	0	0
9. Sidescraper, single straight	3	2.1	5.1
10. Sidescraper, single convex	7	4.8	12.9
11. Sidescraper, single concave	3	2.1	5.1
12. Sidescraper, double straight	0	0	0
13. Sidescraper, double straight convex	0	0	0
14. Sidescraper, double straight concave	1	0.7	1.7
15. Sidescraper, double biconvex	2	1.4	3.4
16. Sidescraper, double biconcave	0	0	0
17. Sidescraper, double convex concave	0	0	0
18. Sidescraper, convergent straight	0	0	0
19. Sidescraper, convergent convex	0	0	0
20. Sidescraper, convergent concave	0	0	0

279  
668

Tool	Number	Total Percentage	Restricted Percentage
21. Sidescraper, asymmetrical	1	0.7	1.7
22. Sidescraper, transverse straight	0	0	0
23. Sidescraper, transverse convex	2	1.4	3.4
24. Sidescraper, transverse concave	1	0.7	1.7
25. Sidescraper, retouched on the ventral surface	2	1.4	3.4
26. Sidescraper, with abrupt retouch	2	1.4	3.4
27. Sidescraper, with thin back	0	0	0
28. Sidescraper, bifacial retouch	0	0	0
29. Sidescraper, with alternate retouch	0	0	0
30. Typical endscraper	2	1.4	3.4
31. Atypical endscraper	3	2.1	5.1
32. Typical burin	1	0.7	1.7
33. Atypical burin	2	1.4	3.4
34. Typical borer	0	0	0
35. Atypical borer	0	0	0
36. Typical backed knife	0	0	0
37. Atypical backed knife	0	0	0
38. Naturally backed knife	1	0.7	1.7
39. Mousterian raclette	1	0.7	1.7
40. Truncated piece	2	1.4	3.4
41. Mousterian tranchet	0	0	0
42. Notched pieces	8	5.5	13.5

Tool	Number	Total Percentage	Restricted Percentage
43. Denticulate	5	3.4	8.5
44. Rec burinante alterne	1	0.7	1.7
45. Flake, retouched on the ventral surface	0	0	
46. Miscellaneous retouched flake, abrupt thick retouch			
47. Miscellaneous retouched flake, alternate thick retouch	17	11.7	
48. Miscellaneous retouched flake, abrupt thin retouch			
49. Miscellaneous retouched flake, alternate thin retouch	48	33.1	
50. Flake, bifacial retouch	0	0	
51. Tagac point	0	0	0
52. Notched triangle	0	0	0
53. Pseudo-microburin	0	0	0
54. Flake, notched end	3	2.1	5.1
55. Cleavers	0	0	0
56. Rabot (plane)	0	0	0
57. Aterian tanged point	0	0	0
58. Tanged piece	1	0.7	1.7
59. Chopper	0	0	0
60. Inverse chopper	0	0	0
61. Chopping tool	0	0	0
62. Miscellaneous piece	4	2.8	6.8
63. Blattspitzen	0	0	0
Total	145	100.3	99.5

(59)

280



Table 6.28 Technical and Typological Indices and Characteristic Groups, Couche 8 (a-d), Abri Bourgeois-Delaunay, Lachaise

Index	Total	Restricted
Levallois	11.79	
Facetting	34.64	
Restricted Facetting	27.55	
Blade (lamellar)	2.35	
Typological Levallois	14.5	0
Sidescraper (Group II)	15.8	40.6
Total Acheulian	0.7	1.7
Unifacial Acheulian	0	0
Bifacial	0.7	0.7
Charentien	6.9	10.9
Quina	0	
Group I: tools # 1 - 4	14.5	0
Group III: tools # 30 - 37, 40	6.9	16.9
Group IV: denticulates	3.4	6.5

Table 6.29 Tool Typology, Couche 8e (8'), Abri Bourgeois-Delaunay, Lachaise

Tool	Number	Total Percentage	Restricted Percentage
1. Typical Levallois flake	18	5.1	
2. Atypical Levallois flake	11	3.1	
3. Levallois point	0	0	
4. Retouched Levallois point	0	0	0
5. Pseudo-Levallois point	0	0	0
6. Mousterian point	1	0.3	0.6
7. Elongated Mousterian point	1	0.3	0.6
8. Limace	0	0	0
9. Sidescraper, single straight	12	3.4	6.9
10. Sidescraper, single convex	22	6.2	12.7
11. Sidescraper, single concave	4	1.1	2.3
12. Sidescraper, double straight	0	0	0
13. Sidescraper, double straight convex	3	0.9	1.7
14. Sidescraper, double straight concave	0	0	0
15. Sidescraper, double biconvex	3	0.9	1.7
16. Sidescraper, double biconcave	0	0	0
17. Sidescraper, double convex concave	1	0.3	0.6
18. Sidescraper, convergent straight	1	0.3	0.6
19. Sidescraper, convergent convex	5	1.4	2.9
20. Sidescraper, convergent concave	2	0.6	1.2



Table 6.3] Tool Typology, Couche 9 (Debenath),  
Abri Bourgeois-Delaunay, Lachaise

Table 6.3a Technical and Typological Indices and Characteristic  
Groups, Couche 8e, (8\*), Abri Bourgeois-Delaunay, Lachaise

Index	Total	Restricted	Tool	Number	Total Percentage	Restricted Percentage
Levallois	6.11		1. Typical Levallois flake	41	13.1	
Facetting	38.38		2. Atypical Levallois flake	26	8.3	
Restricted Facetting	27.35		3. Levallois point	2	0.6	
Blade (lamellar)	1.29		4. Retouched Levallois point	0	0	0
Aypological Levallois	8.2	0	5. Pseudo-Levallois point	1	0.3	0.4
Sidescraper (Group II)	22.2	46.7	6. Mousterian point	2	0.6	0.8
Total Acheulian	2.2	4.6	7. Elongated Mousterian point	0	0	0
Unifacial Acheulian	1.7	3.5	8. Limace	0	0	0
Bifacial	0.6	1.1	9. Sidescraper, single straight	17	5.4	7.1
Charentien	7.8	16.7	10. Sidescraper, single convex	27	8.7	11.3
Quina	0		11. Sidescraper, single concave	8	2.6	3.3
Group I: tools # 1 - 4	8.2	0	12. Sidescraper, double straight	1	0.3	0.4
Group III: tools # 30 - 37, 40	8.4	17.4	13. Sidescraper, double straight convex	0	0	0
Group IV: denticulates	4.2	8.7	14. Sidescraper, double straight concave	1	0.3	0.4
			15. Sidescraper, double biconvex	0	0	0
			16. Sidescraper, double biconcave	3	1.0	1.3
			17. Sidescraper, double convex concave	0	0	0
			18. Sidescraper, convergent straight	0	0	0
			19. Sidescraper, convergent convex	8	2.6	3.3
			20. Sidescraper, convergent concave	0	0	0

283

Table 6.32 Technical and Typological Indices and Characteristic Groups, Couche 9 (a,b) (Debenath), Abri Bourgeois-Delaunay, Lachaise

Index	Total	Restricted
Levallois	8.32	
Facetting	43.26	
Restricted Facetting	36.27	
Blade (lamellar)	3.16	
Appological Levallois	22.1	0
Sidescraper (Group II)	32.0	41.8
Total Acheulian	2.9	3.7
Unifacial Acheulian	1.6	2.5
Bifacial	1.0	1.2
Charentien	15.7	20.5
Quina	0	
Group I: tools # 1 - 4	22.1	0
Group III: tools # 30 - 37, 40	9.9	12.9
Group IV: denticulates	8.3	10.8

Table 6.33 Typology, Couche 9c (9<sup>a</sup>), Debenath, Abri Bourgeois-Delaunay, Lachaise

Piece	Number
1,2. Levallois flakes	16
9. Sidescraper, simple straight	5
10. Sidescraper, simple convex	9
11. Sidescraper, simple concave	1
15. Sidescraper, double biconvex	1
17. Sidescraper, double convex-concave	1
23. Sidescraper, transverse convex	1
25. Sidescraper, retouched on the bulbar surface	1
30. Typical endscraper	3
33. Atypical burin	1
40. Truncated piece	1
42. Notched piece	8
43. Denticulate	4
44. Bec burinante alterne	1
45. Piece retouched on the ventral side	1
54. Flake, notched end	2
59. Choppers	1
62. Miscellaneous	1
63. Blattspitzen	1

287

Table 6.34 Piece Typology, Couche 9c (9') Debenath  
Abri Bourgeois-Delaunay, Lachaise.

Piece	Number
Flakes	150
Bledes	0
Points	0
Trimmed flakes	0
Tools	42
Discs	0
Polyhedra	0
Nuclei	14
Debris	23
Hammerstones	0
Miscellaneous	<u>193</u>
Total	422

Table 6.35 Tool Typology, Couche 9 (David)  
Abri Bourgeois-Delaunay, Lachaise

Tool	Number	Total Percentage	Restricted Percentage
1. Typical Levallois flake	105	4.1	
2. Atypical Levallois flake	270	10.6	
3. Levallois point	7	0.3	
4. Retouched Levallois point	3	0.1	0.2
5. Pseudo-Levallois point	47	1.9	3.0
6. Mousterian point	24	0.9	1.5
7. Elongated Mousterian point	4	0.2	0.3
8. Limace	1	0.0	0.1
9. Sidescraper, single straight	119	4.7	7.6
10. Sidescraper, single convex	282	11.1	18.0
11. Sidescraper, single concave	51	2.0	3.3
12. Sidescraper, double straight	9	0.4	0.6
13. Sidescraper, double straight convex	14	0.6	0.9
14. Sidescraper, double straight concave	4	0.1	0.3
15. Sidescraper, double biconvex	26	1.0	1.7
16. Sidescraper, double biconcave	3	0.1	0.2
17. Sidescraper, double convex concave	12	0.5	0.8
18. Sidescraper, convergent straight	15	0.6	1.0
19. Sidescraper, convergent convex	49	1.9	3.1
20. Sidescraper, convergent concave	3	0.1	0.2

Table 6.36 Tool Typology, Couche 10,

## Abri Bourgeois-Delaunay, Lachaise

Tool	Number	Total Percentage	Restricted Percentage	Tool	Number	Total Percentage	Restricted Percentage
1. Typical Levallois flake	6	5.9		21. Sidescraper, asymmetrical	2	2.0	2.5
2. Atypical Levallois flake	7	6.9		22. Sidescraper, transverse straight	0	0	0
3. Levallois point	0	0	0	23. Sidescraper, transverse convex	2	2.0	2.5
4. Retouched Levallois point	0	0	0	24. Sidescraper, transverse concave	0	0	0
5. Pseudo-Levallois point	1	1.0	1.2	25. Sidescraper, retouched on the ventral surface	1	1.0	1.2
6. Mousterian point	1	1.0	1.2	26. Sidescraper, with abrupt retouch	3	3.0	3.7
7. Elongated Mousterian point	0	0	0	27. Sidescraper, with thin back	0	0	0
8. Limace	0	0	0	28. Sidescraper, bifacial retouch	0	0	0
9. Sidescraper, single straight	3	3.0	3.7	29. Sidescraper, with alternate retouch	0	0	0
10. Sidescraper, single convex	10	9.9	12.3	30. Typical endscraper	2	2.0	2.5
11. Sidescraper, single concave	2	2.0	2.5	31. Atypical endscraper	0	0	0
12. Sidescraper, double straight	0	0	0	32. Typical burin	1	1.0	1.2
13. Sidescraper, double straight convex	0	0	0	33. Atypical burin	0	0	0
14. Sidescraper, double straight concave	0	0	0	34. Typical borer	0	0	0
15. Sidescraper, double biconvex	1	1.0	1.2	35. Atypical borer	0	0	0
16. Sidescraper, double biconcave	0	0	0	36. Typical backed knife	1	1.0	1.2
17. Sidescraper, double convex concave	1	1.0	1.2	37. Atypical backed knife	3	3.0	3.7
18. Sidescraper, convergent straight	1	1.0	1.2	38. Naturally backed knife	5	5.0	6.2
19. Sidescraper, convergent convex	0	0	0	39. Mousterian raclette	0	0	0
20. Sidescraper, convergent concave	0	0	0	40. Truncated piece	9	8.9	11.1
				41. Mousterian tranchet	0	0	0
				42. Notched pieces	13	12.9	16.0

Tool	Number	Total Percentage	Restricted Percentage
21. Sidescraper, asymmetrical	50	2.0	3.2
22. Sidescraper, transverse straight	11	0.4	0.7
23. Sidescraper, transverse convex	30	1.2	1.9
24. Sidescraper, transverse concave	4	0.2	0.3
25. Sidescraper, retouched on the ventral surface	26	1.0	1.7
26. Sidescraper, with abrupt retouch	10	0.4	0.6
27. Sidescraper, with thin back	12	0.5	0.7
28. Sidescraper, bifacial retouch	11	0.4	0.7
29. Sidescraper, with alternate retouch	3	0.1	0.2
30. Typical endscraper	13	0.5	0.8
31. Atypical endscraper	24	0.9	1.5
32. Typical burin	13	0.5	0.8
33. Atypical burin	18	0.7	1.2
34. Typical borer	9	0.4	0.6
35. Atypical borer	24	0.9	1.5
36. Typical backed knife	7	0.3	0.4
37. Atypical backed knife	12	0.5	0.7
38. Naturally backed knife	38	1.5	2.4
39. Mousterian raclette	21	0.8	1.3
40. Truncated piece	29	1.1	1.8
41. Mousterian tranchet	0	0	0
42. Notched pieces	112	4.4	7.2

Tool	Number	Total Percentage	Restricted Percentage
43. Denticulate	226	8.9	14.5
44. Bec burinante alterne	15	0.6	1.0
45. Flake, retouched on the ventral surface	60	2.4	
46. Miscellaneous retouched flake, abrupt thick retouch	132	5.2	
47. Miscellaneous retouched flake, alternate thick retouch			
48. Miscellaneous retouched flake, abrupt thin retouch			
49. Miscellaneous retouched flake, alternate thin retouch	364	14.3	
50. Flake, bifacial retouch	38	1.5	
51. Tayac point	7	0.3	0.4
52. Notched triangle	0	0	0
53. Pseudo-microburin	0	0	0
54. Flake, notched end	12	0.4	0.8
55. Cleavers	2	0.1	0
56. Rabot (plane)	0	0	0
57. Aterian tanged point	0	0	0
58. Tanged piece	0	0	0
59. Chopper	0	0	0
60. Inverse chopper	0	0	0
61. Chopping tool	2	0.1	0.1
62. Miscellaneous piece	115	6.1	9.9
63. Blattspitzen	27	1.1	1.7
64. Foliated bifacial points	1	0.0	0.1
<b>Total</b>	<b>2539</b>	<b>101.0</b>	<b>101.5</b>
	(1563)		

### 6.3.5 Human Remains at Lachaise

Many human bones have been found in Lachaise, ranging from the pre-Neanderthal stage to the modern forms.

#### 6.3.5.1 Suard

In 1950, a calotte was discovered by Bordes, along with many other remains in layers V to VIII. According to Piveteau (in Debénath, 1974), these are a group of pre-Neanderthals. Debénath has found teeth embedded in mandibles, a tibial diaphysis, two calottes, a temporal and occipital bone. The skulls show marked platycephaly, thick bones, a cranial capacity of 1063 cc, all of which are pithecanthropine characteristics, but the temporal region is Neanderthalian, while the occipital bun is transitional, and the taurodont molars could be attributed to either species. Therefore Suard seems to contain hominids which are transitional from H. erectus to H. sapiens neanderthalensis (Figure 6.15, 6.16).

#### 6.3.5.2 Bourgeois-Delaunay

In 1967-1968, Debenath unearthed the remains of three or four individuals, represented by one canine, three molars in a maxilla, a mandible, a calotte, an occipital, and temporal bone, and femur diaphysis, all embedded in the base of layer 11. These can be considered classic Neanderthals with long low cranial vaults made of thick bones. Small mastoid processes and ellipsoidal auditory meati complement the massive mandible with broad rami, containing taurodont molars.

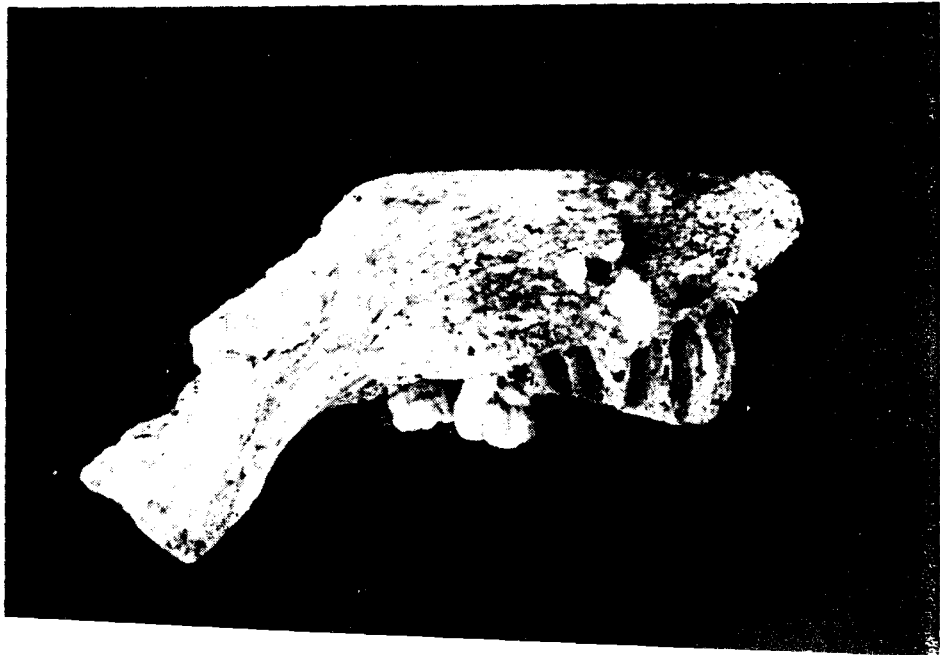
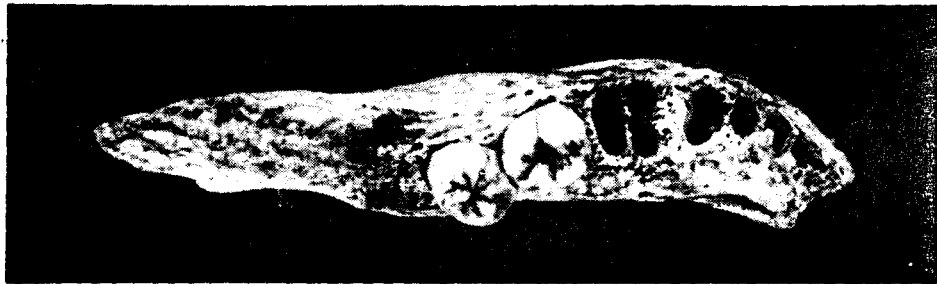
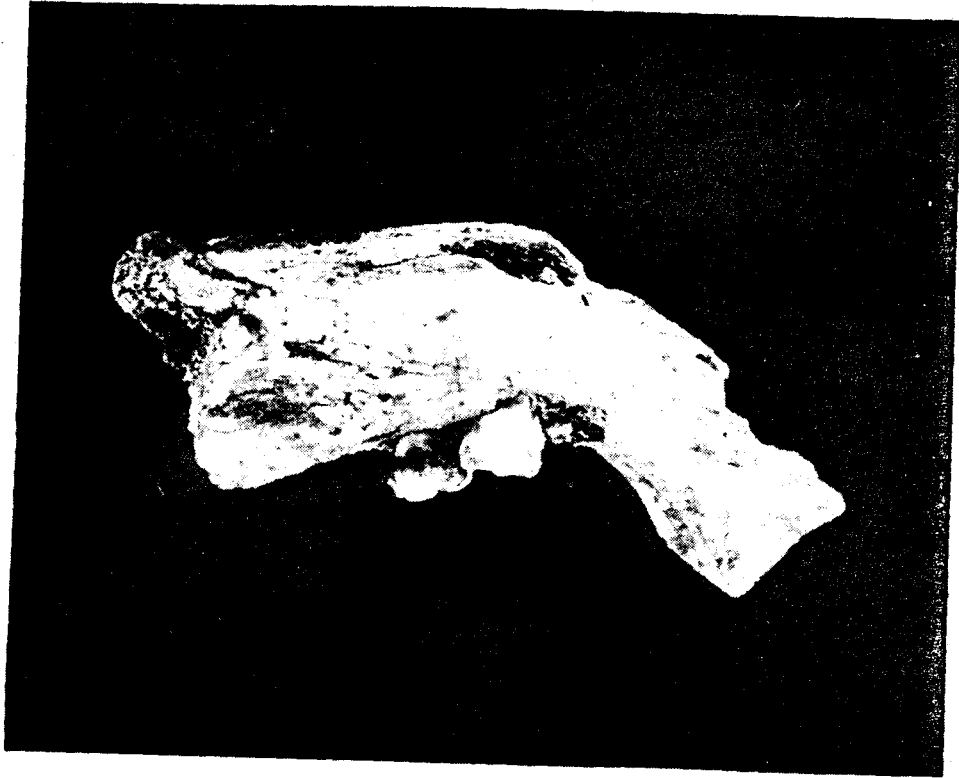


Figure 6.15

Human remains from Abri Suard;

The left half of an adult mandible was found at the base of couche 53. Both the condyle and the coronoid process are missing, while part of the gonial region and ramus border are destroyed.

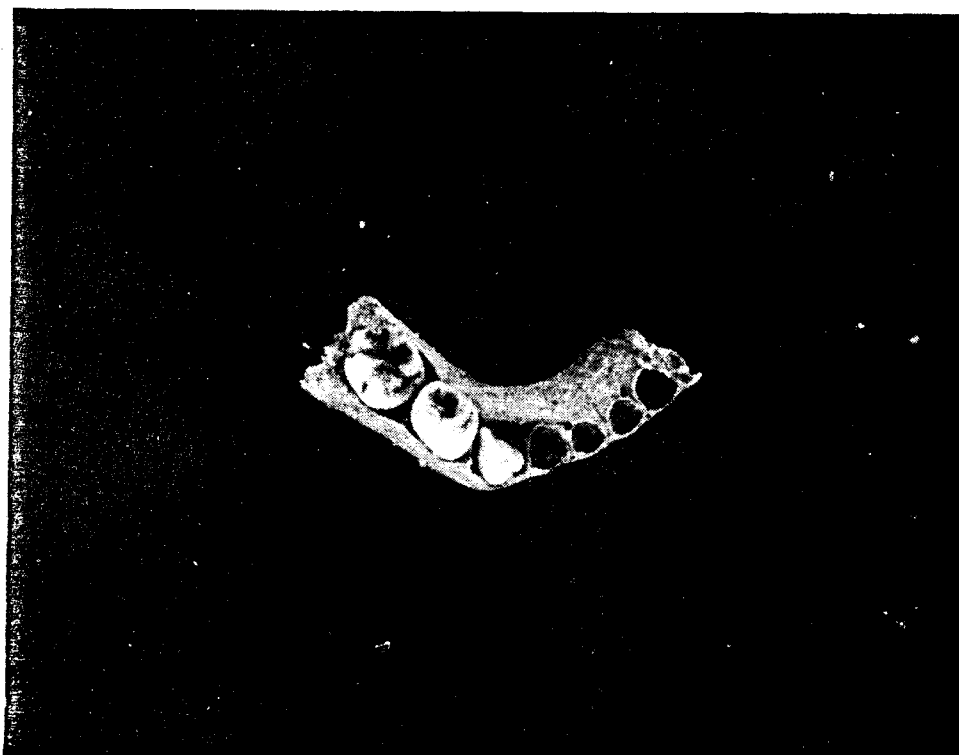
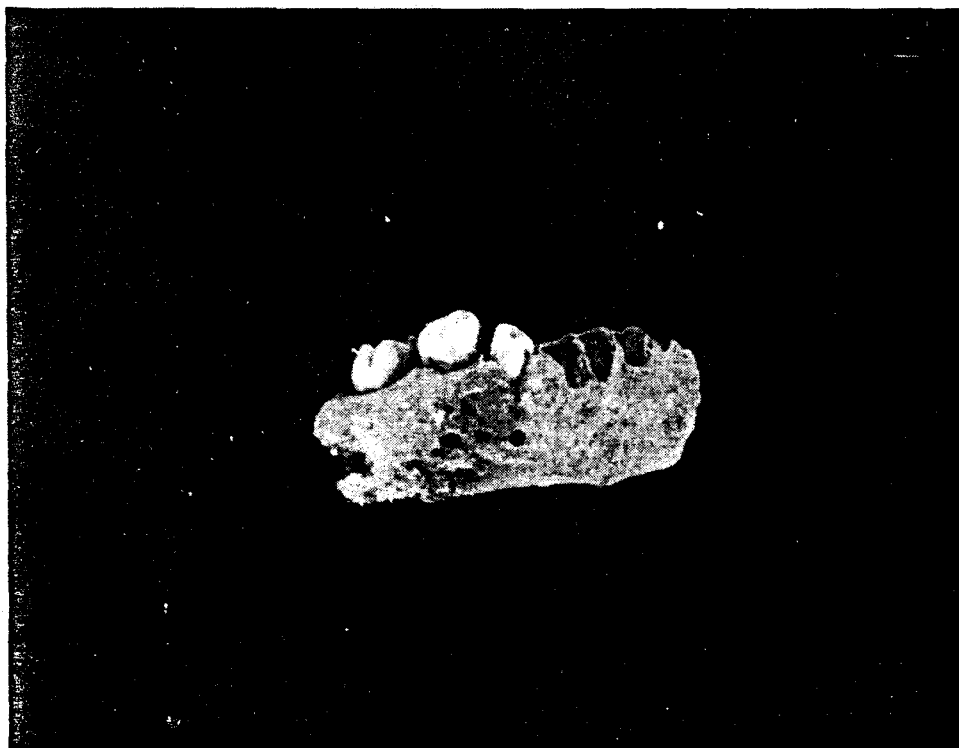
Two teeth, the second and third molars, are present, but badly worn. The third molar is noticeably rotated from its usual position. Situated between the second premolar and the first molar mid-way down the body, the mental foramen is large (after Débénath, 1974).



**Figure 6.16**

**An infant mandible from Lachaise.**

**Also found in couche 53, this infant mandible is broken behind the second premolar on the right side and behind the canine on the left side. Although the incisors are missing, the canine and premolars are present. Because these are deciduous, the child could have been no more than about 8 years, but older than 2 years (after Débenath, 1974).**



### 6.3.6 Paleoenvironments

Although the pollen analyses are incomplete, these along with the faunal and sedimentological data have enabled Debenath (1974) to interpret the paleoenvironments in the cave. Table 6.38 lists the faunal and palynological data, and the paleoclimates.

#### 6.3.6.1 Fauna

Some of the faunal assemblages raise some interesting questions. For instance, in layer 10, Bourgeois-Delaunay, the large number of bear bones suggests that either cave bear was a very popular meal for the human inhabitants, or that there were alternating occupations of bears and humans. Because the bear bones are relatively intact, while the others are badly broken, it is probable cave bears did occupy the cave when humans were not present.

Layer 2 in Bourgeois-Delaunay contains very few reindeer, compared with Aurignacian deposits in other caves, usually deposited under cold conditions. Perhaps this Aurignacian I industry is not contemporaneous with others in the Perigord.

In Suard, layers III-VIII, the association of reindeer with horses and antelope is not consistent with the Würmian date the archeologists would have. The fauna appear to be Riss III, as such a fauna at Combe-Grenal are. Layer 1, however, was deposited under much milder conditions than the lower layers.

#### 6.3.6.2 Interpretations

Using the data in Table 6.38, and the sedimentological analyses, Debenath (1974) interprets deposits to have the chronology listed in Table 6.2.

Table 6.38 Paleoenvironmental Data for Lachaise

A. Bourgeois-Delaunay

layer	Fauna	Pollen	Climate	"Age"
13	?	Scotch pine 8% gradually increasing to 15% with more species, hazel, ash, beech	Cold, dry	?
12	?	5% trees, all scotch pine	Very cold	?
11	?	88% trees, oak, elm hazel, alder, linden, birch	Warm, wet	Riss/ Wurm
10	<u>U. squalens</u> (7%), bovids, horses, fox, mammoth, reindeer, elk, roe deer, hyena	at base: only pine 20% at top: hazel, willow, ash	Cool, wet, becoming wetter	W
9'	<u>U. squalens</u> (6%), horses (20%), bovids, wolves, hyena, reindeer (5%), elk, rhinoceros	Very similar to 10	as in 10	U R M
9	<u>U. squalens</u> (33%), horses (40%), bovids, wolves, fox, hyena, roe deer, Irish elk, rhinoceros, pigs, elephant, reindeer, deer	15% trees, pine mostly	as in 10	I
8'	<u>U. squalens</u> (23%), horses (41%), otherwise as in couche 9	?		
8	Very poor: <u>U. squalens</u> , horses, bovids, elk, reindeer, rhinoceros	?		
7	?	68% trees, scotch pine, hazel, willow oak, some elm, alder	Warm, wet	Wurm I/II

Layer	Fauna	Pollen	Climate	"Age"
6	Very similar to 9, but with fewer horses	?		W
4	Hyena, bovids, rhinoceros, elephant, <u>Felis spalaea</u> , wolves, pigs, ibex, moles	? ? A A		U R M
3	<u>Equus calabus</u> , rhinoceros, <u>U. spalaeus</u> , hyena	?		I
2	Reindeer (18%), horses (59%), bovids, pigs, elk, ibex, Irish elk, elephant, rhinoceros, hare, <u>E. hydruntinus</u>	?		I
<b>B. Suard</b>				
54	?			
53'	?	10-35% trees, fir, beech, cedar	humid	?
53	Horse (44%), rhinoceros (4%), bison, cattle, reindeer (22%), elk (7%), wolves	73% trees, pine, fir, hazel, willow	warm, wet	Riss II/III
52	Horses (73%), rhinoceros (6%), bison, cattle, reindeer (8%), elk (11%), wolves	5% pine	cold	R
51	Horses (64%), rhinoceros (4%), bison, cattle, reindeer (22%), elk (9%), elephant, wolves	12% trees, pine, elm, alder, hazel, birch, willow	humid	I
50b	?	?	warmer more humid	S S
<u>Plancher superieur</u>	?	4% pine, chicory	as 52	I I I
		90% trees, oak, hazel, elm, willow pine	Cool, dry	
			Warm, wet	

Layer	Fauna	Pollen	Climate	"Age"
VIII -	Reindeer (58 - 73%), horses (26% in IV, V-VI), elk (16%	?	?	Riss
III	in VIII), antelope			III
II	Reindeer, horses, deer	?	?	?
I	Horses, deer, <u>E. hydruntinus</u> , bovids, reindeer	?	?	?



Unlike some caves in the Charente, Lachaise did not experience many roof collapses, except at the outermost edges. In addition, it is a deep cave, well-protected from the elements. Therefore, it was an ideal place to camp (Figure 6.17). The cave may also have been preferred over other local caves, because it is approximately at the same level as the river banks, making it an excellent spot from which to ambush game. Whatever the reason, the many levels of human occupation indicate it was a popular place to live, used by people since Acheulian times.

#### 6.3.7 Other Absolute Dates for Lachaise

Layer 51 was estimated to be  $126.0 \pm 15.0$  Ka using the thermoluminescence of a granite pebble (Schoverer et al., 1975 in Schwarcz and Debenath, 1978). Preliminary analyses by U/Th were performed by Ada Dixon on samples 77LC1, 2, and 3, collected by Debenath. These yielded ages of  $106.0 \pm 10.0$ ,  $145.0 \pm 16.0$ , and  $185.0 \pm 30.0$  for layers 7, 11, and 53' respectively (Schwarcz and Debenath, 1978).

#### 6.3.8 Sample Description

Table 6.39 lists the sample descriptions, including thin-section analysis for all the samples from Lachaise, both those from the 1977 collection made by Debenath, and the 1979 collection made by the author with the assistance of Debenath. Figures 6.18 through 6.24 show the samples, while sample locations are shown in Figure 6.4 and 6.25.

Table 6.39. Sample Descriptions, Lachaise

SAMPLE	LOCATION	DESCRIPTION	THICKNESS	DETRITUS	POROSITY	CRYSTALS	LAYERING	COMMENTS
77LC1	BD c. 7 sq ?	Transparent white fst, 1 mm lam macroxtln	3 cm	5% clay	< 5% ang. XO	spar, 1/10-1/2 mm x1/20-1 cm // lam	Clay concentrated on lam, spar length	Spars much shorter on laminae and near edges of sample
77LC2	BD c. 11 sq ?	Transparent white fst, Yellow coloured bands 1 mm thick macroxtln	5 cm	< 5% clay	5-10% ang XO	spar, 1 mm x 1-4 cm, // lam	Clay concentrated on lam	
77LC3	S c. 53' sq ?	Yellow-white stg medium grained, with embedded soda straws	2 cm high	-	-	-	-	
79LC11	BD c. 7 Sq P8	Transparent tan stg, faint growth lam 1 mm thick, white outer rind macroxtln	15 cm high 15 cm diam at base	< 5% clay	< 5% ang XO, only on growth lam	spar, 2 mm x 1-5 cm, // lam	slightly higher poro- sity, more clay on lam	Slight variation in spar length from layer to layer
79LC12	BD c. 7 sq Q8	Transparent white stg with tan base, extreme bottom white, macroxtln faint growth lam 1 mm	10 cm high	5% clay?	10% ang XO most on growth lam	spar, 1 mm x 2 mm - 2 cm, // lam	Slightly more clay on lam, tiny spars on lam 1/5 mm long	Laminations vary in thick- ness laterally
79LC13	BD c. 11 sq H5	Opaque white fst, 2 orange bands present with varying porosity in the 3 sections microxtln	variable 7-9 cm	5% clay	5% ang XO	spar, 1/2 mm x 1 cm, // lam some small polyg on hiatus	hiati have clay con- centrated there, lam where crystal edges meet	

SAMPLE	LOCATION	DESCRIPTION	THICKNESS	DETRITUS	POROSITY	CRYSTALS	LAYERING
79LC14	BD c. 11 sq E or G8	White to tan opaque fst with 3 hiati in growth macroxtln	variable 11-14 cm	<5% clay in all sections	variable	variable	Clay on hiati
14A	bottom	faint growth lam	4 cm		15%	av. 0.5 mm ang X1 polyg random	
14B	lower middle	faint growth lam	3-4 cm		10%	spar 1 mm x ang X1 1 cm, // lam	
14C	upper middle		1-3 cm		10-15%	av. 0.5 mm ang X1 polyg, random	
14D	top		4 cm		10%	spar 1/2 mm x ang X1 1 mm, // lam	
79LC15	S pl sup sq X18	Transparent stg pair, dark brown at top, light brown middle, white base, thin lam macroxtln	8, 10 cm high	10% clay mostly on growth lam	<5% ang X0	spar, no grain boundaries visible rextlz? orient ?	clay concentrated on lam
79LC16	S pl sup sq ?R25?	Transparent stg variable white, tan and brown, 3 major hiati, other faint lam Hiati marked by sand lam 1 mm thick	23 cm high	<5% clay all on growth lam	5% ang X0	spar, much as 79LC15 rextlz? orient?	clay concentrated on lam
79LC17	Did not arrive in Canada						

SAMPLE	LOCATION	DESCRIPTION	THICKNESS	DETRITUS	POROSITY	CRYSTALS	LAYERING	COMMENTS
79LC18	S pl sup? sq ?	Tan to light brown fst under stg, 1 hiatus in middle of centre slightly convo- main cham luted lam in bottom half, also darker	10 cm	0%	10% on hiatus 5% in layers ang IO	spar, 1/2 mm x 2 cm, some polyg on hiatus, // lam, random on hiatus	small crystals on hiatus, more porous on hiatus	
79LC19	S ?pl sup???	Transparent white stg, faint growth lam, macro- near xtl, base is white-brown puits convoluted fst with soda sq ?? straws in base, base sepa- rated from stg by growth hiatus, outer rind opaque	12 cm high 6 cm diam at base	0%	0%	huge, larger than thin section random	none present	Whole piece seems to be made of several large irre- gular blocks each one a single crystal
79LC20	couloir BD/S = BD 11? = S pl sup?	tan stg, separated from variable base by growth hiatus convoluted filled with sand, base is tan at top, black in middle, orange at bottom	8 cm high stg base 4-6 cm thick	20% clay + opaque-min in black, 30% clay in stg. orange 5% clay	10% ang IO (black), 15% rd X1 stg, 25% ang X1 orange.	spar, 1/10 mm x 1/2 mm black, 1/10 polyg random stg, spar, 1/2 x 1 mm orange // lam	clay content, porosity, and colour changes	Black region contains bone, microfauna (20%) occur in stg, éboulis in stg.

ABBREVIATIONS:

BD = Bourgeois-Delaunay  
S = Suard  
c. = couche  
sq = square  
lam = laminations

fst = flowstone

stg = stalagmite

stc = stalactite

ang. = angular pore  
shape

rd = rounded pores

av = average

polyg = polygonal shaped crystals

orient=orientation

rextlz = recrystallized

// lam = oriented parallel to

growth laminations

min = mineral

diam = diameter

pl sup = plancher supérieur

xtln = crystalline

Connectadness of the Pores

IO = unconnected

X1 = partially connected

X2 = connected

X3 = well connected

X4 = a sponge-like porosity

CORRELATION OF DATA FROM LACHAISE, BD C. 7  
USING SAMPLES 77LC1

SAMPLE	AGE (KA)	ERRGR (KA)	YIELDS		TH-230	TH-230	U-234	(U-234)	CONCENTRATIONS	
			U-232 (%)	TH-228 (%)	U-234	TH-232	U-238	(U-238)0	U-238 (PPM)	TH-232 (PPM)
77LC1-1	102.3	+ 12.4 - 11.6	63.18	30.22	+ .646	9.6	1.018	1.043	.27	.06
					- .032	+ 2.2	+ .038	+ .003		
77LC1-2	99.5	+ 11.0 - 10.0	41.78	11.81	+ .603	≥ 1000.0	1.054	1.042	.27	0.00
					- .039		+ .035	+ .003		
-----										
AVERAGES	101.5	+ 12.0 - 11.2					1.032	1.042	.27	
							+ .037	+ .050		

CORRELATION OF DATA FROM LACHAISE, BD C. 7  
USING SAMPLES 79LC11, 79LC12

SAMPLE	AGE (KA)	ERROR (KA)	YIELDS		TH-230	TH-230	U-234	(U-234)	CONCENTRATIONS	
			U-232 (%)	TH-228 (%)	U-234	TH-232	U-238	(U-238)0	U-238 (PPM)	TH-232 (PPM)
79LC11-1	58.5	+ 7.4 - 7.2	34.55	16.96	+ .483	5.6	1.108	1.109	.23	.07
					- .026	+ .9	+ .030	+ .003		
79LC11-2	5.78	+ .9 - .9	10.98	27.10	+ .060	8.0	1.1538	1.0948	.498	.01
					- .005	+ 3.0	+ .043	+ .000		
79LC11-3	75.3	+ 8.5 - 9.1	11.24	20.18	+ .526	15.6	1.117	1.115	.43	.05
					- .031	+ 4.9	+ .057	+ .004		
79LC12-1	72.1	+ 5.5 - 5.3	47.51	83.97	+ .511	15.1	1.076	1.114	.28	.03
					- .021	+ 2.7	+ .033	+ .002		
79LC12-2	-		39.25	0.00	-	-	1.1075	-	.048	-
							+ .073			
-----										
AVERAGES	70.7	+ 6.3 - 6.0					1.093	1.112	.28	
							+ .035	+ .044		

S NOT INCLUDED IN THE AVERAGE DATE

+ THORIUM CORRECTION USED CALCULATED AT R = 1.25

+ REPRESENTS THE YOUNGEST AGE POSSIBLE NOT THE LOWER ERROR LIMIT CALCULATED AT R = 1.25

+ REPRESENTS THE OLDEST AGE POSSIBLE, NOT THE UPPER ERROR

Table 6.43

CORRELATION OF DATA FROM LACHAISE- 80  
USING SAMPLES EAST SIDE 79LC13

SAMPLE	AGE (KA)	ERROR (KA)	YIELDS		TH-230	TH-230	U-234	(U-234)	CONCENTRATIONS		
			U-232 (%)	TH-228 (%)	U-234	TH-232	U-238	(U-238) 0	U-238 (PPM)	TH-232 (PPM)	
79LC13A-1	55.0*	+ 34.3	29.52	2.98	.456	6.2	1.058*	1.139*	.048	.02	
		- 31.2			.113	2.5	.145	.016			
79LC13A-2	79.8	+ 4.7	28.12	56.51	.552	12.9	1.118	1.147	.37	.05	
		- 4.5			.017	1.3	.027	.032			
-----											
AVERAGES	79.8	+ 4.7					1.118	1.143	.37		
		- 4.5					.027	.036			
-----											
SAMPLE	AGE	ERROR	YIELDS		TH-230	TH-230	U-234	(U-234)	CONCENTRATIONS		
	(KA)	(KA)	U-232 (%)	TH-228 (%)	U-234	TH-232	U-238	(U-238) 0	U-238 (PPM)	TH-232 (PPM)	
79LC13B-1	83.5	+ 4.8	64.27	50.72	.560	19.8	1.121	1.163	.04	.00	
		- 4.6			.018	2.9	.023	.003			
79LC13B-2	94.3	+ 5.6	54.27	54.13	.589	26.1	1.139	1.168	.31	.02	
		- 5.3			.022	5.5	.035	.003			
-----											
AVERAGES	89.1	+ 5.2					1.129	1.165	.17		
		- 5.0					.028	.039			
-----											
SAMPLE	AGE	ERROR	YIELDS		TH-230	TH-230	U-234	(U-234)	CONCENTRATIONS		
	(KA)	(KA)	U-232 (%)	TH-228 (%)	U-234	TH-232	U-238	(U-238) 0	U-238 (PPM)	TH-232 (PPM)	
79LC13C-1	120.6	+ 9.7	37.53	40.93	.686	≥ 1000.0	1.167	1.234	.25	0.00	
		- 8.9			.030		.050	.008			
79LC13C-2	109.2	+ 5.1	25.30	60.87	.643	25.9	1.100	1.136	.46	.04	
		- 5.8			.021	3.4	.031	.003			
-----											
AVERAGES	113.8	+ 7.5					1.100	1.195	.34		
		- 7.0					.043	.054			

\* NOT INCLUDED IN THE AVERAGE DATE

+ THORIUM CORRECTION USED CALCULATED AT R = 1.25

Table 6.44

CORRELATION OF DATA FROM LACHAISE, OO C. 11  
USING SAMPLES 77LC2, 79LC14A-C

SAMPLE	AGE (KA)	ERROR (KA)	YIELDS		TH-230		U-234		CONCENTRATIONS	
			U-232 (%)	TH-228 (%)	U-234	TH-232	U-234 U-238	(U-234) (U-238) G	U-234 (PPM)	TH-232 (PPM)
77LC2-1	123.4	+ 17.7	60.29	17.41	+ .703	+ 15.4	+ 1.029	+ 1.031	.23	.03
		- 16.1			+ .039	+ 7.6	+ .041	+ .007		
77LC2-2	153.0	+ 27.5	48.64	15.52	+ .775	+ 20.4	+ 1.056	+ 1.048	.21	.03
		- 23.4			+ .048	+ 14.2	+ .038	+ .011		
77LC2-3 2	240.5	+ 36.4	59.40	44.71	+ .904	+ 47.1	+ .995	+ 1.112	.23	.01
		- 27.6			+ .033	+ 24.0	+ .031	+ .018		
77LC2-4	145.6	+ 12.9	37.79	27.40	+ .746	+ 29.5	+ 1.100	+ 1.086	.22	.02
		- 11.6			+ .030	+ 11.3	+ .040	+ .005		
79LC14A-1P	159.3	+ 32.0	28.83	38.71	+ .802	+ 9.7	+ 1.136	+ 1.089	.39	.11
		- 25.3			+ .053	+ 7	+ .080	+ .012		
79LC14A-2	163.7	+ 13.6	20.54	49.63	+ .787	+ 52.8	+ 1.041	+ 1.090	.41	.02
		- 12.2			+ .027	+ 11.4	+ .032	+ .006		
79LC14B-1	151.7	+ 17.7	54.39	74.59	+ .772	+ 20.1	+ 1.032	+ 1.087	.23	.03
		- 15.5			+ .035	+ 2.8	+ .045	+ .007		
79LC14C-1	106.3	+ 6.8	33.11	39.48	+ .631	+ 30.0	+ 1.037	+ 1.077	.45	.03
		- 6.4			+ .023	+ 8.0	+ .029	+ .002		
79LC14C-2	146.4	+ 9.1	67.60	86.74	+ .748	+ 1000.0	+ 1.054	+ 1.080	.06	0.00
		- 7.5			+ .019		+ .022	+ .003		
79LC14D-1	150.8	+ 15.2	18.83	46.96	+ .759	+ 28.6	+ 1.045	+ 1.087	.35	.03
		- 13.4			+ .034	+ 6.8	+ .047	+ .006		
-----										
AVERAGES	151.0	+ 16.1					+ 1.057	+ 1.087	.22	
		- 14.0					+ .040	+ .006		

† NOT INCLUDED IN THE AVERAGE DATE

\* THORIUM CORRECTION USED CALCULATED AT R = 1.25

Table 6.45

CORRELATION OF DATA FROM LACHAISE, S PL SUP  
USING SAMPLES 79LC15

SAMPLE	AGE (KA)	ERROR (KA)	YIELDS		TH-230	TH-230	U-234	(U-234)	CONCENTRATIONS	
			U-232 (%)	TH-228 (%)	U-234	TH-232	U-238	(U-238)0	U-238 (PPM)	TH-232 (PPM)
79LC15-1	119.3	+ 18.2	17.56	28.14	.713	8.7	1.127	1.177	.25	.07
		- 16.3			± .044	± 1.5	± .063	± .013		
79LC15-2	87.6	+ 14.9	6.60	20.32	.611	6.9	1.025	1.162	.38	.11
		- 13.7			± .046	± 1.1	± .077	± .010		
79LC15-3	74.5	+ 8.9	8.58	55.97	.525	14.8	1.023	1.156	.67	.08
		- 8.4			± .035	± 2.4	± .071	± .006		
-----										
AVERAGES	119.3	+ 18.2 - 16.3					1.127 ± .063	1.177 ± .097	.25	

CORRELATION OF DATA FROM LACHAISE, S PL SUP  
USING SAMPLES 79LC16

SAMPLE	AGE (KA)	ERROR (KA)	YIELDS		TH-230	TH-230	U-234	(U-234)	CONCENTRATIONS	
			U-232 (%)	TH-228 (%)	U-234	TH-232	U-238	(U-238)0	U-238 (PPM)	TH-232 (PPM)
79LC16-1	57.3	+ 5.6	38.88	26.89	.453	8.0	1.045	1.053	.39	.07
		- 5.4			± .022	± 1.2	± .039	± .047		
79LC16-1 R	45.3	+ 9.5	38.88	27.10	.368	11.9	1.045	1.051	.39	.04
		- 9.1			± .041	± 6.4	± .039	± .046		
79LC16-2	246.1	+ 83.2	14.94	37.69	.954	37.7	1.311	1.621	.18	.02
		- 49.2			± .071	± 21.0	± .113	± .362		
79LC16-3	9.2	+ 2.4	20.59	11.48	.081	≥ 1000.0	1.454	1.460	.20	0.00
		- 2.4			± .021		± .056	± .060		
79LC16-4	89.2	+ 21.6	3.18	20.40	.578	29.6	1.371	1.476	.25	.02
		- 18.3			± .086	± 23.2	± .271	± .377		

\* NOT INCLUDED IN THE AVERAGE DATE

+ THORIUM CORRECTION USED CALCULATED AT R = 1.25



Table 6.46

CORRELATION OF DATA FROM LACHAISE, S PL INF  
USING SAMPLES 79LC18

SAMPLE	AGE (KA)	ERROR (KA)	YIELDS		TH-230	TH-230	U-234	(U-234)	CONCENTRATIONS		
			U-232 (%)	TH-228 (%)	U-234	TH-232	U-238	(U-238) 0	U-238 (PPM)	TH-232 (PPM)	
79LC18A-1	94.5	+ 6.0	8.59	43.90	.586	35.1	1.074	1.094	.11	.01	
		- 5.7			± .023	± 5.1	± .039	± .032			
79LC18A-2	105.6	+ 9.7	22.13	25.38	.667	8.0	1.125	1.097	.42	.12	
		- 9.1			± .026	± .7	± .038	± .034			
79LC18B-1	110.4	+ 7.3	38.52	40.92	.663	16.4	1.042	1.039	.11	.01	
		- 6.9			± .021	± 1.8	± .021	± .033			
79LC18B-2 ≥ 350.0\$*	≥ 350.0\$*	(≥ 350.0\$*)	15.36	25.97	2.352	20.5	1.373\$	-	.09\$	.04	
					± .123	± 2.7	± .089				
-----											
AVERAGES	103.0	+ 7.3					1.072	1.037	.21		
		- 6.9					± .028	± .040			

\* NOT INCLUDED IN THE AVERAGE DATE

+ THORIUM CORRECTION USED CALCULATED AT R = 1.25

± REPRESENTS THE YOUNGEST AGE POSSIBLE NOT THE LOWER ERROR LIMIT CALCULATED AT R = 1.25

Table 6.47

CORRELATION OF DATA FROM LACHAISE, COUCHE 53'  
USING SAMPLES 77LC3

SAMPLE	AGE		YIELDS		TH-230		U-234	(U-234)	CONCENTRATIONS	
	(KA)	(KA)	U-232 (%)	TH-228 (%)	U-234	TH-232	U-238	(U-234)0	U-238 (PPM)	TH-232 (PPM)
77LC3-1	≥ 350.0	+ - 295.9	57.56	56.11	+ 1.045 - .089	+ 11.1 - 3.1	+ 1.006 - .082	-	.12	.03
77LC3-2	162.7	+ 31.1 - 25.1	43.33	47.01	+ .796 - .051	+ 17.4 - 5.5	+ 1.090 - .069	+ 1.066 - .015	.13	.02
77LC3-4	190.2	+ 73.1 - 47.3	50.40	32.53	+ .846 - .078	+ 15.7 - 10.8	+ 1.041 - .089	+ 1.071 - .037	.14	.02
-----										
AVERAGES	246.8	+ 27.9 - 42.4					+ 1.042 - .081	+ 1.102 - .148	.13	

\$ NOT INCLUDED IN THE AVERAGE DATE

+ THORIUM CORRECTION USED CALCULATED AT R = 1.25

Table 6.48

CORRELATION OF DATA FROM LACHAISE, SUARD PITS  
USING SAMPLES 79LC19

SAMPLE	AGE		YIELDS		TH-230		U-234		CONCENTRATIONS	
	(KA)	ERROR (KA)	U-232 (%)	TH-228 (%)	U-234	TH-232	U-238	(U-234) (U-238) D	U-238 (PPM)	TH-232 (PPM)
79LC19-1	8.2	+ 1.7 - 1.7	30.07	30.69	+ .094 - .008	+ 5.1 - 1.5	+ 1.152 - .039	+ 1.155 - .001	.47	.03
79LC19-1 R	9.3	+ 2.2 - 2.2	30.07	27.53	+ .106 - .010	+ 5.1 - 1.7	+ 1.152 - .039	+ 1.156 - .001	.47	.03
79LC19-2	-		10.39	0.00	-	-	+ .962 - 0.000	-	.45	-
79LC19-3	10.7	+ 1.0 - 1.0	49.61	54.73	+ .108 - .005	+ 8.8 - 1.7	+ 1.092 - .023	+ 1.094 - .000	.45	.02
AVERAGES	9.7	+ 1.5 - 1.5					+ 1.092 - .029	+ 1.030 - .034	.46	

‡ NOT INCLUDED IN THE AVERAGE DATE

\* THORIUM CORRECTION USED CALCULATED AT R = 1.25

‡ REPRESENTS THE YOUNGEST AGE POSSIBLE NOT THE LOWER ERROR LIMIT CALCULATED AT R = 1.25

\* REPRESENTS THE OLDEST AGE POSSIBLE, NOT THE UPPER ERROR

Table 6.49

CORRELATION OF DATA FROM LACHAISE, COULOIS  
USING SAMPLES 79LC20

SAMPLE	AGE		YIELDS		TH-230		U-234		CONCENTRATIONS	
	(KA)	ERRCR (KA)	U-232 (%)	TH-228 (%)	U-234	TH-232	U-238	(U-234) (U-238) %	U-238 (PPM)	TH-232 (PPM)
79LC20-1	-		10.46	0.00	-	-	1.024 + 0.000	-	.25	-
79LC20-2	86.68	+ 14.0 - 12.5	4.84	5.92	.556 + .056	≥ 1000.0	1.1803 + .078	1.1293 + .006	.213	0.00
79LC20-3	37.3	+ 2.9 - 2.9	23.64	51.53	.352 + .013	5.2 + .4	1.062 + .029	1.112 + .001	.28	.06
79LC20-4	19.28	+ 14.8 - 13.0	2.24	1.63	.163 + .107	≥ 1000.0	1.2053 + .174	1.1063 + .005	.668	0.00
79LC20-5	50.8	+ 8.9 - 8.6	49.64	9.35	.429 + .032	6.3 + 1.8	1.136 + .023	1.116 + .003	.39	.09
-----										
AVERAGES	39.4	+ 3.8 - 3.8					1.101 + .021	.986 + .036	.34	

† NOT INCLUDED IN THE AVERAGE DATE

\* THORIUM CORRECTION USED CALCULATED AT R = 1.25

↓ REPRESENTS THE YOUNGEST AGE POSSIBLE NOT THE LOWER ERROR LIMIT CALCULATED AT R = 1.25

+ REPRESENTS THE OLDEST AGE POSSIBLE, NOT THE UPPER ERROR

**Figure 6.18**

**79LC11, Couche 7, Bourgeois-Delaunay:**

**A. The upper surface of Couche 7.**

The pen marks the location of  
79LC11.

**B. Close-up of the remaining portion  
of the stalagmite.**

**(photos courtesy of H. Schwarcz)**



A



B

Figure 6.19

79LC13, Couche 11, Bourgeois-Delaunay:

Three different portions can be seen in the  
flowstone; the middle one pinches out toward  
the ruler.

Figure 6-19





Figure 6.20

79LC15 and 79LC16, Plancher Supérieur, Suard:

A. 79LC15

B. 79LC16



A



B

Figure 6.21

79LC17, couche 53<sup>a</sup>, Suard:

Unfortunately, this sample did not arrive,  
but it is comparable to 77LC3.





Figure 6.22

79LC18, Plancher Supérieur, Suard.

- A. Before the sample was removed.
- B. After the sample was removed. Note the soda straw in the middle, and the bone breccia at the base (courtesy of H. Schwarcs).
- C. A tool embedded in the base of the sample. Also note the bones and soda straw in the base of the sample.



B



C

Figure 6.23

79LC19, near the puits, Abri Suard.

Figure 6.24

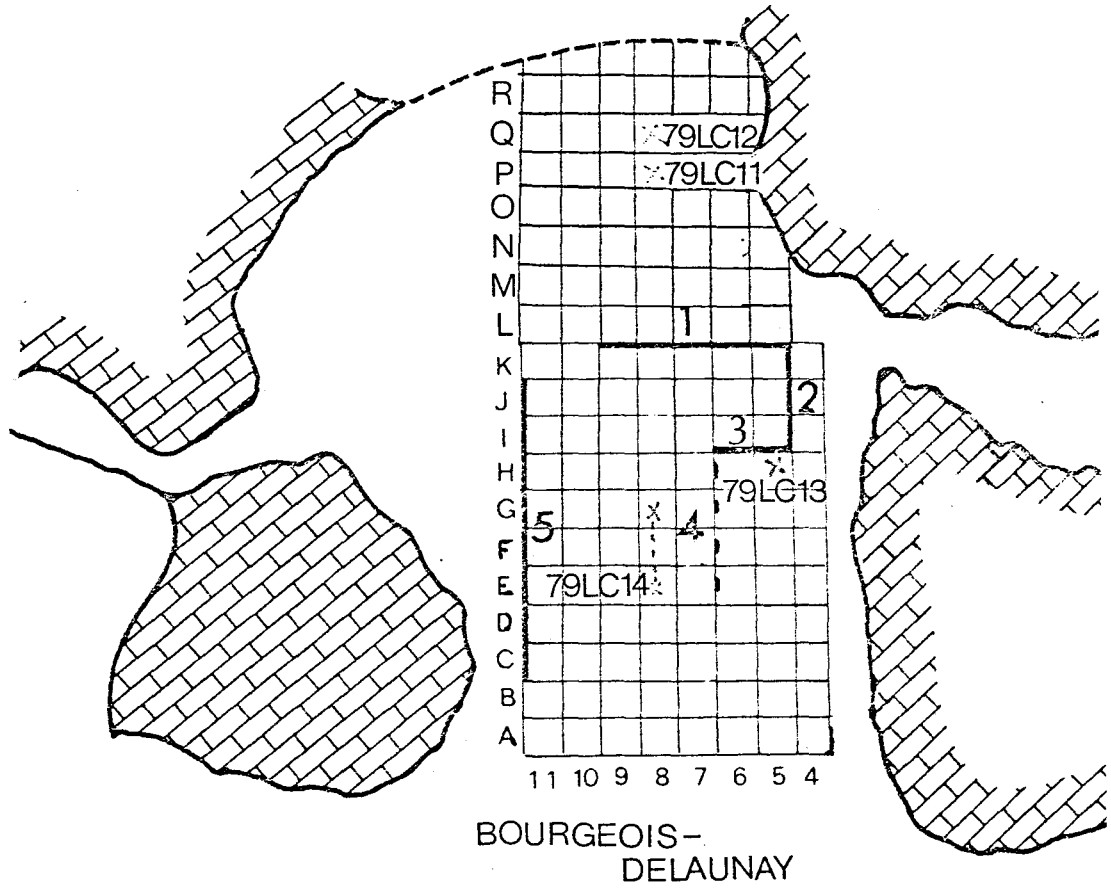
79LC20, in the couloir, comparable to  
couche 11, Bourgeois-Delaunay, and the  
Plancher Supérieur, Suard.





Figure 6.25

Sample locations in Bourgeois-Delaunay.  
Thickened lines indicate the location of  
cuts made by Débenath (adapted from Débenath,  
1974).



#### 6.3.8.1 Bourgeois-Delaunay

79LC11 and 79LC12 were stalagmites collected from layer 7. Unfortunately, David had removed all of the overlying layers 2 to 6. Therefore, the relationship of the stalagmites to layer 6 is unclear, but there is no evidence that the growth of these stalagmites continued after the deposition of layer 6. Furthermore, they grew on the surface of the flowstone that forms layer 7 with no obvious break in calcite deposition.

79LC13 is a sample of flowstone collected by the writer from what appeared to be layer 11. It lay within a block of sediments which was being excavated at the time of its collection. Covered by brown silty sand, and underlain by similar material, the sample was approximately 1 m below the level at which layer 7 sits elsewhere in the cave. Layer 7 was not present directly above 79LC13.

79LC14 was selected by Debénath specifically to represent layer 11, although it was not in situ at the time of its collection. Both 79LC13 and 79LC14 display growth laminations marked by colour bands but no obvious concentrations of detritus. In thin section, there is a slight increase in detrital content visible on these laminations.

#### 6.3.8.2 Suard

Both 79LC15 and 79LC16 are stalagmites collected in Suard from the surface of the plancher supérieur. There was no obvious break in calcite deposition between the growth of the plancher and that of the stalagmites. 79LC16, however, did have a strongly mar-

ked lamination about 5 mm from its outer rim, which represent a hiatus in deposition marked by a layer of sand. Although there are no sediments presently overlying these samples, they could have been removed by David.

Because no conclusive date had been previously determined by Schwarcz and Debénath (1979) for 77LC3, from layer 53', the plancher inférieur, a new sample was collected. Unfortunately, it was never shipped from France.

79LC18 was collected from the plancher supérieur topping David's witness section. It is the flowstone which formed the base of the stalagmite. No sample was collected from the stalagmite atop it because such sampling would have destroyed this magnificent specimen. Embedded in the base of the sample was a flint flake, bones, and calcite éboulis. Above that, the sample was of pure calcite. See Figure 6.22.

79LC19 was a stalagmite which was collected from a plancher in the back of Suard in a very wet grotto. It is contiguous with the plancher. No clastic sediments cover this area.

#### 6.3.8.3 Couloir

79LC20, from the plancher in the couloir between Suard and Bourgeois-Delaunay, was difficult to relate to any other strata. It occurred approximately 0.5 m below the ceiling and 1 m above the floor. There is a small stalagmite on its surface, which overlies three, and in places four distinguishable flowstone layers. There is an obvious hiatus in deposition marked by an accumulation of sand under the stalagmite

Subsamples taken for analysis were as follows:

- 79LC11: all subsamples contain approximately the outer half of the growth rings, 11-1 and 11-3 from the top, 11-2 from the side.
- 79LC12: 12-1 golden brown basal portion.  
12-2 top 1/3 of stalagmite, centre slice.
- 79LC13: all subsamples are from two adjacent slices; subsamples of equivalent stratigraphic position are labelled with the same letter.
- 79LC14: all subsamples are from one slice; subsamples of equivalent stratigraphic position are labelled with the same letter.
- 79LC15: 15-1 top 5 cm of stalagmite  
15-2 middle group of laminae  
15-3 basal portion
- 79LC16: 16-1 outermost ring separated from rest by sand lamination.  
16-2 middle section, several growth rings wide (it should be younger than 16-3, 16-4).  
16-3, 16-4, middle section, oldest growth bands.
- 79LC18: 18A top 1/2 of the flowstone, all subsamples are equivalent.  
18B bottom 1/2, all subsamples are equivalent.
- 79LC19: all subsamples are equivalent in age.
- 79LC20: 20-1 second layer from bottom, yellowish calcite.  
20-2 bottom orangy layer.  
20-3 black layer, top of flowstone base.  
20-4 stalagmite on top.

79LC20: 20-5 base of flowstone equivalent to 20-1 + 20-2.

### 6.3.9 Results

Tables 6.40 to 6.49 list the results for Lachaise.

#### 6.3.9.1 Bourgeois-Delaunay

Both 79LC11 and 79LC12 were collected from the surface of layer 7. With the exception of 79LC12-2 which has an anomalously high uranium concentration, the three determinations agree well, with an average of  $70.7 \begin{smallmatrix} + 6.3 \\ - 6.0 \end{smallmatrix}$  Ka, which coincidentally is the uncorrected age for 79LC11-1. This is significantly younger than 77LC1, dated at  $101.5 \begin{smallmatrix} + 12.0 \\ - 11.2 \end{smallmatrix}$  Ka. Considering, however, that the former two are stalagmites, while the latter is a piece of flowstone, the ages are consistent. Furthermore, no significant amount of detrital deposition could have occurred between the two periods of deposition.

79LC13, supposedly from layer 11, appears to have been overturned. Furthermore, none of the dates,  $79.8 \begin{smallmatrix} + 4.7 \\ - 4.5 \end{smallmatrix}$  Ka,  $89.1 \begin{smallmatrix} + 5.2 \\ - 5.0 \end{smallmatrix}$  Ka, and  $113.8 \begin{smallmatrix} + 7.5 \\ - 7.0 \end{smallmatrix}$  Ka, agree with those determined on other samples from layer 11, which have an average 152.4 Ka. Instead, these dates for 79LC13 seem more consistent with those of layer 7, noted above. If the sample is indeed from layer 7, then three different periods of deposition occurred to deposit the flowstone which shows two well marked hiatuses.

Although 79LC14 was collected to represent layer 11, and although its age is almost identical with that of 77LC2 from layer 11, the date for 79LC14 is not in agreement with that for 79LC13.

Both 79LC13 and 79LC14 look very similar, but there are three different horizons in the former, which all have significantly different ages, while those in the latter, of which there are four, are indistinguishable from one another. Assuming that 79LC13 is from layer 7, the age of layer 11 is  $151.0 \pm 16.1 - 14.0$  Ka.

#### 6.3.9.2 Suard

Both 79LC15 and 79LC16 come from the plancher supérieur in Suard in two adjoining grottoes. 79LC15 ranges in age from 74.5 to  $119.3 \pm 18.2 - 16.3$  Ka, which is consistent with the age given below for 79LC18. 79LC16, however, is completely inconsistent, yet there is nothing in its crystallography to suggest it might have been leached or reprecipitated. Both 79LC16-2 and 79LC16-3 have uranium concentrations which are low, but  $^{234}\text{U}/^{238}\text{U}$  ratios which are high compared with those of 79LC15. If these two dates are ignored, then the stalagmites in these grottos grew periodically from approximately 120 until 45 Ka. The last period of deposition is marked by a sand-filled hiatus in growth.

79LC18 was collected from the plancher supérieur in David's section. This is contemporaneous with the plancher supérieur in the grottos. 79LC18 averaged  $103.0 \pm 7.3 - 6.9$  Ka. Because the determination for 79LC18B-2 has a low uranium concentration and a high  $^{234}\text{U}/^{238}\text{U}$  ratio, it has been ignored in the average age. There was no apparent hiatus in deposition although one lamination is visible in the sample.

Corresponding to 79LC17, 77LC3 is still a problem. Although Swarcz and Debénath (1979) reported an average date, there is no reason to

disregard any of the dates. Therefore, no conclusions regarding the age of layer 53' are possible.

79LC19 from the back of Suard is a post-Pleistocene stalagmite,  $9.7 \pm 1.5$  Ka BP. It is not comparable with the plancher supérieur, as had been hoped.

#### 6.3.9.3 Couloir

Originally thought to be contemporaneous with both layer 11 in Bourgeois-Dalaunay, and the plancher supérieur in Suard, the plancher in the couloir, represented by 79LC20, is not contemporaneous with either deposit. Because the yields for 79LC20-2 were low, this determination is somewhat doubtful. It may, however, be accurate since this subsample is the base of the multilayered sample. 79LC20-5, 79LC20-3, and 79LC20-4 sequentially overlie the base, with ages of  $50.8 \begin{smallmatrix} + 8.9 \\ - 8.6 \end{smallmatrix}$ ,  $37.3 \pm 2.9$ , and  $19.2 \begin{smallmatrix} + 14.8 \\ - 13.0 \end{smallmatrix}$  Ka respectively, although the low yields for the last make it very unreliable. Therefore, deposition in the couloir may have begun at the same time as deposition in both layer 7 and the plancher supérieur was ending, but it continued periodically until at least 37 Ka, and possibly until 20 Ka.

#### 6.3.10 Conclusions

If it can be assumed that 79LC13 is indeed layer 7, then Figure 6.26 shows the depositional history of Lachaise. Calcite precipitation has been active in the cave during the major interstadials of the Wurm, in addition to the Riss/Würm, and the Riss II/III.

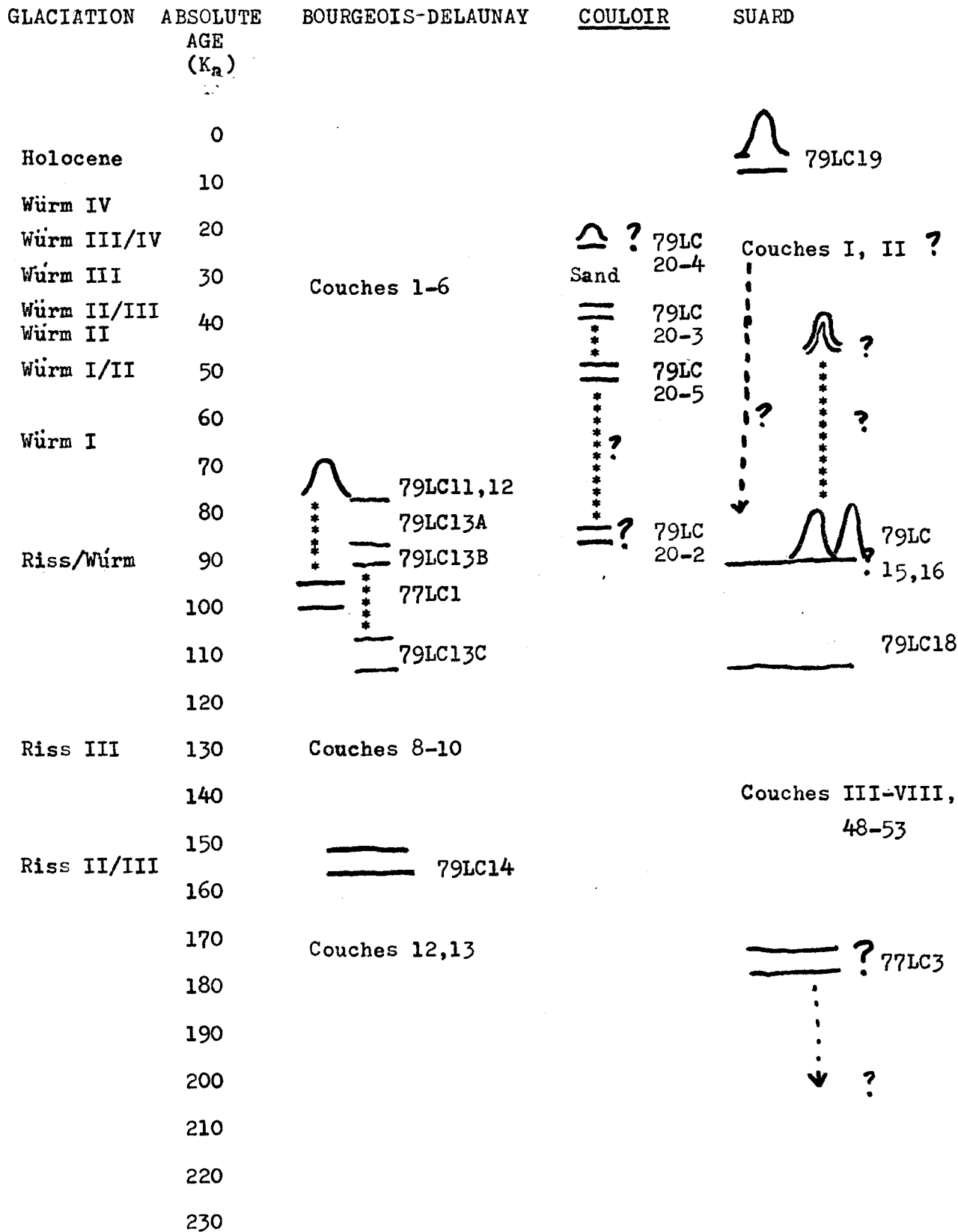


Figure 6.26

An interpretation of the depositional history  
of Lachaise

Note that a question mark indicates an age which  
which is uncertain.

\*  
\*  
\* No deposition occurred during this time.  
\*



In Bourgeois-Delaunay, layers 12 and 13 were deposited prior to the Riss II/III, probably in the Riss II. Both of these deposits have pollen suites which indicate that they were deposited under very cold conditions, which is consistent with a stadial. Layer 11 was deposited during the Riss II/III interstadial, when the area contained many trees. Unfortunately, the glacial isotopic record suggests this should have been a fairly cold time. Perhaps the warm period was very brief and did not last sufficiently long for it to have been preserved in the isotope record.

Overlying layer 11 are layers 10 through 8, all deposited during the Riss III, from 150 to about 115 Ka. The lowermost layers have pollen suites consistent with a cool wet period. Layer 7 was deposited in at least four stages during the Riss/Würm, but no clastic deposition occurred between periods of stalagmitic deposition, presumably because the cave was closed off from the outside, or was washed clean of the clastics before calcite precipitation was renewed each time. Growth of layer 7 spans the period from about 115 until 70 Ka, a time which saw many trees flourishing in the region. Layers 6 through 1 were deposited after 70 Ka.

In Suard, deposition must have begun somewhat earlier, because layer 53', a stalagmitic plancher, was deposited before any in Bourgeois-Delaunay, although the exact date is uncertain. At that time, however, the region boasted many trees. Therefore, layer 53' must have been deposited under very warm conditions, during an interstadial, or interglacial.

Layers 53 to 48 and VIII to III overlying layer 53' are

capped by the plancher supérieur, which was deposited starting at approximately 120 Ka. These layers were all deposited under cool conditions, determined from the pollen. That these predate the Riss/Würm does solve the problem of the high incidence of reindeer, which had caused Debénath (1974) to assign them to the late Riss.

Stalagmitic deposition continued from 120 until at least 100 Ka in the main chamber, and until about 75 Ka in the side grottoes. Deposition was probably equally prolonged in the main chamber since the stalagmite there, which was not dated, is approximately 20 cm tall, suggesting that it grew over several thousand years. In the side grottoes, no sediment deposition occurred until after a final capping of calcite had been added to the plancher supérieur at about 45 Ka, in the Würm I/II. Unless, the stalagmite in the main chamber can be dated, however, it is uncertain if sediments were deposited there between 75 and 45 Ka. Deposition of layers I and II could have been deposited at any time during the Würm. Containing 90% trees, the pollen suite for the plancher supérieur confirms that the period must have been very warm and wet, as an interglacial would have been.

At the back of Ward active deposition began approximately 10 Ka BP, after the end of the Pleistocene, and still occurs presently (Figure 6.5).

The couloir experienced periodic deposition which may have begun contemporaneously with stalagmitic deposition during the Riss/Würm in both Bourgeois-Delaunay and Suard, but continued periodi-

cally until about 50 Ka without any sediment deposition. It is likely that the couloir was blocked off from Bourgeois-Deluanay and Suard during the time. After some deposition of sand another stalagmite grew in the couloir, possibly at about 20 Ka, in the Würm III/IV, following which the couloir was opened and filled with sediments.

Archeologically, these data present a few problems, particularly with respect to the skeletal remains. If the material embedded in the base of layer 11 is truly classic Neanderthal, then it is older than the supposed appearance of the classic Neanderthals by about 70 Ka, although this does agree with the age determined for the Ehringsdorf skull, also a classic Neanderthal (Blackwell, 1978). Furthermore, if the material in layer III is pre-Neanderthal, it may postdate the classic forms. There are three possible solutions to this problem:

1. Layer III is older than layer 11. The plancher supérieur was deposited after a lengthy hiatus. Why, however, was there no deposition in Suard of any plancher equivalent to layer 11, and why was there no sediment deposition after 150 Ka until 100 Ka?
2. The pre-Neanderthal material is actually Neanderthal.
3. There coexisted two contemporaneous populations, one of Neanderthals inhabiting Bourgeois-Delaunay using Acheulian tools, the other pre-Neanderthals in Suard using almost identical tools.

The question will remain unresolved until layer 53' can be precisely

dated.

In Bourgeois-Delaunay, layer 9 contains an industry intermediate between Acheulian and Mousterian. Assuming the rate of sedimentation was constant during the Riss III, then the industry is about 125 Ka old, but most archeologists assume the Mousterian evolved about 80 Ka ago. In Suard, an industry similar to that of layer 9 is present in layers I and II, but this postdates 100 Ka. That an intermediate industry should have lasted so long is unlikely, which raises a question as to the affinities of the industry in layers I and II, both of which are rather poor. The dates of these layers should be more firmly established, since these may be Würm II deposits. Because the grottoes in Suard and the couloir did not experience sediment deposition during the Würm I, it is possible that all of Suard was inactive. If so, then layers I and II could postdate 50 Ka. This question could be resolved by dating the top of the stalagmite atop 79LC18, and any other stalagmitic material which appears to belong to the plancher supérieur near David's section.

Certainly Lachaise still presents problems, but dates on couche 53' and the pillar stalagmite might solve them.

#### 6.4 Montgaudier

Montgaudier, the cave near Vouthon, is one of the most problematic sites in France, if not the world. An immense site, about 750 m<sup>2</sup>, with several different floor levels, and many small abris and caves within the site, Montgaudier has yielded six cultures in the 130 years it has been excavated, and is no closer to

being understood than it was in 1850. Because of its immense size, little has been excavated.

#### 6.4.1 The History of Excavation

Montgaudier was first excavated by E. Lartet, for whom Abri Lartet was named, in about 1850, followed by Vibraye in 1864, Tre-meau de Rochebrune and Bourgeois and Delaunay in 1866-67, Gaudry, for whom Abri Gaudry is named, in 1867, Fermond in 1871-72, Paignon, for whom Abri Paignon is named, Lartet and Gaudry in 1878-79 and 1896, Chauvet, de Nadaillac and Gaudry in 1888, Harle in 1892, Fermond and Curtaillac in 1894-95, de Mortillet in 1907 and 1910, Octobon and Vallade in 1926, and David and Pintaud in 1957-59. The site was then abandoned until 1966 when I. Duport, a gendarme from Angouleme, started to work the site. Unfortunately, because he is not a professional archeologist, the work has been largely done by himself, and has not progressed very far, although he has worked the site most of the year since 1966.

#### 6.4.2 General Description

The complex of abris known as Montgaudier is located on the left bank of the Tardoire about two kilometres downstream from Montbron (Figure 6.1). Rather than one simple abri, the site comprises several different abris on different levels. At present, there are five principal areas recognized, each on a slightly different level above the river, each with its own peculiarities.

The main entrance to the complex is at the present river level through the Grand Porche (Figure 6.27). Looking NNE toward

Figure 6.27

Montgaudier, near Vouthon.

The plan view of Montgaudier showing the test pits and excavations made recently (after Débenath, 1974).



the river, the Grand Porche measures 13 m across and 10 m high. A test pit was opened in this section in 1966 along with three more recent test pits oriented north, east and west, as shown in Figure 6.27.

Toward the back of the Grand Porche, the Balcony is elevated above the floor of the Grande Porche by about 8 m, sitting atop fluvial deposits which have filled the cave (Debénath, 1974). Above the Balcony are a group of small grottos which were excavated at some unknown time. In the northwest section is a small grotto, Cave Bear Alley, notable because it contains a fauna of cave bears, U. deningeri, and hyena, along with a stalagmitic plancher.

Just to the north of Cave Bear Alley, Abri Lartet opens to the northwest overlooking the valley from a height of about 12 m. Once covered by a more extensive roof than at present, this abri has been extensively excavated by Duport since its initial discovery in 1968.

Oriented to the ESE is a huge abri at about the same level as the Balcony. A talus slope stretches 20 m in front of Abri Gaudry (also known as the Tardoire part), and is continued in the form of a meadow around which the Tardoire flows. Part of this abri was excavated in 1966 and 1968.

Between the Grand Porche and Abri Gaudry, opening on the same level as the meadow is Abri Paignon, excavated since 1971. All the data which follows regarding the archeology, stratigraphy, and paleoenvironments, unless otherwise stated comes from Debénath, (1974), Debénath and Duport (1971), and Duport (1973, 1974, 1976, 1977).

Figure 6.28

An overview of Montgaudier:

A. Montgaudier as Gaudry pictured it, c. 1880:

A. The main entrance

B. Lateral arcades (Abri Gaudry & Balcony)

C. The home of a large bear

D. The monticule overlooking the valley.

E. The upper meadow 32 m above the Tardoire  
River (T).

B. Abri Gaudry today.

C. The Balcony looking through the gate at the  
main entrance.

D. Abri Lartet from the Grand Porche.

(Gaudry's sketch after Duport, 1977; photo B courtesy  
of H. Schwarcz)



all out of the valley.

A

1

B





C



D

### 6.4.3 Stratigraphy

The stratigraphy of Montgaudier is one of the most complex of any of the cave sites, because of the interaction of the different levels, in addition to the interaction of fluvial deposits with rock falls and stalagmitic deposition, complicated by slump deposits and human occupations at several different times in different parts, from the late Acheulian to the Bronze Age. Consequently, in some areas, Mousterian deposits overly Magdalenian!

#### 6.4.3.1 The Grand Porche

In the east cut, the sequence consists of 5 m of sands covered by a thin breccia of large rocks. Just below the breccia is a thin lens of iron and manganese salts. The lowest portion comprises fluviially deposited gravels and sands. Several levels of sand have been cemented into a sandstone. Much of the sediment has been derived from the carbonates. At the top of the sequence are fragments of a stalagmitic plancher.

In the north cut, there is about 5 m of silty sand very similar to the east cut. These deposits have been interpreted (Debénath, 1974) as an initial cave deposit partially removed and redeposited with other fluvial sediments.

During the 1966 excavation, four layers were defined:

1. Yellow silt with large calcareous eboulis (allochthonous) and quartz and iron.
2. Similar to 1, but containing more gravel and éboulis.
3. Similar to 1 and 2, but with fewer éboulis, no cementation, and no illuvial concretions. Ferrous elements

suggest fluvial deposition, but frost did affect the deposit. None of the quartz is windblown.

4. Similar to the others, but with more *éboulis* than 3.

In the west cut eight levels comprise about 10 m of sediments. In the upper four, large pieces of stalagmitic planchers and calcareous *éboulis* are found in the sandy silts. The lower layers, also sandy silts, lack *éboulis*. Laterally along the cut the stratigraphy is modified when several silty layers are interspersed between layers 7 and 8. Differing principally in colour from white to reddish-brown, these beds contain a layer of plaquettes sandwiched between two silt layers.

To the extreme west directly beneath Abri Lartet is a heterogeneous group of silty layers with *éboulis* that together measure 10 m thick. As the base is an ancient debris fall below which was found an in situ succession of Mousterian layers for which the stratigraphy comprised seven layers of varicoloured sands and silts underlying the fallen roof debris, one which measured 14 m<sup>2</sup>. Beneath this, and more toward the main entrance was a sequence of sands and silts underlying a 9 m<sup>2</sup> block of *éboulis*. In the thirteen layers of various colours were pre-Mousterian artefacts.

#### 6.4.3.2 The Balcony

In the Balcony sequence, slump blocks, fluvial deposits, and Magdalenean cultures combine. Three series have been studied here. In series A, the 0.8 m thick sequence is:

1. Fine silty mud with few *éboulis*. Magdalenean culture.
2. Silt rich in carbonate. Sterile.

3. Stalagmitic plancher.

4. Sterile silt.

Series B contains two layers of arched pieces, while series C has two layers of fluvial sediments.

#### 6.4.3.3 Abri Lartet

Since 1971, most of the excavation in Lartet has been concentrated in squares D-G 1-7. In the western part of the abri (see Figure 6.29), the stratigraphy is as follows from the top, as shown in Figure 6.30:

1. Soil and vegetation.
2. Red breccia with calcareous blocks, Mousterian artefacts, and faunal remains.
- 2'. Red breccia with fragments of stalagmites, and Mousterian industry.
3. Sterile brown silty sand.
4. Yellow breccia with stalagmite fragments and large calcareous *éboulis*.
5. Yellow sandy silt with small *éboulis*.
6. Very indurated breccia, with an indeterminate industry and faunal remains.

The total thickness represents about 2 m. From the bottom upward, the effect of cryoclastic action increases, as in the Grand Porche; it is difficult to relate the stratigraphy on one side with that on the other, particularly because so little has been excavated. This entire sequence contains a Mousterian assemblage.

Figure 6.29

Plan view of Abri Lartet:

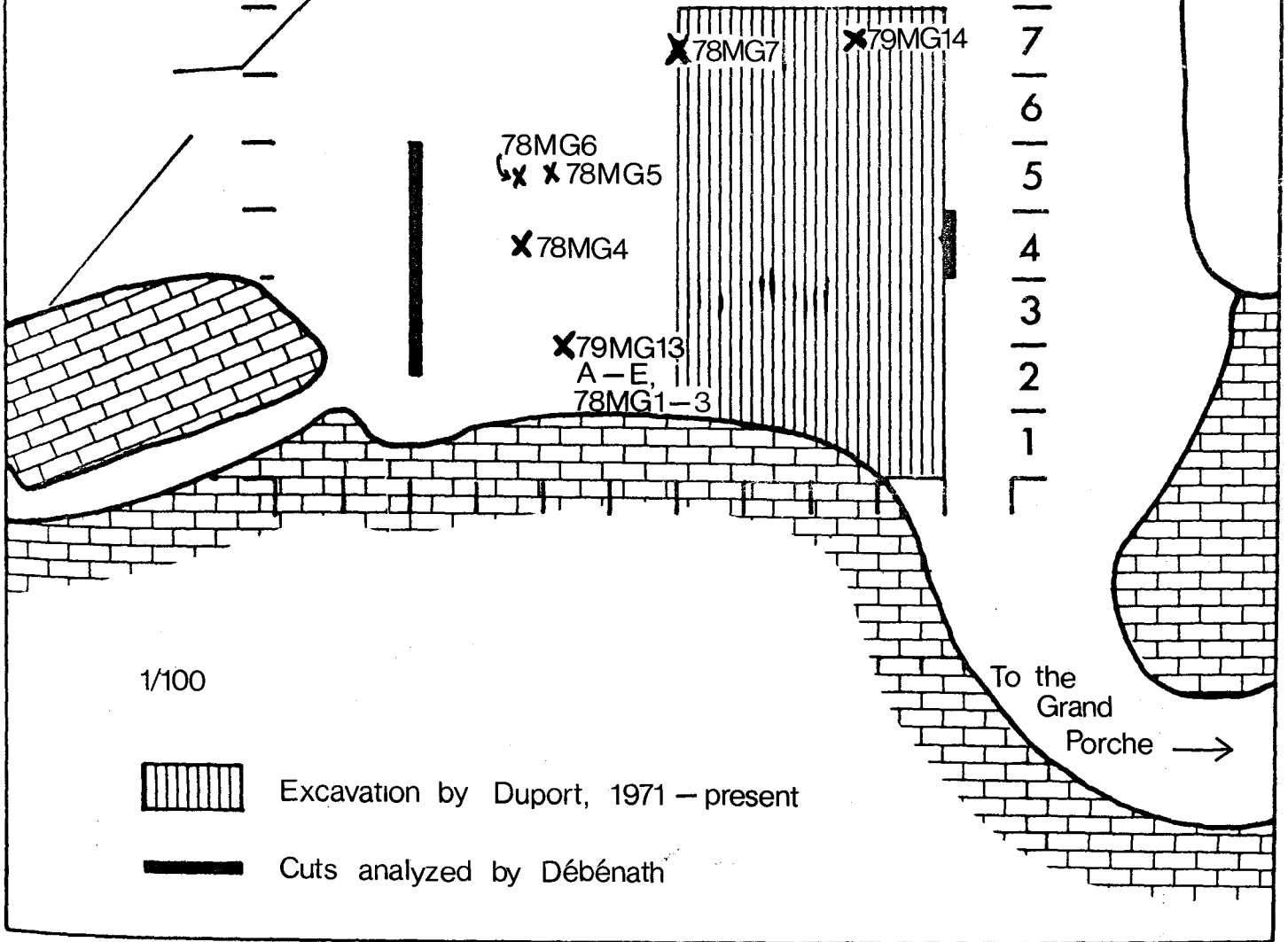
X marks the location of samples collected for  
U/Th dating (adapted from Débenath, 1974).





X I Y I Z I A B C D E F G I H

10  
9  
8  
7  
6  
5  
4  
3  
2  
1



1/100



Excavation by Duport, 1971 - present



Cuts analyzed by Débénath

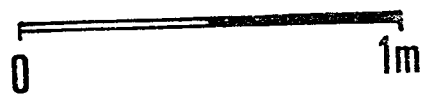
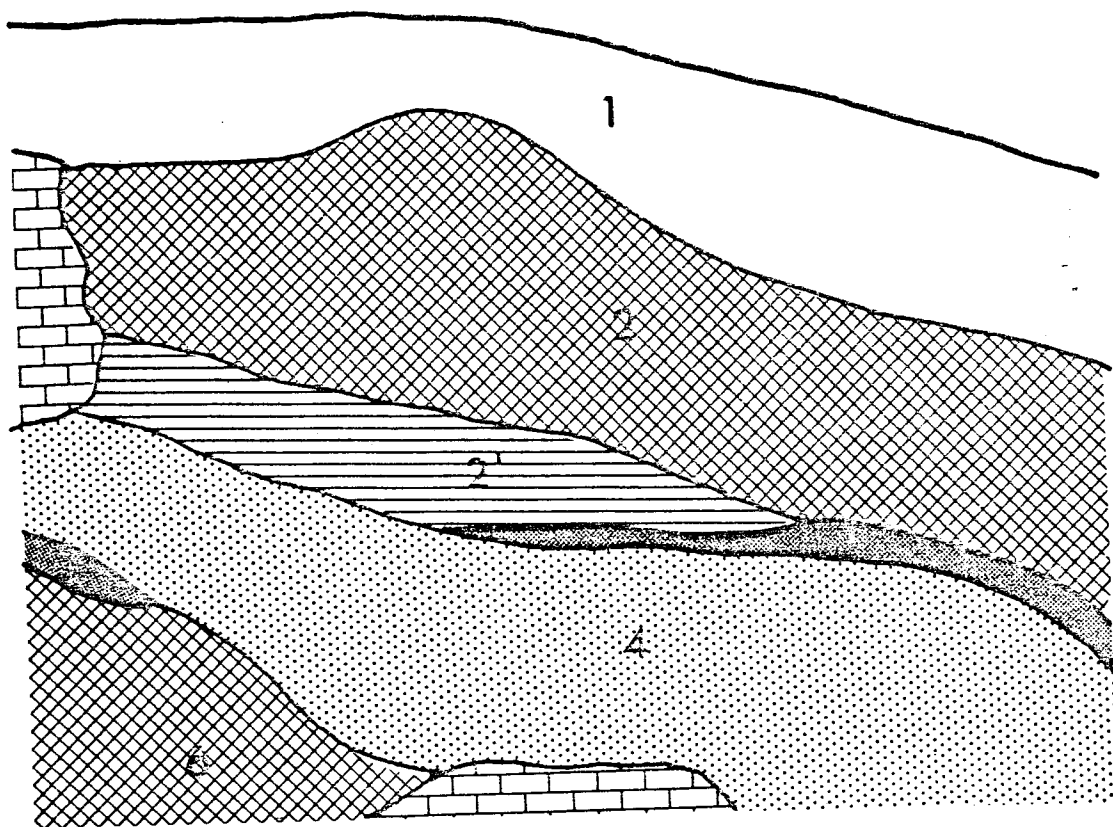
To the Grand Porche →

Figure 6.30

Stratigraphy of the west cut in Abri Lartet  
(after Débenath, 1974)

S-SO

N-NE



## 6.4.3.4 Abri Gaudry

Much controversy has existed about the stratigraphy in Abri Gaudry, because it is a talus slope with Magdelanean interbedded with Mousterian. In 1971, Duport clarified the stratigraphy as follows

0. Breccia of stalagmites and fallen éboulis blocks.
1. Yellowy-orange silty sand with many small limestone fragments. At the base large blocks up to 0.3 m.  
Final Magdelanean with engraved bones.
- 2A. Very similar to 1, but more yellow in colour.
- 2B. Light yellow sand with small limestone fragments and slight lamination.
- 2C. Red silt with polyhedral structures developed.
3. Sterile red silt.
- 4A. Cryoturbated sand with cryoclastic éboulis, brecciated in the lower portion.
- 4B. Very similar to 4A, but with smaller éboulis.
5. Small éboulis in a matrix of brown sandy silt, Upper Paleolithic (Aurignacian) artefacts.
6. Silt with traces of hearths and burnt bones.
7. Sterile yellow sand.
8. Stalagmitic plancher, broken but in situ.
9. Series of varicoloured sterile muddy silt layers.

## 6.4.3.5 Abri Paignon

The entire Paignon sequence is below that of Abri Gaudry, but is not necessarily older, because of possible slumping of the

Gaudry material. Of the two excavations, the Paignon cut comprises approximately 4 m of sediments, while the Prairie cut contains more than 3 m of fill. The stratigraphy of the former is as follows:

1. An altered layer (0.2 m).
2. Reddish-brown silty mud with medium-sized calcareous *éboulis* and larger blocks up to several decimeters in size particularly at the base. Magdalenian artefacts with engraved bones (2.0 m).
3. Very similar to 2, except there are no large blocks, more brown, with Solutrean artefacts (0.2 m).
4. Light grey sandy silt with *éboulis*, Upper Perigordian artefacts (0.8 m), with three sublayers:
  - 4A1. More *éboulis*.
  - 4A2. Enriched in manganese.
  - 4B. More silty with phantoms of *éboulis*.
5. Light grey silty mud with rare *éboulis* (0.5 m).
6. A succession of sandy layers becoming more silty toward the base.
7. Either a large rock fall or the substrate.

The Prairie cut, however, has quite a different stratigraphy from that above. From the top, it is:

1. An altered layer (0.2 m).
2. Red muddy sand with *éboulis* at the bottom (0.8 m).
3. Yellow sand with *éboulis* (0.5 m).
4. Fluvial deposit which is the former bed of the Tardoire (1.5 m).

5. A more silty level, the base of which was not found. Nowhere else in the excavation has the bed of the Tardoire been found.

#### 6.4.4 Archeology

Within Montgaudier, there is evidence of human occupation during at least six cultural periods, from the Acheulian to the Magdalanian. Because of the stratigraphic problems of the site, however, the relationships between these cultures and within a given culture for different areas of the cave are still problematic.

##### 6.4.4.1 Lower Paleolithic

Few details have been published for this culture found under the debris fall in the Grand Porche. The industry is made on pebbles and flint flakes. Fauna in the level includes cave bear, large bovids, horses, deer, rhinoceros, some bones of which have been nicked.

##### 6.4.4.2 The Mousterian

Although Mousterian artefacts have been found in most parts of the site, most areas have too few to allow a more precise classification of the industry. Such is the case in the Grand Porche, where the fauna include reindeer, bear, cattle, horses, and bovids. In Abri Gaudry, layer unspecified (Debenath, 1974), the industry is Quina type, found in the Foyer (see Figure 6.27).

In Abri Lartet, however, the Mousterian levels are in situ, not having been disturbed by previous excavation. At present, only two levels have been extensively excavated. Tables 6.51 through 6.55 list the characteristics of the industries. Both can be clas-

Table 6.50 Tool Typology, Couche 1, Abri Lartet,  
Mongaudier

<u>Tool</u>	<u>Number</u>	<u>Percentage</u>	<u>Restricted Percentage</u>
1. Levallois flake	3	4.8	
2. Atypical Levallois flake	8	12.7	
7. Elongated Mousterian point	2	3.2	3.8
9. Sidescraper, simple straight	8	12.7	15.4
10. Sidescraper, simple convex	16	25.4	30.8
13. Sidescraper, double straight convex	1	1.6	1.9
15. Sidescraper, double biconvex	2	3.2	3.8
19. Sidescraper, convergent convex	1	1.6	1.9
21. Sidescraper, asymmetrical	2	3.2	3.8
23. Sidescraper, tranverse convex	1	1.6	1.9
25. Sidescraper, on the ventral surface	1	1.6	1.9
26. Sidescraper, abruptly retouched	1	1.6	1.9
30. Typical endscraper	1	1.6	1.9
31. Atypical endscraper	1	1.6	1.9
38. Naturally backed knife	5	7.9	9.6
40. Truncated flake	1	1.6	1.9
42. Notched piece	2	3.2	3.8
62. Miscellaneous	5	7.9	9.6
<b>Total:</b>	<b>63</b>	<b>97.0</b>	<b>95.8</b>

Table 6.51 Piece Typology, Couche 2, Abri Lartet,  
Montgaudier

<u>Piece</u>	<u>Number</u>	<u>Percentage</u>
Flakes	147	56.8
Blades	3	1.2
Points	2	0.8
Trimmed flakes	19	7.3
Tools	63	24.3
Discs	0	0
Polyhedra	0	0
Nuclei	4	1.5
Debris	3	1.2
Hammerstones	1	0.4
Miscellaneous pebbles	<u>22</u>	<u>8.5</u>
<b>Total</b>	<b>259</b>	<b>102.0</b>

Table 6.57. Technical and Typological Indices and Characteristic  
Groups, Couche 1, Abri Lartet, Montgaudier

Index	Total	Restricted
Levallois	12.5	
Facetting	23.4	
Restricted Facetting	23.4	
Blade (lamellar)	3.8	
Archaeological Levallois	17.5	0
Sidescraper (Group II)	55.5	67.3
Total Acheulian	0	0
Unifacial Acheulian	0	0
Bifacial	0	0
Charentien	19.0	-
Quina	5.4	-
Group I: tools # 1 - 4	17.5	0
Group III: tools # 30 - 37, 40	4.7	5.8
Group IV: denticulates	0	0



Table 6.23 Piece Typology, Couche 2, Abri Lartet, Montgaudier

Piece	Number	Percentage
Flakes	230	43.2
Blades	2	0.4
Points	0	0
Trimmed flakes	136	25.6
Tools	115	21.6
Discs	0	0
Polyhedra	0	0
Nuclei	8	1.5
Debris	2	0.4
Hammerstones	0	0
Miscellaneous: pebbles	38	7.1
basalt	1	0.2
	<u>532</u>	<u>100.1</u>

Table 6.24 Tool Typology, Couche 2, Abri Lartet, Montgaudier

Tool	Number	Percentage	Restricted Percentage
1. Levallois flake	3	2.6	
2. Atypical Levallois flake	11	9.6	
8. Limaces	2	1.7	2.0
9. Sidescraper, simple straight	14	12.2	13.9
10. Sidescraper, simple convex	38	33.0	37.6
13. Sidescraper, double straight convex	1	0.9	1.0
15. Sidescraper, double biconvex	2	1.7	2.0
17. Sidescraper, double convex concave	4	3.5	4.0
18. Sidescraper, convergent convex	1	0.9	1.0
19. Sidescraper, convergent convex	4	3.5	4.0
21. Sidescraper, asymmetrical	6	5.2	6.0
23. Sidescraper, transverse convex	3	2.6	3.0
26. Sidescraper, abruptly retouched	1	0.9	1.0
27. Sidescraper, with thin back	1	0.9	1.0
29. Sidescraper, with alternate retouch	1	0.9	1.0
31. Atypical endscraper	2	1.7	2.0
38. Naturally backed knife	6	5.2	6.0
42. Notched piece	4	3.5	4.0
43. Denticulate	3	2.6	3.0
44. Bec burinante alterne	1	0.9	1.0
62. Miscellaneous	<u>7</u>	<u>6.1</u>	<u>7.0</u>
Total:	115	100.1	101.5

Table 6.128 Technical and Typological Indices and Characteristic Groups, Couche 2, Abri Lartet, Montgaudier

Index	Total	Restricted
Levallois	7.9	
Facetting	30.3	
Restricted Facetting	21.1	
Blade (lamellar)	0	
Archaeological Levallois	12.1	-
Sidescraper (Group II)	66.0	75.2
Total Acheulian	0	0
Unifacial Acheulian	0	0
Bifacial	0	0
Charentien	20.0	-
Quina	3.8	-
Group I: tools # 1 - 4	12.2	-
Group III: tools # 30 - 37, 40	1.8	2.0
Group IV: denticulates	2.6	3.0

Table 6.129 Tool Typology, Couche 4, Abri Paignon, Montgaudier

<u>Tool</u>	<u>Number</u>	<u>Percentage</u>
Endscrapers	5	6.9
Burins	31	43.1
Awls	6	8.3
Bec	3	4.2
Truncated piece	1	1.4
Retouched blades	10	13.8
Solutrean tanged point	1	1.4
Notched piece	1	1.4
Denticulate	1	1.4
Triangle	1	1.4
Backed blades	11	15.3
Total:	72	98.6

Table 6.129 Piece Typology, Couche 4, Abri Paignon, Montgaudier

<u>Piece</u>	<u>Number</u>	<u>Percentage</u>
Flakes (quartz)	389	59.5
Flakes (other rocks)	16	2.4
Blades, not retouched	57	8.7
Bladelets, not retouched	58	8.9
Burin spalls	37	5.7
Nuclei	3	0.5
Tools	72	11.0
Total	654	96.7

sified as Ferrassie (Charentian) Mousterian. Figure 6.31 shows incised and engraved bones found in Abri Lartet, something very rare for Mousterian assemblages. Debénath (1974) feels that layer 1 is an altered portion of layer 2 caused by the penetration of tree roots into the level.

Also within Abri Lartet, is a lithified Mousterian soil about 30 m<sup>2</sup> containing numerous bones, many splintered, from bovids, horses, reindeer, and the skeletons of pigs (see Figure 6.32) in perfect condition. Until the excavation of this is completed, it is impossible to determine if this industry is different from layer 2 with which it is connected. The presence of the pigs in such good condition compared with the state of the other bones, suggests a cult was active which is hitherto unknown in the Mousterian.

#### 6.4.4.3 Perigordian and Aurignacian

Some Aurignacian tools have been found in layer 5 in Abri Gaudry, but there has been insufficient work done there to describe the industry.

In layer 4 of Abri Paignon, 654 pieces of an Upper Perigordian industry were found, listed in Tables 6.56, and 6.57.. Typical tools included Noailles burins, truncated pieces, blades, and burins on truncation, some of which are shown in Figure 6.33.

#### 6.4.4.5 Solutrean

Although some Solutrean tools have been found in Montgaudier, Debénath (1974) does not think there is enough to indicate that the Solutrean actually existed at the site. No Solutrean retouched flakes have been found, and only 1 laurel leaf of unknown origin,

Figure 6.31

Incised and engraved bones from Montgaudier:

- 1, 2, 3, 4, 5. Traces of defleshing, Abri Lartet, Mousterian levels (actual size).
6. Worked bone (22 mm long), Abri Lartet, Mousterian levels.
7. Traces of utilization on a horse leg bone, Abri Lartet, Mousterian levels (actual size)
8. Incised bone, Abri Lartet, Mousterian levels (1/3 actual size).
9. Utilized bone, Abri Lartet, Mousterian levels (1/3 actual size).
10. Incised bone, actual size.
11. Incised bone, Abri Lartet, Mousterian levels (actual size).
12. Utilized bone, Abri Lartet, Mousterian levels (actual size).

(after Duport, 1977; Debenath, 1974, Debenath & Duport, 1971)

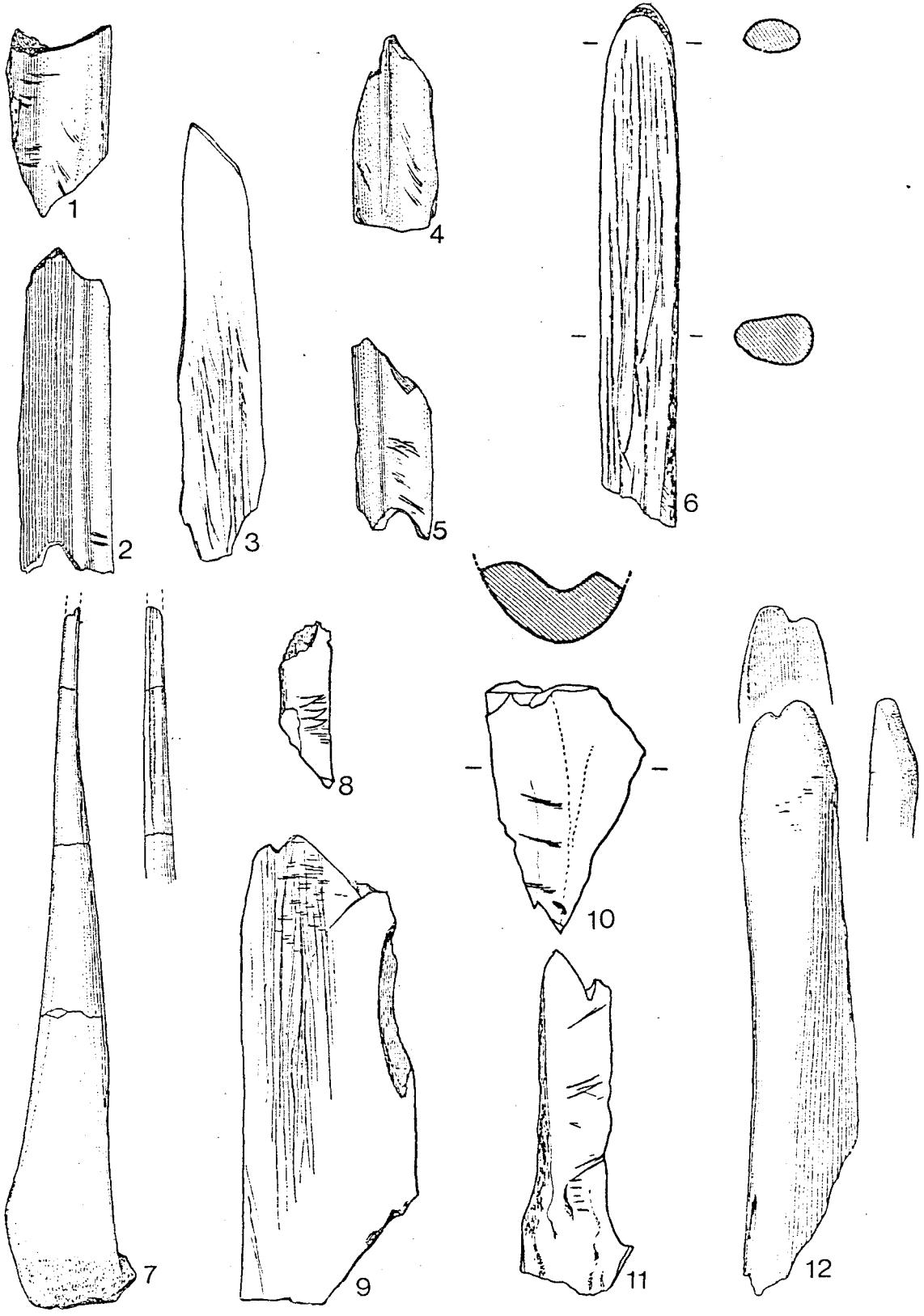


Figure 6.32

Pig skeletons in Abri Lartet (photo courtesy of  
H. Schwarcz).

Figure 6.32



in addition to one laurel leaf from the Grand Porche, of a type very rare in France. In layer 3 of Abri Paignon four tanged points were found of the Solutrean type, one made on a white porcelain-like flint similar to those of Placard. At present, it is impossible to say whether there was a brief Solutrean occupation, or if the Magdalenean people brought the Solutrean tools into Montgaudier, as has happened at other sites. Some of the Solutrean pieces are shown in Figure 6.33.

#### 6.4.4.5 Magdalenean

Because the Magdalenean was one of the first cultures found in Montgaudier, and many of the first excavations were solely for the purpose of finding Magdalenean art, results from these early days are impossible to use. Magdalenean material has been found in most parts of the complex, except Abri Lartet.

Found by Paignon in 1886, in the lower levels of the Grand Porche, the exact location of which is unknown, the Baton de Commandement (staff of office) is engraved on one side with two seals chasing a salmon, or possibly a whale, while the other side is covered by two eels. Remembering that Montgaudier is about 100 km from the present seacoast (more from the coast during Magdalenean times), the find becomes very significant, perhaps explicable by one of the following:

1. There was a trade network which connected Montgaudier with other peoples on the coast.
2. The Magdaleneans visited both the coasts and Montgaudier during their nomadic rounds.



Figure 6.33

The Upper Paleolithic at Montgaudier:

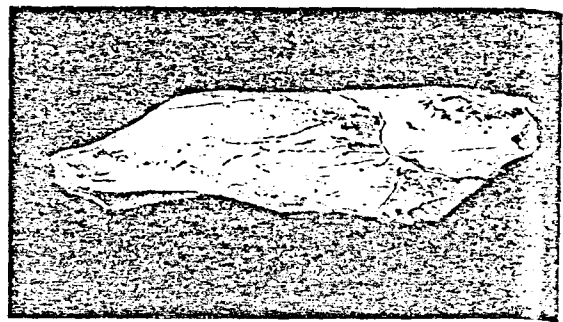
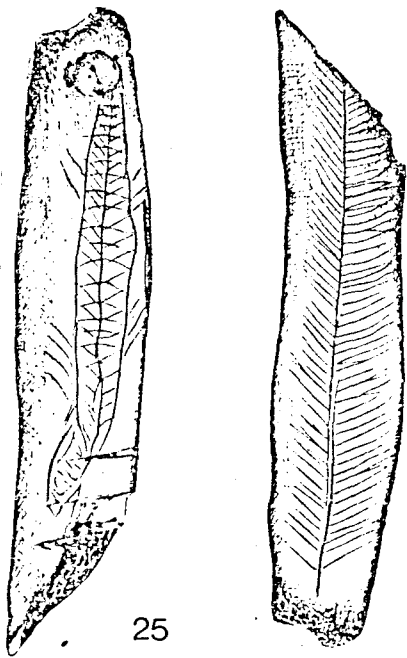
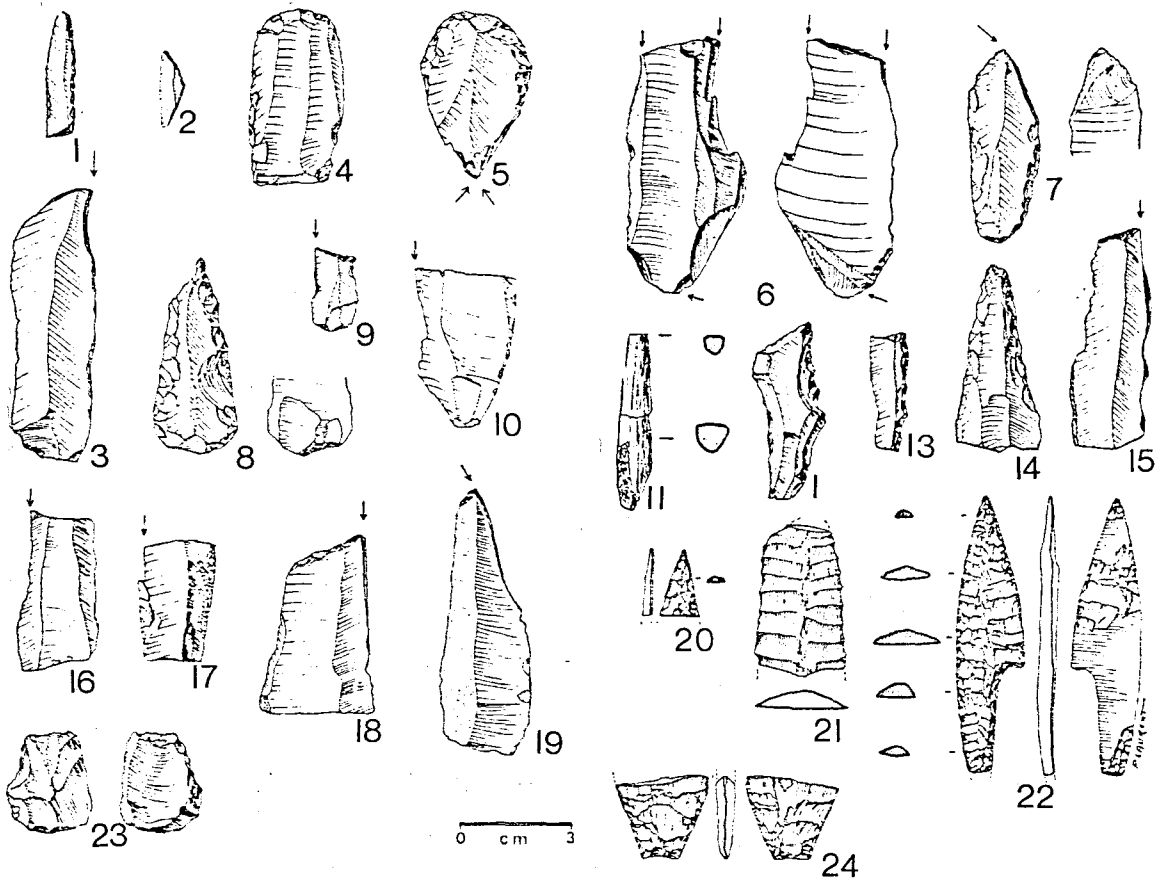
1. Backed bladelet, Paignon couche 2.
2. Triangle, Paignon couche 2.
3. Burin on break, Paignon couche 3.
4. Endscraper on a blade, Paignon couche 4.
5. Endscraper-burin, Paignon couche 4.
6. Multiple dihedral burin, Paignon couche 4.
- 7, 15, 18, 19. Burins on truncation, retouched obliquely, Paignon couche 4.
8. Endscraper-awl, Paignon couche 4.
9. Noailles burin, Paignon couche 4.
- 10, 16, 17. Dihedral burins on the angle of break, Paignon couche 4.
11. Sagaie in bone, Paignon couche 4.
12. Denticulate, Paignon couche 4.
13. Truncated piece, Paignon couche 4.
14. Retouched blade, retouched on two edges, Paignon couche 4.
20. Distal piece of a tanged point, Paignon, top of couche 4.
21. Fragment of laurel leaf point, location unknown
22. Solutrean tanged point, Paignon, top of couche 4.
23. Esquillée piece, Paignon couche 4.
24. Laurel leaf fragment, Grand Porche 1966 pit.
25. Engraved horse rib, location unknown.
26. Engraved bone, Gaudry couche 2
27. Incised reindeer rib, Gaudry couche 2.

Upper Perigordian: Paignon couche 4.

Solutrean: loose pieces in Grand Porche, top of  
Paignon couche 4.

Magdalanean: Paignon couches 2 and 3, Gaudry couche  
2.

(after Duport, 1973; Debenath, 1974; Duport, 1977)



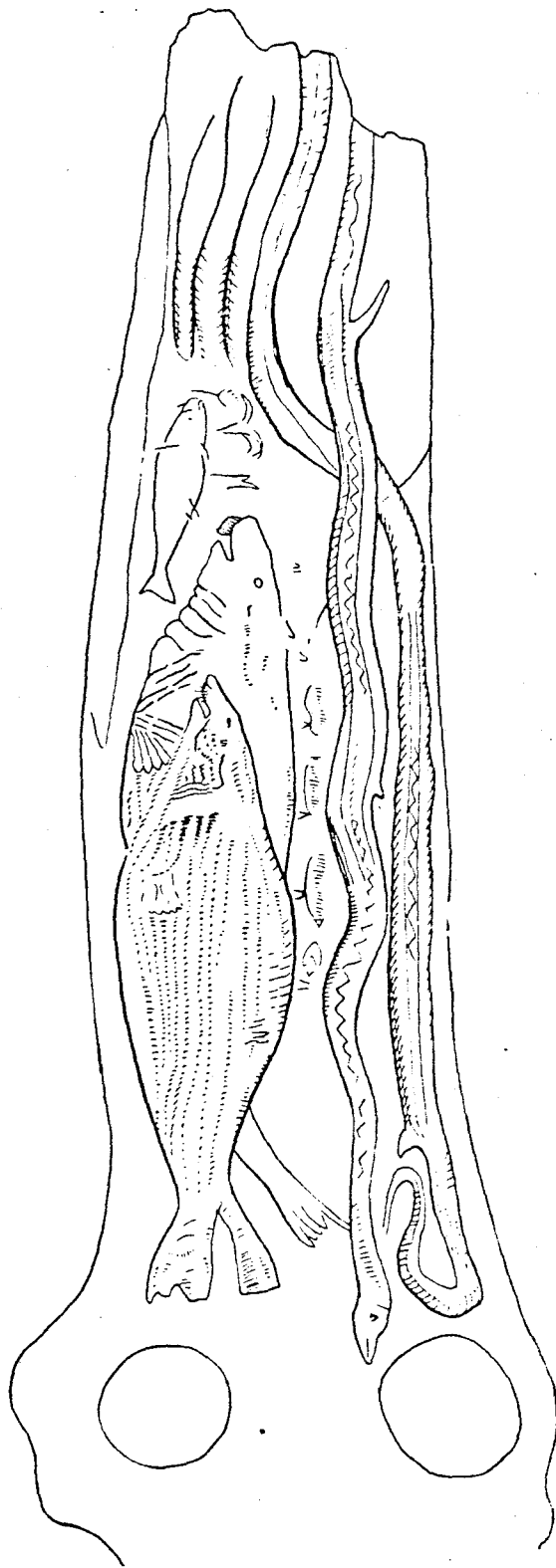
26

27

25

Figure 6.34

The Baton de Commandement, Montgaudier (after  
Duport 1977, 1973)



3. It was a prize of war, or a part of a dowry, or some such accident which brought it from the coast area.

Figure 6.34 shows both sides of the baton.

In layer 2 Abri Paignon, the Magdalenean artefacts include backed bladelets, triangles, an incised femur diaphysis, and burin spalls, which indicate a Magdalenean later than the first phase. Layer 3, consisting of only a few blades, bladelets, and two burins is too poor to characterize.

In the Grande Porche, the industry consists of an ivory sagaie (Figure 6.35), with a concial base, circular in section, incised by a rectilinear marking along the shaft. The point is missing.

In the Balcony five giant pieces were discovered under the debris of an ancient rock fall, in series B. The length of these pieces varies from 25 to 32 cm, averaging about 2 kg in weight (Figure 6.35), while flakes removed from them averaged 14 cm. Duport (1976) attributes these to final Magdalenean.

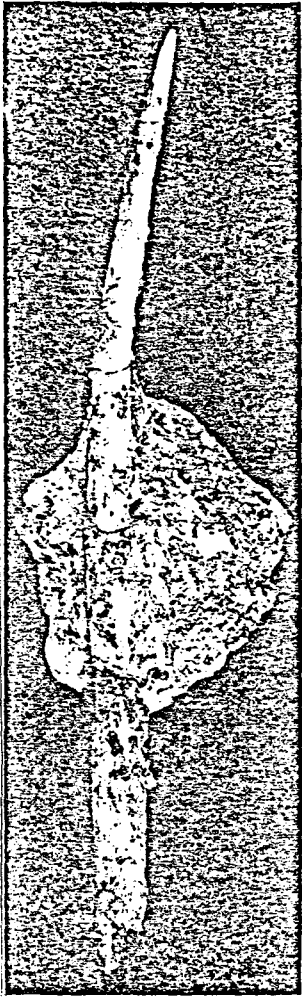
In Abri Gaudry, Pintaud found several engraved and incised bones, including a scapula of a reindeer engraved with horses and reindeer (Figure 6.36), a pebble engraved with a Venus lacking a head and legs (Figure 6.35).

Within layer 2 in Abri Paignon, two Bronze Age sepulchres were found. This is the latest archeological material found in the cave complex.

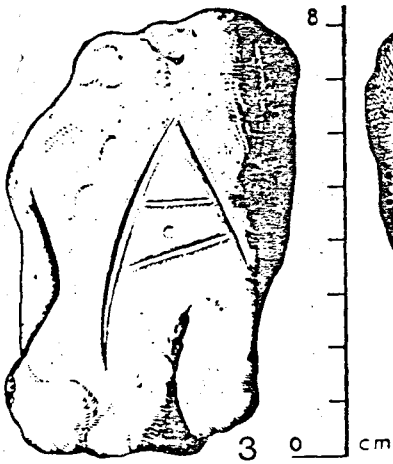
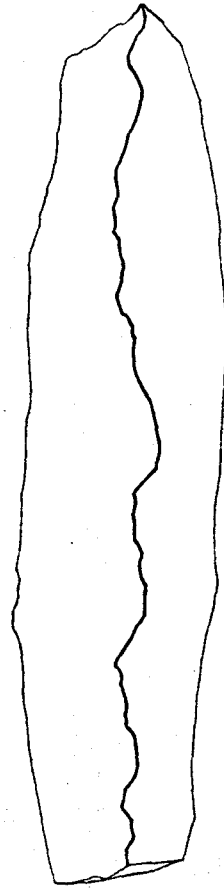
Figure 6.35

Magdalenean pieces from Montgaudier:

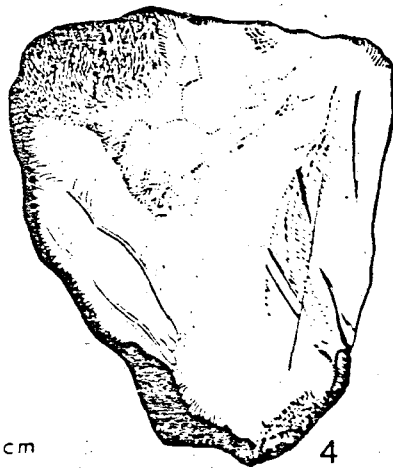
1. Ivory sagaie, Grand Porche.
  2. Giant piece (24.7 mm long), Balcony.
  3. Pebble engraved with a headless, footless Venus, Gaudry, Pintaud excavation.
  4. Obverse of 3.
  5. Engraving on a horse bone, Gaudry couche 2.
- (after Duport, 1973, 1977).



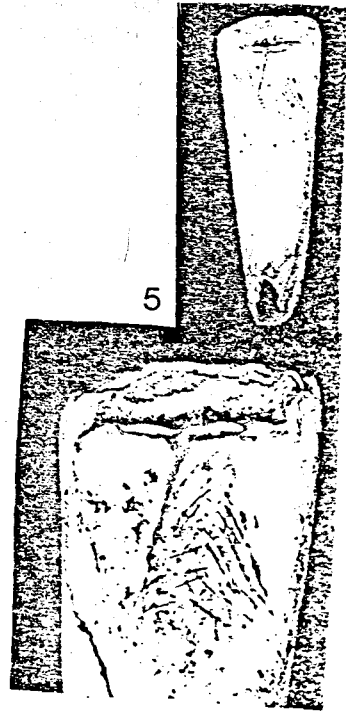
2



3



4



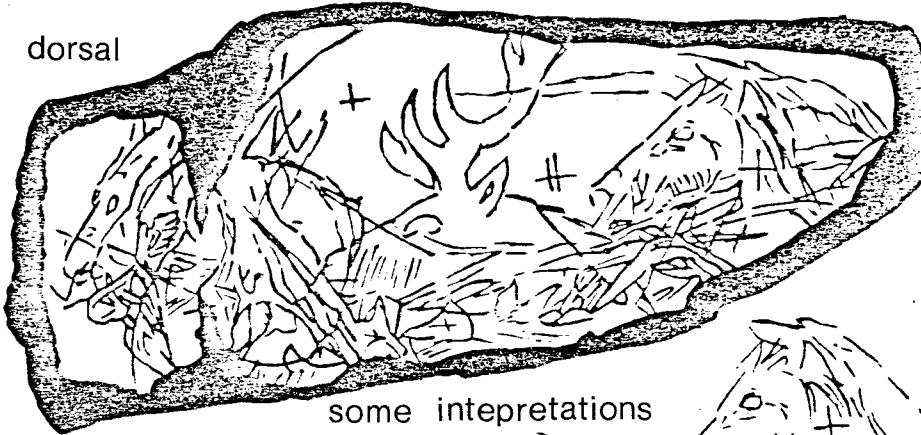
5

Figure 6.36

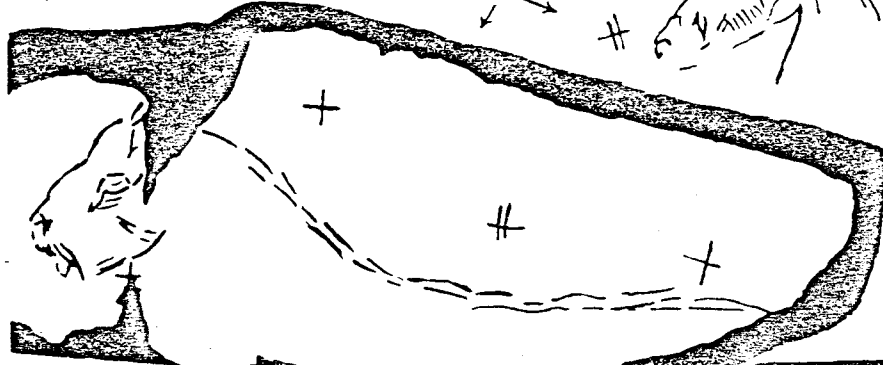
Magdalenean engraved reindeer scapula with some interpretations of the drawings. The crosses are not present on the piece, but are for orientation of the interpretations (after Duport, 1973, 1977).



dorsal



some interpretations

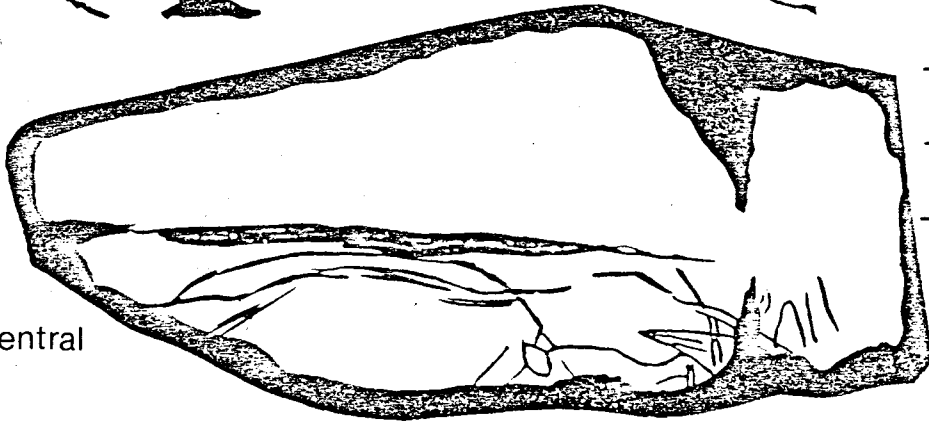


RcP 1939

5 cm

0

ventral



#### 6.4.5 Human Remains at Montgaudier

Few human remains have been found in Montgaudier, none of which are very important evolutionarily. Associated with Mousterian facies, are a fibula, several vertebrae, and a temporal bone, the latter found in layer 4 of the west cut in the Grand Porche. It is probably Neanderthal (Duport, 1977). In layer 3, also in the west cut, extreme west section, Duport (1977) found a Neanderthal mandible. With only the chin region and a few teeth remaining, its affinities are less than certain, but it did lack a true chin (Figure 6.37). Two crania, lumbar vertebrae, and other bone fragments have been found in layer 2 Abri Gaudry. While one cranium is almost complete containing two teeth and lacking only the lower portion of the maxilla, the other comprises only part of a calotte and the back of the face. Another cranial fragment with incisions was found in Abri Paignon layer 2, associated with Magdalenian tools.

#### 6.4.6 Paleoenvironments

Table 6.57 shows Debénath's (1974) interpretation of the paleoenvironments at Montgaudier. These interpretations are based almost entirely on the sedimentological studies, aided by a few distinctive fauna, and the one pollen study finished for the west cut in the Grand Porche. In most cases, the industry associated with the deposit was used to date the material!

Because U. spalaeus was found in the Grand Porche, these sediments must be younger than the Mindel, but the interpretation is uncertain as to which period they really belong. The presence

Figure 6.37

The mandible from Montgaudier:

A. The mandible.

B. The west cut where it was found.

In couche 3, square E'6, an X marks its  
location.

(after Duport, 1974)



Table 6.56 Paleoenvironments at Montgaudier

Glaciation	Climate	Grand Porche	Balcony	Lartet	Gaudry	Paignon
Holocene	warm		Fluvial seds.			
Wurm IV	cold	North cut, east cut	Series B		2A	2 top 2 middle 2 bottom 3 top 3 bottom
	warm				2B	
	cold				2C	
	warm					
	cold					
	warm					
	cold					
Wurm III/IV	warm				3	4 top
Wurm III	cold				4	4 bottom
	warm				5	
	cold				6	5
Wurm II/III	warm				7	6??
	cold				8	
	warm			1?	9	
Wurm II	cold	extreme west Moust.		2		
	warm			2'		
	cold			3		
Wurm I/II				4?	Moust. foyer?	
Wurm I				5?		
Riss/Wurm				6?		
⋮						
Mindel			Cave Bear Alley			

of the arched pieces in the Balcony, associated with the Magdalenean sagaie has been used to date the sediments in the Balcony, and the north and east cuts of the Grande Porche as Würm IV, while the fluvial sediments in the Balcony are thought to represent the initial Holocene warming phase.

In Lartet, there is progressively more cryoclastic action toward the top of the section. Because reindeer are abundant, and a Ferrassie Mousterian is present, these are considered to be Würm II sediments. These, also should roughly correspond to those in the extreme western part of the Grand Porche, which have slid down the slope from Lartet as a block.

In Abri Gaudry, the industries have been used to date the deposits within the period from the Würm II to the Würm IV. A lack of cryoclastic debris in layer 7 and 9 supposedly corresponds to the warmer Würm II/III interstadial, while two cold oscillations seen in layer 4 and 6 represent the Würm III. Layer 3 is thought to be a result of the Würm III/IV, and layers 2 and 1 the Würm IV.

In Abri Paignon, Upper Paleolithic material in the layers has been dated as Würm III and IV, by virtue of the industry. Three cold oscillations, therefore, are attributed to the Würm IV.

Finally, in Cave Bear Alley, U. deningeri under the stalagmitic plancher can be no younger than the Mindel.

Overlooking the Tardoire (Figure 6.38), where game would have been abundant, Montgaudier could probably house the camp of a whole tribe, without crowding. If it were chosen as the meeting place for the whole tribe or a multi-tribal group, religious cere-

Figure 6.38

The River Tardoire as seen from Montgaudier.

Figure 6.39

78MG1, couche 3, Abri Lartet (photo courtesy of  
H. Schwarcz)

Figure 6-38

Figure 6-39





monies probably occurred, as happens among modern hunter-gatherer tribes such as the Australian aborigines. This might explain the presence of the pig skeletons in the Mousterian, which are unknown elsewhere, and perhaps the presence of the Baton de Commandement.

#### 6.4.7 Sample Descriptions

In 1978, the initial collection at Montgaudier was made by H. Schwarcz, assisted by Duport. In 1979, the author collected more samples, assisted by Debénath and Duport.

In Lartet, layer 2 forms a sloping pavement which is attached to the southwest wall. Samples 79MG13A-E were all collected from this calcite-cemented sand within 20 cm of each other. They were collected to enable us to try fit different models for the relationship between detrital components in the samples and the dates obtained.

79MG14 was a large piece of speleothem lying loose in layer 4. Because of its long tapered shape it might be a stalactite, although its internal morphology is extremely unusual. For such a long stalactite, the crystals are very small, and the material very friable. Its place of origin is unknown.

In Cave Bear Alley, a stalagmitic plancher covers the bones of many cave bears. On this plancher are several stalagmites. 79MG15 is a pair of flowstone pieces which represent the whole thickness of the plancher, but do not include any stalagmites.

79MG17 and 79MG16 were both collected from layer 2, a stalagmitic plancher in Gaudry. In the case of 79MG16, there was no-

thing to indicate that this plancher had been displaced. It rested on red sediments, as Duport's (1977) stratigraphy suggests it should. 79MG16 was a stalagmite which had grown up from the surface of the plancher. Internally it resembled 78MG8. Just around the corner, in what Duport (personal communication) was certain was also layer 2, a very porous flowstone was embedded in the sediments. Although this sample, 79MG17, looks as if it could be an illuvial concretion as suggested by Debénath (personal communication), it is comparable in appearance to the base of the flowstone from which 79MG16 was collected, which is in situ.

79MG18 was collected from the edge of the pool near the base of the stairs in the Grand Porche. Its relationship to any stratigraphy there is uncertain but it may be equivalent to a part of the west cut nearby.

More detailed sample descriptions are given in Table

6.59.

Many of the subsamples analyzed from Montgaudier were ground because these were roasted before being analyzed. Many of the samples analyzed from the 1978 collection were loose pieces which could not be related to other subsamples with any certainty. Descriptions of the subsamples for the 1979 samples will be listed with the results.

#### 6.4.8 Results

Montgaudier is as much of a problem to date by the U/Th method, as it is to study sedimentologically. Low yields, large

Table 6.59

SAMPLE	LOCATION	DESCRIPTION	THICKNESS	DETRITUS	POROSITY	CRYSTALS	BIOCLAISTS	LAYERING	COMMENTS
78MG1	L c. 3 sq B2	Yellow fst, microxtln faint lam	4 cm	30% clay 20% carb	10% ang X0	Spar // lam, brecciated small random xtls	shells oolites stromato- lite?	clay concentrated on lam, spar edges form on lam	Unsuitable for dating
78MG2	L c. 3 10 cm below 78MG1 sq B2	White microxtln fst, faint lam 1 mm	broken in transit	10% clay ang X0	< 5% random	av. 1/2 mm random	0	clay concentrated on lam	
78MG3	L c. 3, 18 cm be- low 78MG2 sq B2	Calcite cemented soil, reddish-brown	broken in transit	5% fspar 25% carb 5% bone 30% clay	50% rd X0	av. 1/2 mm random	bone	-	Unsuitable for dating
78MG4	L c. 2 sq A4	Tan convolutedly lam fst with stg, lam marked by red sand 41 mm-5 cm thick	4 cm high 6 cm diam	50% clay < 5% bone 10% algae?	30% rd X1	av. 1/2 mm random	bone algae?	sand on lam	
78MG5	L c. 6 sq B5	Very similar to 78MG4, but not as convoluted with less sand in lam, fst with stg.	4 cm	- -	- -	- -	- -	- -	
78MG6	L c. 6 sq A5 cont with 78MG5	Brown to tan fst with stg, finely lam, sand in lam (red)	5 cm	15% silt all on lam	< 5% ang X0	spar, 1/2 mm x 3 mm // lam	-	silt on lam	

SAMPLE	LOCATION	DESCRIPTION	THICKNESS	DETRITUS	POROSITY	CRYSTALS	BIOCLASTS	LAYERING	COMMENTS
78MG7	L c. 3 sq C7	Macroxtln, grey-white transparent fst(?), may be from vein (?)	broken in transit	0%	<5%	Large, av 1 mm x 1 cm, consistent orient	-	-	Relation of xtl orient to growth unknown
78MG8	G c. 2 sq E'42?	Yellow-tan stg (8B) around white opaque chunk of cal- cite(8A)	4-6 cm high	8A: 30% clay, 8B: <5% clay	8A: 25% ang X2 8B: 5% ang X0	8A: av 1/2 mm polyg random, 8B: spar, very large, rextlz?	-	- 8B: spar edges meet	8B grain boundaries hard to distinguish
78MG9	G c. 2 sq F'42?	White, microxtln fst, pool dep?, large pores between growth layers, layers connected by tiny columns of calcite	4 cm	-	-	-	-	-	Too small and porous to have a thin section made,
78MG10	G c. 2 sq A'46	Curtained fst, tan microxtln	6 cm	20% clay around carb (10%)	10% ang- rd X1	1/2 mm long spar radially out from detrital grains	bone		Illuvial concretion? Unsuitable for dating
78MG11	New hall c. 2, sq H52	white-tan opaque fst, microxtln, fine lam	3-6 cm	5% clay	5% ang X0	large // lam, grain boundaries hard to distinguish	-	Clay concentrated on lam	
78MG12	G c.4? sq E48	grey-white microxtln stg orange lam (hiatus?) dark brown rind	10 cm	40% clay 10% carb	30% ang- rd X1	av. 1/5 mm polyg random	-	Clay concentrated on lam, lam have greater porosity	

SAMPLE	LOCATION	DESCRIPTION	THICKNESS	DETRITUS	POROSITY	CRYSTALS	BIOCLASTS	LAYERING	COMMENTS
79MG13	L c.3 sq B2	Brownish-grey microxtln fst with stems, stc, sand em- bedded in it	variable						
13A			3 cm	10% clay	25% ang X0	av ½ mm random	0	-	
13B			4 cm	30% clay	10% ang- rd, X1	av ½ mm polyg random	oolites ? coprolites?	-	
13C			3 cm	30% clay	40% rd X2	av ½ mm polyg random	coprolites?	-	10% of pores filled by 2° growths
13D			3 cm	25% clay 5% fspar	30% ang X0	av ½ mm polyg random	bone	sand on lam	
13E			4 cm	-	-	-	-	-	
79MG14	L c. 4 sq F7	white-tan opaque microxtln stg with very thin growth loose in lam soil	9 cm thick not tapered	<5% ?	15% ang X0	0.1 mm, polyg, random	-	changes in xtl orient	
79MG15	Balcony grotto, overlies bears	tan-brown macroxtln fst with stg with fine growth lam	7 cm thick	<5% ?	<5% ang X0	spar, 1/10 mm x 1/5 - 1 cm, //lam	-	spar edges meet at lam	
79MG16	G c. 2 sq D' 42	Honey-brown macroxtln stg darker near outer edges, white rim, finely lam	6 cm high	15% clay all on lam	<5% ang X0	av. 2 mm polyg, // lam	-	clay all concent- rated on lam	

SAMPLE	LOCATION	DESCRIPTION	THICKNESS	DETRITUS	POROSITY	CRYSTALS	BIOCLASTS	LAYERING	COMMENTS
79NG17	G c. 2 sq A44??	Fan microxtln fst with thin growth lam, areas of very porous texture	9 cm	10% clay	10% in dense, 50% in porous parts	av 1/5 mm polyg random	-	xtl orient changes, some clay concentrated on lam	
79NG18	Grand porche c. 10 sq ? West cut	Honey-brown fst with white growth lam, transparent, macroxtln, near present pool,	5 cm	5% clay	<5% ang X0	spar, 1 mm x 4 cm, // lam	-	all clay concen- trated on lam.	

ABBREVIATIONS:

L = Lartet	fst = flowstone	av = average	min = mineral	Connectedness of the Pores
G = Gaudry	stg = stalagmite	polyg = polygonal shaped crystals	diam = diameter	X0 = unconnected
dep = deposit	stc = stalactite	orient = orientation	pl sup = plancher supérieur	X1 = partially connected
2° = secondary	ang. = angular pore shape	rextlz = recrystallized	xtln = crystalline	X2 = connected
c. = couche	rd = rounded pores	// lam = oriented parallel to growth laminations		X3 = well connected
sq = square				X4 = a sponge-like porosity
lm = laminations				

amounts of detrital thorium, and ages  $\geq 350$  Ka were common, although roasting did improve the yields in some cases. Tables 6.60 to 6.68 give the dating results, while Figures 6.39 to 6.46 shows the samples, and Figure 6.47 shows the sampling localities.

#### 6.4.8.1 Abri Lartet

Layer 2 in Abri Lartet is represented by 78MG4, which gave low yields until it was roasted. The single date, however, is not likely to be correct, because the correction for detrital thorium was made using an initial ratio of 2.5. The uncorrected age was greater than 350 Ka, as was the corrected age for the normal ratio of 1.25.

In layer 3, several of the samples with excellent yields resulted in dates of  $\geq 350$  Ka. Although the parameters appear normal, these dates are much too old for Mousterian layers. The one date of  $82.2 \begin{matrix} + 14.3 \\ - 13.9 \end{matrix}$  Ka may be an accurate date for this layer, but the sample did contain detrital carbonate and bioclastic material. Unless this date can be confirmed by another date with good yields, this date is almost meaningless.

From layer 4, 79MG14 resulted in an age of  $123.5 \begin{matrix} + 24.5 \\ - 21.4 \end{matrix}$  Ka with good yields when roasted. Although one date is not sufficient to establish the age for any layer, especially in Montgaudier, if the age is accurate, this level is much older than expected.

In layer 6, two determinations for 79MG6 both resulted in dates of  $\geq 350$  Ka. The high detrital thorium concentrations make any meaningful dates on this level impossible to obtain.

Table 6.60

CORRELATION OF DATA FROM MONTGAUGIER L C. 2,  
USING SAMPLES 78MG4

SAMPLE	AGE (KA)	ERROR (KA)	YIELDS		TH-230	TH-230	U-234	(U-234)	CONCENTRATIONS	
			U-232 (%)	TH-228 (%)	U-234	TH-232	U-238	(U-238) 0	U-238 (PPM)	TH-232 (PPM)
78MG4-1	-		0.00	2.43	-	+ 2.0 - .9	-	-	-	.18
78MG4-2	-		0.00	3.06	-	+ 1.0 - .2	-	-	-	.32
78MG4-3	183.5±	+ 63.8 - 31.1	48.21	56.01	+ 1.078 - .074	+ 1.4 - .1	+ .733± - .046	+ .553± - .144	.20±	.35

‡ NOT INCLUDED IN THE AVERAGE DATE

\* THORIUM CORRECTION USED CALCULATED AT R = 25

Table 6.61

CORRELATION OF DATA FROM MONTGAUGIER L C. 3  
USING SAMPLES 78MG1, 78MG2, 78MG3, 78MG7, 79MG13

SAMPLE	AGE (KA)	ERROR (KA)	YIELDS		TH-230	TH-230	U-234	(U-234)	CONCENTRATIONS	
			U-232 (%)	TH-228 (%)	U-234	TH-232	U-238	(U-238) 0	U-238 (PPM)	TH-232 (PPM)
78MG1-1	82.2±	+ 14.3 - 13.2	15.78	20.70	+ .701 - .028	+ 2.4 - .1	+ .917± - .025	+ .835± - .028	.40±	.34
78MG2-1	87.0±	+ 79.9 - 58.9	4.33	7.31	+ .603 - .207	+ 8.9 - 14.0	+ 1.273± - .174	+ 1.348± - .354	.15±	.04
78MG2-3	-		0.00	4.94	-	+ 4.0 - 1.3	-	-	-	.07
78MG2-4	≥ 350.0±	(≥ 350.0±)	67.46	66.81	+ 1.027 - .023	+ 20.6 - .8	+ 1.012± - .024	-	.27±	.04
78MG7-1	≥ 350.0±	(≥ 350.0±)	33.16	20.14	+ 1.404 - .062	+ 16.1 - 1.8	+ .990± - .036	-	.19±	.05
78MG7-2	190.9±	+ 80.7 - 47.6	5.87	23.63	+ .846 - .081	+ 11.4 - 2.3	+ 1.013± - .103	+ 1.022± - .192	.16±	.04

‡ NOT INCLUDED IN THE AVERAGE DATE

\* THORIUM CORRECTION USED CALCULATED AT R = 1.25

‡ REPRESENTS THE YOUNGEST AGE POSSIBLE NOT THE LOWER ERROR LIMIT CALCULATED AT R = 1.25



CORRELATION OF DATA FROM MONTGAUDIER L.C.I  
 USING SAMPLES 78MG1, 78MG2, 78MG3, 78MG7, 79MG13

SAMPLE	AGE (KA)	ERROR (KA)	YIELDS		TH-230		U-234	(U-234)	CONCENTRATIONS	
			U-232 (%)	TH-228 (%)	U-234	TH-232	U-238	(U-238) 0	U-238 (PPM)	TH-232 (PPM)
78MG1-1	82.21+ - 13.2	+ 14.3 - 13.2	15.78	20.70	+ .701 - .028	+ 2.4 - .1	+ .917\$ - .025	+ .895\$ - .028	.40\$	.34
78MG2-1	87.0\$+ - 58.3	+ 79.9 - 58.3	4.33	7.31	+ .683 - .207	+ 8.9 - 14.0	+ 1.273\$ - .174	+ 1.348\$ - .304	.15\$	.04
78MG2-3	-	-	6.60	4.94	-	+ 4.0 - 1.3	-	-	-	.07
78MG2-4	≥ 350.0\$+ (≥ 350.0+)	(≥ 350.0+)	67.46	60.81	+ 1.027 - .023	+ 20.6 - .8	+ 1.012\$ - .024	-	.27\$	.04
78MG7-1	≥ 350.0\$+ (≥ 350.0+)	(≥ 350.0+)	33.16	20.14	+ 1.404 - .062	+ 16.1 - 1.8	+ .990\$ - .036	-	.19\$	.05
78MG7-2	190.9\$+ - 47.6	+ 80.7 - 47.6	5.87	23.63	+ .846 - .081	+ 11.4 - 2.3	+ 1.013\$ - .103	+ 1.022\$ - .192	.16\$	.04
79MG130-1	≥ 350.0\$+ (≥ 350.0+)	(≥ 350.0+)	33.46	9.60	+ 1.283 - .081	+ 2.4 - .2	+ 1.009\$ - .038	-	.23\$	.38

‡ NOT INCLUDED IN THE AVERAGE DATE

+ THORIUM CORRECTION USED CALCULATED AT R = 1.25

+ REPRESENTS THE YOUNGEST AGE POSSIBLE NOT THE LOWER ERROR LIMIT CALCULATED AT R = 1.25

+ REPRESENTS THE OLDEST AGE POSSIBLE, NOT THE UPPER ERROR

Table 6.62

CORRELATION OF DATA FROM MONTGAUDIER L C. 4,  
USING SAMPLES 79MG14

SAMPLE	AGE (KA)	ERROR (KA)	YIELDS		TH-230	TH-230	U-234	(U-234)	CONCENTRATIONS	
			U-232 (%)	TH-228 (%)	U-234	TH-232	U-238	(U-238)0	U-238 (PPM)	TH-232 (PPM)
79MG14-1	0.03+	0.0	8.65	5.08	6.876	12.2	.7208	.7208	.088	.10
					+ 1.552	+ 6.0	+ .178	+ .178		
79MG14-2	123.53+	24.5	40.85	52.60	.764	4.7	1.2258	1.3158	.088	.05
					+ .051	+ .6	+ .071	+ .122		

\* NOT INCLUDED IN THE AVERAGE DATE

+ THORIUM CORRECTION USED CALCULATED AT R = 1.25

↓ REPRESENTS THE YOUNGEST AGE POSSIBLE NOT THE LOWER ERROR LIMIT CALCULATED AT R = 1.25

\* REPRESENTS THE OLDEST AGE POSSIBLE, NOT THE UPPER ERROR

Table 6.63

CORRELATION OF DATA FROM MONTGAUDIER L C. 6,  
USING SAMPLES 78MG5, 78MG6,

SAMPLE	AGE (KA)	ERROR (KA)	YIELDS		TH-230	TH-230	U-234	(U-234)	CONCENTRATIONS	
			U-232 (%)	TH-228 (%)	U-234	TH-232	U-238	(U-238)0	U-238 (PPM)	TH-232 (PPM)
78MG5-1	-		0.00	25.41	-	+ 2.5 - .5	-	-	-	.06
78MG5-2	-		0.00	31.73	-	+ 2.9 - .5	-	-	-	.04
78MG5-3	≥ 350.03+	0.0+	17.48	24.05	+ .996 - .065	+ 1.3 - .1	+ .9998 - .061	-	.208	.49
78MG5-4	≥ 350.03+	47.6+	40.26	64.16	+ .951 - .087	+ 2.2 - .2	+ .8488 - .078	-	.088	.09

\* NOT INCLUDED IN THE AVERAGE DATE

+ THORIUM CORRECTION USED CALCULATED AT R = 1.25

↓ REPRESENTS THE YOUNGEST AGE POSSIBLE NOT THE LOWER ERROR LIMIT CALCULATED AT R = 1.25

\* REPRESENTS THE OLDEST AGE POSSIBLE, NOT THE UPPER ERROR

Table 6.64

CORRELATION OF DATA FROM MONTGALDIER G. C. 2,  
USING SAMPLES 78MG8, 78MG9, 78MG10, 79MG16, 79MG17

SAMPLE	AGE (KA)	ERROR (KA)	YIELDS		TH-230	TH-230	U-234	(U-234)	CONCENTRATIONS	
			U-232 (%)	TH-228 (%)	U-234	TH-232	U-238	(U-238) U	U-238 (PPM)	TH-232 (PPM)
78MG8-2	-		0.00	10.66	-	4.3 + 1.4	-	-	-	.04
78MG8A1-1	172.0§	+ 19.7 - 16.8	21.71	9.29	+ .811 + .036	+ 218.4 + 242.7	+ 1.112§ + .016	+ 1.172§ + .015	1.75§	.02
78MG8B-1	39.9 +	+ 3.9 - 3.8	39.92	57.33	+ .380 + .016	+ 4.7 + .4	+ 1.151 + .039	+ 1.119 + .002	.13	.04
78MG9-1	≥ 350.0§	+ *****	8.80	21.78	+ .969 + .054	+ 11.1 + 1.4	+ .992§ + .050	-	.23§	.06
78MG9-2	≥ 350.0§	(≥ 350.0+)	37.78	36.93	+ 1.155 + .059	+ 59.6 + 35.4	+ .985§ + .047	-	.24§	.01
78MG9-3	≥ 350.0§	(≥ 350.0+)	33.05	41.26	+ 1.049 + .066	+ 21.2 + 5.3	+ 1.041§ + .060	-	.23§	.04
79MG16-1	29.0	+ 13.0 - 9.2	11.72	8.28	+ .236 + .068	≥ 1000.0	+ 1.020 + .106	+ 1.115 + .005	.13	0.00
79MG16-2	47.4 +	+ 28.1 - 26.2	2.15	4.87	+ .370 + .105	+ 21.0 + 80.9	+ .985 + .248	+ 1.121 + .016	.15	.01
79MG16-3	22.4	+ 16.4 - 14.3	2.08	11.23	+ .147 + .115	≥ 1000.0	+ .861 + .500	+ 1.113 + .008	.27	0.00
79MG17-2	164.6§	(≥ 350.0+) - 41.6	44.72	1.78	+ .796 + .107	+ 92.3 + 79.8	+ 1.075§ + .014	+ 1.169§	1.47§	.04
-----										
AVERAGES	36.8	+ 7.7 - 7.1					+ 1.106 + .078	+ 1.119 + .087	.14	

§ NOT INCLUDED IN THE AVERAGE DATE

+ THORIUM CORRECTION USED CALCULATED AT R = 1.25

+ REPRESENTS THE YOUNGEST AGE POSSIBLE NOT THE LOWER ERROR LIMIT CALCULATED AT R = 1.25

+ REPRESENTS THE OLDEST AGE POSSIBLE, NOT THE UPPER ERROR

= THIS IS A COMBINATION DATE DERIVED FROM COMBINING THE U AND TH DATA FROM TWO DIFFERENT SUBSAMPLES, AND AS SUCH, SHOULD BE REGARDED AS QUESTIONABLE AT BEST.

Table 6.65

CORRELATION OF DATA FROM MONTGAUDIER G C. 4,  
USING SAMPLES 78MG12

SAMPLE	AGE (KA)	ERROR (KA)	YIELDS		TH-230	TH-230	U-234	(U-234)	CONCENTRATIONS	
			U-232 (%)	TH-228 (%)	U-234	TH-232	U-238	(U-238) <sup>§</sup>	U-238 (PPM)	TH-232 (PPM)
78MG12-1	160.2 <sup>‡</sup>	+ 202.6 - 68.1	13.11	3.35	+ .777 - .202	+ 41.4 - 162.9	+ 1.096 <sup>‡</sup> - .037	+ 1.055 <sup>‡</sup> - .056	.24 <sup>‡</sup>	.02
78MG12-2	≥ 350.0	+ - 304.3 <sup>‡</sup>	30.24	12.65	+ 1.020 - .065	+ 19.8 - 4.6	+ 1.000 - .048	-	.16	.03
78MG12-2 R	281.1	+ (≥ 350.0 <sup>‡</sup> ) - 66.1	30.29	12.65	+ .939 - .059	+ 19.8 - 4.6	+ 1.060 - .050	1.073	.17	.03
78MG12-3	≥ 350.0 <sup>‡</sup>	+ - 285.9 <sup>‡</sup>	27.61	8.60	+ 1.039 - .094	+ 18.2 - 6.2	+ 1.055 <sup>‡</sup> - .055	-	.18 <sup>‡</sup>	.03
78MG12-4	215.8	+ 30.0 - 23.9	46.74	59.85	+ .879 - .031	+ 17.1 - 2.0	+ 1.042 - .030	+ 1.065 - .011	.21	.03
-----										
AVERAGES	245.4	+ 33.0 - 33.4					+ 1.035 - .041	+ 1.097 - .092	.18	

§ NOT INCLUDED IN THE AVERAGE DATE

+ THORIUM CORRECTION USED CALCULATED AT R = 1.25

+ REPRESENTS THE YOUNGEST AGE POSSIBLE NOT THE LOWER ERROR LIMIT CALCULATED AT R = 1.25

Table 6.66

CORRELATION OF DATA FROM MONTGAUDIER NEW HALL  
USING SAMPLES 78MG11

SAMPLE	AGE (KA)	ERROR (KA)	YIELDS		TH-230	TH-230	U-234	(U-234)	CONCENTRATIONS	
			U-232 (%)	TH-228 (%)	U-234	TH-232	U-238	(U-238)0	U-238 (PPM)	TH-232 (PPM)
78MG11-1	-		0.00	42.85	-	+ 18.2 - 3.0	-	-	-	.03
78MG11-2	212.1	+ 48.1 - 33.1	36.16	37.44	+ .855 - .050	+ 28.2 - 12.1	+ .905 - .048	+ .967 - .010	.10	.01
78MG11-3	-		0.00	8.42	-	+ 8.5 - 1.7	-	-	-	.06
78MG11-4	220.8	+ 137.9 - 66.8	11.92	31.84	+ .890 - .082	+ 6.0 - .8	+ 1.091 - .118	+ .966 - .027	.22	.11
78MG11-5	≥ 350.0	+ (≥ 350.0) -	13.54	30.03	+ 1.099 - .081	+ 7.3 - .8	+ .969 - .067	-	.17	.08
78MG11-6	≥ 350.0	+ - 267.7	26.02	54.61	+ .984 - .056	+ 6.6 - .6	+ 1.045 - .058	-	.14	.07
-----										
AVERAGES	289.7	+ 39.7 - 89.3					+ .982 - .064	+ .904 - .116	.14	

‡ NOT INCLUDED IN THE AVERAGE DATE

+ THORIUM CORRECTION USED CALCULATED AT R = 1.25

+ REPRESENTS THE YOUNGEST AGE POSSIBLE NOT THE LOWER ERROR LIMIT CALCULATED AT R = 1.25

+ REPRESENTS THE OLDEST AGE POSSIBLE, NOT THE UPPER ERROR

Table 6.67

CORRELATION OF DATA FROM MONTGALDIER GMCTTC,  
USING SAMPLES 79MG15

SAMPLE	AGE (KA)	ERROR (KA)	YIELDS		TH-230	TH-230	U-234	(U-234)	CONCENTRATIONS	
			U-232 (%)	TH-228 (%)	U-234	TH-232	U-238	(U-238) 0	U-238 (PPM)	TH-232 (PPM)
79MG15-1	296.2	( $\geq 350.0$ ) - 36.6	50.40	59.49	+ .944 - .027	+ 42.4 - 4.1	+ 1.012 - .018	+ 1.073	.65	.05
79MG15-2	140.38	+ 139.0 - 65.4	2.11	1.89	+ .775 - .166	+ 5.8 - 1.4	+ .9778 - .067	+ 1.0478 - .025	1.078	.43
79MG15-3	129.2	+ 11.0 - 10.0	12.65	21.18	+ .700 - .030	$\geq 1000.0$	+ 1.111 - .027	+ 1.046 - .002	.73	0.00
-----										
AVERAGES	252.4	+ 43.2 - 29.6					+ 1.032 - .020	+ 1.055 - .046	.66	

! NOT INCLUDED IN THE AVERAGE DATE

\* THORIUM CORRECTION USED CALCULATED AT R = 1.25

+ REPRESENTS THE YOUNGEST AGE POSSIBLE NOT THE LOWER ERROR LIMIT CALCULATED AT R = 1.25

\* REPRESENTS THE OLDEST AGE POSSIBLE, NOT THE UPPER ERROR

Table 6.68

CORRELATION OF DATA FROM MONTGALDIER, GP  
USING SAMPLES 79MG18

SAMPLE	AGE (KA)	ERROR (KA)	YIELDS		TH-230	TH-230	U-234	(U-234)	CONCENTRATIONS	
			U-232 (%)	TH-228 (%)	U-234	TH-232	U-238	(U-238) 0	U-238 (PPM)	TH-232 (PPM)
79MG18A-1	86.1	+ 11.4 - 11.1	15.79	28.69	+ .592 - .039	+ 10.1 - 2.3	+ 1.125 - .072	+ 1.242 - .012	.01	.00
79MG18B-1	78.4	+ 9.7 - 9.1	24.10	58.69	+ .541 - .038	+ 19.6 - 4.8	+ 1.245 - .087	+ 1.276 - .010	.01	.00
-----										
AVERAGES	80.3	+ 10.4 - 9.8					+ 1.222 - .081	+ 1.278 - .110	.01	

! NOT INCLUDED IN THE AVERAGE DATE

\* THORIUM CORRECTION USED CALCULATED AT R = 1.25

Figure 6.40

78MG4, couche 2, Abri Lartet, Montgaudier,  
as seen from both sides (photo courtesy of  
H. Schwarcz).

Figure 6.40





Figure 6.41

Couche 6, Abri Lartet, Montgaudier:

- A. 78MG5
- B. 78MG6
- C. The sloping pavement forming couche 6.
- D. The trench in which samples 78MG1 through 78MG7, and 78MG13A-E were collected.

(photos courtesy of H. Schwarcz).





C



D

Figure 6.42

78MG11, New Hall, Abri Gaudry, Montgaudier  
(photos courtesy of H. Schwarcz).

Figure 6.43

78MG12, couche 4, Abri Gaudry, Montgaudier  
(photo courtesy of H. Schwarcz).

Figure 6.42  
Figure 6.43



Figure 6.44

79MG14, couche 4, Abri Lartet, Montgaudier.

Figure 6.45

79MG15, stalagmitic plancher, Cave Bear Alley,  
the Balcony, Montgaudier.

Figure 6-44  
Figure 6-45



Figure 6.46

Couche 2, Abri Gaudry, Montgaudier:

A. 79MG16

B. 79MG17





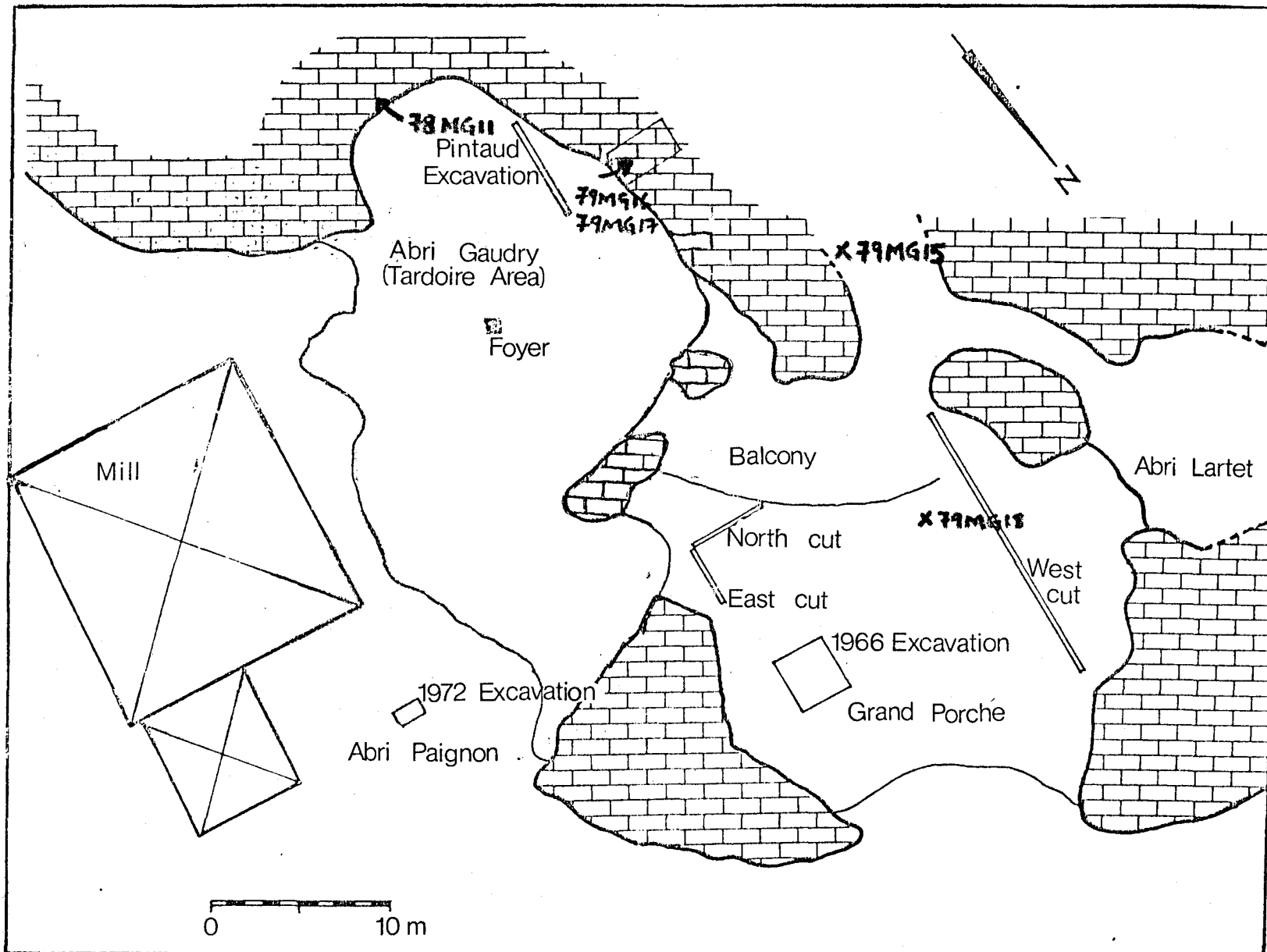
A



B

Figure 6.47

Sample locations within Montgaudier (adapted  
from Débenath, 1974).



## 6.4.8.2 Abri Gaudry

In Abri Gaudry, Magdalenian layers sandwich a plancher, layer 2, from which five samples were collected, 78MG8, 78MG9, 78MG10, 79MG16, and 79MG17. Ignoring the date for 78MG8A, which is an allochthonous eboulis encrusted by 78MG8B, all the dates agree well, averaging  $36.8 \begin{smallmatrix} + 7.7 \\ - 7.2 \end{smallmatrix}$  Ka, certainly somewhat older than the Wurm IV age expected for the Magdalenian. Although the youngest of the ages listed is the least certain because of the poor yields, the agreement of the four ages makes the date fairly reliable. The extremely high uranium concentrations for 78MG8A and 79MG17 suggest that 79MG17 contains redissolved calcite equivalent in age to that of 78MG8A ( $172.0 \begin{smallmatrix} + 19.7 \\ - 16.8 \end{smallmatrix}$  Ka). The date for 79MG17 corroborates this hypothesis.

78MG12, from layer 4, is significantly older than the expected age for a post-Aurignacian deposit. Ignoring the dates with poor yields, the average age is  $245.4 \begin{smallmatrix} + 35.0 \\ - 33.4 \end{smallmatrix}$  Ka. As these fragments of speleothem embedded in the layer could not be traced to a source, they may have spalled off the roof, in which case, the age would be valid.

## 6.4.8.3 New Hall

The tiny room opened by Duport in 1978 referred to as the New Hall contained a stalagmite 1 m tall, from the base of which was collected 78MG11. Dates for this sample range from 212 to  $\geq 350$  Ka. Because all the parameters are consistent, it is difficult to decide what the true age should be, but the average date  $289.7 \begin{smallmatrix} \geq 350.0 \\ - 89.3 \end{smallmatrix}$  Ka spans the entire range of the individual dates.

Therefore, the average date may be considered correct. Although Duport (personal communication) feels that the deposits in the New Hall should be equivalent to layer 2 in Abri Gaudry, such is obviously not the case. This date, however, does correspond to that of 78MG12 in layer 4.

#### 6.4.8.4 Cave Bear Alley

79MG15 resulted in two radically different ages for samples which are equivalent. The yields for both are good, while none of the parameters seems to be unusual. At present, there is no way to decide which age is correct. Therefore, the cave bears underneath, U. deningeri, are still undated.

#### 6.4.8.5 The Grand Porche

In the Grand Porche near the stairs which lead to the Balcony is a small pool which fills with water when the water table is high. In it was a stalagmitic plancher which may correspond to that seen in the west cut nearby, shown in Figure 6.47, between couches 5 and 7. Although the two dates represent the top and bottom, there is no significant difference in the ages for which the average is  $80.9 \pm \begin{matrix} 10.4 \\ 9.8 \end{matrix}$  Ka, confirming Debénath's (1974) belief that the sequence is an early Würm I deposit.

#### 6.4.9 Conclusions

The chronology of Montgaudier, as a whole, is largely unresolved. The few dates, mostly unconfirmed or problematic, do little to answer the questions which exist regarding the site.

During the Mindel or Mindel/Riss, roof deposition and sta-

stalagmite deposition occurred in both Abri Gaudry and the New Hall, averaging 245 and 290 Ka respectively. The large uncertainty in the latter average would allow these deposits to have been contemporaneous. They may also be contemporaneous with deposition of the stalagmitic plancher in Cave Bear Alley.

Two unconfirmed dates for stalagmitic deposition in Lartet are 82 Ka for layer 2 and 123 Ka for layer 4. If these dates are confirmed, then the sequence of Mousterian layers almost completely predates the Würm I glacial. These dates would explain the increasing intensity of the cryoturbation in this section upward as being a result of the cooling trend at the beginning of the Würm I. The great abundance of reindeer, however, is unusual for a Würm I deposit. Therefore, until the dates can be confirmed, the question is unanswered.

Deposition of stalagmite in the Grand Porche occurred at 80 Ka, near the end of the Riss/Würm. Although the relationship is uncertain, this may represent stalagmites comparable to those in the west cut. If this is true, it also implies that the Mousterian culture at Montgaudier is older than was previously thought, predating the beginning of the Würm I.

Although the Magdalenian has been well dated elsewhere by  $^{14}\text{C}$ , the dates obtained here are not consistent with that estimate. While the  $^{14}\text{C}$  dates suggest that the Magdalenian should have existed between 17 and 12 Ka (Smith, 1964), the U/Th dates for layer 2 in Abri Gaudry, suggest that deposition of that layer occurred at approximately 37 Ka. Yet, there is nothing to suggest that the

plancher was not in situ. A possible resolution to this conflict is that the lower culture has been incorrectly identified. Insufficient details for this industry, however, have been published to test this hypothesis. Pollen studies for this layer have shown a warm oscillation in between two cold periods. Deposition of the stalagmitic plancher probably corresponds to the warm oscillation.

### 6.5 Conclusions

Except for a period of stalagmitic deposition 80 Ka, and one at 38 Ka, Montgaudier appears to have experienced no stalagmitic deposition in common with Lachaise. In Lachaise, each major warm period was marked by stalagmitic deposition in at least one part of the cave. Montgaudier, on the other hand seems to have been very dry throughout much of its history. The deposition of speleothem at approximately 250 Ka may correspond to that of layer 53' in Lachaise, but until the date of the latter is confirmed, this is uncertain.

The Charente, however, appears to have experienced warmer wetter conditions during the periods 150 Ka, 120 to 70 Ka, 50 to 35 Ka, 20 Ka, and 10 Ka. The last three correspond to well dated interstadials, the Würm I/II and Würm III/IV, and the Holocene initial warming respectively.

Mousterian cultures in the Charente predate the Würm I, having evolved about 125 Ka BP, while the Neanderthals must have appeared in Europe prior to 150 Ka BP. This surprising because the Neanderthals are usually thought to have evolved at the same

time as the Mousterian industries first appear, the development of the new industry being contingent upon the increased brain capacity of the new hominids. Clearly, however, the Neanderthals were quite content with the Acheulian industries for several thousand years before they modified their tool culture.



## THE SITES IN THE DORDOGNE

Along the Dordogne River in southwestern France are located some of the most famous of the Paleolithic sites, as shown in Figure 7.1. Throughout the upper Pleistocene, hominids inhabited the local caves seasonally, leaving behind artefacts which today represent some of the most studied cultural remains, and some of the more controversial. Located along the Dordogne are two caves and one abri which have been dated by the U/Th method, Pech de l'Azé, Abri Vaufrey and Grotte Treize (also known as Grotte de l'Eglise). While the first has been extensively studied by Bordes, the second is only partially complete, with no faunal or pollen analyses yet completed. Both of these contain hominid cultural remains, but the third seems to have only served as a home for the cave bears.

## 7.1 Geography

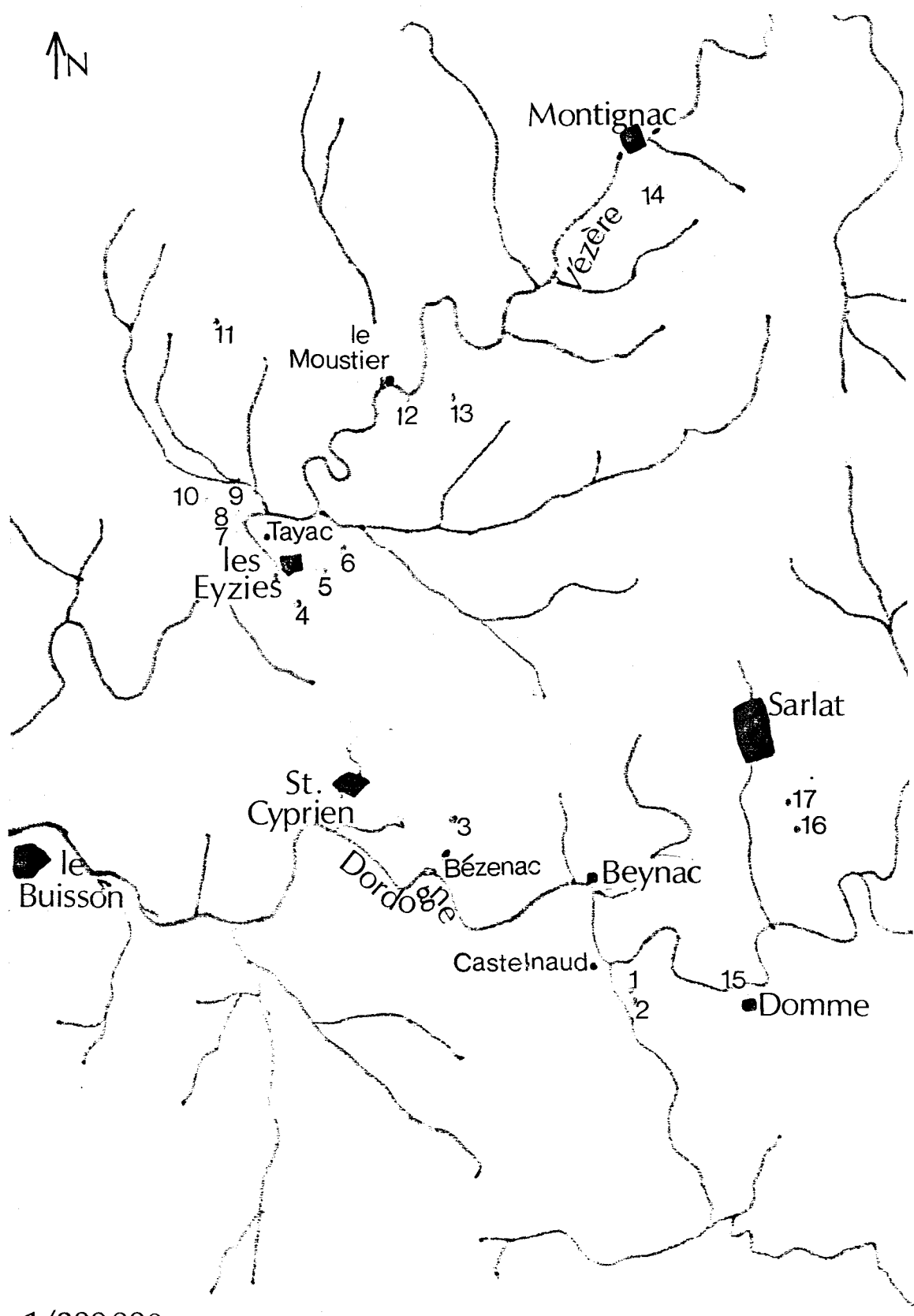
The French department of the Dordogne can be divided into several geographically distinct regions. Bordering the river near Bergerac are the Landais, a rolling region of alluvial plains and more elevated areas of Quaternary and Tertiary sediments, and the Bergeracois, an area of plateaus and small buttes with slight undulations in its Tertiary rocks. Further east, the Pays de Belvès et de Saint-Alvère is a heavily eroded karst region in the chalky Campanian calcites. The bluffs formed in this region by the river's

Figure 7.1

The Perigord, France.

Caves and archeological sites in the region:

1. Abri Vaufrey
2. Grotte Treize
3. Le Flageolet
4. La Mouthe
5. Font-de-Gaun
6. Combarelles
7. Grotte de Grand Roc
8. Laugerie, lower site
9. Laugerie, upper site
10. Carpe-Dien
11. Rouffignac
12. La Roque St. Christophe
13. Le Moustier
14. Lascaux
15. Combe-Grenal
16. Pech-de-l'Aze
17. Caminade



1/200,000

ersion can be seen especially well at les Cingles de Limeuil et de Trémolat. In the extreme east, the Périgord Noir or le Sarladais is a region of hills and valleys surrounded by cliffs, particularly noticeable near Beynac and les Eyzies, as shown in Figure 7.2.

The entire region is dominated by the Dordogne River, an armoured allogenic river, and its tributary, the Vézère. Diciduous and grassland species form the natural vegetation, which has been extensively removed for agriculture, especially in the river valley. Corn, tobacco, grapes, hay, and mixed cash crops are the major crops along with cattle, goats (raised mainly for cheese), and sheep. Rainfall averages 75 cm very little of which falls as snow. Winter temperatures seldom dip below 0°C, while summer temperatures average 25°C.

## 7.2 Geology

Within the southern Dordogne, most of the exposed strata consist of limestones of upper Mesozoic age, covered locally by red ferruginous clastics of the Tertiary and Quaternary (see Figure 7.3).

The fault system seen in the Charente (Chapter 6.2) continues into the western Dordogne trending NW-SE, with one major fault passing through St. Cyprien. From this major fault, a profusion of minor faults trend perpendicularly away from the main fault, forming weaknesses along which many small caves, including Abri Vaufrey, have formed.

Figure 7.2

The escarpments of the Dordogne:

- A. Cliffs formed in the Jurassic limestones,  
along the Céou River south of Beynac.
- B. The Upper Conician (Cretaceous) cliffs,  
along the Vézère 1 km east of les Eyzies



Along the axis of the St. Cyprien fault, Upper Jurassic strata are exposed as a window within the surrounding Cretaceous south of Beynac. These Upper Jurassic beds are formed of Callovian-Oxfordian reefs surrounded by massive lower Kimmeridgian limestones overlain by friable marls of the upper Kimmeridgian and fine-grained Portlandian limestones. At the end of the Jurassic, the seas covering Europe withdrew allowing karstic erosion to attack the Jurassic strata. This erosion ended with a local Cretaceous immersion.

The upper Cretaceous strata, which are the uppermost units in the stratigraphic column over half of the Perigord, consist of a transgressive bituminous shale overlain by massive limestones and marls of the Cenomanian, overlain by Turonian crystalline limestones with rudists and ooliths, followed by the Coniacian glauconitic marls. The upper Coniacian bioclastic limestones form the cliffs along the Vezere near les Eyzies (Figure 7.2B). The Santonian and Campanian microcrystalline glauconitic limestones with some interbedded shales, underly the final Cretaceous strata, the Maestrichtian yellow limestones (Laville, 1975).

When the Cretaceous seas retreated to the west, the Perigord was again subject to karstic erosion in the Tertiary. Originating in the Massif Central to the north, iron-rich Siderolithic sands and clays were deposited in the Dordogne Valley. At the beginning of the Eocene, the Pyrenees orogeny ended following which the Perigord Sand was deposited as a part of the clastic wedge. The final result of this history is a group of intercalated Upper

Mesozoic beds of compact, resistant, massive limestones and karstically eroded, porous, soft marls and bioclastic limestones in which caves and abris abound.

### 7.3 Pech de l'Azé

Pech de l'Azé, a complex of caves and abris known since the nineteenth century, has been extensively studied by François Bordes. In addition to a child's skull, the sites contain several Mousterian cultural layers, a few Acheulian layers, and travertine deposits within its many stratigraphic levels, which have been paleoclimatologically analyzed in minute detail. All of the data which follows regarding the history, sedimentology, paleoclimates and archeology is taken from Bordes (1972, 1976) and Laville (1975).

#### 7.3.1 The History of Excavation

Pech de l'Azé has been known to the locals in the Dordogne having been partially leveled in order to be used as a sheep pen in medieval times. Probably many of the deposits in Pech I were destroyed then. In 1816 and 1818, François Jouannet described the cave as being of the greatest antiquity. In 1828, Abbé Audierne described the interior of Pech I including the cemented bone breccias on the walls. Edouard Lartet and H. Christy found flints in 1864, which they thought were comparable to those in Combe-Grenal and le Moustier.

In 1906, the first proper excavation at Pech I was dug by by Louis Capitan and Denis Peyrony. In addition to finding an ar-



cheological layer, they found a Neanderthal child's skull. Subsequently, the 1906 collection was lost. In 1929-30, Professor Raymond Vaufrey (for whom Abri Vaufrey was named) excavated at Pech I, publishing a preliminary report on the work in 1933. Finally, in 1948-53, Bordes excavated both Pech I and II, the latter of which had not been disturbed, and returned in 1967-69 with several specialists, H. Laville (sedimentology), F. Prat (paleontology), and M.-M. Paquereau (palynology). Excavation at Pech IV began recently.

### 7.3.2 General Description

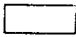


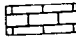



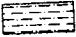


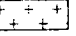
Located about 5 km east of Sarlat (see Figure 7.1), on the road from Sarlat to Gourdon, Pech de l'Azé Cave is located in the Coniacian (Cretaceous) strata of the Sarladais region. The south flank of the hill in which the cave is located is a dry valley which joins a tributary of the Dordogne. About 50 m above the valley floor are the openings to the main cave: Pech I, the more southerly, opens to the southeast, while Pech II faces southwest. Some 20 m north of Pech II, a small grotto, Pech III, opens to the southwest. This cave may be a diverticule of the main cave. Finally, Pech IV is located 100 metres south of Pech I. Figure 7.4 shows the main cave openings, Pech I and II.

### 7.3.3 Stratigraphy

Pech III was filled by the backdirt from the 1953 excavations, while the sedimentology of Pech IV has not been completed. Therefore, the sedimentology of Pech I and II only can be given in detail. Figure 7.5 shows the stratigraphy of Pech IV.

Figure 7.3

Geology of the Dordogne:

-  Quarternary  
(alluvial terraces: muds, silts, and sands)
-  Tertiary  
(lacustrine or marine: limestones and molasses)
-  Tertiary  
(continental: muds, sands, and gravels)
-  Upper Cretaceous  
(limestones, silty limestones)
-  Upper Jurassic  
(oolitic limestones, silty limestones, marls, biogenic limestones)
-  Middle Jurassic  
(limestones)
-  Lower Jurassic (Liassic)  
(marls, limestones, siltstones)
-  Permo-Triassic  
(shales, siltstones)
-  Silurian or unmetamorphosed crystalline rocks
-  Metamorphic rocks  
(gneiss, schist, myloites)
-  Granites

(adapted from Laville, 1975)



Figure 7.4

Plan view of Pech de l'Aze I and II

(after Laville, 1975)

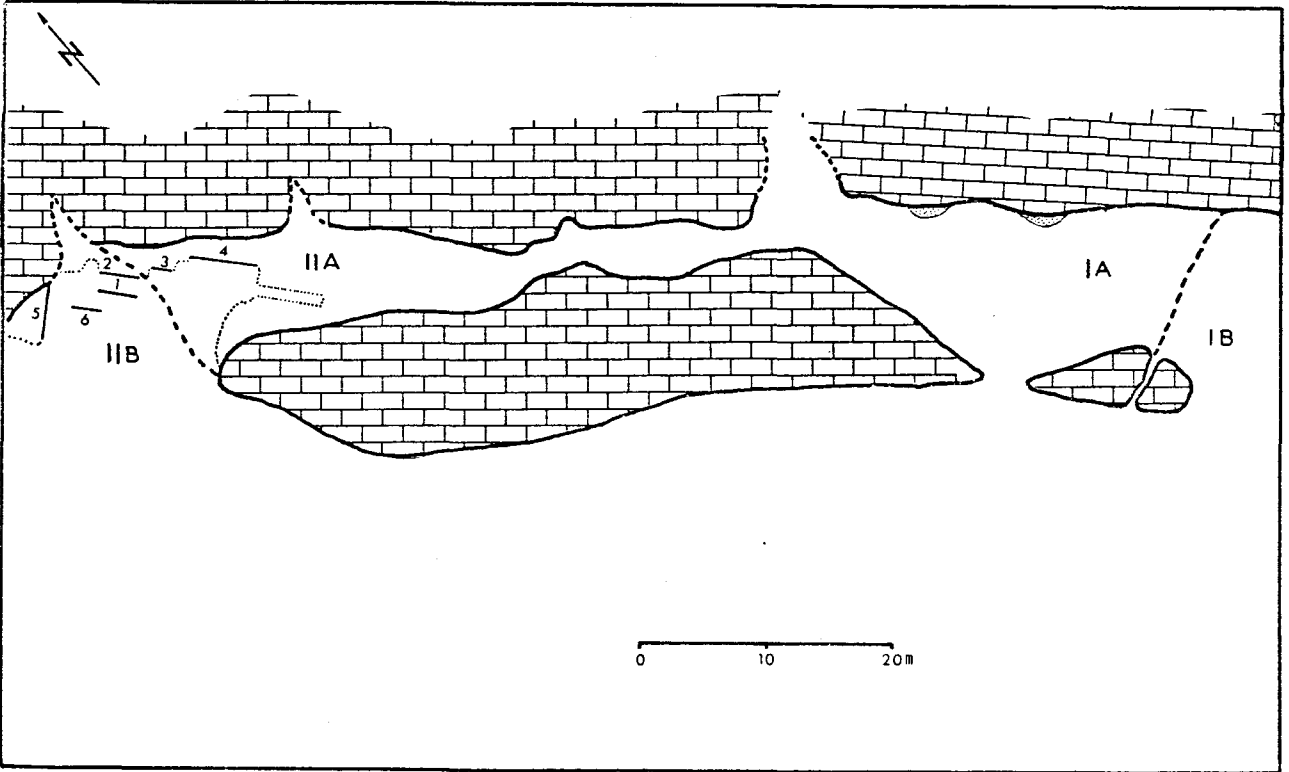


Figure 7.5

The stratigraphy in Pech de l'Azé IV:

- A. The top portion of the cut
- B. To the right of A. Note the difference in colour of the two adjacent sections. The darker one has weathered for one winter.
- C. Directly below A.

(photo courtesy of H.P. Schwarcz)

Figure 7.5



A



B



C

## 7.3.3.1 Pech de l'Azé I

The stratigraphy of Pech I, as can be seen in Figure 7.6, is complex, with a portion of the sediments having apparently slumped, perhaps due to solifluction, or the formation of a sink beneath the southern part of the cut. The strata are, from top:

1. Light yellow sand with small éboulis at the top; sterile but stratified.
2. Pavement of flat limestone slabs, perhaps natural, perhaps man-made.
3. Yellow sand with lenses of ashes; Mousterian of Acheulian Tradition A.
4. Black ashes from 1 to 25 cm thick hearths somewhat consolidated by calcite concretions, directly covered by large éboulis; Mousterian of Acheulian Tradition A found only behind a wall of calcite blocks about 1 m high.
5. Eboulis mixed with yellow sand; some bones and tools Mousterian of Acheulian Tradition A-B transitional
- A. Reddish soil, perhaps water-laid; bones and Mousterian of Acheulian Tradition; found only in the southern part of the cut.
6. (also B) Ash layer with hearths, and small éboulis; Mousterian of Acheulian Tradition B.
7. (also C) Eboulis from roof collapse with traces of fire; Mousterian of Acheulian Tradition B (final), and



Figure 7.6

The stratigraphic section in Pech de l'Azé I

A. The cut along AA'(noted in 7.5B)

B. A plan of the excavations

Dotted: Vaufrey's excavations

Cross-hatched: Bordes' excavations

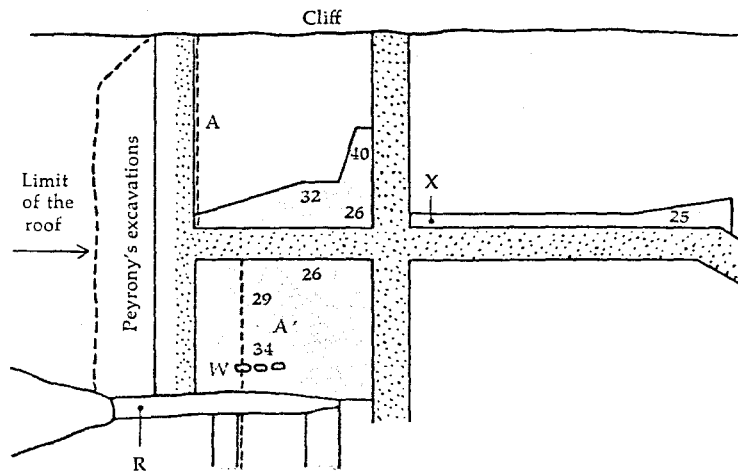
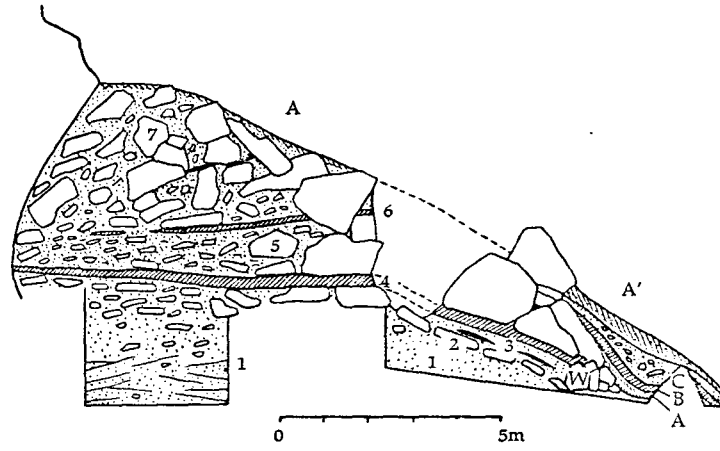
AA': The line of the section

W: Cave wall

R: Rocky ridge continuing the cave wall

X: Spot with many hand axes flakes

(after Bordes, 1972)



bones.

8. Modern soil with tools in secondary positions.

Above the Mousterian levels in the back of the cave are 16 levels of silty sands with numerous éboulis and a few tools of apparently Mousterian or Acheulian tradition.

Also within Pech I are two suspended breccias, shown in Figure 7.6, which contain both travertine and tools. Both breccias are calcite cemented yellow unweathered sand with no traces of fire nor internal bedding indicators (Bordes, 1972). Breccia 1, the closer to the entrance (see Figure 7.4), may be comparable to layer 4B in Pech II, while Breccia 2 may be equivalent to 4C2. Both breccias along with the two isolated blocks of breccia analyzed contained tools and bones and some pollen.

7.3.3.2 Pech de l'Aze II

The detailed stratigraphy of Pech II is given in Table 7.1 along with the palynology, faunal analysis, archeology, and paleoclimatic interpretation. Figure 7.7 shows both the section in detail and the overview of Pech II.

7.3.3.3 Pech de l'Aze IV

The stratigraphy in Pech IV has not yet completely described. What is known follows, from the top:

- A1. Vegetation, roots, with one flint, pottery (Iron Age?).
- A2. Sterile brown sand with éboulis.
- B, C. Sterile brown sand with traces of Mousterian.
- D, E. Red sand with éboulis
- F. Rich in éboulis, subdivided into four sublayers, Mous-

Figure 7.7

Pech de l'Azé I:

A. The stratigraphic section

B. The opening to Pech II

(courtesy of H. Schwarcz)

Figure 7-7



A



B

Table 7.1 The Strata of Pech II: Sedimentology,  
Archeology, Palynology, And Faunal Analysis

LAYER	THICKNESS	"AGE"	CLIMATE	SEDIMENTOLOGY
1	1.0 m	Würm I		Red sand
2A	0.3 m	Würm I	Warmer and more humid than in 2D	Yellow sand with limestone fragments
2B	0.2 m	Würm I	Warmer and more humid than in 2D	Yellow sand with limestone fragments
2C	0.25 m	Würm I	Warmer and more humid than in 2D	Yellow sand with limestone fragments
2D	0.15 m	Würm I	Climatic minimum: cold and dry	Yellow sandy clay with rare limestone fragments
2E	0.35 m	Würm I	Colder and drier than 2F	Yellow soils with numerous sharp-edged limestone fragments
2F	0.30 m	Würm I	Colder and drier than 2G	Yellow clay-like sand with small limestone fragments
2G1	0.25 m	Würm I	Temperate but damp	Yellow soil with scattered limestone fragments
2G2	0.10 m	Würm I	Climatic minimum: cold	Yellow soil with numerous small rounded $\epsilon$ boulis
2G3	0.10 m	Würm I	Warmer and damper than in 3	Yellow soil with numerous small $\epsilon$ boulis
3	0.3 m	Würm I	Cold and damp at first, becoming drier upward	Light brown sandy clay
4A1	0.10 m	Würm I	Becoming colder upward, damp	Reddish brown sandy clay with rare limestone fragments, soliflucted
4A2	0.10 m	Würm I	Climatic optimum	Reddish brown sandy clay with rare limestone fragments
4B	0.10 m	Würm I	Mild and fairly humid	Reddish brown sandy clay

FAUNA	FLORA	ARCHAEOLOGY
Too poor to determine		Undetermined
Red deer*		Mousterian (Quina ?) < 50 artefacts
Red deer*		Mousterian (Quina ?) < 50 artefacts
Red deer*		Mousterian (Quina ?) < 50 artefacts
Too poor to determine	Steppic grasses, no deciduous trees	Mousterian (Quina ?) < 50 artefacts
Reindeer* bovids	Steppic grasses 10% trees	Mousterian (Quina ?) < 50 artefacts
Too poor to determine	Grasses, 12% trees	Mousterian (Quina ?) < 50 artefacts
Red deer, roe deer, wild boar, reindeer, ibex	Grasses, hazel, oak, 33% trees	Quina Mousterian
Red deer, roe deer wild boar, some reindeer, ibex	Grasses, 10% trees	Quina Mousterian
Red deer; bovids; reindeer*	Grasses, pine, hazel, birch, alder, willow, some rare elms, linden, beech, 23% trees	Quina Mousterian
Wild boar; red deer; more reindeer, ibex than 4A1	Willows, birch, alders, hazel in lower 3, dis- appear upward as prairie grasses and steppes appear, 17 up to 8% trees	Typical Mousterian 1,261 artefacts
As in 4A2 but with more reindeer	Progressively fewer trees upward, hazel, pine willow, birch reappear	Typical Mousterian 179 artefacts
Wild boar, ibex, red deer, reindeer, hyena, cave bear	Oak, birch, hornbeam, maple shrubs, ferns, 57% trees	Typical Mousterian 337 artefacts
Red deer (59/28%), horses (29/24%), bovids (7/12), ibex, roe deer, reindeer, badger, wolf, Merck's rhinoceros	Hazel, oak, alder, 50% trees	Denticulate Mousterian 6,039 artefacts Lots of traces of fire

Table 7.1 (continued)

LAYER	THICKNESS	"AGE"	CLIMATE	SEDIMENTOLOGY
4C1	0-0.05 m	Würm I	Mild	Red soil
4C2	0.05-0.10 m	Würm I	Mild but variable	Alternation of red clay-like sands with brown clay
4D	0.20 m	Würm I	Warmer and damper than 5	Yellow soil with angular limestone fragments, upper portion cryoturbated polygonal soil with rounded limestone fragments
5	0.75 m	Würm I	Cold and humid but seasonal becoming warmer and drier up- ward	Large limestone blocks from debris fall and roof collapse
X	0.20 m	Riss III	Very cold and dry, drier at top	Weathered red sandy soil
6	0-0.2 m	Riss II	Colder and drier than in 7	Weathered reddish sandy soil with fragments of stalactites, calcareous éboullis
7A	0-0.3 m	Riss II	Warmer than in 7B but very humid	Yellowish sandy silt with abundant ferruginous fragments
7B	0.4-0.6 m	Riss II	Cold but humid	Yellow sandy silt with abundant ferruginous fragments
7C	0.1-0.2 m	Riss II	A bit warmer than in 7B, humid	Yellow sandy silt with some ferruginous fragments, cryoturbated
8E1	0.10 m	Riss I/II (start)	Warmer and more humid than 8E2	Reddish brown silt with rare éboullis
8E2	0.0 m	Riss I	Cold but humid	Reddish brown sandy silt with abundant éboullis
9	0.15 m	Riss I	Cold and dry	Light brown sand with rounded éboullis, often calcite cemented, heavily disturbed by cryoturbation 3/or running water
10	5.80 m	Mindel- Riss (?)	Impossible to determine	Rocky sand



FAUNA--	FLORA	ARCHAEOLOGY
Sterile	Undetermined	Sterile
Red deer (73/?) <sup>†</sup> , horses (10/?), bovids (8/?), roe deer, chamois, fox, rabbit, wolves	Fine, willow, birch, alder, hazel, trees rise to 43% upward	Typical Mousterian 2,638 artefacts Much evidence of fire
Rabbit; red deer; horses, bovids, rhinoceros, chamois, 1 reindeer bone	Pine, some alder, birch, higher in the layer 5-10" trees	Typical Mousterian ? Levallois technique present
Almost sterile	Steppic grasses with some pine	Almost sterile
Almost sterile	Steppic grasses with rare pines	Almost sterile
As in ?	Prairie grasses, some pine, hazel, birch, alder, willow, 10" trees	Acheulian (?) very poor
Horses; red deer; roe deer; ibex badger, rabbits, wolves	Prairie grasses, hazel, alder, willow, beech, rare elm, oak, linden	(?) very few flakes, some Levallois technique
Red deer; roe deer; bovids; boar, horses, wolves, hobcat, Merck's rhinoceros, fox, rabbit, cave bear ( <u>Deningeri spelaeus</u> )	Pine, hazel, willow, birch, firs, spruce, cedar, prairie grasses	Acheulian (Southern ?) 167 artefacts
Red deer; roe deer; horses; bovids, cave bear, boar, Merck's rhinoceros, hyena, panther	Pine, birch, hazel, alder, willow, grasses 25" trees	Acheulian (Southern ?) 321 artefacts
Red deer; bovids; horses; roe deer, primitive cave bear, Merck's rhinoceros, wolves, badger, rabbits	Pine, juniper, some birch, rare hazel, spruce, balsam, grasses, 12" trees	Acheulian (Southern ?) (with 822 560 artefacts) 1 engraved bone
As in 8B1	Pine, juniper, birch, firs, grasses, 50 trees	As in 8B1
Red deer; bovids; roe deer, <u>Megaceras</u> (Irish giant elk), horses, wolves, rabbit, Merck's rhinoceros, 1 elephant bone ( <u>Elephas antiquus?</u> )	Steppic grasses, few pines, < 50 trees <u>Lycopodium</u>	Acheulian (Abbevillian ?) 330 artefacts
Sterile	"Archaic flora"	Sterile

(adapted from Bordes, 1972; Laville, 1973)

terian of Acheulian Tradition.

Beneath layer F4 was a gully which probably was formed in the Wurm I/II.

- G. Mousterian artefacts.
- H. Sand with Mousterian artefacts.
- I1. Sand with Typical Mousterian artefacts.
- I2. Sand rich in Eboulis with Typical Mousterian artefacts.
- J1. Reddish-brown sand with large éboulis, Mousterian.
- J2. Rounded éboulis, cryoturbated. Mousterian (Typical?).
- J3a. Red porous sand with rare éboulis, Asinipodian.
- J3b. As in J3a, but more grey.
- J3c. As in J3a, but grey in colour.
- K. Large éboulis.
- X. Dark brown sand with Typical Mousterian artefacts.
- Y. Red sand with Typical Mousterian artefacts.
- Z1. Sand with Typical Mousterian artefacts.
- Z2. Granules.
- W. Limestone basement.

#### 7.3.4 Archeology

As noted above the archeology for Pech II is summarized in Table 7.1, but will be discussed in more detail below. For Pech IV, no final results have been published.

##### 7.3.4.1 Pech de l'Azé I

As noted above, layer 1 and 2 were sterile. Layer 3 is essentially the same as layer 4 which is described in detail

apparently found just under the porch of Pêche I near the wall. At present, there are several possibilities for the actual level in which it was located. From Peyrony's description, it was probably somewhere in the upper layers, 5 to 7, because these are transitional Mousterian-Upper Paleolithic, while the Acheulian which Peyrony claimed lay below the level with the skull could be **layer 4, Mousterian of Acheulian Tradition**. The fauna Peyrony describes, however, seems more similar to Pech II, especially **layer 2**, but unlike anything in Pech I. A fluorine test shows the skull to be about ten times richer in fluorine than the bones in **layers 5 through 7**. Therefore, the skull may be from other deposits in Pech I which have not survived since 1909.

### 7.3.6 Paleoenvironments

Because it is an abri, Pech de l'Azé was constantly changing during the deposition of the sediments. As discussed before, an abri gradually extends further into the cliff, but simultaneously, the roof will collapse, resulting in a wedge of deposits (Figure 2.5).

According to the paleoclimatological data listed in Table 7.1, Pech II appears to contain deposits which are older than any found in Pech I. While the former sediments are relatively dated from the late Mindel/Riss (or early Riss I) until the Würm I, the latter apparently are the result of deposition in the Würm II, although none of the layers contain many faunal remains, excepting reindeer. Pollen studies of layers 4 and 5 show both to have been deposited in a cold climate. The breccias, however, seem to have

Figure 7.13

The history of Pech de l'Azé I and II:

- A. After the Riss/Wurm, a soil developed on top of the Riss deposits (1).
- B. After the Wurm I, Wurm I sediments (2) are deposited over the interglacial soil.
- C. Water entering the cave via overhead cracks in the Wurm I/II removes most of the Pech I sediments, except the breccias. Some sediments in Pech II are partially removed, or disturbed, as are the sediments in the passage connecting the two caves.
- D. By the end of the Wurm II, new Wurm II sediments (3) have been deposited in Pech I.

(after Bordes, 1972)

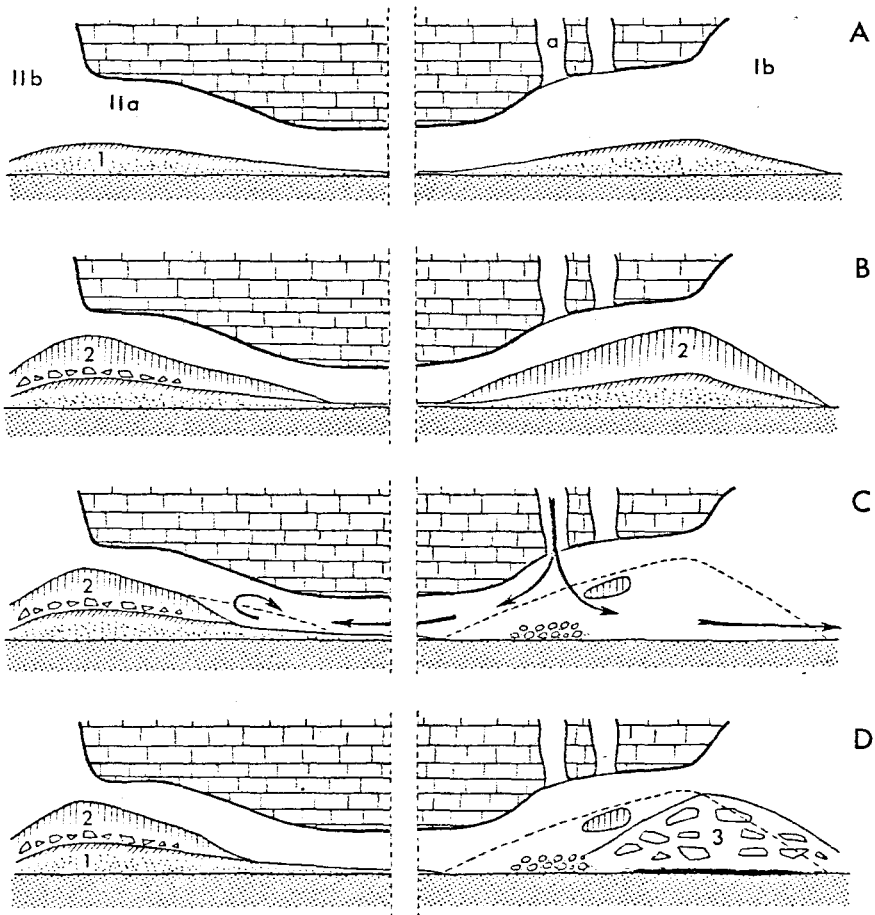
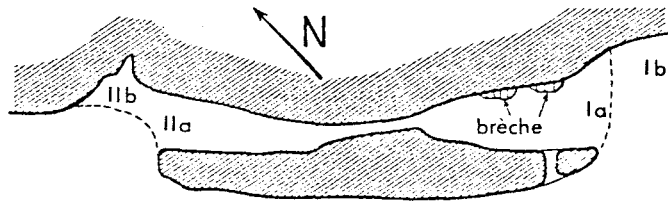


Table 7.29 Sample Descriptions from Pech de l'Azé

SAMPLE	LOCATION	DESCRIPTION	THICKNESS	DETRITUS	POROSITY	CRYSTALS	BIOCLASTS	LAYERING	COMMENTS
77PA1	P IV, below A	Calcite-cemented brown sand with flints, charcoal, bone	4 cm	-	-	-	Bone	-	No dates attempted.
77PA2	P IV, moved	Fragments of stg crust, fell into site from where?	-	-	-	-	-	-	
77FA 3	P IV	Bone fragments							No dates possible.
77PA4	P I, outer breccia	Opaque orangy-white microxtln fst with red sand lam, much loose material	5-6 cm	variable 10-40% clay 10% sand	variable 5-30% ang XO	variable ½ mm - ½ cm polyg, random	-	More clay, sand on lam, xtls smaller on lam	
77PA5	same as PA4	White opaque fst with sand on lam	5 cm	10% clay 5% sand	40% ang X1	spar, ½ x 2 mm, // lam	-	lam have more clay, pores	
77PA6	same as PA4	Transparent macroxtln white fst, pool deposit	2 cm	-	-	-	-	-	
77PA7	P I, inner breccia	White translucent macroxtln fst (stg boss), very thinly lam, 2 or 3 growth hiati	? loose pieces	-	-	-	-	-	
77FA8	same as PA7	White-yellow transparent macroxtln fst (stg boss) with orange lam	6 cm	-	-	-	-	-	

SAMPLE	LOCATION	DESCRIPTION	THICKNESS	DETRITUS	POROSITY	CRYSTALS	BIOCLASTS	LAYERING	COMMENTS
77PA9	P I, base inner breccia	Orangy-white transparent macroxtln fst with red silt lam	8 cm	-	-	up to 2 cm long spars	-	-	
77PA10	P I, top inner breccia	Orange-white microxtln fst with orange silt lam	5 cm	40-50% clay	30% ang X0	½ mm polyg random	bone	More clay on lam, less carb eboulis on lam	Unsuitable for dating.
77PA11	P I, inner breccia?	White transparent macroxtln stg with faint lam	4 cm	-	-	-	-	-	
77PA12	P II, B2 block in c. 4D	White opaque macroxtln stc? with red sand in pockets no lam visible	broken 3 cm??	40% clay	10% ang X0	1/10 mm polyg random	-	Clay concen- trated on lam	
77PA13	P II, c. 3	Orangy-beige microxtln fst between calcite cemented sand (orange), fst has 2 or 3 lam, some bone at bottom	2 pieces 0.5, 2.5 cm	35% sand	20% ang X0; in sand 75% X3	½ mm polyg random, some (5%) spar // lam	-	More clay and pores on lam	
77PA14A	P II, B1 block in c. 4?	Orange-white microxtln fst with orange silt lam 2 mm apart	2 cm	10% clay	40% ang X1	½ mm polyg random		More clay and pores on lam	
77PA14B	same as PA14A	Grey microxtln fst with con- voluted lam and vugs of red silt	5 cm	25-30% clay & silt	50% ang X4	1/10 mm polyg random	-	More clay and pores on lam	

SAMPLE	LOCATION	DESCRIPTION	THICKNESS	DETRITUS	POROSITY	CRYSTALS	BIOCLASTS	LAYERING	COMMENTS
77PA14C	same as PA14A	Chalky white fst with faint lam	8 cm	10% clay & sand	variable X2 10-30% ang	½ mm - 1 mm, random, polyg	-	Porosity greater on lam	
77PA14D	same as PA14A	Brown microxtln fst with 2 lam full of red silt	2-4 cm	10% clay & sand	25% ang X0	½ mm polyg, random	-	More detritus pores on lam	
77PA15	P II, c. 8 (?)	Orange-white microxtln fst with thin lam, porous	1-1.5 cm	-	-	-	-	-	
77PA16	P II, c. 6 (?)	White macroxtln fst convoluted, faintly lam, surrounded by calcite-cemented red sand	fst: 4-6 cm; sand: av 10 cm						
16A	fst			5% clay	5% ang	spar, ½ mm x X0 1 mm, // lam	-	Clay concentrated on lam	
16B	fst			30% sand (qtz & carb)	25% ang X0	spar, ½ mm x 1 mm // lam	-	Detritus concentrated on lam	
16A&B	cemented sand			10% clay 50% qtz 5% carb	high	-	-	-	
77PA17	P II, c 6 ?	Orange-brown fst with thin lam	1.5 cm	-	-	-	-	-	Too little to date
77PA18	same as PA17	same as PA17		-	-	-	-	-	Too little to date



SAMPLE	LOCATION	DESCRIPTION	THICKNESS	DETRITUS	POROSITY	CRYSTALS	BIOCLASTS	LAYERING	COMMENTS
78PA19	P II, c. 8 (?)	White-tan microxtln fst with thin lam, some silt on lam	6 cm	0	15% ang X0	½ mm polyg random	-	Slightly smal- ler xtlns on lam	
78PA20	P II, c. 6 (?)	White opaque microxtln fst with yellow sand lam	4 cm	45%	20% ang X1	½ mm polyg random	-	Greater poro- sity on lam	

ABBREVIATIONS:

P = Pech	fst = flowstone	av = average	min = mineral	Connectiveness of the Pores
dep = deposit	stg = stalagmite	polyg = polygonal shaped crystals	diam = diameter	X0 = unconnected
2° = secondary	stc = stalactite	orient=orientation	pl sup = plancher supérieur	X1 = partially connected
c. = couche	ang. = angular pore shape	rextlz = recrystallized	xtln = crystalline	X2 = connected
sq = square	rd = rounded pores	// lam = oriented parallel to growth laminations		X3 = well connected
lm = laminations				X4 = a sponge-like porosity

Figure 7.14

77PA1, calcite cemented sand in the Würm  
layers in Pech de l'Aze IV (photo courtesy  
of H. Schwarcz)

Figure 7.14



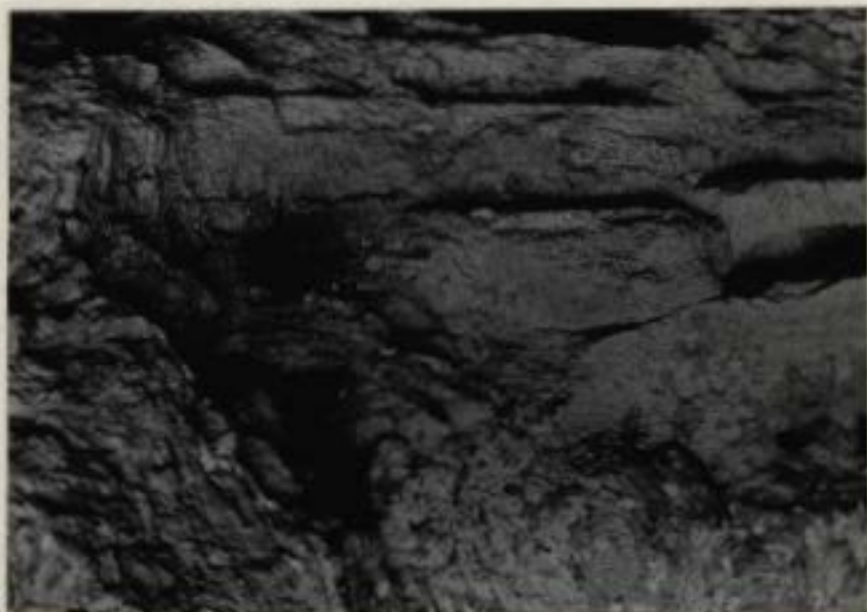
Figure 7.15

The outer breccia mass, Pech de l'Azé I:

- A. The breccia mass (I) suspended from the roof.
- B. Detail of the mass.
- C. The cavity from which 77PA4, and 77PA5 come.
- D. More detail of the cavity.

(photos courtesy of H. Schwarcz)





C



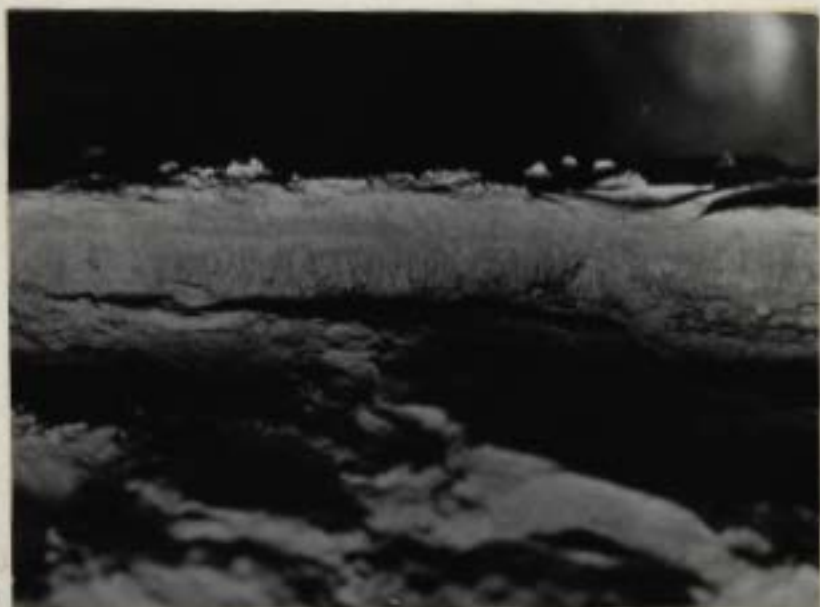
D

Figure 7.16

The inner breccia mass, Pech de l'Azé I.

- A. 77PA9, a flowstone layer in the mass.
- B. The denser-looking mass is the boss from which 77PA7, 77PA8, and 77PA11 came. 77PA10 came from the surrounding dirtier material.

(photos courtesy of H. Schwarcz)



A



B



Figure 7.17

Couches 3 and 4, Pech de l'Azé II, site of  
77PA12 and 77PA13 (photo courtesy of H.  
Schwarcz).

Figure 7-17



Figure 7.18

77PA14, couche 4, Pech de l'Azé II:

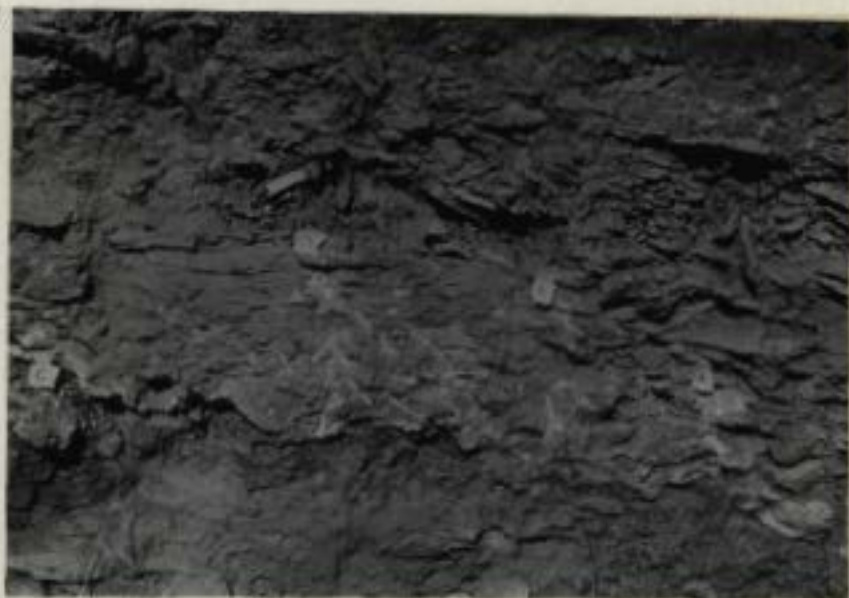
A. Close-up of the sample in situ.

B. Relative positions of all the subsamples.

(photos courtesy of H. Schwarcz)



A



B

Figure 7.19

77PA15, couche 9, Pech de l'Azé II:

The actual location of the sample was around  
the corner from the picture (photo courtesy of  
H. Schwarcz).

Figure 719



Figure 7.20

77PA16, Pech de l'Azé II:

- A. Location of 77PA16 in couche 6.
- B. The section.
- C. The sample as it appeared before shipping.
- D. Obverse of C.

(photos courtesy of H. Schwarcz)

Figure 7.20



A

B







C



D

in Tables 7.2 through 7.8. Both are Mousterian of Acheulian Tradition A. In both layers A and 5, the industry is the transitional form between Mousterian of Acheulian Tradition types A and B. Layers 5 through 7 show an evolution of the tradition, as the Levallois technique becomes less important, but the incidence of blades increases, a pattern which occurs at the Mousterian-Upper Paleolithic boundary. Concomitant with this change is an increase in the numbers of characteristic Upper Paleolithic tool types, and backed knives, some of which are proto-Chatelperron types (early Perigordian types). Figure 7.8 shows some of the tools found in Pech I.

The breccias contain what appears to be Denticulate Mousterian, but none contain sufficient tools to be certain. Found on top of Breccia 1, one burin represents the only Upper Paleolithic in Pech I.

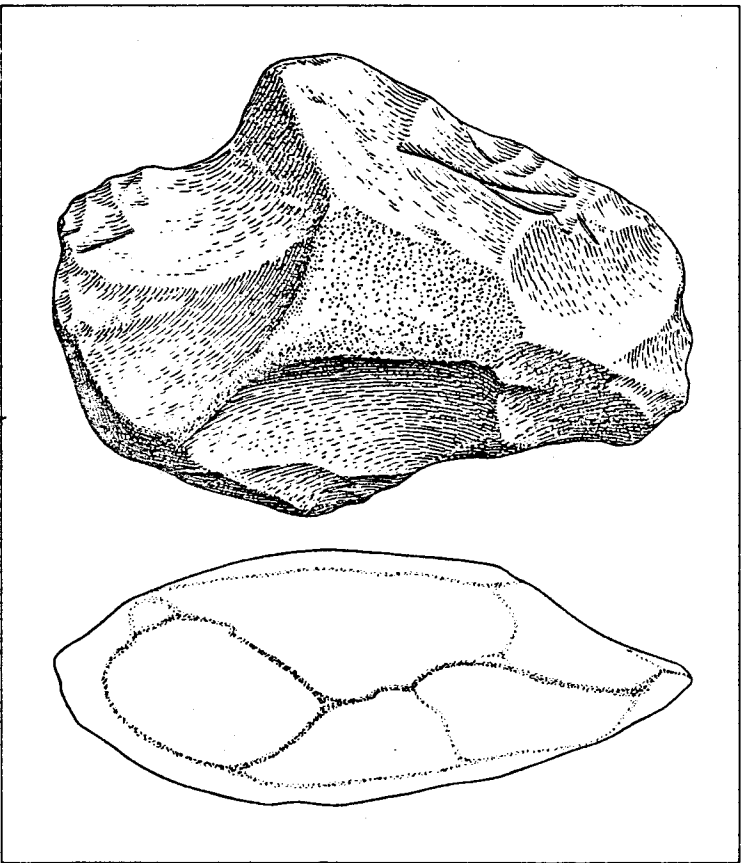
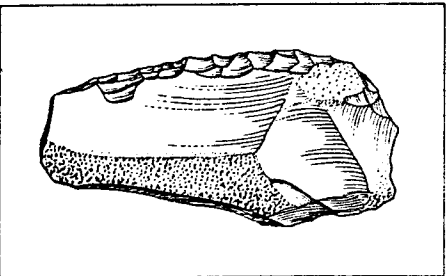
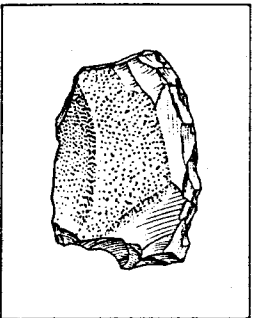
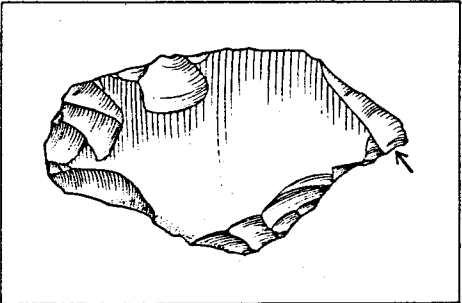
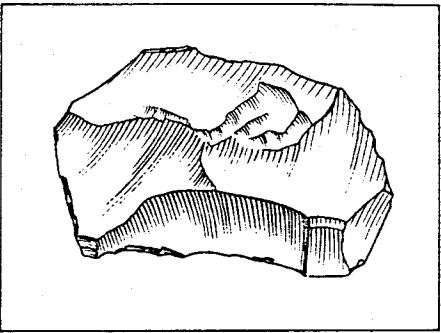
#### 7.3.4.2 Pech de l'Azé II

Layer 10 in Pech II is sterile, but layer 9 contains an Acheulian industry of 330 pieces. Of these, 113 were retouched tools, including endscrapers, borers, burins, backed knives, notched pieces, denticulates, sidescrapers, and handaxes. Table 7.10 listed the pertinent indices. Layer 8 as a whole contained 560 artefacts (228 tools). As an industry, layer 8 is similar to layer 9, a middle Acheulian. Found near the top of layer 8, an engraved bone, shown in Figure 7.9, represents the oldest known engraving. All other engraved bones are at the oldest Upper Paleolithic.

Layer 7 can be divided into 3 sublayers, the bottom of which

Figure 7.8

Tools from Pech I (after Bordes, 1972)

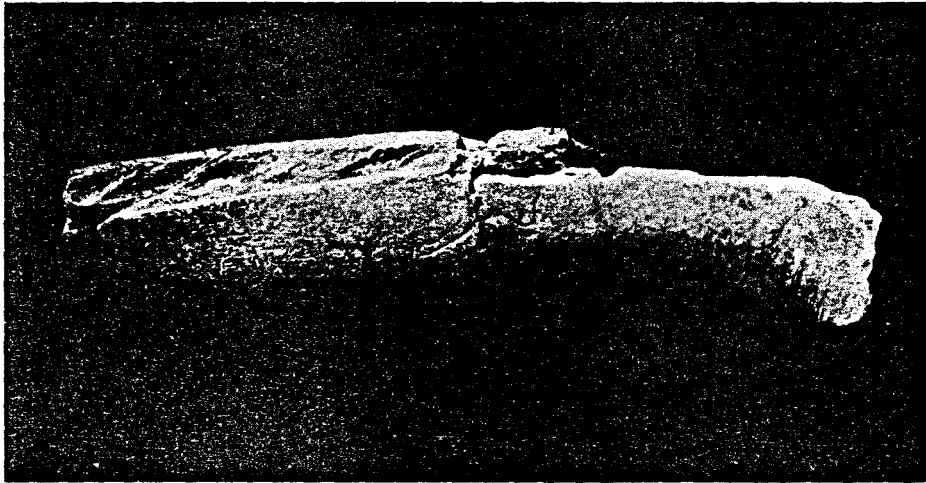


**Figure 7.9**

**Worked bones from Pech de l'Azé II:**

- A. An engraved bone from an Acheulian level, one of the earliest engraved bones ever found (couche 8).
- B. A pierced bone from couche 4A, a rare piece in a Mousterian level.

(after Bordes, 1972)



A



B

Figure 7.10

Tools from Pech II, Mousterian of Achuelian  
Tradition A

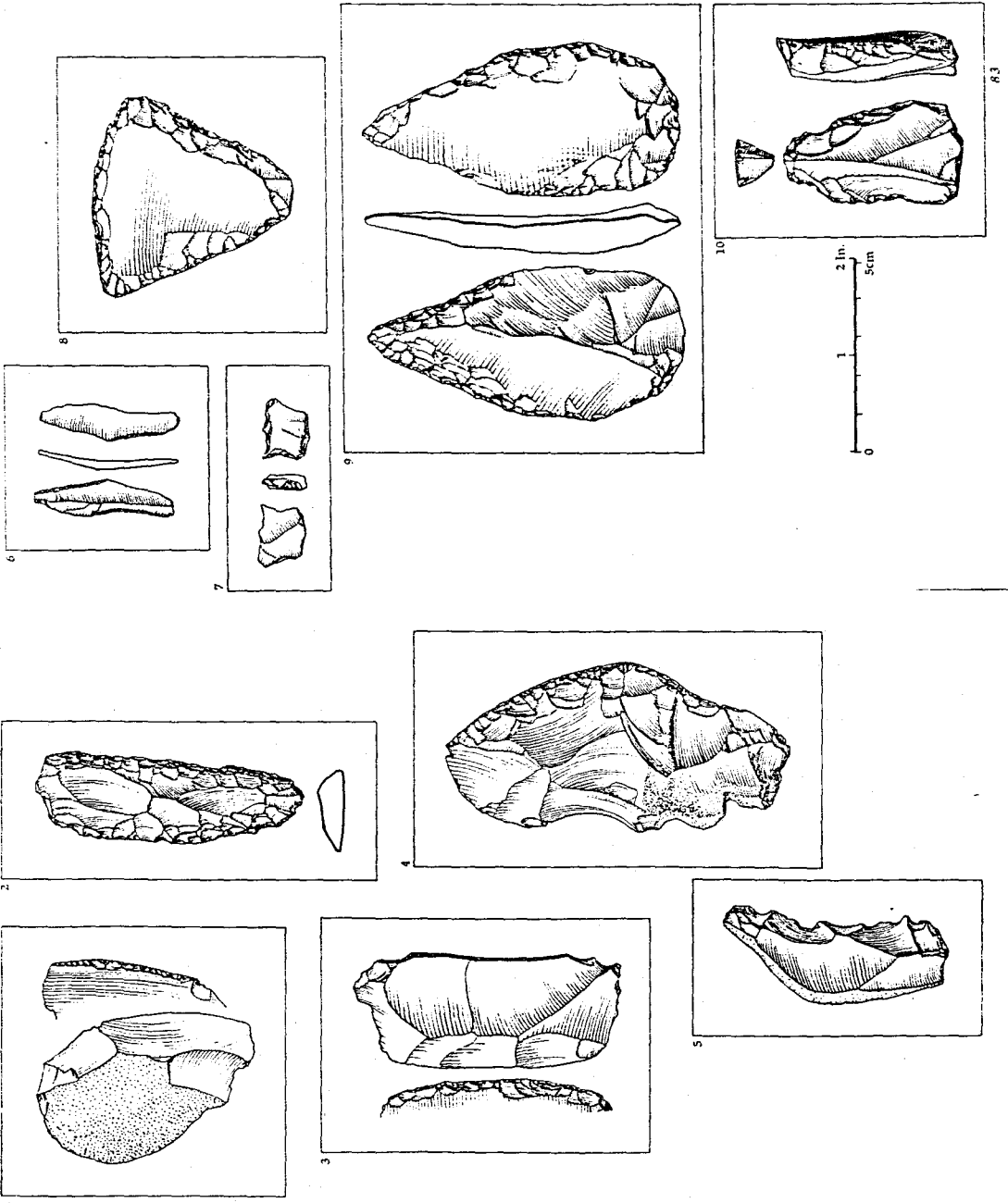




Figure 7.11

Tools from Pech II, Mousterian of Acheulian  
Tradition B (after Bordes, 1972)

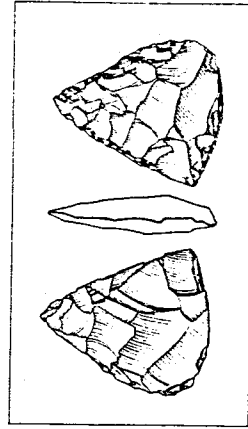
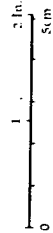
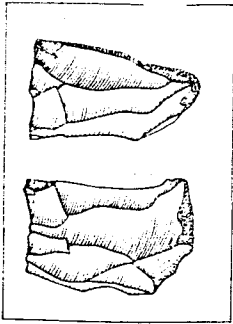
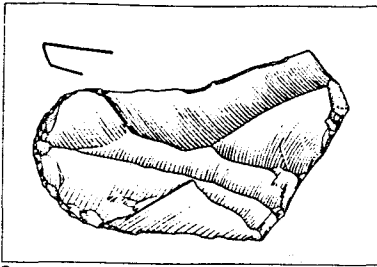
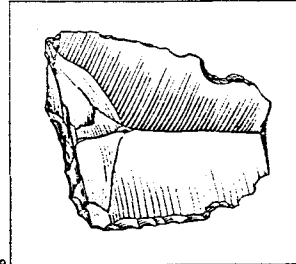
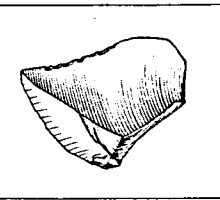
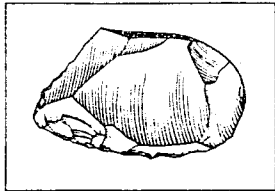
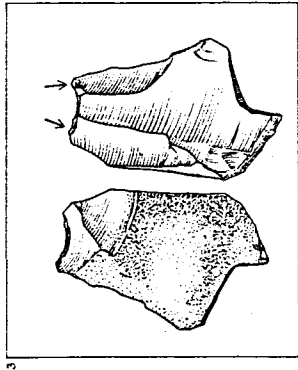
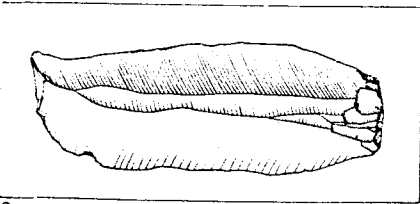
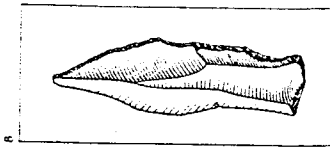
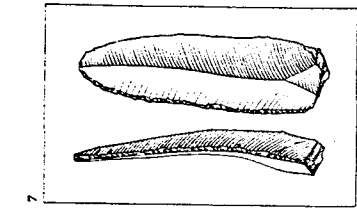
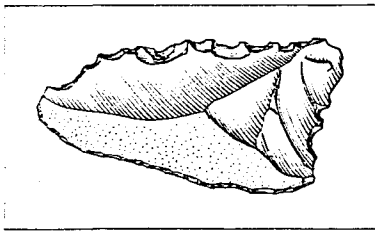
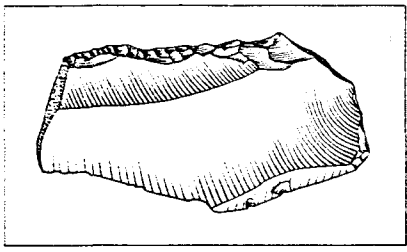


Table 7.2 Tool Typology, Couche 4,  
Pech de l'Aze I

Tool	Number	Total Percentage	Restricted Percentage
1. Typical Levallois flake	36	0.9	
2. Atypical Levallois flake	135	3.4	
3. Levallois point	5	0.1	
4. Retouched Levallois point	0	0	0
5. Pseudo-Levallois point	37	0.9	1.5
6. Mousterian point	20	0.5	0.8
7. Elongated Mousterian point	3	0.1	0.1
8. Limbo	1	0.0	0.0
9. Sidescraper, single straight	142	3.6	5.6
10. Sidescraper, single convex	257	6.6	10.2
11. Sidescraper, single concave	61	1.6	2.4
12. Sidescraper, double straight	8	0.2	0.3
13. Sidescraper, double straight convex	23	0.6	0.9
14. Sidescraper, double straight concave	1	0.0	0.0
15. Sidescraper, double biconvex	23	0.6	0.9
16. Sidescraper, double biconcave	2	0.1	0.1
17. Sidescraper, double convex concave	8	0.2	0.3
18. Sidescraper, convergent straight	6	0.2	0.2
19. Sidescraper, convergent convex	30	0.8	1.2
20. Sidescraper, convergent concave	0	0	0

Table 7.2 (continued)

Tool	Number	Total Percentage	Restricted Percentage
21. Sidescraper, asymmetrical	37	0.9	1.5
22. Sidescraper, transverse straight	7	0.2	0.3
23. Sidescraper, transverse convex	18	0.5	0.7
24. Sidescraper, transverse concave	2	0.1	0.1
25. Sidescraper, retouched on the ventral surface	154	3.9	6.1
26. Sidescraper, with abrupt retouch	22	0.6	0.9
27. Sidescraper, with thin back	6	0.2	0.2
28. Sidescraper, bifacial retouch	27	0.7	1.1
29. Sidescraper, with alternate retouch	56	1.4	2.2
30. Typical endscraper	33	0.8	1.3
31. Atypical endscraper	32	0.8	1.2
32. Typical burin	20	0.5	0.8
33. Atypical burin	38	1.0	1.5
34. Typical borer	23	0.6	0.9
35. Atypical borer	33	0.8	1.3
36. Typical backed knife	15	0.4	0.6
37. Atypical backed knife	28	0.7	1.1
38. Naturally backed knife	92	2.3	3.7
39. Mousterian raclette	163	4.2	6.5
40. Truncated piece	48	1.2	1.9
41. Mousterian tranchet	6	0.2	0.2
42. Notched pieces	264	6.7	10.5

Table 7.2 (continued)

Tool	Number	Total Percentage	Restricted Percentage
43. Denticulate	459	11.7	18.2
44. Bec burinante alterne	39	1.0	1.5
45. Flake, retouched on the ventral surface	102	2.6	?
46. Miscellaneous retouched flake, abrupt thick retouch			
47. Miscellaneous retouched flake, alternate thick retouch	127	3.2	
48. Miscellaneous retouched flake, abrupt thin retouch			
49. Miscellaneous retouched flake, alternate thin retouch	973	24.8	
50. Flake, bifacial retouch	22	0.6	
51. Tayac point	19	0.5	0.8
52. Etched triangle	21	0.5	0.8
53. Pseudo-microburin	4	0.1	0.2
54. Flake, notched end	32	0.8	1.2
55. Cleavers	10	0.3	0.4
56. Rabot (plane)	0	0	0
57. Aterian tanged point	0	0	0
58. Tanged piece	1	0.0	0.0
59. Chopper	0	0	0
60. Inverse chopper	0	0	0
61. Chopping tool	1	0.0	0.0
62. Miscellaneous piece	184	4.7	7.3
63. Blattspitzen	0	0	0
64. Bifacial foliate	1	0.0	0.0
<b>Total</b>	<b>3918</b>	<b>99.9</b>	<b>99.5</b>
	(2518)		

Table 7.3 Piece Typology, Couche 4, Fach de 1'Aze I

Piece	Number	Percentage
Flakes	3522	
Blades	314	
Points	49	
Trimmed flakes	24875	
Tools	2518	
Discs	8	
Polyhedra	0	
Nuclei	275	
Debris	3262	
Hammerstones	0	
Miscellaneous (pigments)	276	
Palette	1	
<b>Total</b>	<b>35100</b>	

Table 7.4 Raw Materials, Couche 4

Material	Number
Flint	33777
Quartz	725
Basalt	284
Cobbles	34
Other:	
Red ochre	23
Yellow ochre	4
MnO <sub>2</sub>	249
Bone (utilized)	4

Table 7.5 Nuclei Form, Couche 4,  
Pech de l'Aze I

Shape	Number
Discoidal	79
Globular	33
Prismatic	4
Irregular	57
Levallois flake	18
Levallois blade	00
Levallois point	1
Detritus	0
Miscellaneous	80
Pyramidal	3

Table 7.6 Characteristic Techniques, Couche 4,  
Pech de l'Aze I

Non-Levallois						
	Smooth	Facetted	Dihedral	Broken	Displaced	Convex
Flakes	1414	615	692	2297	261	463
Points	0	2	27	1	0	8
Blades	222	94	64	192	16	43
Total:	6411					

Table 7.7 Characteristic techniques, Couche 4,  
Pech de l'Aze I

Levallois						
	Smooth	Facetted	Dihedral	Broken	Displaced	Convex
Flakes	64	103	40	108	16	85
Points	1	4	3	0	0	3
Blades	23	48	6	58	8	19
Total:	589					

Table 7.8 Technical and Typological Indices and Characteristic  
Groups, Couche 4, Pech de l'Aze I

Index	Total	Restricted
Levallois	8.41	
Facetting	57.35	
Restricted Facetting	36.77	
Blade (lamellar)	11.32	
Typological Levallois	4.5	0
Sidescraper (Group II)	22.6	35.3
Total Acheulian		
Unifacial Acheulian	1.1	1.7
Bifacial		
Charentien		
Quina		
Group I: tools # 1 - 4	4.5	0
Group III: tools # 30 - 37, 40	1.9	10.7
Group IV: denticulates	11.7	18.2
Handax	3.8	5.8

Table 7.9 Technical and Typological Indices and Characteristic  
Groups, Couche A, Pech de l'Azé I

Index	Total	Restricted
Levallois	13.5	
Facetting	54.1	
Restricted Facetting	27.0	
Blade (lamellar)	13.1	
Aypological Levallois		
Sidescraper (Group II)		
Total Acheulian		
Unifacial Acheulian		
Bifacial		
Charentien		
Quina		
Group I: tools # 1 - 4		
Group III: tools # 30 - 37, 40		
Group IV: denticulates		

Table 7.10 Technical and Typological Indices and Characteristic  
Groups, Couche 9, Pech de l'Azé II

Index	Total	Restricted
Levallois	3.5	
Facetting	35.5	
Restricted Facetting	?	
Blade (lamellar)	?	
Aypological Levallois	?	
Sidescraper (Group II)	20.0	
Total Acheulian	?	
Unifacial Acheulian	4.0	
Bifacial	?	
Charentien	?	
Quina	?	
Handax	9.1	
Group I: tools # 1 - 4	?	
Group III: tools # 30 - 37, 40	27.0	
Group IV: denticulates	?	

is an Acheulian with 321 artefacts (Table 7.11), of which 116 are retouched tools. **Layer** 7A contains only a few flakes, but some of these show Levallois technique suggestive of the Mousterian, while **layer** 7B contains 167 artefacts (62 tools), including some sidescrapers, denticulates, and notched pieces, but few Upper Paleolithic types, prepared on flakes 40% of which are Levallois type, again suggestive of the Mousterian. **Layer** 6 appears similar to 7B, but contains very few tools, while **layer** X is sterile.

Several different types of hearths can be found in the Acheulian strata. Near the front of the cave are small elementary hearths with thin ash layers indicating the fires were of short duration. Hearths paved by flat calcite blocks probably were used repeatedly. These hearths, which average  $1 \text{ m}^2$  in size, are also found deeper within the cave as are the dug-out hearths. Dugout hearths are known in the Upper Paleolithic, but these represent the earliest, averaging 20 to 30 cm across the "channel". Dugout hearths are associated with **layer** 7b where the possible technological shift also occurs.

Both **layers** 4D and 5 are almost sterile, except for a few scattered pieces, and some badly crushed pieces in **layer** 4D, the cryoturbated portion. **Layer** 4C2, however, contains 2638 artefacts representing a Typical Mousterian assemblage (Table 7.12). Figure 7.10 shows some of the tools from **layer** 4C2, including a very unusual composite burin-endscraper, rare for the Mousterian. **Layer** 4C1 where present is sterile. In **layer** 4B, 6039 artefacts were found belonging to a Denticulate Mousterian (Table 7.13). In 4A2 only 337 artefacts were found, while in **layer** 4A1 179 were found.

Table 7.11 Technical and Typological Indices and Characteristic  
Groups, Couche 7c, Pech de l'Azé II

Index	Total	Restricted
Levallois	8.5	
Facetting	34.5	
Restricted Facetting	?	
Blade (lamellar)	?	
Aypological Levallois	?	
Sidescraper (Group II)	22.4	
Total Acheulian	6.5	
Unifacial Acheulian	?	
Bifacial	?	
Charentien	?	
Quina	?	
Group I: tools # 1 - 4	?	
Group III: tools # 30 - 37, 40	9.3	
Group IV: denticulates	?	

Table 7.12 Technical and Typological Indices and Characteristic  
Groups, Couche 4C2, Pech de l'Azé II

Index	Total	Restricted
Levallois	9.5	
Facetting	50.8	
Restricted Facetting	33.5	
Blade (lamellar)	6.0	
Aypological Levallois	?	10.2
Sidescraper (Group II)	?	37.8
Total Acheulian	?	
Unifacial Acheulian	?	
Bifacial	?	
Charentien	?	
Quina	0	
Group I: tools # 1 - 4	?	
Group III: tools # 30 - 37, 40	9.3	
Group IV: denticulates	13.1	



Table 7.12 Technical and Typological Indices and Characteris  
Groups, Couche 4B, Pech de l'Azé II

Index	Total	Restricted
Levallois	9.4	
Facetting	48.9	
Restricted Facetting	24.0	
Blade (lamellar)	9.4	
Aypological Levallois	12.5	
Sidescraper (Group II)	14.5	
Total Acheulian	?	
Unifacial Acheulian	?	
Bifacial	?	
Charentien	?	
Quina	0.8	
Group I: tools # 1 - 4	?	
Group III: tools # 30 - 37, 40	6.9	
Group IV: denticulates	40.3	

Table 7.14 Technical and Typological Indices and Characteristic  
Groups, Couche 3, Pech de l'Azé II

Index	Total	Restricted
Levallois	29.1	
Facetting	73.6	
Restricted Facetting	64.6	
Blade (lamellar)	9.3	
Aypological Levallois	23.5	
Sidescraper (Group II)	29.1	
Total Acheulian	?	
Unifacial Acheulian	?	
Bifacial	?	
Charentien	?	
Quina	0	
Group I: tools # 1 - 4	?	
Group III: tools # 30 - 37, 40	18.2	
Group IV: denticulates	?	

Both assemblages appear to be Typical Mousterian, as is that of **layer 3**, represented by 1261 artefacts (Table 7.14), and one piece of red ochre. Of all the sublevels in **layer 2**, only couche 2G1-2 contains more than 50 artefacts. **Layer 2** may be a Quina Mousterian, but insufficient tools are present to be certain.

It is curious that the Denticulate Mousterian deposits of 4B are found near the mouth, while those of the Typical Mousterian in 4C2 are found deeper inside. Also noted in several of the layers were groups of limestone blocks assembled obviously by humans, but for some unknown purpose. Found the composite layer 4A (4A1-2), a bone from an animal the size of a red deer has been bored, something rarely seen in Mousterian cultures.

#### 7.3.4.3 Pech de l'Azé IV

**Layer Z** contained 3851 artefacts of which 271 were tools, from a Typical Mousterian industry, as was **layer Y** with 1756 artefacts (214 tools). In **layer X**, 13,703 artefacts were found (857 tools), also from a Typical Mousterian.

In **layer J3**, J3c contained 3330 artefacts (222 tools), J3b 9674 (941), and J3a 9548 (601). All of these have been attributed by Bordes (1976) to a local variation not seen previously, because of the large number of naturally backed knives, the presence of Kombewa flakes, the small size of many of the flakes, and the small number of sidescrapers, and points. Unlike the Micromousterian which is simply a small version of the Mousterian constrained by the size of the flint nodules, this is a purposefully small industry. Bordes (1976) calls it the Asinipodian (Latin for Pech de l'Azé).

Table 7.15 Technical and Typological Indices and Characteristic Groups, Couche F1, Pech de l'Azé IV

Index	Total	Restricted
Levallois	5.4	
Facetting	36.9	
Restricted Facetting	21.3	
Blade (lamellar)	5.2	
Aypological Levallois		18.4
Sidescraper (Group II)		?
Total Acheulian		9.9
Unifacial Acheulian		8.5
Bifacial		1.4
Charentien		?
Quina		?
Group I: tools # 1 - 4		18.0
Group III: tools # 30 - 37, 40		17.0
Group IV: denticulates		21.3

Table 7.16 Technical and Typological Indices and Characteristic Groups, Couche F2, Pech de l'Azé IV

Index	Total	Restricted
Levallois	5.4	
Facetting	37.2	
Restricted Facetting	21.9	
Blade (lamellar)	5.8	
Aypological Levallois		19.9
Sidescraper (Group II)		5.9
Total Acheulian		10.0
Unifacial Acheulian		7.3
Bifacial		2.7
Charentien		?
Quina		?
Group I: tools # 1 - 4		19.9
Group III: tools # 30 - 37, 40		15.1
Group IV: denticulates		22.4

Table 7.17 Technical and Typological Indices and Characteristic  
Groups, Couche F3, Pech de l'Azé IV

Index	Total	Restricted
Levallois	8.9	
Facetting	41.7	
Restricted Facetting	26.2	
Blade (lamellar)	6.9	
Aypological Levallois		27.4
Sidescraper (Group II)		?
Total Acheulian		6.2
Unifacial Acheulian		4.1
Bifacial		2.1
Charentien		?
Quina		?
Group I: tools # 1 - 4		27.4
Group III: tools # 30 - 37, 40		6.4
Group IV: denticulates		24.8

Table 7.18 Technical and Typological Indices and Characteristic  
Groups, Couche F4, Pech de l'Azé IV

Index	Total	Restricted
Levallois	9.3	
Facetting	38.5	
Restricted Facetting	27.6	
Blade (lamellar)	5.8	
Aypological Levallois		24.8
Sidescraper (Group II)		25.6
Total Acheulian		2.6
Unifacial Acheulian		1.2
Bifacial		1.4
Charentien		?
Quina		?
Group I: tools # 1 - 4		24.8
Group III: tools # 30 - 37, 40		6.5
Group IV: denticulates		24.3

Table 7.19 Technical and Typological Indices and Characteristic  
Groups, Couche II, Pech de l'Azé IV

Index	Total	Restricted
Levallois	15.9	
Facetting	70.8	
Restricted Facetting	65.4	
Blade (lamellar)	11.2	
Aypological Levallois		?
Sidescraper (Group II)		69.4
Total Acheulian		0
Unifacial Acheulian		0
Bifacial		0
Charentien		?
Quina		?
Group I: tools # 1 - 4		?
Group III: tools # 30 - 37, 40		?
Group IV: denticulates		2.8

Table 7.20 Technical and Typological Indices and Characteristic  
Groups, Couche I2, Pech de l'Azé IV

Index	Total	Restricted
Levallois	25.5	
Facetting	56.3	
Restricted Facetting	49.6	
Blade (lamellar)	17.1	
Aypological Levallois		45.4
Sidescraper (Group II)		52.6
Total Acheulian		0
Unifacial Acheulian		0
Bifacial		0
Charentien		?
Quina		?
Group I: tools # 1 - 4		45.4
Group III: tools # 30 - 37, 40		5.0
Group IV: denticulates		4.3

Table 7.22 Technical and Typological Indices and Characteristic  
Groups, Couche J3a, Pech de l'Azé IV

Index	Total	Restricted
Levallois	23.5	
Facetting	56.5	
Restricted Facetting	50.0	
Blade (lamellar)	6.4	
Aypological Levallois		73.0
Sidescraper (Group II)		14.7
Total Acheulian		0.1
Unifacial Acheulian		0.1
Bifacial		0
Charentien		?
Quina		?
Group I: tools # 1 - 4		73.0
Group III: tools # 30 - 37, 40		4.9
Group IV: denticulates		13.7

Table 7.21 Technical and Typological Indices and Characteristic  
Groups, Couche J3, Pech de l'Azé IV

Index	Total	Restricted
Levallois	25.3	
Facetting	56.4	
Restricted Facetting	48.4	
Blade (lamellar)	7.7	
Aypological Levallois		66.6
Sidescraper (Group II)		27.7
Total Acheulian		?
Unifacial Acheulian		?
Bifacial		?
Charentien		?
Quina		?
Group I: tools # 1 - 4		66.6
Group III: tools # 30 - 37, 40		?
Group IV: denticulates		14.5

Table 7.23 Technical and Typological Indices and Characteristic  
Groups, Couche J3B, Pech de l'Azé IV

Index	Total	Restricted
Levallois	23.2	
Facetting	53.9	
Restricted Facetting	47.2	
Blade (lamellar)	5.8	
Aypological Levallois		68.7
Sidescraper (Group II)		9.9
Total Acheulian		2.6
Unifacial Acheulian		2.1
Bifacial		0.5
Charentien		?
Quina		?
Group I: tools # 1 - 4		68.7
Group III: tools # 30 - 37, 40		8.2
Group IV: denticulates		14.4

Table 7.24 Technical and Typological Indices and Characteristic  
Groups, Couche J3c, Pech de l'Azé IV

Index	Total	Restricted
Levallois	21.0	
Facetting	61.2	
Restricted Facetting	52.1	
Blade (lamellar)	4.2	
Aypological Levallois		57.2
Sidescraper (Group II)		12.7
Total Acheulian		0.5
Unifacial Acheulian		0.5
Bifacial		0
Charentien		?
Quina		?
Group I: tools # 1 - 4		57.2
Group III: tools # 30 - 37, 40		12.8
Group IV: denticulates		16.4

Table 7.25 Technical and Typological Indices and Characteristic  
Groups, Couche X, Pech de l'Azé IV

Index	Total	Restricted
Levallois	15.5	
Facetting	54.1	
Restricted Facetting	46.5	
Blade (lamellar)	7.0	
Aypological Levallois		38.6
Sidescraper (Group II)		44.4
Total Acheulian		1.0
Unifacial Acheulian		0.5
Bifacial		0.5
Charentien		?
Quina		?
Group I: tools # 1 - 4	38.6	
Group III: tools # 30 - 37, 40	10.5	
Group IV: denticulates	9.2	

Table 7.26 Technical and Typological Indices and Characteristic  
Groups, Couche Y, Pech de l'Azé IV

Index	Total	Restricted
Levallois	17.2	
Facetting	51.5	
Restricted Facetting	41.8	
Blade (lamellar)	7.3	
Aypological Levallois		39.8
Sidescraper (Group II)		30.3
Total Acheulian		0
Unifacial Acheulian		0
Bifacial		0
Charentien		?
Quina		?
Group I: tools # 1 - 4	39.8	
Group III: tools # 30 - 37, 40	13.5	
Group IV: denticulates	12.4	



Table 7.27 Technical and Typological Indices and Characteristic

Groups, Couche Z, Pech de l'Aze IV

Index	Total	Restricted
Levallois	16.6	
Facetting	56.0	
Restricted Facetting	47.8	
Blade (lamellar)	9.6	
Typological Levallois		35.1
Sidescraper (Group II)		48.4
Total Acheulian		0
Unifacial Acheulian		0
Bifacial		0
Charentien		?
Quina		?
Group I: tools # 1 - 4		35.1
Group III: tools # 30 - 37, 40		7.9
Group IV: denticulates		8.7

The very top of layer J3a, is called J3, but it is a Typical Mousterian. Layer J1 and J2 were too poor to characterize, except as Mousterian. Layer I2, one of the richest with 1,010 tools among 10,890 artefacts, also contained some Kombewa flakes, but is still considered to be a Typical Mousterian. Layer I1 is also a Typical Mousterian represented by 1074 artefacts (116 tools). Both layer G and H were too poor to describe in any detail, although both were Mousterian.

Containing 22,698 artefacts of which 953 were tools, layer F4 represents a Mousterian of Acheulian Tradition A, while F3 (3540 artefacts, 252 tools) is an intermediate form between A and B, which is found in layer F1 (5297; 356) and F2 (3259; 215).

Layers A through E were too poor to describe. Tables 7.15 through 7.27 list the pertinent indices for the layers in Pech IV. Figures 7.11 and 7.12 shows some of artefacts.

#### 7.3.5 Human Remains at Pech de l'Azé

In 1909, Capitan and Peyrony found a young child's skull. Although definitely Neanderthal, some of the features appear to be more modern, but not unduly so for any Neanderthal child. The skull was found under 3 m of limestone blocks in an archaeological layer 1 m thick, 10 cm from the top, surrounded by bones and teeth from bovids, horses, red deer, goat, and reindeer, in addition to an "Upper Mousterian Tradition" according to Capitan and Peyrony (Bordes, 1972). In 1909, "Upper Mousterian" implied Quina type, or perhaps Typical Mousterian. Bordes (1972) says the skull was

Table 7.30

CORRELATION OF DATA FROM PECH IV,  
USING SAMPLES 77PA1, 77PA2, 77PA3

SAMPLE	AGE (KA)	ERROR (KA)	YIELDS		TH-230	TH-230	U-234	(U-234)	CONCENTRATIONS	
			U-232 (%)	TH-228 (%)	U-234	TH-232	U-238	(U-238) 0	U-238 (PPM)	TH-232 (PPM)
77PA2-1	21.78 <sup>+</sup> - 21.7	+ 66.1 - 21.7	3.24	31.19	+ .421 - .216	+ 1.8 - .2	+ 1.4328 <sup>‡</sup> - 1.023	+ 1.4533 <sup>‡</sup> - 1.226	.068	.06

‡ NOT INCLUDED IN THE AVERAGE DATE

+ THORIUM CORRECTION USED CALCULATED AT R = 1.25

↓ REPRESENTS THE YOUNGEST AGE POSSIBLE NOT THE LOWER ERROR LIMIT CALCULATED AT R = 1.25

\* REPRESENTS THE OLDEST AGE POSSIBLE, NOT THE UPPER ERROR

Table 7.31

CORRELATION OF DATA FROM PECH I OUTER BRECCIA  
USING SAMPLES 77PA4, 77PA5, 77PA6

SAMPLE	AGE (KA)	ERROR (KA)	YIELDS		TH-230	TH-230	U-234	(U-234)	CONCENTRATIONS	
			U-232 (%)	TH-228 (%)	U-234	TH-232	U-238	(U-238) 0	U-238 (PPM)	TH-232 (PPM)
77PA4-1	-		0.00	5.09	-	+ 4.8 - 6.6	-	-	-	.02
77PA5-1	37.28 <sup>+</sup> - 9.3	+ 9.3 - 9.3	6.30	19.26	+ .346 - .036	+ 6.4 - 3.2	+ 2.7958 <sup>‡</sup> - .415	+ 2.2068 <sup>‡</sup> - .042	.053	.02
77PA5-3	99.0 - 16.8	+ 19.3 - 16.8	20.56	25.95	+ .639 - .078	≥ 1000.0	+ 2.087 - .351	+ 2.435 - .097	.04	0.00
77PA6-1	36.58 <sup>+</sup> - 15.4	+ 17.0 - 15.4	3.22	59.29	+ .317 - .100	+ 11.8 - 2.8	+ 1.1528 <sup>‡</sup> - .496	+ 2.2948 <sup>‡</sup> - .073	.138	.01
AVERAGES	99.0	+ 19.3 - 16.8					+ 2.087 - .351	+ 2.435 - .539	.04	

‡ NOT INCLUDED IN THE AVERAGE DATE

+ THORIUM CORRECTION USED CALCULATED AT R = 1.25

↓ REPRESENTS THE YOUNGEST AGE POSSIBLE NOT THE LOWER ERROR LIMIT CALCULATED AT R = 1.25

\* REPRESENTS THE OLDEST AGE POSSIBLE, NOT THE UPPER ERROR

Table 7.32

CORRELATION OF DATA FROM PEGH I INNER BRECCIA  
USING SAMPLES 77PA7, 77PA8, 77PA9, 77PA10, 77PA11

SAMPLE	AGE (KA)	ERROR (KA)	YIELDS		TH-230	TH-230	U-234	(U-234)	CONCENTRATIONS	
			U-232 (%)	TH-228 (%)	U-234	TH-232	U-238	(U-238) 0	U-238 (PPM)	TH-232 (PPM)
77PA10-2	-		0.00	65.25	-	+ 1.0 - .0	-	-	-	.50
77PA7-1	-		0.00	40.36	-	+ 8.6 - 3.0	-	-	-	.01
77PA7-2	-		0.00	2.99	-	+ 4.3 - 3.5	-	-	-	.05
77PA7-3	-		0.00	3.02	-	+ 20.5 - 93.9	-	-	-	.02
77PA8-3	108.3	+ 66.1 - 42.0	18.56	5.09	+ .648 - .183	≥ 1000.0	1.304 + .083	1.305 + .074	.10	0.00
77PA11-2	105.8	+ 24.8 - 22.4	15.88	13.98	+ .668 - .062	+ 10.8 - 6.9	1.281 + .094	1.303 + .031	.09	.02
77PA11-3	≥ 350.0§	- 0.0+	7.58	71.83	+ .966 - .123	+ 37.0 - 14.1	.897§ + .135	-	.09§	.01
77PA8-1	128.4	+ 21.3 - 18.5	23.86	51.99	+ .726 - .054	+ 23.6 - 8.4	1.248 + .101	1.323 + .028	.09	.01
77PA11-1	136.5	+ 59.8 - 43.1	11.31	29.87	+ .770 - .112	+ 8.8 - 3.8	1.177 + .216	1.335 + .075	.09	.03
77PA9-1	134.9	+ 32.1 - 26.3	27.93	32.81	+ .760 - .069	+ 10.4 - 2.6	1.274 + .127	1.329 + .042	.05	.01
77PA9-2	-		60.99	0.00	-	-	+ 1.165 - .128	-	.18	-
-----										
AVERAGES	128.7	+ 34.6 - 27.2					+ 1.225 - .121	+ 1.371 - .205	.12	

§ NOT INCLUDED IN THE AVERAGE DATE

+ THORIUM CORRECTION USED CALCULATED AT R = 1.25

Table 7.33

CORRELATION OF DATA FROM PECH II, C. 4  
USING SAMPLES 77PA14A-D

SAMPLE	AGE --- (KA)	ERROR ----- (KA)	YIELDS		TH-230	TH-230	U-234	(U-234)	CONCENTRATIONS	
			U-232 (%)	TH-232 (%)	U-234	TH-232	U-234	(U-234)	U-234 (PPM)	TH-232 (PPM)
77PA14A-1	≥ 350.0‡ (≥ 350.0‡)		40.37	62.85	.948 + .158	1.0 + .1	1.309‡ + .233	-	.02‡	.09
77PA14A-2	201.6‡ (≥ 350.0‡) - 0.0		28.70	40.42	1.060 + .096	1.0 + .1	1.056‡ + .092	1.098‡	.06‡	.21
77PA14B3-1	-		0.00	13.44	-	1.1 + .1	-	-	-	.50
77PA14C-1	156.9‡ (≥ 350.0‡) - 130.0		8.08	2.79	.847 + .245	3.6 + 2.5	1.101‡ + .192	1.156‡	.10‡	.08
77PA14C-2	≥ 350.0‡ - 41.9‡		36.38	35.01	1.013 + .049	6.0 + .4	1.025‡ + .047	-	.08‡	.04
77PA14D-1	-		0.00	18.67	-	1.9 + .3	-	-	-	.13

‡ NOT INCLUDED IN THE AVERAGE DATE

+ THORIUM CORRECTION USED CALCULATED AT R = 1.25

‡ REPRESENTS THE YOUNGEST AGE POSSIBLE NOT THE LOWER ERROR LIMIT CALCULATED AT R = 1.25

+ REPRESENTS THE OLDEST AGE POSSIBLE, NOT THE UPPER ERROR

= THIS IS A CONSTRUCTION DATE FROM THE DATA

Table 7.34

CORRELATION OF DATA FROM PECH 22, BL 02, C 40  
USING SAMPLES 77PA12

SAMPLE	AGE (KA)	ERROR (KA)	YIELDS		TH-230	TH-230	U-234	(U-234)	CONCENTRATIONS	
			U-232 (%)	TH-228 (%)	U-234	TH-232	U-238	(U-238)0	U-238 (PPM)	TH-232 (PPM)
77PA12-1	≥ 350.0\$+	- 9.2+	5.96	11.70	+ 3.532 - 6.157	+ 22.8 - 43.5	+ .762\$ - 1.781	-	.02\$	.01
77PA12-2	63.2\$+ (≥ 350.0+)	- 3.0	6.72	42.23	+ .823 - .124	+ 1.5 - .1	+ 1.172\$ - .227	1.205\$	.02\$	.16

\$ NOT INCLUDED IN THE AVERAGE DATE

\* THORIUM CORRECTION USED CALCULATED AT R = 1.25

+ REPRESENTS THE YOUNGEST AGE POSSIBLE NOT THE LOWER ERROR LIMIT CALCULATED AT R = 1.25

\* REPRESENTS THE OLDEST AGE POSSIBLE, NOT THE UPPER ERROR

Table 7.35

CORRELATION OF DATA FROM PECH II, C. 3  
USING SAMPLES 77PA13

SAMPLE	AGE (KA)	ERROR (KA)	YIELDS		TH-230	TH-230	U-234	(U-234)	CONCENTRATIONS	
			U-232 (%)	TH-228 (%)	U-234	TH-232	U-238	(U-238)0	U-238 (PPM)	TH-232 (PPM)
77PA13-2	-		21.18	0.00	-	-	+ .906\$ - 0.600	-	.14\$	-
78PA13-3	103.5\$+	+ 29.6 - 25.3	22.60	35.78	+ .729 - .065	+ 3.5 - .3	+ 1.208\$ - .110	1.278\$ - .170	.06\$	.05

\* NOT INCLUDED IN THE AVERAGE DATE

+ THORIUM CORRECTION USED CALCULATED AT R = 1.25

+ REPRESENTS THE YOUNGEST AGE POSSIBLE NOT THE LOWER ERROR LIMIT CALCULATED AT R = 1.25

\* REPRESENTS THE OLDEST AGE POSSIBLE, NOT THE UPPER ERROR

- THIS IS A CORRELATION DATE DERIVED FROM CORRELATING THE U AND TH DATA FROM THE DIFFERENT

Table 7.36

CORRELATION OF DATA FROM PECH II, C 6,  
USING SAMPLES 77PA16A, 77PA16B, 77PA17, 77PA18

SAMPLE	AGE (KA)	ERROR (KA)	YIELDS		TH-230	TH-230	U-234	(U-234)	CONCENTRATIONS	
			U-232 (%)	TH-228 (%)	U-234	TH-232	U-238	(U-238)0	U-238 (PPM)	TH-232 (PPM)
77PA16A-1	236.3± <sup>(≥ 350.0*)</sup>	- 91.1	12.90	10.33	+ 1.031 - .121	+ 3.4 - .5	+ 1.760± - .294	2.475±	.05±	.08
77PA16B-1	75.3± <sup>(≥ 350.0*)</sup>	- *****	15.24	14.99	+ .837 - .062	+ 1.0 - .1	+ 1.449± - .116	1.555±	.10±	.39
77PA16B-2	≥ 350.0±	.....	5.59	32.91	+ .918 - .073	+ 1.1 - .0	+ .940± - .082	-	.03±	.07

CORRELATION OF DATA FROM PECH II, C 6,  
USING SAMPLES 77PA20

SAMPLE	AGE (KA)	ERROR (KA)	YIELDS		TH-230	TH-230	U-234	(U-234)	CONCENTRATIONS	
			U-232 (%)	TH-228 (%)	U-234	TH-232	U-238	(U-238)0	U-238 (PPM)	TH-232 (PPM)
77PA20-1	61.0± <sup>+</sup>	+ 52.8 - 39.7	1.32	6.77	+ .458 - .269	+ 17.0 - 25.0	+ 1.323± - .750	+ 1.384± - .965	.09±	.01
77PA20-2	50.1± <sup>+</sup>	+ 12.9 - 12.4	7.62	35.55	+ .523 - .044	+ 2.9 - .2	+ 1.500± - .172	+ 1.576± - .219	.12±	.10

± NOT INCLUDED IN THE AVERAGE DATE

+ THORIUM CORRECTION USED CALCULATED AT R = 1.25

+ REPRESENTS THE YOUNGEST AGE POSSIBLE NOT THE LOWER ERROR LIMIT CALCULATED AT R = 1.25

+ REPRESENTS THE OLDEST AGE POSSIBLE, NOT THE UPPER ERROR

± THIS IS A COMBINATION DATE DERIVED FROM COMBINING THE U AND TH DATA FROM TWO DIFFERENT SUBSAMPLES, AND AS SUCH, SHOULD BE REGARDED AS QUESTIONABLE AT BEST.

Table 7.37

CORRELATION OF DATA FROM PECH II, C. 8,  
USING SAMPLES 77PA15, 78PA19

SAMPLE	AGE (KA)	ERROR (KA)	YIELDS		TH-230	TH-230	U-234	(U-234)	CONCENTRATIONS	
			U-232 (%)	TH-228 (%)	U-234	TH-232	U-238	(U-238)0	U-238 (PPM)	TH-232 (PPM)
77PA15-1	247.73 <sup>‡</sup> - 73.8	(2 350.0*)	36.80	66.36	+ .993 - .103	+ 10.5 - 1.8	+ 1.5045 - .171	2.0118	.058	.02
78PA19-2	-	-	0.00	51.64	-	+ 2.6 - .2	-	-	-	.01

‡ NOT INCLUDED IN THE AVERAGE DATE

+ THORIUM CORRECTION USED CALCULATED AT R = 1.25

+ REPRESENTS THE YOUNGEST AGE POSSIBLE NOT THE LOWER ERROR LIMIT CALCULATED AT R = 1.25

+ REPRESENTS THE OLDEST AGE POSSIBLE, NOT THE UPPER ERROR

‡ THIS IS A COMBINATION DATE DERIVED FROM COMBINING THE U AND TH DATA FROM TWO DIFFERENT SUBSAMPLES, AND AS SUCH, SHOULD BE REGARDED AS QUESTIONABLE AT BEST.



been deposited in the early Würm I or late Riss III, as the bottom has experienced a very cold climate, followed by a **cool damp climate**, with 21 to 35% trees present, comparable to 4B or 4C in Pech II.

From the paleoclimatological reconstructions above, Bordes (1972) has reconstructed the history of the cave, shown in Figure 7.13. Both caves were filled by sediments in the Riss and Würm I. During the Würm I/II, the sediments in Pech I were completely washed out except for the breccias adhering to the wall. Pech I was subsequently filled by Würm II sediments, while deposition in Pech II did not occur. From the end of the Würm II until the Middle Ages the cave was relatively untouched by either humans or the processes of erosion or sedimentation.

Table 7.28 shows the paleoclimatic interpretation for Pech IV, compared with the other two. Based upon the industries at Pech IV, Bordes (1976) has attributed the section to the Würm: layers Z through G to the Würm II, and F through A to the Würm I.

### 7.3.7 Results

Unfortunately, few definitive results have been obtained for Pech de l'Azé. Like Montgaudier, poor yields and large amounts of detritus plagued the analysis. In general, the uranium concentrations were also very low. Only one sample improved when it was roasted, 78PA20. Table 7.29 lists the sample descriptions, while Tables 7.30 through 7.37 list the results. Figures 7.14 to 7.20 show the samples collected by H. Schwarcz, some with the help of M. Aitken and F. Bordes.

## 7.3.7.1 Pech de l'Azé IV

Of the three samples from Pech IV, only one was suitable for dating, but it gave an age with a large error, and a low uranium yield. Therefore, 77PA2 may be Würmian, but it is not certain until more dates can be obtained.

## 7.3.7.2 Pech de l'Azé I

In the outer breccia mass, three samples were collected from the middle of the mass, 77PA4-6. None of the dates totally agree. The date with the best yields is 77PA5-3,  $99.0 \begin{matrix} + 19.3 \\ - 16.8 \end{matrix}$  Ka, which is consistent with an age between the Riss III and Würm as implied by the sedimentological and pollen analysis. Interestingly, the other two dates correspond to the Würm I/II, the time that the rest of sediments in Pech I were supposedly washed out leaving only the breccias. If the dates are correct, then they may represent a period of recrystallization of these layers.

In the inner breccia, Figure 7.16, 77PA10 was collected from the dirtier travertine surrounding the stalagmitic boss, while 77PA7, 77PA8, and 77PA11 come from the boss, and 77PA9 from the basal flowstone beneath the boss. Although 77PA10 gave no result, all the other dates agree well with an average of  $128.7 \begin{matrix} + 34.6 \\ - 27.2 \end{matrix}$  Ka. Therefore, the inner breccia is a late Riss or Riss/Würm deposit, similar in age to the outer breccia.

## 7.3.7.3 Pech de l'Azé II

77PA15 was a stalagmitic crust in layer 3, in Pech II. Although the error is rather large, the date of  $103.5 \begin{matrix} + 29.6 \\ - 25.3 \end{matrix}$  Ka seems reliable; but unconfirmed. If the date is accurate, then

the supposed Würm I sediments are actually Riss/Würm.

77PA12, from block B2 embedded in couche 4D in Pech II did not give any result, but was full of detrital thorium. Part of a stalactite from layer 4, 77PA14A-D, also gave no reliable reliable dates, but had large amounts of  $^{232}\text{Th}$ .

Layer 6 contained a paper-thin stalabmitic growth which was sampled, 77PA16, 77PA17, and 77PA18, while 78PA20 was also collected from layer 6. None of the ages from 77PA16, either A or B, can be used because there is a higher concentration of detrital thorium in them than that of  $^{238}\text{U}$ . 77PA20 seems to be quite young, the dates ranging from  $50.1 \pm 12.9$  to  $61.0 \pm 52.8$  Ka, but with poor yields, it is uncertain if this represents the true age. Bordes' interpretation for layer 6 was Riss II, not Würm I.

Layer 8 and 9 were sampled respectively as 77PA15 and 78PA19, the former a stalactite, the latter also likely a roof spall. If a single age can be believed, then the roof spall was deposited on the roof in the Mindel,  $247.7 \pm 350.0$  Ka ago, to fall into the deposit at some later time.

### 7.3.8 Conclusions

As far as can be determined from the few dates listed above, the history of Pech de l'Azé was much as Bordes (1972) describes it.

In Pech I, sediments and stalagmites were deposited from at least 130 Ka until 100 Ka in the Riss/Würm, but most were later washed out by a Würm I/II flood. Sediments accumulated in Pech II and IV, but neither are well dated.

The dates on the breccia masses mean that the Mousterian tools embedded in them are much older than is conventionally assumed for a Mousterian culture. If the upper part of the outer breccia is comparable to layer 4 in Pech II, then the date of 103 Ka for layer 3 agrees extremely well with that of the outer breccia. If that is the case, most of Pech II is also older than expected, but many problems still remain in Pech II.

Unfortunately, there is little travertine in Pech which makes it extremely difficult to obtain more material for dating while most of the samples collected were so small that only a few dates could be obtained. Therefore, many of the problems which exist may remain unsolved.

#### 7.4 The Castelnaud Caves

Abri Vaufrey and Grotte 13 are just two of the many caves and abris found in the cliffs overlooking the Dordogne above Castelnaud. Several of the caves including Vaufrey contain archeological material, others such as Grotte 13 contain faunal remains. All are the result of karstic erosion along the St. Cyprien Fault in the "Jurassic window". Laville (1975) has studied Grotte 13 in detail, but only preliminary reports mention Vaufrey (Bordes, 1972).

##### 7.4.1 The History of Excavation

Abri Vaufrey has probably been known to the locals for several centuries, because it is clearly visible from the valley (Figure 7.21). In 1930, R. Vaufrey also excavated at Vaufrey,

Figure 7.21

The cliffs near Vaufrey:

The upper picture shows the exposed cliff faces, which are maintained through debris falls, resulting from undercutting erosion of the softer strata in the lower picture.



Figure 7.22

Stoping of the roof in Abri Vaufrey.

Figure 7.23

Three caves near Abri Vaufrey all parallel-trending with arrowhead profiles (courtesy of C. Pierce).

Figure 7.22

Figure 7.23





Figure 7.22  
Figure 7.2.3



but abandoned it in favour of Africa. Although he did excavate rather extensively, little was ever published. He also "discovered" and named about 30 other caves and abris along the local cliffs, including Grotte 13.

Above Vaufrey on the cliff top is a Boy Scout camp. For many years the scouts used Vaufrey and several of the other caves for camping, and exploring. In the early 1970's, J.-P. Rigaud began to excavate there. Although he erected a fence to keep the Boy Scouts out, much damage had already been done.

#### 7.4.2 The Formation of the Caves

Two different karst processes have been acting to produce the Castelnaud caves. Undercutting erosion attacking the softer strata in the cliffs at about the level of Vaufrey has kept the cliff faces above exposed, as their edges periodically collapse and are added to the scree slopes at their base. Until the scree reaches the level of the softer strata and covers them, the cliff faces will continue to be exposed, as shown in Figure 7.21A.

Figure 7.21B shows the extent of the undercutting at present. These softer strata are also causing the roof of Abri Vaufrey to stope upward, as small abris erode into the rocks just above the roof (Figure 7.22), and then collapse into the sediments below as *éboulis*.

Within the cliffs, small faults perpendicular to the St. Cyprien Fault have produced weakness along which karst solutions have premeated to form many caves, all trending parallel to one

another, each with a characteristic arrowhead profile (Figure 7.23) Vaufrey, however, has two faults spaced about 15 m apart which are responsible for its great width, and more complex profile. Figure 7.24 shows the two faults which together cause Vaufrey to be shaped like the distal end of an arrowhead.

### 7.4.3 Abri Vaufrey

Containing mainly Mousterian artefacts, Vaufrey is problematic as far as dating is concerned. Much of the sedimentary fill has been soliflucted, cryoturbated, or redeposited.

#### 7.4.3.1 General Description

Located in the cliffs overlooking Castelnaud about 50 m below the top of the cliffs, Vaufrey is a lofty abri about 12 m in height. Originally, it was almost completely filled with sediments. Although the bedrock has been found in parts of the back, 20 m of excavation at the front have still not reached the bottom.

At the back of the cave are two small grottoes formed along the two faults which are the reason for the abri's formation (Figure 7.24).

#### 7.4.3.2 Stratigraphy

The stratigraphy in Vaufrey, as shown in Figure 7.25, is from the top:

- O. Stalagmitic cap, very thin.
- I. Thermoclastic plaquettes with little interstitial silt, bones, and Quina Mousterian
- II. Dark brown loam with few éboulis, and two Mousterian

Figure 7.24

The two faults on which Abri Vaufrey is situated.

Figure 7.24



Figure 7.25

A diagrammatic representation of the stratigraphy  
in Vaufrey (Bordes, 1972).



cultural levels.

- III. Light yellow silt with very altered éboulis. At the base is a stalagmitic plancher. Mousterian artefacts.
- IV. Muddy silt with éboulis and two archeological levels (Mousterian). The base has been soliflucted into V and VI, while much of the level is soliflucted material from II and III. A burnt horizon which has also been soliflucted can be seen in the section. (Figure 7.26).
- V. Dark brown sand with thermoclastic éboulis, cemented, with Typical Mousterian. Figure 7.26.
- VI. Light brown, very similar to V, with large éboulis near the front of the abri. Typical Mousterian
- VII. Calcareous sand with rare éboulis, yellow, with Typical Mousterian.
- VIII. Yellow calcareous sand without éboulis, Typical Mousterian.
- IX. Yellow sand with plaquettes, soliflucted. Typical Mousterian. Figure 7.27.
- X. Typical Mousterian.
- XI. Subdivided into 3 layers:
  - a. Typical Mousterian
  - b. Mousterian of Acheulian Tradition
  - c. Acheulian, not in situ, has been deposited flu-  
vially.
- XII. Eboulis, sterile.
- XIII. Fluviially deposited bear bones, U. deningeri.
- XIV. Sand.



Figure 7.26

Couches 4 through 6:

Note on the upper picture the solufuction of  
the black horizon in couche 4, and the eboulis  
in couche 6 at the -190 cm mark.

Figure 7.2b



Figure 7.27

Couche 9, filled by plaquettes spalled from  
the roof.

Figure 7-27

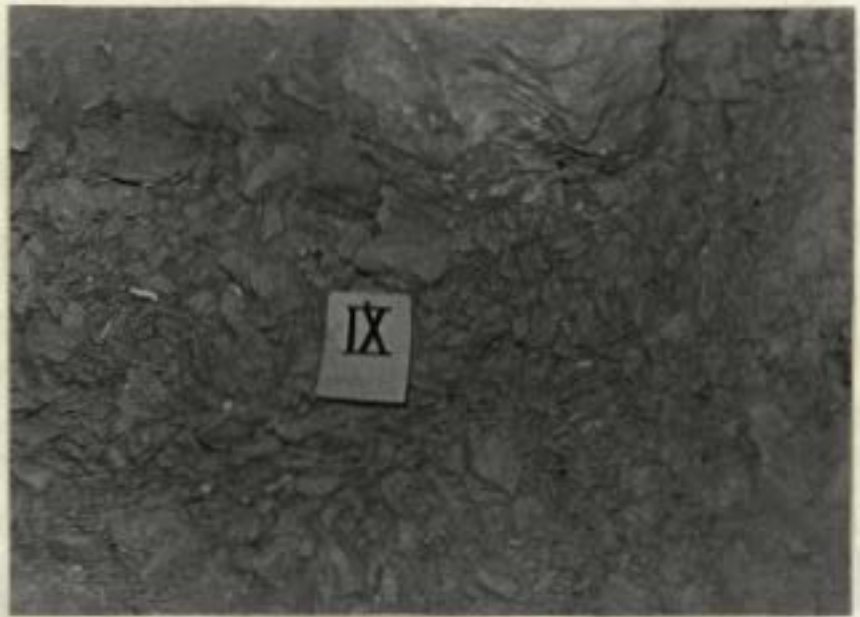


Figure 7.28

The stratigraphy of Vaufrey in the pit at  
the back: the lower figure continues down  
from the one above (courtesy of H. Schwarcz).



Figure 7-28

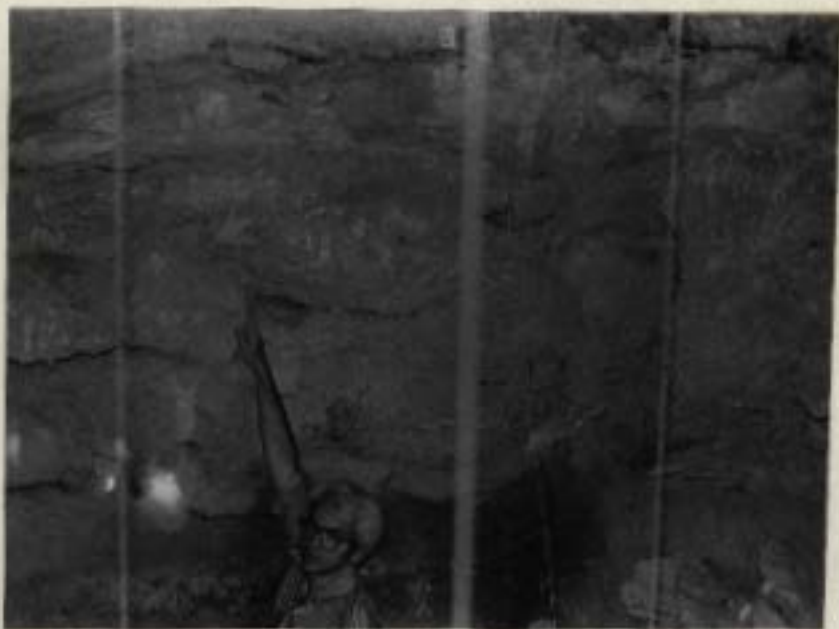


Figure 7.29

The view from the cliffs at Castelnaud:

The top picture looks along the Céou, tributary  
to the Dordogne, shown in the bottom photo.



Figure 7.29



Figure 7.2<sup>8</sup> shows the section near the back of the cave from layer I to XI.

#### 7.4.3.3 Archeology and Faunal Remains

Until more detail is published little can be added to the details listed with the stratigraphy. The Acheulian material, which is accompanied by few faunal remains, has a different patina from that of the Mousterian material. The Mousterian material is associated with a fauna of bovids, horses, and rhinoceros in layer XIb, and red deer, rhinoceros, and horses in the other layers. Layer I also contained ibex.

#### 7.4.3.4 Human Remains

Sometime between Vaufrey's and Rigaud's excavations, the Boy Scouts reputedly found a skull, presumably a Neanderthal. Unfortunately, all traces of the skull have been lost. (It probably sits in some aging Boy Scout's closet.) In addition one tooth, maybe Neanderthal, was found in layer I.

#### 7.4.3.5 Paleoenvironments

The basal sand in Vaufrey is thought to predate the Mindel, because of the U. deningeri bones above it. It may even be Villefranchian. The bones, however, were deposited in the Mindel, and subsequently redeposited. Layers XI through I, by virtue of their Mousterian industries and the low incidence of reindeer are thought to be from the Wurm I. Considering the thickness of the sequence, this is surprising. Regardless of the age, it is obvious why Vaufrey was chosen as a camp: From the cliffs, one can see for several miles along both the Dordogne and the Ceou to spot game (Figure 7.29).

Figure 7.30

The stalagmitic mound in Abri Vaufrey, from which samples 78AV1A-E are taken. (courtesy of H. Schwarcz).

Figure 7.30

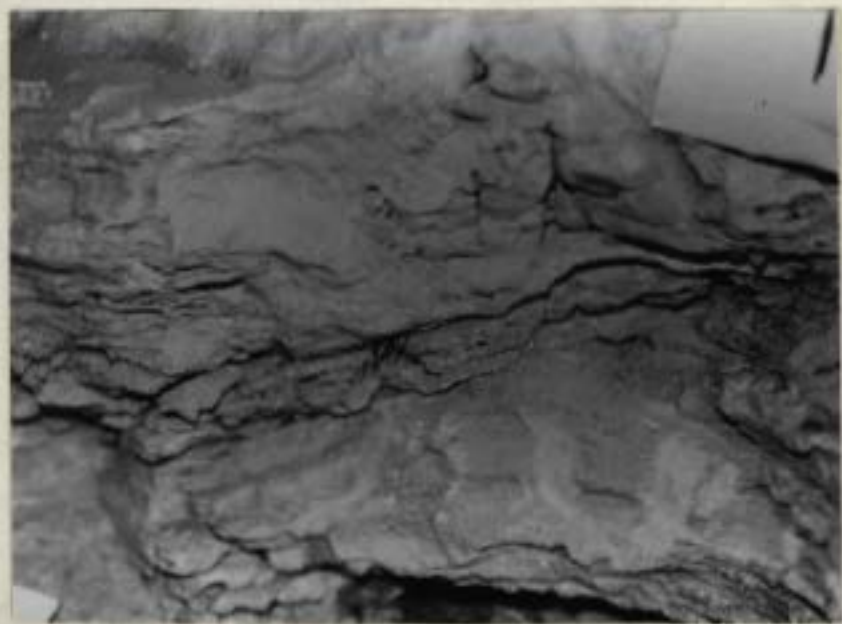
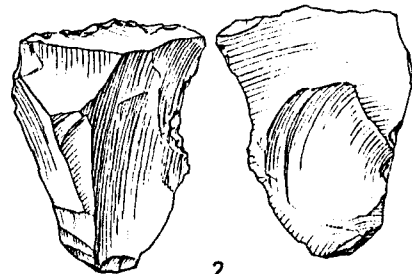
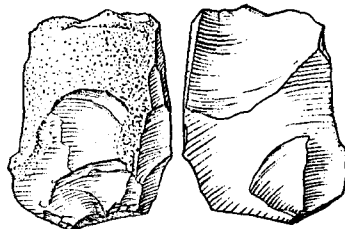
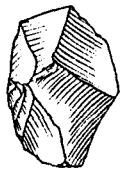
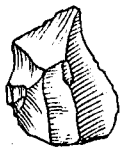
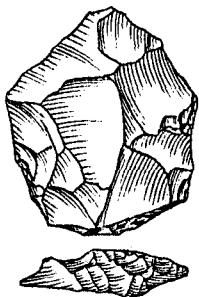
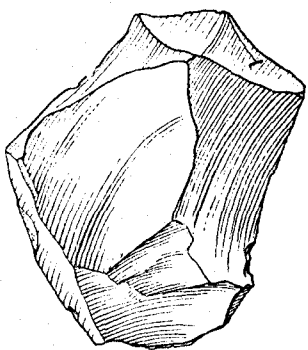


Figure 7.12

Tools from Pech IV (after Bordes, 1976).



2

3

4

1

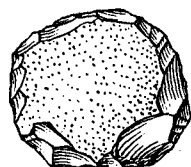
2



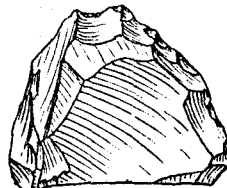
5



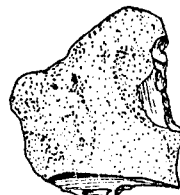
6



7



3



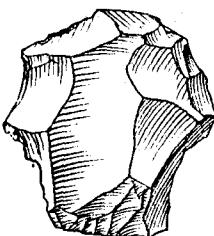
4



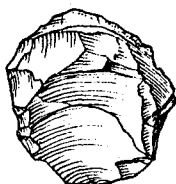
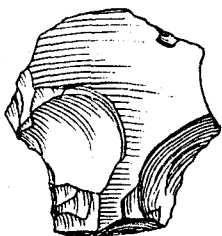
5



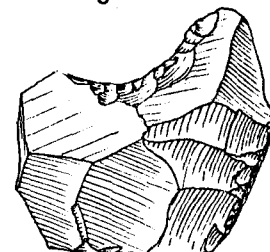
6



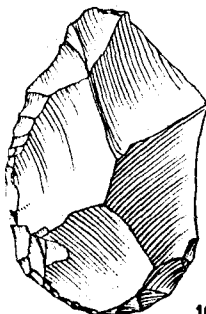
8



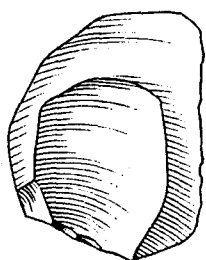
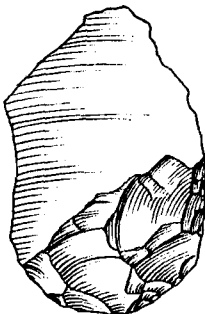
9



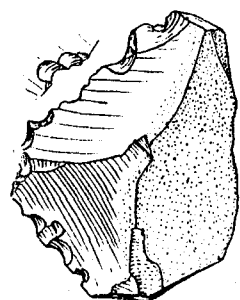
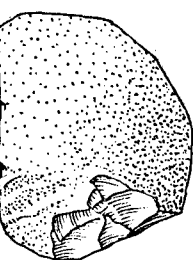
7



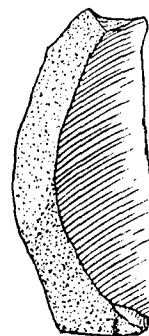
10



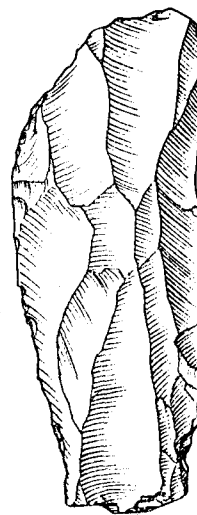
11



8



9



10



#### 7.4.3.6 Sample Descriptions

In 1978, H. Schwarcz, assisted by J.-Ph. Rigaud, collected several samples from Abri Vaufrey. Because preliminary results for these samples were discouraging, more samples were collected in 1979 by the author. It had been hoped prior to the 1979 collection that it would be possible to test the theory that soda straws are penecontemporaneous with the sediments in which they are found. Therefore, several soda straws were collected, but none of these were sufficiently large to attempt to analyze. Several new samples collected from the excavations proved to be wall rock, or sand cemented by calcite. There is very little travertine in Vaufrey suitable for dating.

One sample, 78AV9 (renamed 79AV15) was not transported from France. This probably would have been the best to analyze. 79AV18 was a small stalagmitic mound in the sediments of couche 7, which appeared as if it was in situ, lying flat, with the stalagmite up. No other stalagmitic material, however, was found in this level in the area. 79AV21 was a piece included in the shipment by the archeologists; therefore, its context is unknown. All other samples were unsuitable for dating.

During shipment, the majority of the 1978 samples were badly broken. Therefore, much of the material dated was from loose pieces. For the remainder of the material, relative positions are known, but mean nothing because only one date could be calculated for the sample.

#### 7.4.3.7 Results

Although Abri Vaufrey was not expected to be a problem to date by the U/Th method, results have been dismal. Roasting the samples helped to recover the uranium from some samples which had had low uranium yields for unroasted samples, but most still proved to be undatable. Tables 7.39 through 7.43 list the analytical data, while 7.38 gives the sample descriptions.

In layer III, a stalagmitic mound was sampled in five slightly different positions, 78AV1A-E, shown in Figure 7.30. Although 21 different attempts were made to date the samples, only four gave ages, three of which were from roasted samples. In all cases, the amount of detrital  $^{232}\text{Th}$  equaled or exceeded the that of  $^{238}\text{U}$  in the sample. Therefore none of the dates are reliable.

78AV5, 78AV6, and 79AV18 all come from layer VII. Excepting 78AV6-3 for which the  $^{232}\text{Th}$  concentration equals that of  $^{238}\text{U}$ , and 78AV6-4 for which the uranium concentration is higher than for any other subsample of 78AV6, the dates do agree. In fact even the lower limit of 78AV6-3 is in agreement. It is questionable, however, as the age for 78AV6-4 is so much younger and really should not be disregarded for any strong reason. Even disregarding this age, the average of  $149.3 \pm 62.0$  Ka is unreliable because the large amounts of detrital thorium have caused the corrected age noted above to be significantly younger than the uncorrected ages which average approximately 200 Ka.

Four samples were collected from layer IX, 78AV2, 78AV3,



SAMPLE	LOCATION	DESCRIPTION	THICKNESS	DETRITUS	POROSITY	CRYSTALS	BIOCLASTS	2° GROWTHS	LAYERING	COMMENTS
78AV5	sq J9, c 7 top	White microxtln fst with brown lam slightly convo- luted	6 cm	0%	10% ang X0	spar, 1/10 x 2/10 mm // lam	-	-	Xtl edges meet to form lam	
78AV6	sq I6, c 7	Chalky beige microxtln opaque fst with 1-2 mm lam, roof spall?	5 cm	-	-	-	-	-	-	
78AV7	sq G7 c 9 base	Loose pieces of sparry grey- brown trnsparent calcite xtls	up to 3 cm across	-	-	-	-	-	-	
78AV8	sq G7 c 10 top	White-beige microxtln fst with thin lam	2 cm	-	-	-	-	-	-	
78AV9	sq K10	Sample did not arrive.	-	-	-	-	-	-	-	
78AV10	sq K6 fst cap	White microxtln fst with faint lam	6 cm	30% clay 5% qtz	20% ang X1	av 1/2 mm random	-	-	More clay, pores on lam	
78AV11	Grotto sq J4 + 20 cm	Tan-brown microxtln .fst with faint lam	2 cm	50% clay 5% carb (biocl)	25% rd X2	1/5 mm random	bone	50% pores (=10% of total)	More clay, pores on lam x 2/20 mm radially into pores; unsuitable for dating	Sparry 2° growth av 1/20
78AV12	Grotto sq J4 + 30 cm	White microxtln fst with faint areas of very white dense calcite	3 cm	10% clay	30% ang X3	1/10 mm random	bone ?	5% of pores (=2% total)	-	
78AV13	sq K-L10 c J-4	Brown calcite cemented breccia of sand and eboulis	4 cm	10% clay 5% qtz 15% carb	60% ang -rd X4	variable: bone 1/10 - 1 mm random	bone	45% total		Unsuitable for dating

CORRELATION OF DATA FROM VALFREY, COUCHE 3,  
USING SAMPLES 78AV1A, 78AV1B, 78AV1C, 78AV1D, 78AV1E

SAMPLE	AGE (KA)	ERROR (KA)	YIELDS		TH-230		U-234 U-238	(U-234) (U-238)10	CONCENTRATIONS	
			U-232 (%)	TH-228 (%)	U-234 U-234	TH-232 TH-232			U-238 (PPM)	TH-232 (PPM)
78AV1A-1	-		0.00	27.52	-	7.5 3.4	-	-	-	.02
78AV1A-2	-		0.00	28.27	-	≥ 1000.0	-	-	-	0.00
78AV1A-3	-		0.00	29.38	-	4.7 .7	-	-	-	.06
78AV1B-1	- +		0.00	5.09	-	2.6 .5	-	-	-	.15
78AV1B-2	-		0.00	1.30	-	≥ 1000.0	-	-	-	0.00
78AV1B-3	-		0.00	11.36	-	2.9 .8	-	-	-	.09
78AV1C-1 12 350.03+	- +	19.3 18.6	41.45	15.20	1.083 .101	3.2 .6	1.3378 .111	-	.088	.11
78AV1C-2	-		0.00	14.31	-	5.6 2.0	-	-	-	.06
78AV1C-3	46.0 +	19.3 18.6	37.35	14.64	.506 .064	2.7 .6	1.625 .145	1.611 .040	.07	.07
78AV1C-4 ≥ 350.03+	- +	0.0+	15.79	30.87	1.084 .170	3.8 .7	1.3193 .243	-	.058	.06
78AV1C-5	-		0.00	30.75	-	2.5 .3	-	-	-	.15
78AV1C-6	-		0.00	65.76	-	2.6 .2	-	-	-	.10
78AV1D-1	-		0.00	4.35	-	5.2 2.8	-	-	-	.04
78AV1E-1	-		9.87	0.00	-	-	.972 0.000	-	.12	-
78AV1E-2	-		0.00	8.29	-	10.5 5.3	-	-	-	.01
78AV1E-3	-		0.00	23.12	-	10.6 4.0	-	-	-	.01
78AV1E-4	-		0.00	28.44	-	12.9 3.3	-	-	-	.01
78AV1E-5	50.6 +	8.6 8.4	13.28	46.00	.469 .035	4.2 .5	1.707 .148	1.619 .018	.01	.01
78AV1E-6	-		0.00	36.00	-	4.3 .6	-	-	-	.05
78AV1E-7	-		0.00	39.69	-	3.3 .5	-	-	-	.08
AVERAGES	49.5	+ 11.2 - 10.9					1.537 .122	1.455 .192	.07	

1 NOT INCLUDED IN THE AVERAGE DATE

+ THORIUM CORRECTION USED CALCULATED AT R = 1.25

+ REPRESENTS THE YOUNGEST AGE POSSIBLE NOT THE LOWER ERROR LIMIT CALCULATED AT R = 1.25

+ REPRESENTS THE OLDEST AGE POSSIBLE, NOT THE UPPER ERROR

CORRELATION OF DATA FROM VAUFREY, COUCHE 7,  
USING SAMPLES 78AV5, 78AV6, 78AV18

SAMPLE	AGE (KA)	ERROR (KA)	YIELDS		TH-230	TH-230	U-234	(U-234)	CONCENTRATIONS	
			U-232 (%)	TH-232 (%)	U-234	TH-232	U-238	(U-238)0	U-238 (PPM)	TH-232 (PPM)
78AV5-1	-		8.58	0.00	-	-	2.660 + 0.000	-	.02	-
78AV5-2	-		0.00	10.63	-	+ 5.3 - 1.9	-	-	-	.04
78AV5-3	157.8	+ 66.3 - 43.1	8.54	55.80	+ .814 - .131	+ 40.1 - 57.0	+ 1.984 - .710	+ 1.733 - .165	.02	.00
78AV5-4	-		0.00	41.03	-	+ 4.5 - .8	-	-	-	.02
78AV5-5	-		0.00	7.26	-	≥ 1000.0	-	-	-	0.00
78AV5-6	-		0.00	36.94	-	+ 19.9 - 15.8	-	-	-	.01
78AV5-7	157.2	+ 50.7 - 38.3	21.96	33.09	+ .860 - .084	+ 5.3 - .7	+ 1.043 - .102	+ 1.732 - .132	.05	.03
78AV6-2	103.03	+ 19.8 - 17.7	4.25	23.88	+ .670 - .061	+ 10.3 - 2.3	+ 1.4365 - .201	+ 1.6295 - .047	.078	.02
78AV1E-4	-		0.00	28.44	-	+ 12.9 - 3.3	-	-	-	.01
78AV1E-5	50.6	+ 8.6 - 8.4	13.28	46.00	+ .469 - .035	+ 4.2 - .5	+ 1.707 - .148	+ 1.619 - .018	.01	.01
78AV1E-6	-		0.00	36.00	-	+ 4.3 - .6	-	-	-	.05
78AV1E-7	-		0.00	39.69	-	+ 3.3 - .5	-	-	-	.06
AVERAGES	49.5	+ 11.2 - 10.9					+ 1.537 - .122	+ 1.455 - .192	.07	

‡ NOT INCLUDED IN THE AVERAGE DATE

+ THORIUM CORRECTION USED CALCULATED AT R = 1.25

\* REPRESENTS THE YOUNGEST AGE POSSIBLE NOT THE LOWER ERROR LIMIT CALCULATED AT R = 1.25

+ REPRESENTS THE OLDEST AGE POSSIBLE, NOT THE UPPER ERROR

Table 7.41

CORRELATION OF DATA FROM VALFREY, COUCHE 9,  
MINE SAMPLES 78AV3, 78AV7, 78AV8

SAMPLE	AGE (KA)	ERROR (KA)	YIELDS		TH-230	TH-230	U-234	(U-234)	CONCENTRATIONS	
			U-232 (%)	TH-232 (%)	U-234	TH-232	U-238	(U-238) G	U-238 (PPM)	TH-232 (PPM)
78AV3-1	214.8	+ 63.2 - 40.9	20.56	7.01	+ .895 - .070	+ 53.2 - 73.2	+ 1.161 - .066	+ 1.331 - .092	.08	.00
78AV3-2	216.1	+ (> 350.0+) - 95.0	27.11	4.20	+ .906 - .150	+ 15.7 - 29.2	+ 1.238 - .062	+ 1.332	.08	.02
78AV3-3	-		0.00	35.87	-	+ 75.3 - 80.0	-	-	-	.00
78AV3-4	-		0.00	29.82	-	+ 22.2 - 40.7	-	-	-	.00
78AV3-5	> 350.0+ (≥ 350.0+)		46.69	44.26	+ 1.630 - .560	+ 4.9 - 1.9	+ 1.278 - .466	-	.018	.01
78AV3-6	42.18	+ 34.2 - 31.8	12.74	35.95	+ .553 - .092	+ 2.1 - .4	+ 1.681 - .386	+ 1.204 - .031	.048	.06
78AV7-3	190.6	+ (> 350.0+) - 190.6	12.04	37.32	+ .893 - .244	+ 5.2 - 2.1	+ 1.094 - .370	+ 1.309	.03	.02
78AV7-4	-		0.00	42.02	-	+ 13.1 - 4.3	-	-	-	.01
78AV3-1	-		0.00	8.67	-	+ 1000.0	-	-	-	0.00
78AV3-3	245.7	+ (> 350.0+) - 70.3	53.06	74.91	+ .953 - .082	+ 6.5 - 1.1	+ 1.180 - .103	+ 1.361	.05	.03
AVERAGES	226.3	+ 152.5 - 105.8					+ 1.181 - .115	+ 1.344 - .428	.06	

CORRELATION OF DATA FROM VAUFREY, COUCHE 9,  
USING SAMPLES 78AV2

SAMPLE	AGE (KA)	ERROR (KA)	YIELDS		TH-230	TH-230	U-234	(U-234)	CONCENTRATIONS	
			U-232 (%)	TH-228 (%)	U-234	TH-232	U-238	(U-238)0	U-238 (PPM)	TH-232 (PPM)
78AV2-2	≥ 350.0\$+	- 15.5+	6.32	8.43	+ 1.697 - .700	+ 4.0 - 1.8	+ .862\$ - .443	-	.02\$	.02
78AV2-3	≥ 350.0\$+ (≥ 350.0+)		47.67	28.26	+ 1.053 - .124	+ 6.6 - 2.5	+ .849\$ - .087	-	.05\$	.02

‡ NOT INCLUDED IN THE AVERAGE DATE

+ THORIUM CORRECTION USED CALCULATED AT R = 1.25

+ REPRESENTS THE YOUNGEST AGE POSSIBLE NOT THE LOWER ERROR LIMIT CALCULATED AT R = 1.25

+ REPRESENTS THE OLDEST AGE POSSIBLE, NOT THE UPPER ERROR

Table 7.42

CORRELATION OF DATA FROM VAUFREY, COUCHE 10,  
USING SAMPLES 78AV10

SAMPLE	AGE (KA)	ERROR (KA)	YIELDS		TH-230	TH-230	U-234	(U-234)	CONCENTRATIONS	
			U-232 (%)	TH-228 (%)	U-234	TH-232	U-238	(U-238)0	U-238 (PPM)	TH-232 (PPM)
78AV10-1	≥ 350.0\$+	- 0.3+	4.15	5.08	+ 1.098 - .200	+ 7.2 - 4.5	+ 1.209\$ - .20E	-	.09\$	.05
78AV10-2	-		0.00	5.61	-	+ 10.2 - 13.6	-	-	-	.02
78AV10-3	22.8\$+	+ 7.3 - 7.2	6.44	30.14	+ .353 - .029	+ 2.2 - .2	+ 1.375\$ - .123	+ 1.400\$ - .139	.15\$	.10

‡ NOT INCLUDED IN THE AVERAGE DATE

+ THORIUM CORRECTION USED CALCULATED AT R = 1.25

+ REPRESENTS THE YOUNGEST AGE POSSIBLE NOT THE LOWER ERROR LIMIT CALCULATED AT R = 1.25

+ REPRESENTS THE OLDEST AGE POSSIBLE, NOT THE UPPER ERROR

Table 7.43

CORRELATION OF DATA FROM VAUFREY, COUCHE Z,  
USING SAMPLES ABOVE DATUM, 78AV11, 78AV12

SAMPLE	AGE (KA)	ERROR (KA)	YIELDS		TH-230	TH-230	U-234	(U-234)	CONCENTRATIONS	
			U-232 (%)	TH-228 (%)	U-234	TH-232	U-238	(U-238) $\mu$	U-238 (PPM)	TH-232 (PPM)
78AV11-1	-		14.70	0.00	-	-	1.642 $\pm$ 0.000	-	.09 $\pm$	-
78AV11-2	$\geq 350.0\pm$	- 9.3 $\pm$	14.38	26.04	+ 1.263 .198	+ 2.0 .2	+ 1.542 $\pm$ .340	-	.05 $\pm$	.14
78AV12-1	187.5 $\pm$ ( $\geq 350.0\pm$ )	- 101.5	11.69	6.72	+ .919 .151	+ 3.8 1.9	+ 1.296 $\pm$ .167	1.502 $\pm$	.04 $\pm$	.04
78AV12-3	95.0 $\pm$	+ 14.2 - 13.1	20.78	37.92	+ .703 .032	+ 3.1 .1	+ 1.039 $\pm$ .043	+ 1.051 $\pm$ .058	.34 $\pm$	.25

\* NOT INCLUDED IN THE AVERAGE DATE

+ THORIUM CORRECTION USED CALCULATED AT R = 1.25

\* REPRESENTS THE YOUNGEST AGE POSSIBLE NOT THE LOWER ERROR LIMIT CALCULATED AT R = 1.25

+ REPRESENTS THE OLDEST AGE POSSIBLE, NOT THE UPPER ERROR

78AV7, and 78AV10. 78AV2 gave no useful results, but solutional vugs along its laminations and the low  $^{234}\text{U}/^{238}\text{U}$  ratio compared with other samples in the abri suggest it has been leached of  $^{234}\text{U}$ , which would account for the age of  $\approx 350.0$  Ka. The other samples, however, show some agreement when the data with the concentration of  $^{232}\text{Th}$  greater than that of  $^{238}\text{U}$  are rejected (78AV3-5, 78AV3-6). The good yields for 78AV8-3 lend credence to the average age of  $226.3 \pm 152.5$  Ka, although the error is large.

The data from layer X are very peculiar. Although the uranium yield for 78AV10-3 is low, the other parameters seem reasonable compared to those for other samples in the abri; yet the age seems to be much too young. More dates on this sample are necessary before anything conclusive can be said about the date.

From the small grotto above the datum come 78AV11 and 78AV12. Although 78AV11-2 was roasted, it still gave no useful date because the concentration of  $^{232}\text{Th}$  was much greater than that of  $^{238}\text{U}$ . Nor are the results listed for 78AV12 very reliable because of the high concentrations of  $^{232}\text{Th}$ . Although the age of  $95.0 \pm 14.2$  Ka for 78AV12-2, a roasted sample, may represent the actual age, with only one date the determination is not certain.

Several other samples were collected from Abri Vaufrey, but most were either too small to date, or contained noticeable amounts of calcite detrital fragments. Conceivably, the samples dated may have contained carbonate detritus as well, although it was noted only in 78AV1B and 78AV11, neither of which gave results.

#### 7.4.3.8 Conclusions

None of the results from Abri Vaufrey, except those for layer IX, are very reliable. Unfortunately, the material in layer IX consists of stalactitic plaquettes spalled from the roof, and hence, the age represents that of the deposition of the calcite on the roof, not that of the strata in which the plaquettes are deposited. Therefore, there are no dates for the deposition of the sediments in Vaufrey. Perhaps, layer VII is about 150 Ka, placing it in the late Riss, a date in partial agreement with those derived for the Mousterian tools embedded in the breccias at Pech de l'Azé, while the stalagmitic plancher in the grotto may be about 100Ka old.

Therefore, Abri Vaufrey experienced deposition of stalactites in the late Mindel or early Mindel/Riss, about 250 Ka ago, which later fell into the sediments below. At some time, the cave was filled with sediments, mostly éboulis from the roof, and occupied by people who left Mousterian artefacts behind, some of which might be as old as Rissian. The stalagmitic material in the cave is high in detrital  $^{232}\text{Th}$ , low in uranium, and has  $^{234}\text{U}/^{238}\text{U}$  ratios which average 1.3 - 1.4. More work is necessary but difficult to accomplish because much of the remaining material from the samples collected is too full of detrital thorium to date, and the cave has been closed, its excavations finished as of 1979. Therefore, the problem of dating Abri Vaufrey may remain unsolved.



#### 7.4.4 Grotte Treize

About 200 m south of Abri Vaufrey in the cliffs overlooking Castelnaud is a deep cave called Grotte Treize (13), also known as Grotte de l'Eglise. Although there are no archeological materials inside, there are numerous faunal remains, and large amounts of travertine. All stratigraphic data comes from Laville (1975).

##### 7.4.4.1 General Description

The entrance to Grotte 13, which opens at approximately the same level as that of Vaufrey is about 1.7 m high, giving access to a foyer about 7 m square. In the south wall is a small passage 1 m high, opening below the level of the floor in the foyer. Further west this deepens where it has been excavated by Laville (1975). This passage, the Main Gallery, extends west for 15 m at a level about 2 m below the stalagmitic plancher which floors both the foyer and Shanty's Nose, although the latter slopes upward toward the rear of the room. Figure 7.31 is a map of Grotte 13.

To the north off Shanty's Nose are Diverticules 1 and 2. Diverticule 1, a room with active stalactites (Figure 7.33), is partially filled by a shallow pool masking the excavations made by Laville. Diverticule 2 is reached through a narrow squeeze. Beyond Shanty's Nose, the caves continues on a lower level, connecting eventually with Grotte Douze (12).

##### 7.4.4.2 Stratigraphy

In section 1 in the Main Gallery, Laville noted the following:

I. Thin (0.5 to 1 cm) plancher.

1. Brown sandy silt with granular structures, locally

Figure 7.31

Plan view of Grotte 13 (after Laville, 1975).

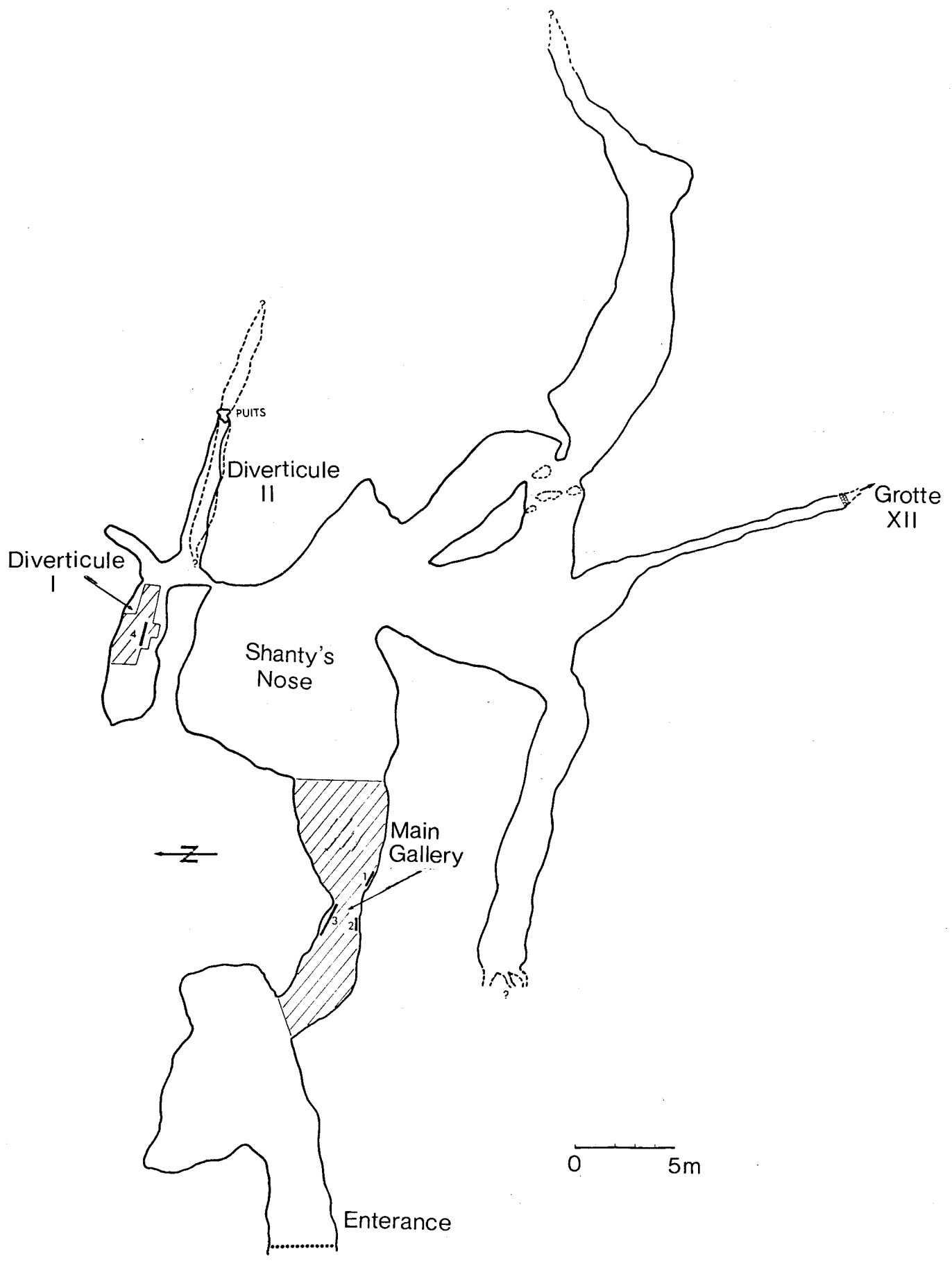


Figure 7.32

Actively growing stalactites in Diverticule 1,  
Grotte 13.

Figure 7.33

The Mindel/Riss boundary, couche II, Main  
Gallery, Grotte 13.

Figure 7.32  
Figure 7.33



divided by a thin more silty layer, containing stalagmitic debris and some éboulis from the walls.

- II. Stalagmitic plancher with lenses of silt and sand, fragments of stalagmites and stalactites. Locally, stalagmites grow up from this layer through layer I
2. Yellow brown sand, very friable, containing stalactites and stalagmites as in II.
  3. Cemented sediment which texturally appears to be as in layer 2. Rich in faunal remains.
  4. Brown silt, foliated, "crackled" (sic), plastic when wet, with rare calcite concretions.
  5. White concreted calcite formed as lenses on the top of layer 6.
  6. Reddish-brown unconsolidated sand, weathered into plaquettes, with many resistant calcareous concretions of irregular form.
  7. Hard compact reddish-brown sand rich in fine gravels, éboulis, and fauna.
  8. Sand like in layer 7, but not undurated. Many plaquettes and fine gravel.
  9. Reddish-brown sand rich in gravel, especially fine white calcite gravel with many large éboulis in the extreme east.
  10. Brown silty sand, foliated with many black bones and a few concretions of iron oxide.
- III. Stalagmitic plancher, discontinuous, formed of plaquettes lying flat. More plaquettes to the east.

11. Brownish-red silt with small éboulis and rare thin lenses of finer silt.
12. Yellowish-brown sand, texturally similar to layer 11, with some concreted gravels.
13. Yellowish-brown compact sand with cemented fragments of the same colour with rare black spots, and much quartz gravel.
14. Yellowish-brown silty sand, locally hardened with rare quartz gravels, illuvial concretions of sand and many black spots.
15. Silty sand identical to layer 14, strongly cemented, layered into plaquettes.
16. Yellowish-brown silty sand with many quartz pebbles and bones, rare illuvial concretions and stalactites. In the west, layer 16 rests on IV, a well-cemented deposit, but in the east, it rests on layer 17.
- 17a. Large sands with some silt, light brown to reddy-yellow in colour, with many quartz pebbles, rare cemented sand aggregates.
- 17b. Porous slightly silty sand, reddish yellow but cut by black and white beds, and obliquely crossed by a black zone.
18. Five distinct layers of reddish-yellow to yellowish-brown sand with many quartz pebbles, black spots at top.
19. Reddish-yellow sand with rare quartz pebbles.
20. Red sandy silt with hardened nodules.

21. Two layers of sandy silt, yellowish-red in colour, the bottom one containing illuvial concretions.

Below **layer 21** is a limestone floor which is either the Jurassic host rock or the top of another stalagmitic plancher.

In Diverticule 1, the stratigraphy is as follows:

0. Superficial clay
1. Upper stalagmitic plancher.
2. Sand with lenses of microfauna either yellow or black.
3. Lower stalagmitic plancher of varying thickness, with some sand lenses and bones of small mammals.
4. A dark brown indurated sand.
5. Black sand with lighter irregularities. Base is deposited in a gulley which washed out part of layers 6 and 8
- 6a. Stalagmitic plancher.
- 6b. Breccia of bones, especially U. deningeri, which pinches out at the edges of the diverticule.
7. Very localized discontinuous white clacite.
8. Fossiliferous sandy silt with many U. deningeri at the base.
9. Compact sand.
10. Silty sand.
11. Silty sand.

Figure 7.33 shows the Mindel/Riss boundary, **layer II** in the Main Gallery, while Figure 7.34 shows the two sections as seen by Laville in the Diverticule, and the Main Gallery.



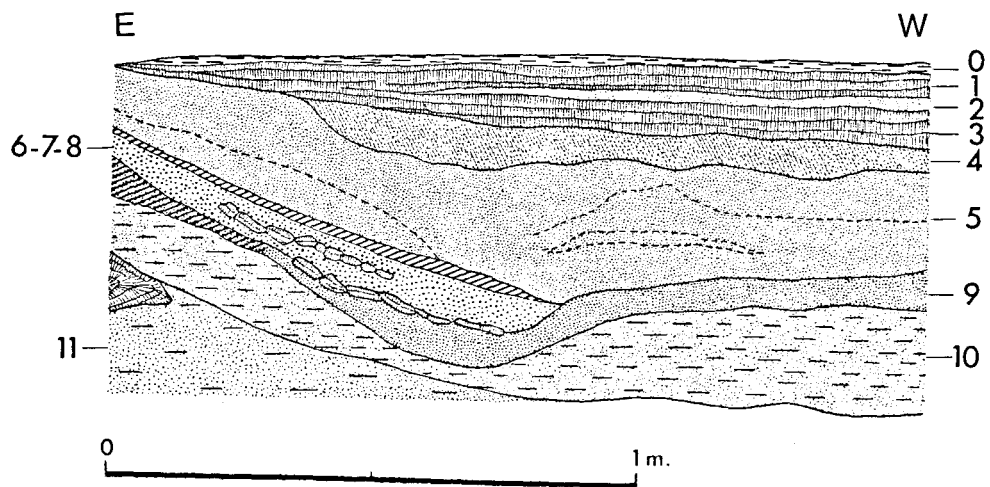
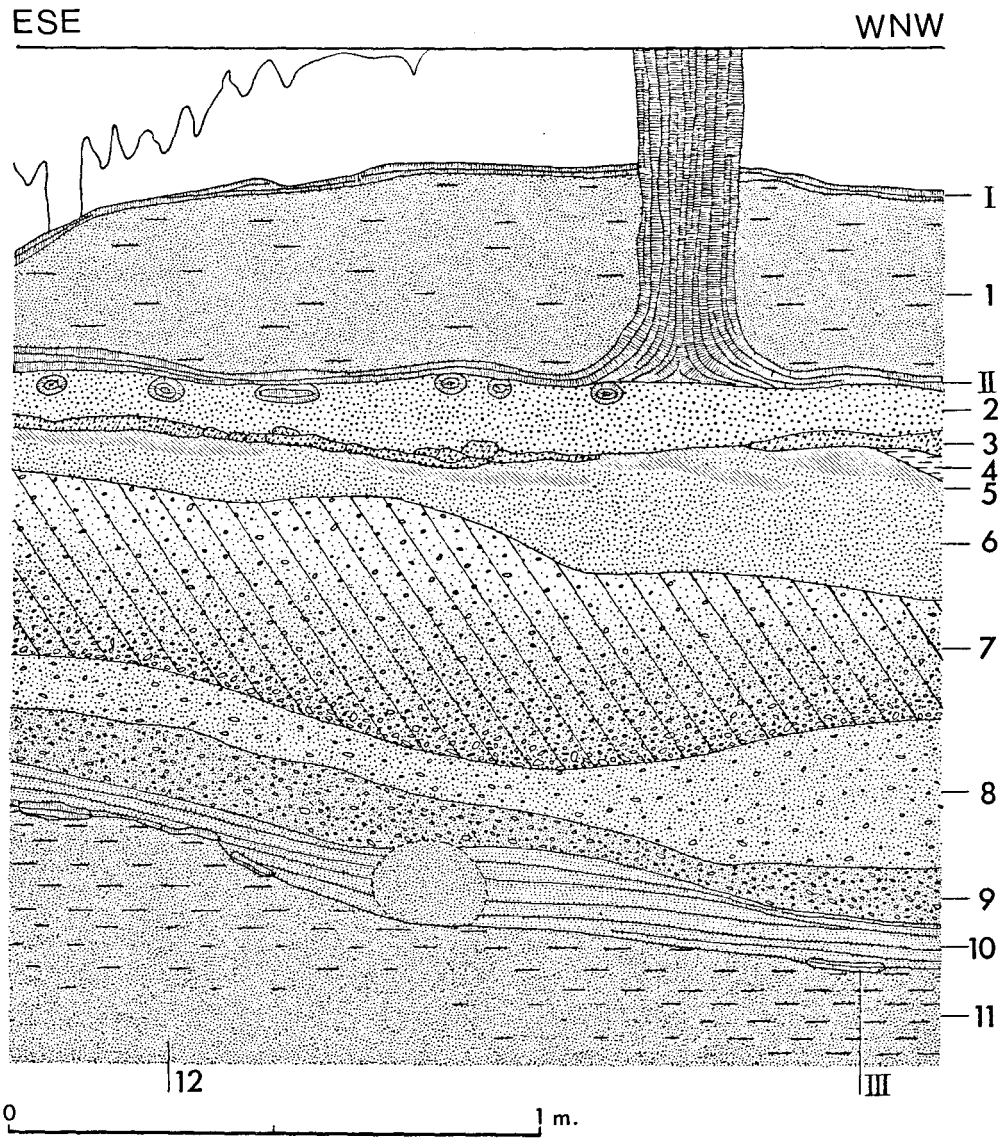
Figure 7.34

The stratigraphy in Grotte 13;

A. The main gallery cut 1

B. Diverticule 1

(after Laville, 1975)



#### 7.4.4.3 Paleoenvironments

Within Grotte 13, cryoclastic action has not affected the sediments, but they are the result of normal karstic pedogenic conditions. Therefore, the sediments give no hints as to the paleoclimatic conditions except that they were moist and warm.

In the Main Gallery, U. deningeri is common throughout layers 2 to 16, with the highest concentrations registered in layers 2-3, 7, 10, and 16. In the diverticule, the greatest concentrations of bear bones, U. deningeri, are found in layer 8 and 10, but occur throughout the section below layer 1. A thar, Hemitragus, is found in both areas, while Canis etruscus and Cervus are found in the Main Gallery.

Several of these species can be used to establish relative dates. Hemitragus indicates a very cold climate, because these goats are usually found only in alpine areas. Meanwhile, Canis etruscus was replaced by the taller Canis lupus in the Mindel/Riss. In Western Europe, U. deningeri evolved in the Günz/Mindel. Therefore, the association is thought by Prat (in Laville, 1975) to be Mindelian. This, however, does not completely agree with the sedimentology. Therefore, Laville (1975) attributes the layers below II to either a very early Mindel/Riss or a Mindel interstadial for the Main Gallery sequence, and the entire section in the Diverticule to the same period.

#### 7.4.4.4 Sample Descriptions

As in Vaufrey, the 1978 collections were made by H. Schwarcz, and the 1979 collection by the author, assisted by J.-Ph. Rigaud. Collection with Grotte 13 was hampered by the pool which filled the excavation made in Diverticule 1 by H. Laville. The pool fills the pit to about the level of layer 1-3, making it impossible to tell the stratigraphy of the material below the sample collected, 79GT6, and also impossible to collect anything from layer 6a. It was not possible to drain the pit because this would have required lowering a pump over the cliff and somehow connecting sufficient piping to carry the water entirely out of the cave. For one sample, this effort was not warranted. If at some future time more excavation is attempted in the Diverticule 1, it might be possible.

79GT7 was collected from approximately the same location as 78GT4, although it was impossible to be certain because several locations looked similar. Both, however, are from the same layer.

Collecting samples in Diverticule was almost impossible. Because of the cramped crawlway, and the shaft there, only one person could navigate the passage at a time. Therefore, the sample 79GT8 was collected by Rigaud's assistant, who knows the crawlway very well. It is impossible to locate its exact position on the map, and the stratigraphy in this region is unknown.

Since most of the samples were very small in both collections all the subsamples analyzed were slices of the sample, cut to include all growth layers.

#### 7.4.4.5 Results

Although the samples from Grotte 13, with the exception of 78GT8, look as if they should be reasonably good for dating, many of the analyses gave low yields, which, coupled with the low uranium concentration, made it difficult to obtain good dates. Many of the samples contained high amounts of  $^{232}\text{Th}$ , in some cases exceeding the amount of uranium. Several samples were roasted to improve the yields. Table 7.47 lists the sample descriptions and Tables 7.44 to 7.46 the analytical data. Figure 7.35 shows 78GT1 and 78GT5.

78GT1, 78GT2, 78GT3, and 78GT5 were all collected from couche II in the Main Gallery. Although they vary slightly in stratigraphic position within the layer, they should all give the same date. 78GT1-3, 78GT1-4, 78GT1-5, 78GT3-3, and 78GT5-3 were roasted before analysis. Excepting 78GT2, which contains too much  $^{232}\text{Th}$  to make the date reliable, there is a bimodal distribution of the dates. 78GT1, which showed solutional pitting on its upper surface averages  $40.6 \pm 6.6$  Ka, while the others average  $124.6 \pm 23.1$  Ka, ignoring 78GT5-2 which has a very high uranium concentration for 78GT5, and a suspiciously low amount of detrital  $^{232}\text{Th}$  for this region, but why this should be so is unknown.

No dates were obtained for layer I in the Main Gallery by roasting or normal analyses. Like the other deposits in the cave, high amounts of detrital  $^{232}\text{Th}$  plague this deposit.

In Diverticule 1, two stratigraphically equivalent subsamples of 79GT6 give significantly different ages. For 79GT6-2 the uranium concentration is very high compared to others in the cave, and

Table 7.44

CORRELATION OF DATA FROM GR. XIII, MG C II,  
USING SAMPLES 78GT1, 78GT2, 78GT3, 78GT5

SAMPLE	AGE (KA)	ERROR (KA)	YIELDS		TH-230	TH-230	U-234	(U-234)	CONCENTRATIONS	
			U-232 (%)	TH-232 (%)	U-234	TH-232	U-238	(U-238) <sub>0</sub>	U-238 (PPM)	TH-232 (PPM)
78GT1-2	-		5.49	0.00	-	-	1.304 + 0.000	-	.15	-
78GT1-3	95.23 <sup>†</sup>	+ 33.3 - 27.1	7.36	40.71	+ .647 - .101	+ 7.4 - 1.0	+ 1.113 <sup>†</sup> - .230	+ 1.405 <sup>†</sup> - .044	.13 <sup>†</sup>	.04
78GT1-3 R	34.0	+ 3.9 - 3.9	10.96	40.71	+ .310 - .020	+ 7.4 - 1.0	+ 2.061 - .183	+ 1.341 - .005	.15	.04
78GT1-4	62.3	+ 15.3 - 14.7	24.88	13.73	+ .494 - .052	+ 7.2 - 3.4	+ 1.629 - .107	+ 1.370 - .020	.08	.03
78GT1-5	35.33 <sup>†</sup>	+ 4.2 - 4.1	6.89	80.57	+ .314 - .023	+ 8.5 - .9	+ 1.161 <sup>†</sup> - .090	+ 1.343 <sup>†</sup> - .035	.23 <sup>†</sup>	.03
78GT2-1	151.71 <sup>†</sup>	+ 210.9 - 151.7	22.48	6.59	+ .899 - .183	+ 2.5 - .9	+ 1.753 <sup>†</sup> - .205	+ 1.473 <sup>†</sup> - .348	.05 <sup>†</sup>	.10
78GT3-3	114.2	+ 7.8 - 7.4	32.62	76.41	+ .738 - .020	+ 5.0 - .1	+ 1.120 - .025	+ 1.428 - .012	.27	.14
78GT5-1	61.3 <sup>†</sup>	+ 22.7 - 19.0	1.68	11.81	+ .440 - .113	+ 75.0 - 158.3	+ .938 <sup>†</sup> - .251	+ 1.353 <sup>†</sup> - .028	.09 <sup>†</sup>	.00
78GT5-2	14.0	+ 3.0 - 2.9	15.30	36.51	+ .121 - .024	+ ≥ 1000.0	+ 1.129 - .105	+ 1.323 - .003	.21	0.00
78GT5-3	124.6	+ 29.7 - 25.3	47.70	49.86	+ .766 - .064	+ 5.2 - .8	+ 1.161 - .092	+ 1.440 - .044	.01	.00
-----							-----	-----	-----	
AVERAGES	81.4	+ 11.8 - 10.6					+ 1.310 - .084	+ 1.324 - .132	.12	

† NOT INCLUDED IN THE AVERAGE DATE

\* THORIUM CORRECTION USED CALCULATED AT R = 1.25

Table 7.45

CORRELATION OF DATA FROM GR. XIII, MG C I,  
USING SAMPLES 78GT4, 78GT7

SAMPLE	AGE --- (KA)	ERROR ----- (KA)	YIELDS		TH-230	TH-230	U-234	(U-234)	CONCENTRATIONS	
			U-232 (%)	TH-228 (%)	U-234	TH-232	U-238	(U-238)0	U-238 (PPM)	TH-232 (PPM)
78GT4-1	-		0.00	4.56	-	+ 1.4 - 1.1	-	-	-	.04
78GT4-3	-		0.00	15.91	-	+ 3.0 - .9	-	-	-	.06
78GT7-1	-		0.00	20.11	-	+ 3.6 - 1.7	-	-	-	.04

‡ NOT INCLUDED IN THE AVERAGE DATE

+ THORIUM CORRECTION USED CALCULATED AT R = 1.25

‡ REPRESENTS THE YOUNGEST AGE POSSIBLE NOT THE LOWER ERROR LIMIT CALCULATED AT P = 1.25

+ REPRESENTS THE OLDEST AGE POSSIBLE, NOT THE UPPER ERROR

Table 7.46

CORRELATION OF DATA FROM GR. XIII, DIV 1 C1-3  
USING SAMPLES 78GT6

SAMPLE	AGE --- (KA)	ERROR ----- (KA)	YIELDS		TH-230	TH-230	U-234	(U-234)	CONCENTRATIONS	
			U-232 (%)	TH-228 (%)	U-234	TH-232	U-238	(U-238)0	U-238 (PPM)	TH-232 (PPM)
78GT6-1	20.4‡+	+ 4.3 - 4.3	19.82	19.47	.218 + .017	5.0 + 1.6	1.338‡ + .059	1.359‡ + .067	.18‡	.03
78GT6-2	5.4‡+	+ 1.9 - 1.9	11.4‡	35.32	.093 + .009	2.5 + .5	1.169‡ + .045	1.172‡ + .046	.34‡	.05

‡ NOT INCLUDED IN THE AVERAGE DATE

+ THORIUM CORRECTION USED CALCULATED AT R = 1.25

+ REPRESENTS THE YOUNGEST AGE POSSIBLE NOT THE LOWER ERROR LIMIT CALCULATED AT R = 1.25

+ REPRESENTS THE OLDEST AGE POSSIBLE, NOT THE UPPER ERROR

Table 7.47 Sample Descriptions from Grotte 13

SAMPLE	LOCATION	DESCRIPTION	THICKNESS	DETRITUS	POROSITY	CRYSTALS	LAYERING	2° GROWTHS	COMMENTS
78GT1	MG c.II	White-grey macroxtln fst with one visible growth lam	2-4 cm	10% clay 5% carb 5% qtz	20% ang X0	variable 1mm - 1cm random,	Clay concent- rated on lam	80% rextlz	Solutional pitting on upper surface, 1 soda straw with radial xtls
78GT2	MG c.II	Grey-white macroxtln fst, porous appearing with a few growth lam	4 cm	variable 0-10%	20% ang X0	Massive av. 1-3 cm random	Clay concent- rated on lam, lam more porous	Relict spars rextlz	
78GT3	MG c II bottom	White transparent macroxtln fst, with 2 major growth hiati, few minor growth lam at bottom, soda straws in base	5 cm	variable 5-25% clay	10-20% ang X0	½ - 1 mm // lam	More clay, smaller xtls on lam	Rextlz?	Dissolved channel on upper surface, filled by Fe-rich sand
78GT4	MG c I	Grey-white stg, uppermost lam marked by yellow silt, brown lam near base, macroxtln, active stg	6 cm	<5%	5% ang X0	Massive, orient undeter- mined	Silt on lam	90% rextlz	
78GT5	MG c II c. II	Beige microxtln stg, yellow stg above silt on some growth rings	4 cm high	10-20% silt, clay	25% ang X0	variable ½ - 4 mm	More clay, silt, smaller xtls on lam	rextlz?	
78GT6	Div 1 c. 1 & 3	Beige-white macroxtln fst with stg, soda straws near base, lam 5 mm apart	variable 1-10 cm	0-50% clay, silt	5-50% ang X0-X3	Variable ½ mm random -2 cm //lam	More clay, pores, smaller xtls on lam	partially rextlz?	
78GT7	MG c I	Grey-white macroxtln fst with soda straws in middle red silt in growth lam	3 cm	10-20% clay, silt	variable 10-40% ang X0	av. ½ mm random	more clay, pores on lam	Relict spars rextlz	



SAMPLE	LOCATION	DESCRIPTION	THICKNESS	DETRITUS	POROSITY	CRYSTALS	LAYERING	2° GROWTHS	COMMENTS
78GT8	Div 2	Dark brown calcite-cemented sand	3-4 cm	20% clay 20 qtz 35 carb 5 fspar	10% ang	very small	-	-	Cement constitutes about 20% of sample, bioclasts present include teeth, bones, also oolites

ABBREVIATIONS:

MG = Main Gallery

Div = diverticule

qtz = quartz

fspar = feldspar

dep = deposit

2° = secondary

c. = couche

sq = square

lm = laminations

fst = flowstone

stg = stalagmite

stc = stalactite

ang. = angular pore shape

rd = rounded pores

av = average

polyg = polygonal shaped crystals

orient = orientation

rectlz = recrystallized

// lam = oriented parallel to growth laminations

min = mineral

diam = diameter

pl sup = plancher supérieur

xtln = crystalline

Connectedness of the Pores

X0 = unconnected

X1 = partially connected

X2 = connected

X3 = well connected

X4 = a sponge-like porosity

Figure 7.35

Couche II, Grotte 13:

A. 78GT1

B. 78GT5

(photos courtesy of H. Schwarcz)

Figure 7.35



the  $^{234}\text{U}/^{238}\text{U}$  ratio is rather low for 78GT6-2, compared to those in layer II of the Main Gallery. Therefore, 79GT6-1 may be an accurate age,  $20.4 \pm 4.3$  Ka, but one determination is not enough to say positively.

Diverticule 2 contained nothing suitable for dating.

#### 7.4.4.6 Conclusions

Although the fauna in layers 2 through 16 in the Main Gallery may be Mindelian, layer II, the stalagmitic plancher is apparently a Riss/Würm deposit which was partially dissolved in the Würm I/II. If this is accurate, however, where are the Mindel/Riss and Riss deposits? Although the cave may have been sealed off from outside sediment sources, why is there no travertine from the Mindel/Riss, if the deposits below layer II are Mindelian? A date for layer III would solve this problem. Layer I is still undated.

In the diverticule, layers 1-3, the stalagmitic plancher may be much younger than expected, as its lone date corresponds to Würm III/IV. Layer 2 was assigned to the Mindel on the basis of one bear bone, from a layer which overlies a layer (5) which obviously has been deposited after fluvial erosion. Furthermore, there are no bear bones in the intervening levels. Therefore, the one bone may have been dissolved out of some other level and redeposited in layer 2. Therefore, the date may be accurate. A date for the stalagmitic plancher in layer 6a would perhaps solve the problem, if that level can be sampled with the pool that now fills the excavation. At present, the pool fills the cut to the top of layer 3.

## 7.5 Conclusions

Generally, for the Dordogne caves as a whole, the uranium concentrations are very low, averaging less than 0.2 ppm in most deposits. Furthermore, travertine deposits are scarce, especially for the two archeological caves. There is, however, some correspondence in the ages determined for the Dordogne caves.

Two, and possibly all three, of the caves studied have experienced deposition of stalagmitic planchers between 125 and 100 Ka. Furthermore, the ages of these deposits in two are bimodally distributed, indicating periods of solution and recrystallization at approximately 35 to 40 Ka. Therefore, the periods of 125 to 100 Ka and 35 to 40 Ka must represent two regional phenomena. Because speleothem is not deposited at subzero temperatures, these periods must have been wet and not extremely cold. Hence, it is probable that the Riss/Würm interglacial dates from 100 to 125 Ka, and the Würm I/II interstadial occurred at 35 to 40 Ka BP. While the former was accompanied by the deposition of speleothems, the latter was marked by solution and recrystallization.

Both Pech de l'Azé and Abri Vaufrey also have experienced deposition of stalactitic travertine on their ceilings approximately 225 to 250 Ka BP, and perhaps as far back as 350 Ka. These roof deposits later spalled off into the lower sediments.

There may have also been a brief period of deposition at about 20 Ka BP.

Because all three caves contain speleothem dating from the

Riss/Würm, all must have been formed prior to that period. Furthermore, two contain stalactites which formed over 200 Ka BP, while the other contains sediments which underly the Riss/Würm deposits. Therefore, all the caves must have been formed long before the Riss/Würm.

The dates established herein agree well with the ages determined for the warm trend in the global deep sea core data, isotope stage 5, dated from approximately 120 to 90 Ka (Broecker and van Donk, 1970), and a warm oscillation noted at 40 Ka. At about 250 Ka, the isotope record shows a warmer interglacial period. Therefore, the data are consistent.

Although the archeologists would claim that the Mousterian at Pech de l'Aze was Würmian, the Mousterian here must predate the beginning of the Würm I by several thousand years. Although it is uncertain, the thick sequence from Abri Vaufrey probably partially predates the start of the Würm as well, as both Pech and Vaufrey contain Typical Mousterian facies in their sections, some of which are pre-Würmian in Pech de l'Aze.

## CONCLUSIONS

In Southern France, there are several regional climatic phenomena which can be correlated between the Dordogne and the Charente regions. Furthermore, the cultures in both regions can be shown to be significantly older than previously assumed.

Both regions experienced stalagmitic plancher deposition in the Riss/Würm interglacial from 125 to 80 Ka BP. These planchers were formed in each of the five sites examined, and in all cases were extensive deposits usually more than 5 cm thick, implying wet conditions throughout the district. Similarly, both regions experienced deposition of stalactites which later spalled off, and some stalagmitic deposition at approximately 250 Ka corresponding to the Mindel/Riss, or a Mindel interstadial. Finally, both regions may have experienced limited deposition in the Würm III/IV.

In both areas, the Würm I/II interstadial has affected the deposits. But in the Charente, speleothem was deposited, while in the Dordogne, previously deposited speleothem was dissolved and recrystallized. Only in the Charente in Lachaise was deposition of speleothem in the Riss II/III seen. Obviously, from the dates of the speleothem in all the caves, they were all formed prior to the Riss.

There is no question from the data presented that the Mousterian culture predates the beginning of the Würm by several thousand years. In Lachaise, an approximate date for its development

is 125 Ka, some 45 Ka before the Würm I. In all four archeological caves, there are Mousterian cultural layers underlying deposits which are Riss/Würm in age. Furthermore, the Neanderthals with which this industry is often associated also predate the Wurm, their appearance predating 150 Ka. Therefore, the Neanderthals had evolved before they developed the Mousterian culture. The two events are not contemporaneous. Therefore, Neanderthals need not be associated with Mousterian cultures, but might be expected to be associated with evolved Acheulian, as well.

Much more remains to be discovered about the travertine in archeological sites. Although the roasting technique has improved the basic method for some archeological samples, many samples remain undatable by both procedures. Certainly the nature of the detrital contaminants in the travertines need to be studied, as does the trace element composition for samples which consistently result in poor yields or dates  $\geq 350$  Ka, which are obviously wrong. Study of the effects of bioclastic contamination, especially by bones and teeth, could provide some insight into the problems encountered in dating calcite-cemented bone breccias, which has proven to be unsuccessful. More work regarding the petrography of fine grained speleothems might reveal features not previously recognized that could give answers to some of these problems. Finally, there many more sites to be dated, both in Europe and in Asia and Africa which have travertines associated with their cultural artifacts. The many analyses done in the McMaster laboratories, and one or two others, have only skimmed the surface.



## REFERENCES

- Bass, W.M. 1971 Human Osteology. Missouri Archeological Society, Columbia.
- Bilsborough, A. 1972. Cranial Morphology of Neanderthal Man. Nature 237: 351-352.
- Binford, L.R. & S. Binford, 1966 A preliminary analysis of functional Variability in the Mousterian of Levallois facies. American Anthropologist 68: 238-295.
- Bordes, F. 1961 Mousterian cultures in France. Science 134: 805-811.
- 1961b La Typologie du Paléolithique ancien et moyen. Bordeaux.
  - 1968 The Old Stone Age. McGraw Hill, New York.
  - 1972a A Tale of Two Caves. Harper-Row New York.
  - 1972b. Fouilles et monuments archeologiques en France metropolitaine. Gallia Préhistoire 15: 487-497.
  - & D. de Sonne ville-Bordes, 1974. The significance of variability in Paleolithic assemblages.
  - 1976 Le gisement du Pech de l'Azé IV. Bulletin de la Société Préhistorique Française 2:293-308.
- Brace, C.L. & A. Montague. Human Evolution, 2nd ed. McMillen, New York
- Brace, CL, H. Nelson, N. Korn. 1971. Atlas of Fossil Man. Holt, Rinehart, Winston, New York.
- Brace, C.L., H. Nelson, N. Korn, M.L. Brace, 1979. Atlas of Human Evolution, 2nd ed. Holt, Rinehart, Winston, New York.
- Bowen, D. 1978 Quaternary Geology. Pergammon Press, London.
- Cherdyntsev, V.V. 1971 Uranium-234, translated by J. Schmorak. Keter, Jerusalem.
- Cherdyntsev, V.V., N. Senina, E.A. Kuzmina, 1975. Die alterbestimmungen det travertin. on Weimar-Ehringsdorf. Abh. des Zentral Geologischen Instituts 23: 7-14.

- Crew, H. 1976. The Mousterian site of Rosh Ein Mor. In Prehistory and Paleoenvironments in the Central Negev, Israel, Vol I. SMU Press, Dallas, 317-351
- Debenath, A. 1974. Thèse: Recherches sur les terrain Quaternaires Charentais et les industries qui leur sont associées. Bordeaux.
- Debenath A. & L. Duport, 1971. Os travaillés et os utilisés de quelques gisements préhistoriques charentais. Memoires de la société Archeologique et Historique de la Charente 1971: 189-202.
- Duport, L. L'Art Préhistorique en Charente. Société Archéologique et Historique de la Charente.
- Duport, L. Découverte d'une portion de mandibule de Néanderthalien dans le gisement de Montgaudier. Memoires de la société Archeologique et Historique de la Charente, 1973-74: 33-36.
- Duport, L. 1977. Dix Années de Fouilles a Montgaudier. Société Archeologique et Historique de la Charente.
- Duport, L. 1976. La grotte de Montgaudier. Valenciennes et les Anciens Pays-bas. IX: 399-404.
- Fagan, B. 1974. Men of the Earth. Little Brown, Boston.
- Faure, G. 1977. Isotope Geology. Wiley, New York.
- Flint, R.F. 1971 Glacial and Quaternary Geology. Wiley, New York.
- Ford, D.C. & R.O. Ewers, 1979. The development of limestone cave systems in the dimensions of length and depth. CJES 18: 1783-1798.
- Gascoyne, M. 1979. Pleistocene Climates determined from Stable Isotope and Geochronologic Studies of Speleothem. PhD Thesis, McMaster, Hamilton.
- Harmon, R. 1975. Late Pleistocene Environments in North America as inferred from Isotopic Variation in Speleothems. PhD Thesis, McMaster, Hamilton.
- Harmon, R., J. Glazek, K. Nowak, 1980.  $^{230}\text{Th}/^{234}\text{U}$  dating of travertine from the Bilzingsleben site. Nature 284: 132-135.
- Howell, F.C. 1952. Pleistocene glacial ecology and the evolution of "classic" Neanderthal Man. Southwestern J. of Archeology 8: 377-410
- 1957. The evolutionary significance of variation and variability of Neanderthal Man. Quarterly Rev. of Biology: 32: 330-347

- Howells, W.W. Neanderthals: names, hypotheses and scientific methods. American Anthropologist 76: 24-38.
- Jelinek, J. 1969. Neanderthal man and Homo sapiens in central and eastern Europe. Current Anthropology 10:475-503.
- Kleindienst, M. 1961. PhD. Thesis, Michigan.
- Langmuir, D. 1978. Uranium solution-mineral equilibria at low temperatures with applications to sedimentary ore deposits. GCA 42: 547-569.
- Laville, H. 1975. Climatologie et Chronologie du Paléolithique en Périgord. Provence.
- Leakey, M. 1971. Olduvai Gorge. Cambridge Press, Cambridge.
- Leakey, R. & R. Lewin, 1977. Origins. Dutton, New York.
- LeGros Clark, W.E., 1965. History of the Primates, 5th ed. Chicago Press, Chicago.
- Leroi-Gourhan, A. 1968. The evolution of Paleolithic art. Old World Archeology. Freeman San Francisco, 12-23.
- Mintz, L.W. Historical Geology, 2nd ed. Merrill, Columbus.
- Moore, G.W., 1952. Speleothem - a new cave term. National Speleological Society News 10:2.
- 1957. The growth of stalactites. Bulletin of National Speleological Society 24: 95-106.
- Roe, D.A. 1964. The British Lower and Middle Paleolithic. PPS XXX; 245-267.
- Schwarcz, H.P. P. Goldberg, B. Blackwell, 1978. U-series dating of archeological sites in Israel, Nature 277: 558-560.
- Schwarcz, H.P. & A. Debénath, 1978. Absolute dating by U-series disequilibrium of human remains at Lachaise du Vouthon (Charente). Comptes Rendus 288: 1155-1157.
- Schwarcz, H.P. 1979. U-series dating of contaminated travertines. McMaster Tech Memo 79-1
- Schwarcz, H.P., Y. Liritzia, A. Dixon, 1980. Absolute dating of travertines from Petralona Cave. Anthropos 7: 152-173.
- Schwarcz, H.P. 1980. Absolute age determination of archeological sites by uranium series dating of travertines. Archeometry 22: 3-24.

- Shackleton, N.J. & N.D. Opdyke, 1976. Oxygen isotope and paleomagnetic survey of Pacific core V28-239. GSA Memoir 145: 449-464.
- de Sonneville-Bordes, D. & J. Perrot. 1956. Lexique typologie du Paléolithique supérieur. Société Préhistorique Française.
- Smith, P. 1964. Solutrean culture. Old World Archeology. Freeman San Francisco, 24-32.
- Szabo, B.J. & K.W. Butzer, 1979. U-series dating of lacustrine limestones from pan deposits with final Acheulian assemblage at Rooidam, Kimberly District, South Africa. Quaternary Research 11: 257-260.
- Thomas, D.H. 1971 On the use of cumulative curves and numerical taxonomy. American Antiquity 36: 206-209.
- Thompson, P. 1973. Speleochronology and Late Pleistocene Climates inferred from C,C,H, U, and Th isotopic variations in Speleothems. PhD Thesis, McMaster, Hamilton.
- Trinkaus, E. & W.W. Howells. 1979. The Neanderthals. Sci Am 1979 6: 118-133.
- Weast, R.C. ed. 1972 Handbook of Chemistry and Physics, 53rd ed. CRC Press, Cleveland.
- Webb, E. 1978. Problems in the use of the cumulative frequency graph of the comparison of lithic assemblages. XVIII Int. Archeometry Conference, Bonn